Analysis of Protein Modifications in Biopharmaca by Capillary Electrophoresis and High-Performance Liquid Chromatography: Monitoring Deamidation, Charge Variant Distribution, and PEGylation

Inauguraldissertation

zur

Erlangung der Würde eines Doktors der Philosophie

vorgelegt der

Philosophisch-Naturwissenschaftlichen Fakultät

der Universität Basel

von

Alena Ferenc

aus

der Tschechischen Republik

Basel 2019

Genehmigt von der Philosophisch-Naturwissenschaftlichen Fakultät auf Antrag von

Prof. Dr. Peter C. Hauser
PD Dr. Maria Anna Schwarz
ao. Univ.-Prof. i.R. tit. Univ.-Prof. Mag. Dr. Andreas Rizzi

Basel, den

Prof. Dr. Martin Spiess

Dekan

Acknowledgements

Today is the day: writing this note of thanks is the finishing touch on my thesis. It has been a period of intense learning for me, not only in the scientific area, but also on a personal level. Though only my name appears on the cover of this dissertation, a great many people have contributed to its production and have made this dissertation possible. To them I shall always be grateful.

My deepest gratitude is to my supervisor PD Dr. Maria Anna Schwarz for giving me opportunity to be a member of her group. Her passion and dedication for electrophoretic techniques have resulted in a decision to graduate in this field. She has introduced me to capillary electrophoresis and gave me the chance to meet and participate on many attractive projects. This work would not have been possible without her great ideas, advices and patience.

I would like to thank my colleagues from Solvias Company. You supported me greatly and were always willing to help me. I wholeheartedly appreciate everything you have done for me: Dr. Alexander Beck, Delphine Ketterer, Dr. Claudia Michael, Rafael Sande, Dora Bolyan, Dr. Britta Person, Dr. Alexandra Stettler, Kristina Djordjevic, Petra Lombardi, Thomas Gräber, Dr. Philipp Wettstein, Clifford Barrow, Dr. Thomas Kauf, Nadia Howald, Dr. Bärbel Rückert, Dr. Eva Rödel. Some became friends for life.

I am also indebted Prof. Peter C. Hauser, Dr. Dawn Williams, Dr. Steffen Kiessig, Rolf Ketterer and Dr. Jan David. Your guidance and support has been amazing.

Very special thanks go to Andreas and Christa. I just want to say how grateful I am that you were sharing your wisdom with me.

Most importantly, none of this would have been possible without the love and patience of my husband, of my family and my husband's family. I want to extend my thanks to my closest friends who supported me over the last years, especially Markéta Fikrlová, Vendy Zgraggen, Tereza Michlová, Zuzana Zetzema and special family members Denisa Virtelová and Nikola Guldová.

Finally, I appreciate the financial support from Solvias AG that funded parts of the research discussed in this dissertation.

Summary

This thesis focuses on the analysis of protein modifications and protein isoforms in biopharmaceuticals. It evaluates the potential of HPLC-UV, HPLC-ESI-MS, CE-UV and CE-ESI-MS methods, when optimized and used together with specific enzymatic treatments, for characterizing protein modifications like deamidation, modifications leading to a shift in the charge pattern, and on PEGylation.

In a first study, the effect of various forced degradation conditions on asparagine deamidation in peptides and proteins was investigated. Capillary electrophoresis and chromatography were applied to examine this kind of peptide and protein degradation in intact and digested samples. It is demonstrated that both analytical methods provide very good resolution of deamidated species and allow to distinguish between asparagine, aspartate and isoaspartate in intact samples. Although the introduced electrophoretic conditions did not yield the detection of succinimides (whereas they were clearly detected by chromatography), CZE was a preferred choice over chromatography. Using the CZE method, the analysis time was reduced more than three times and the present Asn, Asp, isoAsp variants were separated in close proximity to each other always in the same way (migration order depends on pH value of separation buffer). This fact allowed determination of present deamidation by visual comparison of the UV electropherograms of unstressed and stressed intact samples. Introducing the specific cleavage of aspartates by Asp-N enzyme, the presence of deamidation could be verified using electrophoresis (or chromatography) without employment of MS detection. The electrophoretic (and chromatographic) profiles of unstressed and stressed digested samples were compared. The presence of some new peak(s) in stressed digested sample was commonly a sign of deamidation. The explanation for this observation is the increased presence of aspartates in stressed (deamidated) samples. It was shown that the application of Asp-N digestion is particularly useful for the investigation of forced degradation in peptides. When applying this approach to larger polypeptides and proteins, the results become more complicated to interpret. One of the reasons, why the visual detection of deamidation by the comparison of the data was nearly impossible, was the low level of deamidation in molecules with longer amino acid chain. These molecules are better protected from deamidation and the attempts to produce some deamidated sample were often unsuccessful. To avoid the long incubation times (often needed to induce deamidation in proteins) and frequently observed sample degradation, L-Asparaginase was applied to accelerate the deamidation rate of asparagine. Although the utilization of this method led to faster deamidation in Peptide 1, no acceleration of the deamidation rate could be observed in proteins under the conditions described.

In a second study, charge variants (i.e. isoforms with different net-charge) of two monoclonal antibodies (IgGs) were examined by capillary zone electrophoresis. By means this method, various isoforms with different net-charge could be separated and detected when using bare fused silica capillaries without any additional permanent capillary coating, but using ε-aminocaproic acid (EACA) as additive to the running buffer. An enzymatic cleavage was applied to reduce the complexity of these proteins. Papain digestion followed by electrophoretic analysis led to an improved demonstration of single charge variants. The described strategy also allowed the better localization of changes that occurred in the structure of stressed samples. The developed CZE method with EACA as additive to the background electrolyte was employed for further enzymatic studies using pepsin or lysine hydrolysis and a coupled papain-PNGase digestion.

Finally, in the third study, the application of diverse electrophoretic and chromatographic methods for a study of a PEGylated and glycosylated protein is demonstrated. Considering the possibility of the detection of PEGylated peptides and the quantification of PEG by capillary electrophoresis, this analytical tool was favoured over chromatography. Capillary electrophoresis showed its potential for the investigation of the degree of PEGylation and for the localization of PEGylation sites (followed by calculation of PEG occupancy - PEGocc). For this purpose the findings from previous studies were utilized and the advantages of the introduced methods were taken to achieve an optimal separation.

TABLE OF CONTENTS

1 Aim

In this work we would like to demonstrate the efficiency and performance of capillary electrophoresis when used for the characterization of posttranslational modifications in proteins. This powerful technique allows the separation of a wide variety of analytes in only one type of capillary, whereas with HPLC often various column types have to be chosen to achieve optimal separation. Applying CZE for the investigation of biopharmaceutical drugs, high throughput (short analysis times) can be expected, often with higher resolving capability compared to other analytical methods. CZE as the preferred method will be combined with various other analytical techniques within this work.

With proteins used as biopharmaceuticals, deamidation (i.e. the change of asparagine to aspartate and isoaspartate) has to be controlled as deamidation might have a serious impact on the drugs' functionality. Thus, deamidation in peptides and proteins is subject of our investigation. In the first part of the study, optimum conditions for forced degradation were examined to attain a reproducible production of stressed material. Shortly after that, the mapping of the deamidated species was performed. For investigating the degraded species the commonly used CZE-UV and HPLC-MS methods were employed together with a novel procedure, i.e. the specific cleavage with the enzyme Asp-N for distinguishing between asparagine, aspartate and isoaspartate residues. The possibility to generate faster and more specific formation of aspartate was studied. It is known that L-Asparaginase is able to hydrolyse the asparagine single amino acid to aspartate. Therefore the function of the catalytic effect in peptides and proteins was examined. The aim of this study was to evaluate the potential of these combined methods, i.e. CZE-UV and HPLC-ESI-MS together with Asp-N treatment for monitoring deamidation events on routine basis.

The aim of the second study was to demonstrate how well capillary zone electrophoresis (CZE) could replace capillary isoelectric focusing (CIEF) methods in examining charge variants and charge alterations in monoclonal antibodies. This procedure is aimed at the investigation of intact monoclonal antibodies as well as to the polypeptide chains obtained by enzymatic hydrolysis with papain or other proteolytic enzymes.

Finally, the aim of the third study was demonstrating the potential and the usefulness of capillary zone electrophoresis for characterizing the modifications of proteins by polyethylenglycol poly/oligomers. This characterization covered the determination of the PEGylation degree (quantity of all PEG moieties attached), the localization of the PEG attachment sites and the determination of the PEG occupancy. CZE was evaluated as tool for monitoring protein heterogeneity caused by PEGylation.

2 Introduction

2.1 Protein based biologics

Development and production of pharmaceutical products belongs to the strongest growing areas in industry and business worldwide. With the rapidly aging population, the medical requirements steadily increased in recent decades [1]. To face the challenges of complex oncology or of auto-inflammatory diseases, to address just two examples, the products supplied to market have dramatically changed. Over the last decade, biopharmaceutical companies tended to focus on the discovery and development of protein-based drugs [2, 3]. Especially in oncology, monoclonal antibodies (mAbs) have proved to be an important tool for fighting threatening diseases [4, 5]. The top ten pharmaceutical products by sales worldwide in 2014 are presented in Scheme 1 which shows that five of these ten pharmaceuticals are protein-based drugs, two of them ranking in the top two positions.

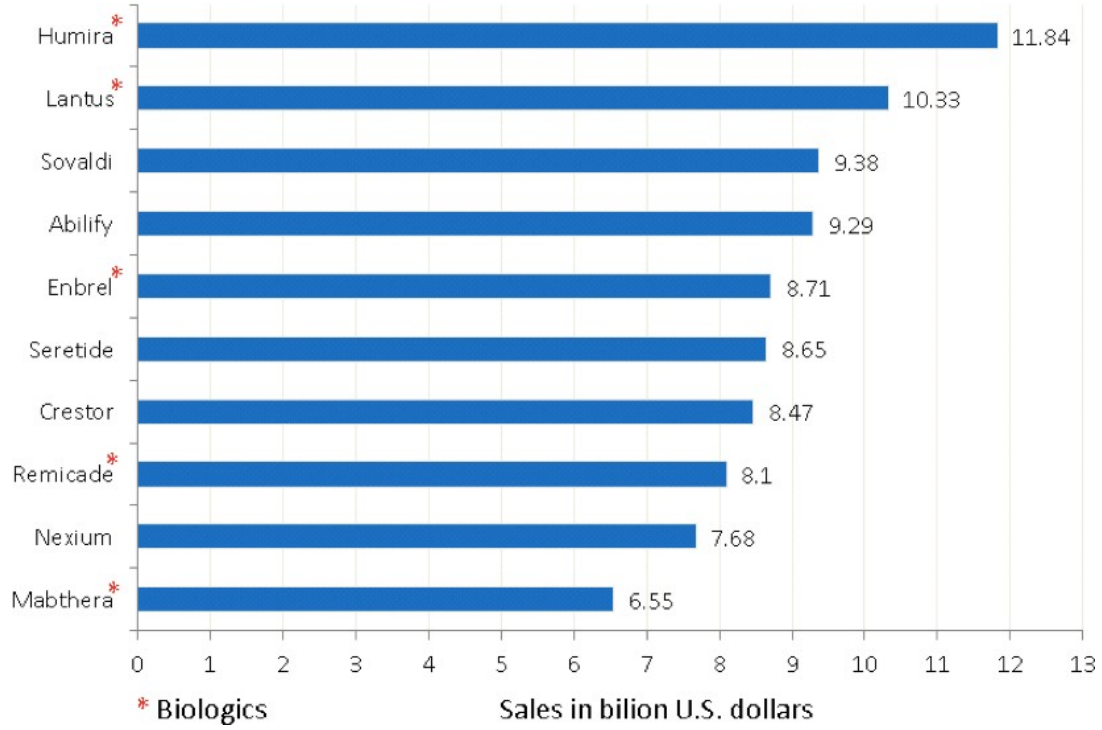

Scheme 1: Overview over the global pharmaceutical market – top ten best-selling products worldwide in 2014 [6].

Without doubt, researchers will succeed also in the future in finding new ways of treating not only widely spread but also rare diseases, and many medical and pharmaceutical products will emerge aimed at improving human life quality. For consumers' protection both, best quality and highest safety of these products have to be assured [7].

Protein therapeutics are obtained in complex production processes, mostly involving cell cultures of microorganisms. Unlike chemical synthesis, reaction pathways are highly interconnected potentially resulting in a large number of side-products and modifications that might impact product quality [8]. Purification, storage and administration as a part of the protein drug lifecycle should also be taken into account. Finally, the aspects of aggregation, fragmentation and degradation have to be considered as they can negatively impact the drug's safety profile [9].

Proteins in cells can undergo various modifications, as for instance co- and post-translational modifications like glycosylation, phosphorylation and methylation, coupling of cysteine-thiols by disulphide bridges etc. [1]. In addition, there might occur chemical degradation or modification by hydrolysis, isomerization, racemization, deamidation, oxidation etc. [10], as well as physical degradation and aggregation, denaturation, precipitation etc. [11, 12]. For biopharmaceuticals (biologica) it is very important to be able to control and demonstrate the product integrity, lot-to-lot manufacturing consistency and long-term product stability (under recommended storage conditions) to ensure the biological function of the product.

Commonly, particularly if the protein is glycosylated, the product shows a certain heterogeneity arising from slight variations in the glycan species attached to the protein (micro-heterogeneity) or from other modifications like deamidation, glycation, C-terminal Lys cleavage, N-terminal glutamine cyclization, etc. [13, 14, 15]. This heterogeneity pattern is influenced primarily by the manufacturing process but also by the storage conditions. In any instance, these variants have to be controlled, since alterations, for example in some glycan epitopes and in surface-charge properties (e.g. deamidation, incorrect disulfide bond formation, partial denaturation etc.) can lead to an unwanted immune response [16, 17]. The availability of a wide set of specific and sensitive test procedures for controlling product integrity, purity and stability, as well as type and concentration of impurities is thus essential.

2.1.1 Structural features relevant in biopharmaceuticals

Modification (degradation) of asparagine to aspartate or isoaspartate residues in proteins (deamidation) can impact in vitro stability and in vivo biological functions. The deamidation reaction kinetics is found to depend on the polypeptide sequence next to the deamidation sites. It probably differs for synthetic peptides and intact proteins, where the higher order structure plays an important role. It is an interesting issue, how deamidation processes can be influenced and how a better stability against deamidation can be achieved. (This question will be addressed in chapter 3.1 of this Thesis.)

Deamidation, phosphorylation, sulfation, acetylation etc., as well as the presence of charged sugars like sialic acids, lead to a set of protein isoforms exhibiting differences in their net charge (charge variants). The charge variant profile (charge heterogeneity) is an important issue when characterizing therapeutic proteins like monoclonal antibodies. (This topic will be addressed in 3.2.)

Biomolecules typically studied in the context of therapeutic use are composed of amino acids, nucleic acids, glycans or complex combinations of these groups of substances. They cover different ranges of molecular weight and often differ in their production. They might range from lower molecular mass (from peptides with approximately 5 to 10 kDa), over proteins (IgGs with approx. 150 kDa) up to large macromolecules (IgMs with about 300 kDa and others over 500 kDa). Often, the therapeutic potential of biomolecules and their biotechnological production efficiency can be enhanced by coupling these proteins to partner compounds building conjugates. Examples cover different types of conjugates, from radionuclide chelators, to protein conjugates with cytotoxic drugs, and e.g. polyethylenglycol (PEG) modified protein drugs [2]. Protein modification with PEG, referred to as PEGylation, is a procedure of growing interest and several PEGylated protein conjugates are commercially available. Attachment of PEG molecules to a protein is a covalent modification that increases the half-life of proteins *in vivo*, improves efficacy of the drugs, and reduces immunogenicity [18, 19, 20]. PEGylation, however, leads to enhanced protein heterogeneity which is difficult to study and to control in detail. Detailed structural characterization of such complex molecules as PEGylated proteins is a demanding task. Determining the linkage sites of PEG to a polypeptide requires sensitive and accurate analytical methods [19]. (This issue is part of the investigations reported in chapter 3.3).

Typically, biological drugs are delivered by transgenic organisms; they are widely expressed in bacterial, fungal and mammalian cell cultures. Bacterial expression systems are very popular for protein expression because of the low costs and the simplicity of cultivating bacteria [21]. However, these prokaryotes lack enzymes typical for humans, and

this fact can cause incorrect disulfide bond formation, very significant changes in post-translational modifications (PTMs) like unmatching or totally absent glycosylation. Therefore, many molecules obtained from bacterial expression systems are in their detailed structure not identical to those gained from mammalian cells. Although the therapeutic action of proteins is widely determined by the amino acid sequence, post-translational modifications as well play a crucial role for protein function, availability and stability. Even small differences in the structure of proteins can lead to protein aggregation, reduced solubility or to differences in the pharmacokinetic and pharmacodynamic properties. In some instances, even the entire loss of function (e.g. caused by missing glycosylation in the case of erythropoietin) might occur, or a change in the strength of action (e.g. observed with aberrant fucosylation in the case of monoclonal antibodies (mAbs) and their antibody dependent cell-mediated cytotoxicity (ADCC) activation effect [22]). Hence, molecules that need this type of modification for their desired function need to be expressed in mammalian or insect cells [23, 24].

Using mammalian cells for protein expression, however, is no guarantee for achieving the desired product. Often, major differences were detected when using two different cell lines, but also production of proteins by different lots of one cell line might lead to a certain variation in the glycopattern, for instance regarding decoration and amount of sialic acids [25].

When considering the growing market of “biosimilars”, it is important to keep in mind that the properties of pharmaceuticals are dependent on the used clone in the cell culture and on the overall manufacturing process including the protein extraction and purification scheme. A certain structural variation of the resulting products has thus to be expected as manufacturing methods and processes cannot be duplicated in all instances [26].

Quality control (QC) and quality assurance (QA) must focus on all these structural features and properties in order to prove and ascertain the quality of drugs, beginning from pre-clinical research up to the clinical application to patients.

2.2 Analytical tools for characterizing biopharmaceuticals

For the extensive physicochemical and biological characterization of protein drugs the use of state-of-the-art analytical methods is necessary. There are several techniques considered as well suited and essential for structural and physicochemical characterization of biologics [27]. Amongst the numerous methods available in the field of bioanalysis, capillary electrophoresis (CE), high-performance liquid chromatography (HPLC), as well as mass spectrometry (MS) have attained the most sincere attention in the context of characterization of protein and nucleic acid based biologics [28, 29, 30].

2.2.1 Capillary electrophoresis

Capillary electrophoresis (CE) is a powerful analytical technique that can be used in several modes of operation. Numerous application areas (DNA, carbohydrates, peptides and proteins, metabolites, enantiomers, inorganic anions, biologics, biotechnological, clinical and forensic samples) use CE in routine analysis for qualitative and quantitative characterization of products [31]. This technology is a widely applied separation technique during the last two decades. The separation unit simply consists of a fused silica capillary with an inner diameter below 100 µm (mostly 50 µm) containing <1 ppm metal oxide (quartz contained 60 ppm). Such materials were developed in the late 1970s [32]. An external coating of polyimide, which gives the capillary full flexibility and stability, protects this fragile capillary.

The high separation efficiency and selectivity of CE in combination with small sample (and solvent) consumption are some of the reasons, why this technique is widely used as analytical tool. The used capillaries should be chemically and physically resistant. With bare silica capillaries, adsorption of analytes onto the inner wall of the capillary might be a problem, particularly with (basic) proteins [33, 34]. Covering/modifying the surface by permanent or dynamic coatings can solve this problem. Coatings have also a major effect on the electroosmotic flow (EOF), a non-selective bulk-flow in the capillary towards the cathode if the capillary surface is net-negatively charged (creating a negative zeta-potential). With bare silica a cathodic EOF is established at pH values above 2.5 to 3, resulting from the dissociation of the silanol groups at the silica surface exhibiting pKa values in the range of 4.5 to 5.5.

Since 1989, fully automated capillary electrophoresis instruments became available [35]. To cope with the tiny peak volumes injected (nanoliters), the small internal capillary diameters (typically 50 µm) and the short light-pathways, highly sensitive detectors are required. Often, the detection is carried out directly on-capillary after removing the polyimide external coating (mostly by burning or scraping). Expansion of the light-path-length can be done by using bubble-cell capillaries or Z-shaped flow-through detection cells [35]. Up to the present, UV/VIS detectors are the most widely adopted detectors in the majority of the commercial systems, though potentially much more sensitive fluorescence detectors (FLD) with laser excitation (LIF) or excitations by light-emission diodes (LedIF) are available and increasingly used. The same holds for the universal contactless conductivity detectors. CZE can also be on-line coupled electrospray ionization (ESI) mass spectrometry (MS), a combination which allows one to profit from the entire potential of modern MS instrumentation and methodology for the purpose of structure elucidation.

Ultraviolet-visible (UV/VIS) detectors can be operated either at one wavelength using only filters for the specified wavelength window. Alternatively, multi-wavelengths detectors based on a photodiode array (PDA) can be implemented; they allow the simultaneous measurement of light absorption at various single wavelengths in the range of 190-600 nm. Their sensitivity is usually lower than single-wavelength instruments. For attaining high sensitivity in CZE, often the application of laser-induced fluorescence (LIF) is required. As with this method, the wavelength of the laser has to match with the excitation wavelength for the analytes, derivatization of the analytes is often necessary for attaining good fluorescence.

Basic principles:

In the most simple and most often used cases, capillary zone electrophoresis (CZE) takes place as electric potential driven migration (electrophoresis) in free homogeneous solution, i.e. without interactions between surfaces, or micellar or polymeric pseudo-stationary phases or sieving gels. Often, selectivity is easily and successfully tuned by use of secondary equilibria involving e.g. protonation/deprotonation or complexation equilibria.

Electrophoretic separation is based on the differential movement of charged species in an electric field. Ions are separated according to the ratio of their charge, q, to their hydrodynamic radius, r, as the electrophoretic mobility of an ion, μ_e, is dependent on q/r in the following way:

$$\mu_{!} = \frac{!}{!\cdot!\cdot!\cdot!} \qquad (2.1)$$

where η is the viscosity of the BGE solution.

The electrophoretic migration velocity, v_e, of an ion results from the mobility of the ion and the electric field strength (E) applied [32, 35]:

$$v_{!} = \mu_{!} \cdot E \qquad (2.2)$$

where E is dependent on the applied voltage, V, and the length of the capillary, L.

$$E = \frac{!}{!} \qquad (2.3)$$

When dealing with non-permanent ions, the *effective* net-charge number, z^{eff}, resulting from protonation/deprotonation or complexation equilibria have to be considered as it determines the *effective* mobility, $\mu^{!""}$, of the ion under the given pH conditions.

$$\mu_{!}^{!!!} = \frac{!!^{!""}}{!\cdot!\cdot!\cdot!} \qquad (2.4)$$

with

$$z_{!}^{!""} = \frac{!}{!!!^{"!"\#!!"}} \qquad (2.5);$$ for acidic analytes (one dissociation step) and

$$z_{!}^{!""} = \frac{!}{!!!^{"!"!!"\#}} \qquad (2.6);$$ for basic analytes (one protonation step)

In presence of a non-selective bulk flow, as e.g. an electroosmotic flow (EOF), the migration velocity and the finally attained selectivity and resolution is affected by this flow as well.

One can define an "*apparent*" mobility, μ^{app}, the mobility that is directly determined from the measured migration time according to the formula

$$t = \frac{!\,!}{!^{!""}\,!} \qquad (2.7)$$

where l indicates the distance from capillary inlet to detector. The apparent mobility, μ^{app}, is the vector sum of the effective mobility, μ^{eff}, (depending on the features of the analyte) and the mobility inferred by the EOF, μ^{EOF}.

$$\mu^{!""} = \mu^{!""} + \mu^{!"\#} \qquad (2.8)$$

If electrophoretic mobility of the ion and the direction of the EOF are towards the same direction (co-migration), the apparent ion migration becomes faster (shorter migration times). In case of counter-migration, apparent ion migration becomes slower (longer migration times) and the selectivity is enhanced in many cases. The strength of the EOF is thus an important parameter to be adjusted for a good CZE separation.

The EOF originates at the capillary wall, under certain conditions, when a buffer solution is placed inside the capillary after applying a voltage. With bare silica, the silanol groups (SiOH) are (at least partially) ionized to negatively charged silanate groups (SiO^-) if the pH value of the background electrolyte is higher than 2.5. Positively charged ions of the BGE are lining up opposite to the silanate ions creating an electric double layer. The loosely bound water-surrounded cations from the outer layer migrate to the cathode (most often is this the direction to the detector) dragging the uncharged molecules of the solvent (water) in this direction creating so the EOF. The velocity of the EOF (v^{EOF}) is given by the following equation:

$$v_{!"\#} = \frac{!}{!\cdot!\cdot!}\zeta \cdot E \qquad (2.9)$$

where ε is the dielectric constant of the solution, η is the solution viscosity, and ζ is the potential established at the capillary wall.

Selectivity and resolution

The separation selectivity in electrophoresis is usually expressed in terms of the selectivity coefficient between pairs of analytes, j and i, and this selectivity coefficient is defined by the ratio of the effective mobilities:

$$r_{!,!} = \left[\frac{!^{""}_{!}}{!^{""}_{!}}\right] \qquad (2.10)$$

Since the effective electrophoretic mobility $\mu^{!""}_{!}$ is given by the actual mobility $\mu^{!"\#}_{!}$ times the degree of dissociation $\alpha_!$ (or protonation), the selectivity coefficient can be written as:

$$r_{!,!} = \left[\frac{!^{"\#}_{!}}{!^{"\#}_{!}}\right]\left[\frac{!_{!}}{!_{!}}\right] \qquad (2.11)$$

In CE systems with EOF, the selectivity coefficient of interest it the “apparent” selectivity, r_{ji}^{app}, which is defined as the ratio of the apparent mobilities:

$$r^{!""}_{!,!} = \left[\frac{!^{""}_{!}}{!^{""}_{!}}\right] \qquad (2.12)$$

This equation allows one to estimate how strong an EOF enhances or decreases the selectivity of a CE system.

Based on the previous definition of the selectivity coefficient, the resolution $R_{!,!}$ between two compounds j and i is obtained by the following equation.

$$R_{!,!} = \frac{!}{!}(r_{!,!} - 1)\sqrt{N_!} \qquad (2.13)$$

where N_i is the so-called number of theoretical plates providing a measure for the efficiency of the system. It should be noticed that the resolution is proportional to ($r_{j,i}^{app}$ – 1).

Most often, electrophoretic separations are based on differences in the pKa values of analytes, which can be tuned by the composition of the running buffer (i.e. background electrolyte, BGE). Differences in pKa values are the major sources for a successful separation in CZE. Systems with 100 000 theoretical plates (under typical conditions a CE separation invokes 50 000 – 500 000 theoretical plates [36, 37]) enable to achieve the separation of two compounds with very subtle differences in the pKa values which might be

even less than 0.01 units. Thus, even compounds with equal actual mobilities can be resolved under BGE conditions that allow one to use small differences in the pKa values. (This is often associated with low effective charge numbers of the analytes leading to long migration times and considerable peak broadening.)

Capillary electrophoresis instrumentation

A schematic drawing of a CE instrument is given in Scheme 2. The instrumental set-up basically consists of the capillary filled with BGE, two buffer vials filled with BGE as well, several injection vials filled with the sample solutions, a high-voltage source with voltages up to 30 kV, a sample/capillary temperature control, a detector and a data acquisition device (computer).

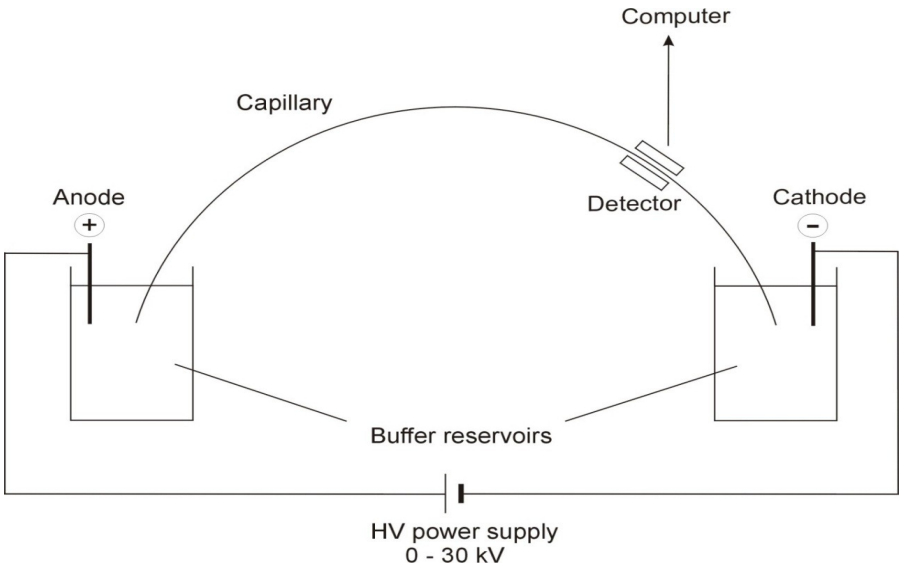

Scheme 2: Capillary electrophoresis system.

Modes of capillary electrophoresis

Capillary electrophoresis comprises a family of techniques, which differ in separation principle/mechanism. The most frequently used modes of CE are: capillary zone electrophoresis (CZE, introduced above), capillary gel electrophoresis (CGE), micellar electrokinetic capillary chromatography (MEKC) – both take place in capillary zone electrophoretic modus, capillary isoelectric focusing (cIEF), capillary isotachophoresis (CITP) and capillary electro-chromatography (CEC), which is a chromatography (for neutral analytes) using EOF for the transport of solutes along the capillary towards the detector or a combination of chromatography and CZE (for ions).

Capillary gel electrophoresis

Capillary gel electrophoresis (CGE) is a capillary electrophoresis method that uses sieving gels and charged surfactants like SDS for denaturation and uniform net-charging of the proteins. In this respect it is the method analogous to SDS/PAGE carried out in capillary format. A constant amount of SDS per unit protein weight (i.e., 1.4 g SDS/g of protein - with a few exceptions) is bound to the denatured proteins mainly by interactions between hydrophobic structures [38] resulting in a detergent-protein complex. Attached SDS masks the intrinsic charge of protein and leads to constant negative charge per unit mass as well as to a similar denatured shape of each complex. Without the sieving gel, SDS-protein complexes would hardly be resolvable by electrophoresis.

CGE-SDS has been applied in protein analysis for more than two decades. By using replaceable and water-soluble linear polyacrylamide as the sieving matrix in the capillary, reproducible and robust analyses of proteins are attained since early 1990s [39]. CGE provides faster and more efficient separations than traditional SDS-PAGE without the need of gel fixation and visualization by staining but with on-column detection connected to data acquisition device [40].

Capillary isoelectric focusing

Isoelectric focusing (IEF) is a separation method that can be applied to amphoteric (at least zwitterionic) analytes. When dealing with a mixture of amphoteric compounds, upon application of an electric field, these “ampholytes” line-up in a capillary according to their pI values forming a pH gradient. The anolyte (often phosphoric acid) terminates at the anodic side, the catholyte (often NaOH or NH_4OH) at the cathodic side. As illustrated in Scheme 3, when inserting amphoteric or polyacidic/basic analytes like peptides and proteins into this IEF system and applying voltage, these compounds will migrate to positions in the pH gradient at which their net-charge will be zero (isoelectric point, pI). At this position, their migration stops because of zero charge [41]. The analytes are thus separated according to differences in their isoelectric points [42]. The system is autofocussing and generates very narrow peaks. With intact proteins, the reduced solubility at the pI might become a problem. Surfactants used for improved solubilisation must not infer any charge to the analytes. Non-ionic surfactants or permanently zwitterionic ones (like CHAPS) are suited for this purpose. IEF is a highly effective high-resolution technique allowing to resolve proteins with pI differences lower than 0.005 pH units [41]. IEF can be carried out in casted gels (e.g. polyacrylamide based) to which ampholyte solutions are added, or in polyacrylamide based gels with immobilized weakly acidic and weakly basic moieties which form an immobilized

pH gradient (IPG strips), or in a capillary format (cIEF) where ampholyte solutions are positioned in the capillary between the anolyte and the catholyte zones.

The latter mentioned form of IEF provides automation, repeatable detection and quantification of various peptides and proteins. When carrying out a cIEF separation the capillary is initially filled with the carrier ampholyte solution and the analytes/proteins. Carrier ampholytes are mixtures of small molecules containing multiple amino- and carboxylate groups, they develop the pH gradient after application of an electric field. For attaining good focusing, it is decisive that the ampholyte species are well distributed in the desired pH range [41]. An ideal carrier ampholyte mixture includes good buffering capacity at the pI ($|pI - pKa| < 1$), high conductivity at the pI of the studied molecule, cover molecular weights between 500-1000 Da and is soluble in common protein precipitants [43, 44, 45].

Free solution isoelectric focusing in a capillary (cIEF) can be performed on standard equipment for capillary electrophoresis, e.g. Beckman Coulter PA800, Agilent 7100 or the "Protein Simple iCE280" instrument can be used. Detection is commonly done by an on-column detector like in normal CZE or, often, also with a whole column UV absorption detector. Such a whole column imaging detection (WCID) avoids disturbances of focused protein zones [46] as it does not need any mobilization of the focused zones towards the detector site. Usually, the detectors are programmed to monitor at 280 nm as at this wavelength the absorption of the ampholytes, which form the pH gradient, is usually low. At 254 nm, the interference with aromatic structures in the ampholytes might be significant.

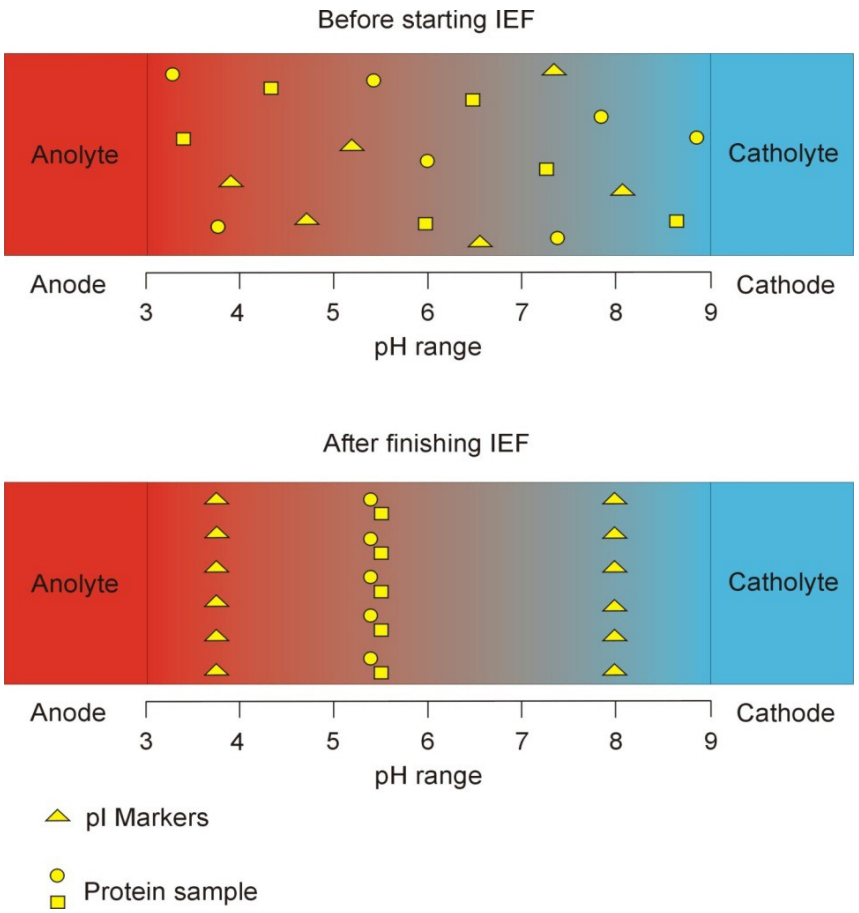

Scheme 3: Isoelectric focusing.

2.2.2 High-performance liquid chromatography of proteins

High-performance liquid chromatography (HPLC) is an analytical tool that is widely applied for investigating in a quantitative way structural features of proteins and protein-based pharmaceuticals. The migration velocity (and thus the retention time) of a compound is determined by its intrinsic affinity for both the mobile phase and the stationary phase. The mobile phase is a liquid flowing through a column packed with solid particles – the stationary phase. The column is a tube of various lengths (usually 30-250 mm) and diameters (generally 2.1-4.6 mm) made from stainless steel or quartz filled with adsorbents (stationary phase) with particle sizes of 3 to 5 µm (HPLC) (and up to 50 µm in classical LC), various shapes (e.g. spherically or irregularly particles, monolithic porous media in shape of a cylinder or down to the shape of membranes) and the chemical nature of their material and surfaces (e.g. silica with all the various surface modifications, alumina, polymers neat or with attached ligands, etc.). Operating pressures are between 50-350 bars [47, 48, 49, 50].

Characterization of biopharmaceutical products is predominantly provided by HPLC in combination with UV-detection. Because of its high resolution, the reversed-phase HPLC technique (RP-HPLC) is well adapted for the analysis of protein samples [51]. The RP chromatographic mode uses a polar (i.e. most often aqueous organic) mobile phase and a

stationary phase that is less polar than the mobile phase. The stationary phase is based on chemically modified silica, using various functional groups to achieve a high selectivity and efficiency (an example of commonly used stationary phase ligands listed from non-polar to the most polar: alkyl, phenyl, fluoro, cyano and silica) [52].

The separation of analytes into single peaks by RP method is based on slight differences in the hydrophobicity of analytes. The use of organic modifier (most often acetonitrile and methanol) and, in the case of peptides, also of an ion-pairing agent (usually trifluoroacetic acid) is mandatory to attain optimal separation conditions [53]. The choice of organic modifier plays an important role because it affects the selectivity of the separation [54]. Organic modifiers can also affect the conformation of the protein, and this might impact protein quantification [55].

Another type of HPLC widely used in protein separation is size exclusion chromatography (SEC). In contrast to RP-HPLC, SEC separations can be carried out under non-denaturing solution conditions and, thus, have no or only minimal impact on higher order structures of proteins [56]. Until now, a variety of materials exhibiting size-exclusion effects was developed. Dextrans cross-linked with epichlorohydrine are known under the trade-name Sephadex. These gels are weakly acidic and tend to adsorb basic analytes, a problem that can be avoided by addition of salt to the eluent. Thanks its inertness, non-swelling behaviour and superior mechanical strength, porous silica became predominant as a column packing material. The utility of porous silica for the analysis of proteins is limited because of the strong ionic interaction due to the acidic surface silanols. Thus, diol-modified surfaces seem to be the best choice to mitigate these interactions and attaining non-adsorbing SEC surfaces for proteins. It is also worth to mention other polymeric resins, such as polyacrylamide-based gels or agarose [57].

Regarding detectors, similarly to CE, by far the most widely adopted detectors in commercial HPLC systems are UV/VIS diode array detectors (DAD) and fluorescence detectors (FLD). In modern commercial instruments, there are many other detectors available, which can be coupled to LC. Examples are (i) conductivity detectors, based on the fact that ionic components conduct electricity, measure the electric resistance which is indirectly proportional to the ions concentration [58]; (ii) multi-angle light scattering detectors [59]**;** (iii) evaporative light scattering detectors [58], (iv) refractive index detector (RID) which is suitable for detecting all analyte components in a sample. An important detection method which can be combined with HPLC, particularly RP-HPLC and SEC, is mass spectrometry (MS). It can easily be on-line coupled to HPLC when using an electrospray ionization (ESI) device.

Protein therapeutics must be “well-characterized” to assure their safety and efficacy. The demand for developing accurate, effective and reproducible methods is driven by the need to support the manufacturing process and product formulation. The development of appropriate analytical methods involves the considering of method benefits, method robustness and reproducibility, available laboratory equipment, needed operation personal, as well as its costs. In addition to HPLC, electrophoretic methods are rapidly becoming the tool of choice in pharmaceutical analysis. Within the last decades, CE manufacturers have invested much effort in improving the weak points in CE in order to develop a technique competitive to HPLC. Therefore, problems like insufficient reproducibility (due to reliance on the EOF), and low concentration sensitivity in optical detection (due to the short light pass) are being solved. In case of the unwanted presence of an EOF, the use of capillary coatings (dynamic or permanent) will be beneficial [60]. The use of more sensitive detection methods like laser-induced fluorescence (LIF) and electrochemical detection (ElD) as well as nano-ESI-MS can help to solve the sensitivity problem often associated with UV detection etc. [61]. (A rather practical problem is that, currently and compared to HPLC, only a few manufacturers of CE instruments are on the market, a situation which limits competition.

The particular advantages of using capillary electrophoresis over HPLC deserve attention and should be described briefly. It is well known that CE separations are highly efficient (very narrow peaks), can be carried out within short analysis time, and time consuming sample pre-treatment is often not required, at least when using UV detection [60].

Based on the small diameter of the capillary, CE separations need only low sample volumes (some nL) and low solvent amounts. (This fact is very environmental-friendly and represents also a non-negligible financial advantage) [36]. A major advantage of CE is that the molecule charge, and thus migration velocity and selectivity, can easily be influenced/optimized by small variations in pH. This is more easily done in CZE than in HPLC. To keep a method reproducible and robust, the adjusting of the pH values of the running buffers have to be done very precisely [62]. It is worth to mention that there is an area in which CE has proved to be an excellent method, even better than all other separation techniques: separation of enantiomers.

Some advantages and constraints of HPLC (RP, SEC, IEX) and CE (CZE, CGE-SDS, cIEF) techniques commonly used for biomolecule analyses and utilised within the studies of this Thesis are listed in Table 1:

Table 1: Benefits and limitations of HPLC and CE analytical techniques in the context of protein analysis.

Assessment of identity and purity of intact proteins

Technique	Benefits	Limitations
RP-HPLC/UV	various column types available	
	fractions can be collected for MS	
CZE/UV	orthogonal to HPLC	limited ability to collect fractions
	one multipurpose fused silica capillary (also coated) small amounts of sample sufficient	
SEC	High-resolution separations of aggregates and impurities based on their size	limited resolution of high molecular weight aggregates and low molecular weight impurities
	various column types	
	fractions can be collected for further analysis	long analysis times compared to CGE-SDS
CGE-SDS	one multipurpose fused silica capillary (eventually coated)	limited ability to collect fractions
	good resolution of high molecular weight aggregates and low molecular weight impurities	necessity of high pressure instruments (stable at 60 psi), frequent capillary blockages, usage of sticky gels demands proper cleaning of instruments
	fast, reproducible and quantitative	expensive commercially available buffers

Peptide mapping

Technique	Benefits	Limitations
RP-HPLC/UV	protein fingerprint can be monitored thorough QA/QC	no mass information (fractions can be collected for further MS analysis)
	reliable, robust methods	long gradients, time consuming
CZE/UV	one multipurpose fused silica capillary (eventually coated)	limited ability to collect fractions
RP-HPLC/MS	peptide mass information	requires experts for use and data analysis
	verification of sequence coverage, site identification of post-translational modifications	
CZE/MS	orthogonal to HPLC	Possible reproducibility issues with separations
		does not provide the same sensitivity as LC/MS

Charge isoform analysis

Technique	Benefits	Limitations
IEX	separation of protein charge variants using various anion and cation resins	long gradients, high buffer consumption, time consuming
	ability to fractionate and collect separated isoforms for further analysis	not directly MS compatible
cIEF	high-resolution separation of protein isoforms	higher resolution separations than IEX
	one multipurpose fused silica capillary (eventually coated)	not MS compatible, no possibility to collect fractions
	faster separation than IEX	expensive equipment
whole-column cIEF	UV light applied over whole column	no LIF detection
	no migration step to the detection window necessary	not MS compatible, no possibility to collect fractions
	faster separation than cIEF	expensive equipment

2.2.3 Mass Spectrometry in hyphenation to separation methods

Mass spectrometry (MS) is a highly effective analytical technique (its origin can be dated to the end of 19th or the beginning of the 20th century [63]) that plays an increasingly significant role in the study of biomolecules [64]. The ability to measure molecular masses with high sensitivity can be exploited in many fields of protein analytics; it is a favoured technique for protein characterization and quality control, routinely used for protein identification as well as for a detection and characterization of posttranslational modifications (PTMs) [64, 65]. Two major types of soft ionization MS methods should be briefly introduced: Matrix-assisted laser desorption ionization (MALDI) and Electrospray ionization (ESI). In MALDI, a mixture of analyte sample (usually less than one microliter) and a MALDI-matrix solution (also about 0.5 to 1 µL) are deposited onto a metal plate for co-crystallization. After drying, the sample/matrix spot becomes irradiated by a sequence of nanosecond laser pulses. By this method, predominantly ions of the type $[M+H^+]^+$ (attachment of a proton), or $[M+Na^+]^+$ and $[M+K^+]^+$ (attachment of an alkali cation) are generated.

The electrospray method has been developed for analysing samples in solution. In ESI, a strong electrical field is applied to create fine charged droplets leading to more efficient ionization. During solvent evaporation by a flow of gas (typically nitrogen) and heat charged droplets are repeatedly reduced in size resulting in production of gas-phase ions. The in this way produced desolvated ions are immediately accelerated into the mass spectrometer by the applied electric fields [66]. Using this technique, larger molecules like peptides and proteins become multiply charged ions during the desolvation process leading to a charge

state distribution (detection in *m/z* ranges of 500 to 3000). For effective ionization in ESI, the analytes have to be to a large extent free of salts and detergents.

By ESI, typically ions of the type $[M+nH^+]^{n+}$ (attachment of a several protons leading to a charge-state distribution) are generated, or $[M+kNa^+]^{k+}$ and $[M+kK^+]^{k+}$ (attachment of a several cations). ESI can generate also negatively charged ions generated by the subtraction of a proton. The ion types are then mostly $[M-nH^+]^{n-}$, again giving a charge-state distribution with several values for n. In the presence of alkali ions, the following ion types can be generated as well: $[M+kNa-nH^+]^{(n-k)-}$. ESI-MS can be utilised for studying thermally labile molecules if their polarity allows the attachment of a charge (positive ion mode) or the detraction of charge (negative ion mode). The technique is described in more detail below in part HPLC-ESI-MS.

Mass spectrometers are rather expensive instruments, particularly used in areas, where alternative analytical techniques cannot provide the level of performance required. All of these instruments measure the mass-to-charge ratio of ions generated from molecules. MS instruments differ by the working principles of the mass analyser employed, i.e. how they achieve mass separation. The most common instruments use time-of-flight (TOF) analyzers, quadrupole (Q) analyzers, ion trap (IT) analyzers, and (in more advanced instruments) orbitrap or ion-cyclotron-resonance- (ICR) analyzers.

In hybrid instruments aimed for tandem mass spectrometry (MS/MS), combinations of these MS separation principles can be used. Examples are ESI-Qq-RTOF, ESI-QqQ, ESI-IT-ICR instruments. In this set up, a quadrupole (q) or an IT analyser is used as collision cell for the fragmentation of selected ions. The analyser following the collision cell is used for mass analysis of the generated fragments [67]. The MS/MS technique is commonly applied in structural analysis of biomolecules, for instance peptide sequencing and analysis of glycosylation or other PTMs.

For peptide sequencing, the peptides become fragmented e.g. by vibrational excitation in the course of collision-induced dissociation (CID) (sometimes also called collision-activated dissociation (CAD)) or by generating impaired electrons e.g. by electron-transfer dissociation (ETD)-based fragmentation [68]. Here, the energy released in the exothermic capture of a thermal electron is used for fragmentation [69]. Peptide sequencing using CID-fragmentation occurs in the collision cell by collision with an inert gas. (The gas can be present constantly or introduced for a short moment especially for this purpose.) In case of CID [70] several peptide bonds along the backbone can be cleaved resulting in the formation of b ions (containing the N-terminus plus one more additional residues) and y ions (containing the C-terminus plus one more additional residues) as shown in Scheme 4.

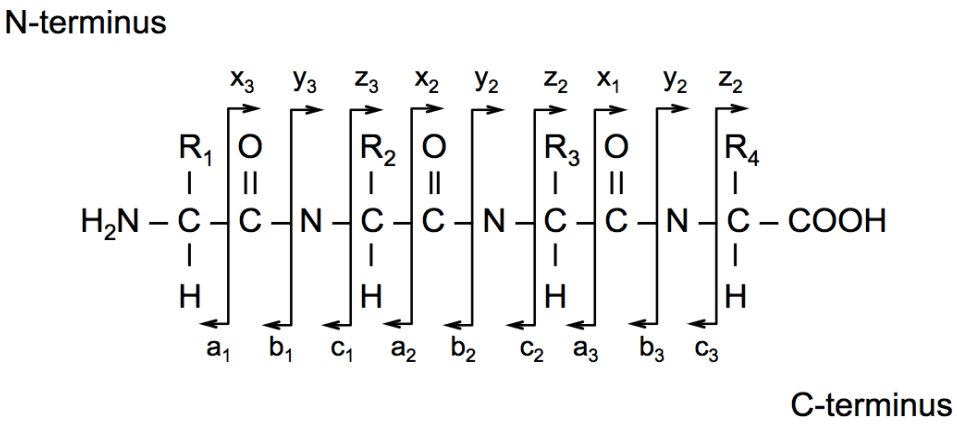

Scheme 4: Nomenclature for ions generated in the fragmentation of peptide molecules by tandem mass spectrometry.

Since CID may result sometimes in undesired cleavages of labile bound PTMs, the development of alternative fragmentation techniques was necessary. Applying the ETD technique, labile modifications (like acetylation, glycosylation, phosphorylation etc.) can be preserved providing the more comprehensive information on the site-specificity of modification.

High-resolution (HRMS) instruments allow one to attain high mass accuracy as well, which is now typically between 3 to 5 ppm (with R values about 40,000 to 60,000) and sub 1 ppm (with R values about several 100,000). Often external calibration or lock masses [71, 72] are needed for assuring such high accuracy. The given numbers refer to the analyses of peptides and small molecules; for intact proteins a mass accuracy 10-20 ppm is a more realistic number [73].

With ESI ionization, large molecules like protein drugs typically acquire multiple charging (charge state distribution). For the molecular weight determination of such molecule the process called deconvolution [64] is commonly used (an algorithm-based process that groups the signals of various intensities into a single peak at the molecular weight of the analyte).

HPLC-ESI-MS

In HPLC-ESI-MS experiments, the sample components of interest are eluted from a HPLC- column, followed by ionization and transfer into mass spectrometer for analysis [64]. Reversed-phase HPLC (using C18 columns) (used for hydrophobicity based separations) directly coupled to a mass spectrometer (MS) became a very widely used technique in the context of protein identification. There, this set up is used for the monitoring of the peptides generated from the protein by enzymatic digestions. For this purpose a mobile phase

gradient with increasing content of organic solvent is routinely employed. The separated peptides are not only characterized according to their molecular masses but also (at least) partially sequenced by CID- or ETD-based fragmentation analysis. Protein identification and identity tests are commonly performed in this way [71].

CE-ESI-MS

Since the end of the 80s, capillary electrophoresis coupled to MS has become an extremely powerful tool for the analysis of protein drugs. CE-MS exhibits interesting possibilities for the characterization of intact proteins, because particularly high separation efficiency can be achieved [74]. Also, relatively mild conditions as low temperature and low concentrations of salts or organic solvents contribute to the creation of high-performance separation systems for protein study, because conformational changes of proteins can be minimised [75].

In contrast to HPLC-MS, coupling of CE with MS is less straightforward. With CE-MS the effluent flow from the capillary is often not sufficient to generate an effective electrospray, particularly when using nano-ESI devices in combination with nano-HPLC-columns or HPLC chips. Therefore, various interfaces for various types of ionization sources (e.g. ESI, MALDI and ICP ionization for protein and peptide CE-MS analysis) have been designed [60, 76]. Coupling of CE to MS is most commonly carried out by ESI using either sheath liquid, sheathless, or liquid junction interfaces [77].

The components of the CE running buffers are an important aspect in CE-ESI-MS analyses. Preferably volatile, low concentrated buffers should be used to achieve a sensitive MS response. However, such buffers might not provide optimal conditions for CE separations. Efficient separations can be obtained by use of volatile buffers in the BGE, comprising acetate, formate anions and ammonium cation [77]. However, as discussed by Haselberg et al. in [76], ammonia, frequently used for the pH adjustment of the BGE, might lead to some extent to ionization suppression which could adversely affect sensitivity.

3 Results

3.1 Study on the deamidation and aspartate isomerization of peptide and protein therapeutics using CZE-UV and HPLC ESI-MS

One of the most common modifications in protein drugs is the deamidation of asparagine. The transformation of this molecule to aspartate can be described as a spontaneous, non-enzymatic reaction and although only minor structural changes can be observed, this process might have a serious impact on the drug functionality. Such medicament alteration may cause severe health problems to the patients and therefore this molecule alteration has to be controlled properly.

This study presents various conditions that can be employed to produce some stressed material (where the asparagine is a subject of the transformation to aspartate). The impact of miscellaneous factors on the deamidation rate of a small model peptide (VYPNGA) is shown in detail and the results are compared with published data of other researchers. The findings from the peptide study were applied for further work with another small peptide (GSNSG) and more structurally complex molecules (Glu1-Fibrinopeptide, Hirudin, Lysozyme, Aprotinin, Interferon, Hemoglobin, BSA, Avastin and Erbitux). The ability to employ CZE-UV system for the determination and quantification of the deamidation products (aspartate and isoaspartate) is studied. The analysis conditions used by Boni et al. [78] and Lai et al. [79] were applied and adapted to achieve the most effective separation. Furthermore, the compliance with the requirements of mass spectrometry was considered.

Under the natural (non-enzymatic) deamidation circumstances (or application of relatively mild stress conditions; as harsh conditions may lead to the protein degradation) long times are often necessary to produce deamidated samples. Considering the catalytic function of L-Asparaginases, which are able to hydrolyse asparagine to aspartate, the enzyme was used in the study of the acceleration of the deamidation rate in peptide (VYPNGA) and various proteins.

The asparagine deamidation sites were investigated by common methods (HPLC-MS, CZE-MS). A novel procedure applied for the examination of deamidated molecules is also described: A utilization of an Asp-N enzyme for the pre-localization of newly formed aspartates by an enzymatic cleavage followed by CZE analysis with UV detection.

3.1.1 Introduction

Structural aspects of deamidation, mechanism and factors involved

In the last decades, biological applications within the pharmaceutical industry are one of the most developing technological areas. The monoclonal antibodies and antibody-domain based molecules represent the majority of protein therapeutics. The specificity of these molecules is determined by amino acid sequences in the complementarity determining regions of variable F_v domain. If asparagine or aspartate participates in antigen recognition, their modifications can lead to loss of functionality. These alterations can be recognized at the beginning of protein designing, which leads often to elimination of this product from the list of potential candidates. Some protein therapeutics can be protected by implementing of formulation strategies that are able to improve the stability of proteins to deamidation and isomerization. Sometimes in the drug development process such candidates are re-engineered and the problematical hot spots are removed. Despite of these protective actions the risk of degradation increases with the storage period and the therapeutic proteins can undergo deamidation. One of the most frequent routes of peptide and protein degradation is deamidation of asparagine and glutamine [80, 81]. This amino acid alteration may result in structural and functional changes, which depending on its position in the amino acid sequence of the affected protein may cause decreased bioactivity or unwanted immune response [82, 83]. Glutamine undergoes deamidation leading to glutamic acid formation with much slower deamidation rate than asparagine [84]. The degradation mechanism of asparagine proceeds via different pathways at acidic and alkaline pHs. Capasso et al. [85] reported that the deamidation pathway in the pH range 5-10 carries on exclusively via succinimide as shown in Scheme 5. The illustrated reaction is a visualization of asparagine joined to other amino acids on both sites in some peptide or protein.

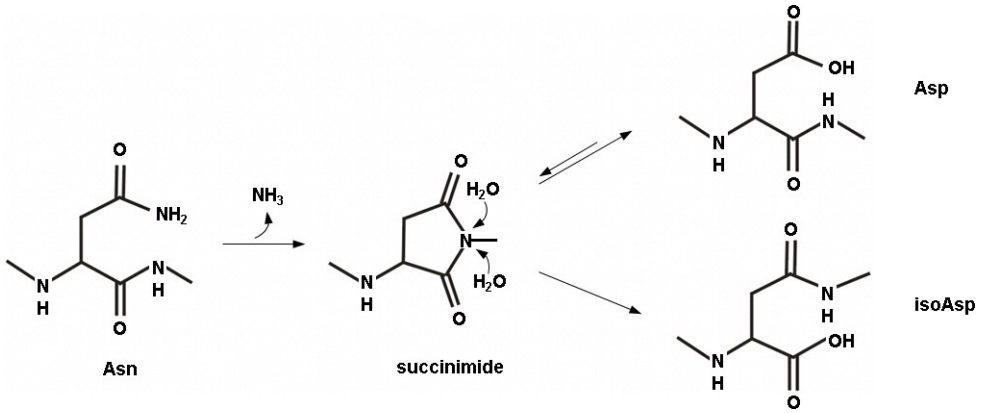

Scheme 5: Asparagine deamidation reaction.

Nucleophilic attack of the adjacent backbone nitrogen on the side chain carbonyl carbon of asparagine (Asn) leads to formation of a 5-membered cyclic succinimide intermediate and the release of ammonia [86]. This intermediate is spontaneously opened by the attack of water on either the α- or β-carbonyl group, resulting either in the formation of aspartate residue (Asp) or an isomerized isoaspartate (isoAsp) [80, 81]. It was observed that the mentioned hydrolytic cleavage of the succinimide intermediate provides a isoaspartate:aspartate product ratio of about 3:1 [80, 87, 88] in peptides (pH range 5-10). Deamidation of peptides or proteins results in a mass increase of 1 Da (see Scheme 5, NH_2 - 16 Da is replaced by OH – 17 Da [80, 89]).

At pH ≥7 glutamine (Gln) deamidation follows the same reaction path as observed by asparagine through formation of a cyclic imide intermediate [81]. The slower rate of glutamine deamidation is explained by ring structure of cyclic imide intermediate. The six-membered ring cyclic imide is less stable than the five-membered ring of succinimide intermediate [84] and the direct hydrolysis of glutamine to glutamic acid (Glu) is favoured.

The deamidation rate of asparagine and glutamine is dependent on buffer type, pH, temperature, ionic strength, primary sequence and structural aspects [80, 90]. Phosphate buffers were found more appropriate to catalyse deamidation [84, 90]. It has been observed that ammonium bicarbonate has also an increased catalytic effect compared to Tris-HCl [91]. At neutral to alkaline pH the rate of asparagine deamidation is affected by the amino acid sequence of the peptide. The more basic pH accelerates the deamidation rate by increasing hydroxide ion concentration [90, 92]. In contrast, acidic buffers do not lead to the typical aspartate and isoaspartate formation since almost exclusively aspartate is formed [87]. Deamidation rate increases with temperature, but too high temperatures may cause decomposition of the deamidation buffer [87, 93, 94]. In the case of Tris-HCl the elevated temperature leads to the formation of formaldehyde, which could form a covalent adduct with tyrosine [94]. Deamidation buffer decomposition could also result in the alteration of pH value, formation of small particles and the elevated risk of protein precipitation. The importance of ionic strength effects on deamidation has not been elucidated completely to date, but was observed in couple of studies. The higher the concentration of deamidation buffer, the faster is the deamidation reaction [95, 96]. Primary sequence plays a crucial role in deamidation. Cumulative evidence from a number of peptides and proteins indicates that these molecules contain deamidation-prone sites also called “hot spots” with N[1]-X motifs. The neighbour amino acid X is relatively small and hydrophilic (X=G, S, H[2]). Glycine was

[1] N – asparagine

[2] G – glycine, S – serine, H - histidine

found as the most destabilizing flanking amino acid, because this small molecule leaves the peptide group exposed and so able to be attacked by nucleophile [80, 87]. The asparagine destabilization is also expected in the proximate presence of serine, but this process is not described as fast as in the presence of glycine [80, 87, 97]. Also histidine, alanine, aspartic acid and arginine were found as semi-destabilizing (peptides including this amino acids deamidate with rate in the intermediate range) [87]. In contrast to these, amino acids with a large, bulky side chains (V, Y, L, P[3] [81]) cause steric hindrance preventing or reducing deamidation of asparagine [87, 97]. Some experiments [98, 99] have shown that secondary structure has influence on deamidation. Asparagines hidden in the middle of alpha-helix or beta-turn are better sheltered from deamidation than the ones closer to the carboxyl end sequence [98]. M. Xie and Schowen [99] explained the protection of asparagine by conformation effects (e.g. different properties of alpha and beta in this regard).

Tertiary and quaternary structure elements of proteins are also inhibiting deamidation rates [98]. Kossiakov [100] investigated the structural features that affect the deamidation process of asparagine in trypsin. Modelling suggested that certain sets of peptide torsion angles are incompatible with deamidation. All deamidated groups in trypsin were conformationally similar; asparagines were followed by serine residues. The non-deamidated asparagine is distinguished from the deamidated asparagines by having a different hydrogen-bonding structure. This interaction hinders the formation of the productive deamidation geometry.

The aspartates present in peptides and proteins (not derived from asparagines by deamidation) are also unstable amino acids as they may undergo isomerization and enantiomerization [78, 101, 102]. This degradation mechanism is similar to the conversion mechanism of asparagine to aspartate and involves the nucleophilic attack of the β-carbonyl carbon by α-nitrogen next amino acid leading to the formation of an aminosuccinimide. The effect of various C-flanking amino acids on isomerization of Asp residue has been studied in peptides, proteins and monoclonal antibodies. As observed by Asn also here the C-terminal glycine and serine facilitate succinimide formation and aspartate isomerization [103, 104, 105].

Separation and identification of deamidated forms

To detect deamidation of asparagine in protein drugs and to separate the newly formed deamidated structures from parent molecules is still a challenging job in protein analysis. Since the additional negative charge and increase in molecular mass are close associated

[3] V – valine, Y – tyrosine, L – leucine, P - proline

with aspartate formation, electrophoretic (isoelectric focusing (IEF), capillary zone electrophoresis (CZE)) as well as chromatographic methods (reversed-phase chromatography (RP-HPLC), ion exclusion chromatography (IEX), hydrophobic and affinity chromatography) are the suitable analytical tool for the separation of deamidated forms [10, 106 and 107].

HPLC is a common analytical technique, which is to date state-of-the-art technology for separation of peptides. Changes in hydrophobicity caused by replacement of an amide by a carboxylic acid can be exploited with RP-HPLC [10, 108]. Long analysis times are needed in order to achieve a good separation profile of not deamidated peptide from its deamidated isoforms (L-Asp, D-Asp, isoAsp and succinimide), since very shallow gradients are applied [109, 110, 111]. Because the alterations can be better detected in peptide pattern than in whole protein, the enzymatic treatment of proteins is used to produce peptide fragments. Afterwards the asparagine deamidation is monitored by peptide mapping. It was observed, that four different isoforms of hexadecapeptide elute in this order: isoAsp, Asn, Asp and succinimide using H_2O/TFA and acetonitrile/TFA as eluents [89]. Despite such methods, separation of asparagine peptide from isoaspartate peptide remains challenging due to the similar selectivity (e.g. asparagine and isoaspartate have the same hydropathy index [112]). Fortunately, isomerization induces structural changes, which might have some influence on retention time of these isomers and lead to separated peaks [89].

Capillary electrophoresis is able to provide superior resolution of peptides and proteins due to its charge-based separation mechanism [33]. In comparison with RP-HPLC, this method offers fast separation without any long equilibration steps, stable capillary to capillary reproducibility (after suppression of EOF) and is also very environmental-friendly because only small amounts of background electrolytes are required [113]. Capillary electrophoretic separation mechanism differs from HPLC. Capillary zone electrophoresis separation mechanism is based on charge-to-mass ratio [114], or better charge-to-hydrodynamic radius, whereas RP-HPLC separation of analytes uses the distribution between stationary and mobile phase, where polarity of the analytes is responsible for the separation of compounds [115]. Upon deamidation the amide in the side chain of the amino acid converts into carboxylic acid, which leads to the formation of an additional negative charge and possibility to separate asparagine-containing peptide from aspartate. By contrast to RP-HPLC, the CE is capable to separate closely related species if they possess even small differences in charge [79]. Asp and isoAsp peptides differ slightly in the pKa values of their carboxylic groups, which causes small charge differences. Separation buffers with pH near the pKa of these carboxylic acids (pH 3.0) should result in resolution in this order: Asn, Asp,

isoAsp [79]. The separation systems that fulfil these requirements are acetic acid and phosphate run buffers and fused silica capillaries [79, 78, 107].

Mass spectrometric identification of deamidated small peptides is straightforward while direct quantitation of aspartate and isoaspartate stays challenging, due to the missing mass difference between aspartate and isoaspartate. The level of isomerization can be determined after methylation, using protein isoaspartate methyltransferase, followed by hydrolysis of methyl ester, which leads to a mass shift of 2 Da [116]. The isoaspartyl methyl esters are labile molecules, which spontaneously cyclize within couple of minutes to form succinimides followed by hydrolysis to Asp or isoAsp. To reach the stable molecule the isoAsp methyl esters are coupled with nucleophilic hydrazines or hydroxylamines resulting in peptide hydrazides [117, 118].

Another elegant approach in aspartate/isoaspartate detection is an utilization of site-specific enzymatic cleavage. Enzyme, which possesses the ability to fulfil this task, is called endoproteinase Asp-N [119]. Asp-N is a metallo (Zn) protease, which hydrolyses peptide bonds on the N-terminal side of aspartate while isoaspartate residues remain undigested [120]. Many researchers have studied the specificity of this enzyme. It has been reported that Asp-N cleaves also on the N-terminal side of cysteic acid residues, if they are not alkylated [120, 121]. It appears that this metalloprotease has some preferences for small hydrophilic residues [122]. Published data about Asp-N digestion of erythrocyte carbonic anhydrase and erythrocyte D-aspartyl/L-isoaspartyl methyltransferase demonstrate cleavage specificity for N-terminal side of glutamyl residue [123]. This enzyme property could be also used for detection of glutamine deamidation to glutamic acid in peptides and proteins. It seems that Asp-N prefers some acidic residues more, than other independently of flanking sequences [123]. Finding of the optimal digestion conditions would contribute to the higher enzyme specificity. Enzyme digestions conditions were therefore a part of the study and are later discussed.

The application of Asp-N enzymatic digest on samples of interest combined with CZE-UV technique might be an interesting approach for a pre-localization of deamidated sites. The strategy, facts and expectations are introduced below.

If one asparagine is present in peptide or protein, which undergoes deamidation/deamidation, isomerization to aspartate and isoaspartate and the Asp-N digest is applied, following situation can be described by Scheme 6.

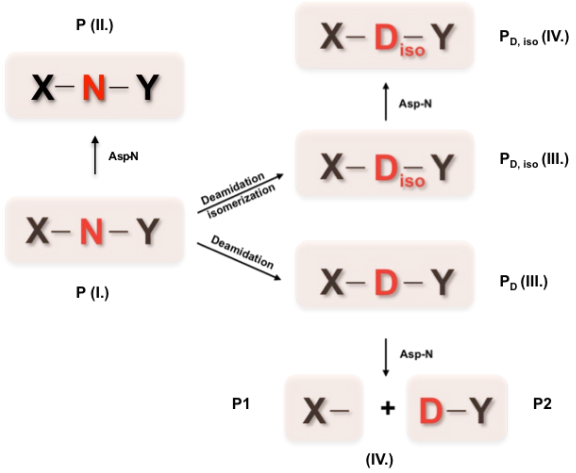

Scheme 6: Deamidation of asparagine and its Asp-N cleavage.

X-N-Y in Scheme 6 represents the peptide P (I.) with one deamidation site (N). Asparagine undergoes deamidation/deamidation, isomerization after incubation and forms newly more acidic X-D-Y/X-D_{iso}-Y variants (III.). If Asp-N is applied, the enzyme will be able to cleave only X-D-Y motifs at the N-terminus of aspartate (II., IV.).

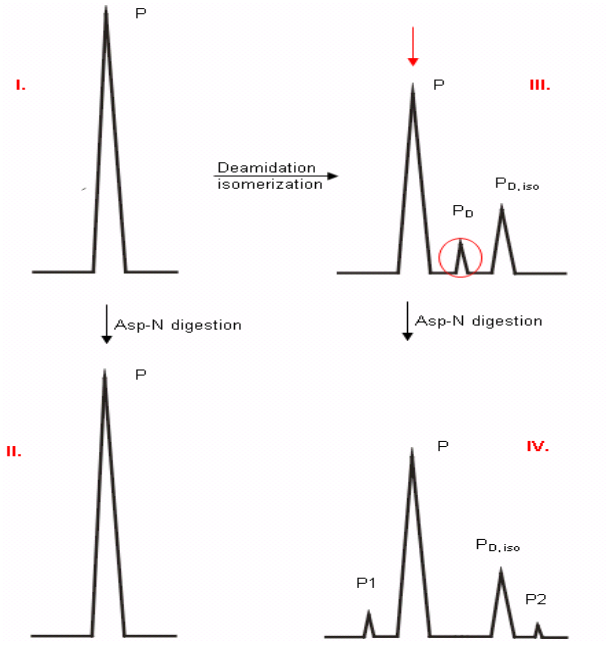

Scheme 7: Visualization of electrophoretic separation of deamidated peptide and its Asp-N cleavage products.

For better illustration of the deamidation process of peptide P followed by Asp-N digestion as depicted in Scheme 6, a respective schematic CZE profile is shown in Scheme 7. The demonstration of peptide separation using an acidic run buffer system, where all ions carry positive charge [79], is explained in four following simplified examples. After incubation of P (upper left panel, I.) a decreased signal of P is observed. At the same time new signals P_D,

$P_{D,\ iso}$ appear (upper right panel, III.). This process might continue during the entire incubation period until the asparagine is completely deamidated.

Asp-N digestion induces no changes in the separation profile, if no aspartates are present in the peptide (lower left panel, II.). In contrast, the aspartate in P_D (upper right panel, III.) is a subject of enzymatic digestion and its signal will disappear with concurrently creation of two new signals P1, P2 (lower right panel, IV.). At the same time $P_{D,\ iso}$ signal will stay unaltered, since the Asp-N enzyme is able to hydrolyse only non-isomerized aspartate [119]. It must be taken into account, that the new appeared signals P1 and P2 are not the quantitative mirror of the P_D peak. The intensities of the observed peaks do not reflect the quantitative amount of the respective peptides using a wavelength of 214 nm. This detection technique is used for monitoring of peptide bonds. Therefore for a semi-quantitative comparison the length of the observed peptides (number of amino acids, responding peptide bonds) should be concerned [124].

Enzymatic deamidation by L-Asparaginase

L-asparaginases are widely used in the treatment of cancer, especially acute lymphoblastic leukemia. This enzyme is capable to perform the hydrolysis of L-asparagine to L-aspartate and ammonia. Using this ability, there is an eventual possibility to induce the deamidation in peptides and proteins without long deamidation procedure. Avoiding the long incubation process would decrease the risk of possible test sample decomposition, targeted deamidation would offer faster results and minimize side effects caused by long incubation.

Until now there is no known example of successful experiment, where the asparaginase was used as a tool to deamidate asparagine within a peptide or protein. All published works discuss about free asparagine conversion to aspartate [125, 126]. Expected enzyme activity is shown in Scheme 8.

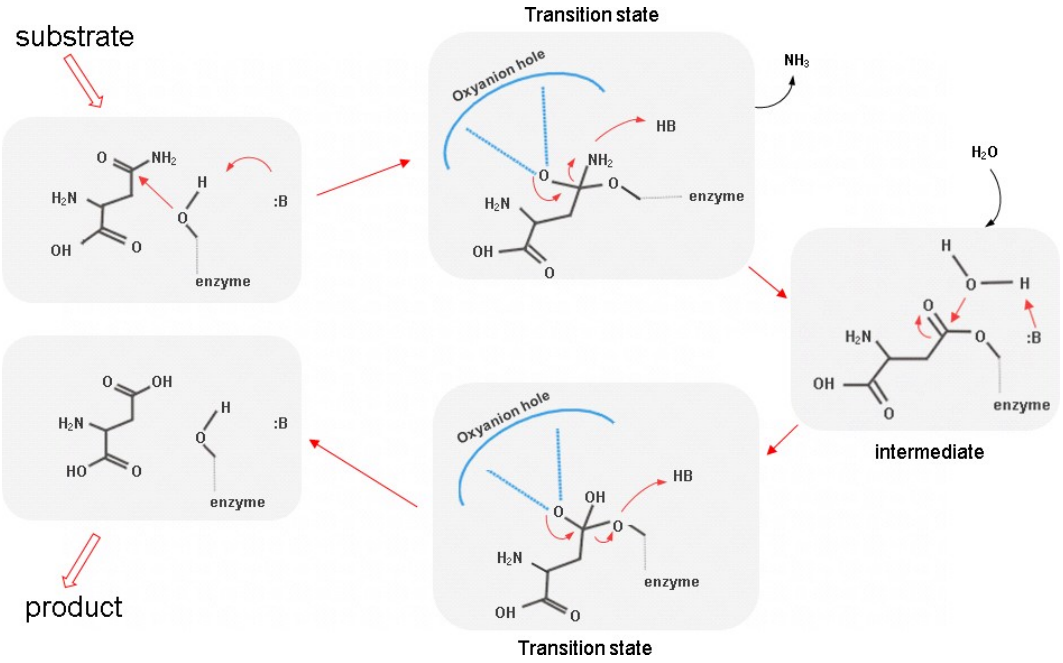

Scheme 8: Hypothetical function of L-Asp.

Michalska and Jaskolski [127] described the catalytic mechanism of asparaginases as follows: “In the first step, the enzyme's nucleophile, activated via a strong O-H...B hydrogen bond to an adjacent basic residue, attacks the C atom of the amide substrate, leading through a tetrahedral transition state to an acyl-enzyme intermediate product. The negative charge that develops on the O atom of the amide group in the transition state is stabilized by interactions with adjacent hydrogen bond donors. The constellation of those donors (which typically are main-chain N-H groups) is known as the "oxyanion hole". The second step of the reaction is similar, but now the attack on the ester C atom is launched by an activated water nucleophile”.

Strategy for the investigation of deamidation

The overall strategy is described in depth in section “Separation and identification of deamidated forms” (page 31-33). Briefly the test sample is exposed to various conditions to induce deamidation, non-deamidated and deamidated samples are analysed (intact and digested by Asp-N) by CZE and HPLC. Upon deamidation, the Asp-N digestion pattern may be different as shown in Figure 3 and Figure 4. This results from multiple presences of cleavable sites in larger peptides and proteins. The careful selection of test samples (see Table 2) should result in better understanding of deamidation behaviour therefore a broad spectrum of samples (e.g. molecules with short/long amino acid chains; molecules with typical N-G, N-S deamidation motifs; molecules with one, two or more possible deamidation sites etc.) was assessed regarding relevance and applicability in the study’s context.

Table 2: Studied samples introduced in detail.

Sample	Amino acid sequence
Peptide 1 (P1)	VYPN^{4}GA [4]
Peptide 2 (P2)	GSN^{3}SG
Glu1-Fibrinopeptide (F)	EGVN^{4}DN^{6}EEGFFSAR [128]
Hirudin (H)	VVYTDCTESGQN^{12}LCLCEGSN^{20}VCGQGN^{26}KCILGSDGE KN^{37}QCVTGEGTPKPQSHN^{52}DGDFEEIPEEYLQ [129]

Literature [80] describes the VYPNGA peptide as an unstable peptide with a deamidation half-life of one day in 150 mM Tris-HCl (pH 7.4 at 37 °C). According to the same literature source, the deamidation rate of GSNSG peptide is significant slower with the deamidation half-time of 15 days using the same degradation conditions. These two peptides will be studied in detail and the acquired knowledge will be applied for further examinations.

3.1.2 Materials and Methods

Materials

Test samples used in this study were purchased from various manufacturers: Peptide 1 (VYPNGA), Peptide 2 (GSNSG) from Bachem; Aprotinin, bovine serum albumin (BSA), Glu1-Fibrinopeptide, Hirudin, Hemoglobin, Lysozyme and Myoglobin from Sigma; Avastin from Roche; Erbitux from Merck; Interferon from Fluka and Protein P from customer.

Acetic acid, ammonium bicarbonate, disodium hydrogen phosphate, dithiothreitol (DTT), ethylenediaminetetraacetic acid (EDTA), hydroxypropyl methylcellulose (HPMC), iodoacetamide (IAA), 1 M Tris-HCl, pH 8.0[5] and zinc acetate were purchased from Sigma. Acetonitrile (ACN), ammonium hydroxide, hydrochloric acid (HCl), sodium hydroxide (NaOH), trifluoroacetic acid (TFA), tris(hydroxymethyl)aminomethane (Tris) were purchased from Fluka. Conditioning solution, SDS-MW gel buffer were purchased from AB Sciex, RapiGest from Waters. Enzymes Asp-N and Lys-C were obtained from Roche, L-Asparaginase from Emelca Bioscience.

Fused silica capillary was obtained from CM scientific, 3 kDa filters from Millipore, air displacement pipettes, thermomixer and centrifuge from Eppendorf.

Methods

Forced deamidation. Stressed samples were prepared in 50 mM ammonium bicarbonate pH 8.0, (except degradation study of Hirudin, following the instructions in [130]: 170 mM disodium hydrogen phosphate, pH 8.0). If not otherwise specified, all test samples were

[4] Summary of standard amino acids and their abbreviations are presented in Table 41.

[5] for all Tris-HCl solutions of pH 8.0

incubated at 40 °C. Concentrations of dissolved samples: Peptide 1 and Peptide 2: 1 mg/mL, Glu1-Fibrinopeptide 2 mg/mL, Hirudin 5 mg/mL.

Asp-N digestion. Asp-N enzyme was added to the peptide at a ratio 1:100, the peptide/enzyme mixture was then diluted to a final concentration of 0.8-2 mg/mL with milli-Q water and incubated at 37 °C (25 °C in case of Peptide 1) for 14-18 h.

Asp-N digestion of Hirudin. Prior to Asp-N digestion, Hirudin sample was incubated after addition of 0.1 % final concentration RapiGest and 50 mM final concentration DTT at 37 °C for 1 h. Alkylation was achieved using 85 mM final concentration IAA. Current buffer was changed to digestion buffer containing 50 mM Tris-HCl, pH 8.0, 2 mM zinc acetate using 3 kDa filters and centrifugation. The Asp-N was added to the sample at a ratio 1:100 (w/w) and the protein/enzyme mixture was diluted to a final concentration of 1.5 mg/mL with the digestion buffer and incubated at 37 °C for 18 h.

Lys-C digestion of Hirudin. Prior to Lys-C digestion, the Hirudin sample was incubated after addition of 50 mM final concentration DTT (37 °C for 1 h). Alkylation was achieved using 80 mM final concentration IAA. Current buffer was changed to digestion buffer containing 50 mM Tris-HCl/2mM EDTA, pH 8.0 using 3 kDa filter and centrifugation. Lys-C enzyme was added to the peptide at a ratio 1:20 (w/w), the protein/enzyme mixture was then diluted to a final concentration of 1.5 mg/mL with the digestion buffer and incubated at 37 °C for 18 h.

L-Asparaginase digestion. One unit of L-asparaginase was added to each 20 µg of peptide/protein in 50 mM Tris-HCl pH 8.6[6]. After gentle homogenization the sample/enzyme mixture was incubated at 40, 50 and 60 °C.

Electrophoretic conditions. CZE was carried out on the PA800 Beckman Coulter (AB Sciex) instrument with temperature controlled autosampler using fused silica capillary (50 cm of length, 50 µm id) with normal polarity (unless otherwise stated). The cathode was at the detector end of the capillary for the analyses with pH of 2.5. The capillary was flushed (by HCl, NaOH and milli-Q water) from appropriate buffer reservoirs using pressure (50 psi) prior to each run. The dynamic coating was applied (conditioning solution, 20 psi) and the capillary was filled with running buffer (3 % AcA, pH 2.5, unless otherwise stated[7]) using pressure (50 psi). The sample was injected using pressure (0.5 psi) for 10-20 s, the constant voltage of 30 kV was applied and the operation temperature of 25 °C was kept.

---

[6] prepared from Tris powder, pH adjusted by 1 M HCl.

[7] acetate running buffers with pH above 2.5 were adjusted by 10 % NH_3.OH.

Electropherograms were UV-monitored at 214 nm and the data were processed with 32 Karat.

Mass spectrometry analyses were carried out in positive mode on Agilent G1600 AX and Bruker microTOF-Q instruments using sheath Liquid: IPA/H_2O 60:40 + 1 % formic acid.[8]

Chromatographic conditions. Reversed phase chromatography was carried out using an Agilent 1200 binary pump system with temperature controlled autosampler and vacuum degasser coupled to Thermo Quadrupole Ion Trap MS LTQ XL (linear ion trap mass). The analytes were introduced onto X-Bridge BEH300 C18 3.5 µm, 2.1 x 150 mm column from Waters and the flow rate was maintained at 0.2 mL/min. The column was equilibrated with mobile phase A (0.1 % TFA in H_2O). Mobile phase A and mobile phase B (0.1 % TFA in ACN) were used to establish the 120 min gradient as shown in Table 3.

The UV chromatograms were obtained by monitoring absorbance at 214 nm and the data were processed with Chromeleon software (Dionex). Peptides were then analysed on the LTQ XL equipped with HESI-probe Version 1 at an electrospray potential of 4.5 kV and capillary temperature of 275 °C, sheath gas pressure 25 psi and auxiliary gas flow 10 arb units. The LTQ XL was set to perform data acquisition in the positive ion mode (m/z full scan range 200-2000). The most intense ion was selected for Zoom Scan and then for MS/MS by using a data dependent scheme and dynamic exclusion. The data were acquired with Thermo Scientific™ Xcalibur Software. Data analysis was performed using Thermo Scientific™ PepFinder™.

Table 3: Gradient.

time [min]	mobile phase B [%]
0	0
5	0
85	50
86	90
96	90
97	0
120	0

[8] CZE MS results provided K. Jooss, University Aalen.

3.1.3 Results and Discussion

3.1.3.1 Forced degradation of Peptide 1 - VYPNGA

As introduced in detail in chapter 3.1.1 (Separation and identification of deamidated forms, Strategy for the investigation of deamidation), chromatography and electrophoresis will be applied for the examination of intact and Asp-N digested unstressed and stressed samples. In this study forced deamidation of Peptide 1 was induced using a degradation buffer consisting of 50 mM ammonium bicarbonate, pH 8.0 and elevated temperature (40°C).

In theory, the partial deamidation of Peptide 1 asparagine leads to the formation of three possible peptide variants: P1 (Asn), $P1_D$ (Asp) and $P1_{D,\ iso}$ (isoAsp) as illustrated in Scheme 9[9]. Masses and pI values of Peptide 1 deamidation variants were calculated using the Expasy software [131] and are summarized in Table 4.

P1: VYPN^{4}GA
$P1_D$: VYPDGA
$P1_{D,\ iso}$: VYPD$_{iso}$GA

Scheme 9: Expected signals after heating stress of Peptide 1 (no enzyme digest) with possible peptide modifications: P1: no deamidation, $P1_D$: N4 position deamidated, $P1_{D,\ iso}$: N4 position deamidated and isomerized.

Table 4: Calculated [131] monoisotopic masses and pI values for undigested Peptide 1: not-deamidated and N4 deamidated.

Peak name / Sequence	Mass [Da]	pI
P1: VYPN^{4}GA	619.30	5.49
$P1_D$:VYPDGA	620.66	3.80

In a first step, LC coupled to MS was used to study the unstressed and forced deamidated Peptide 1. The present signals were identified and investigated for the presence of deamidation of asparagine. After peak detection further experiments were performed using capillary zone electrophoresis and UV detection.

As described in chapter 3.1.1, HPLC in the reversed-phase mode is well suited for the investigation of asparagine deamidation due to subtle differences in hydrophobicity and structure between Asn, Asp and isoAsp [10, 108]. According to Yang and Zubarev [89] four different variants of asparagine containing peptide/protein can be expected after partial deamidation. The separation order of these variants will be following: isoAsp, Asn, Asp and

[9] The presence of succinimides is not demonstrated, because this unstable intermediate product is according to literature quickly hydrolysed to the aspartyl or the isoaspartyl residue.

succinimide when using H_2O/TFA and acetonitrile/TFA as eluents. Nilsson et al. [132] introduced another elution order of these peptide/protein forms: Asn, isoAsp, Asp and succinimide in presence of low pH buffers (pH 2). They observed a co-elution of Asn and isoAsp as well as separated aspartate in the more hydrophobic region than Asn signal.

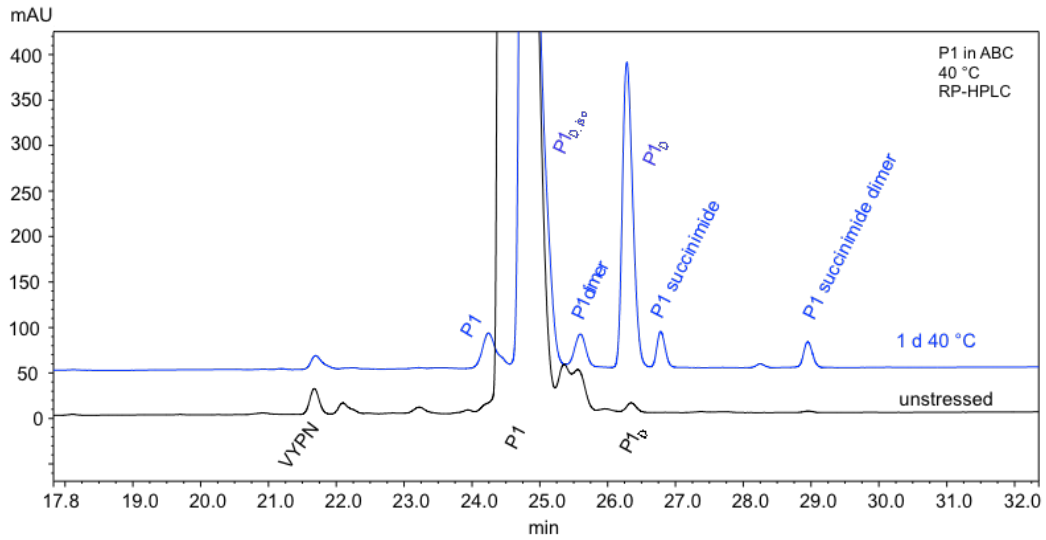

Figure 1: RP-HPLC: Zoomed UV-chromatogram (214 nm wavelength) overlay from 18-32 min for Peptide 1. From bottom to top: unstressed (black), 24 h 40 °C (blue). Experimental conditions: X-Bridge BEH300 C18, 3.5 µm, 2.1 x 150 mm column, H_2O/ACN with 0.1 % TFA, flow rate 0.2 mL/min, column temperature 50 °C.

Figure 1 shows an overlay of two HPLC/UV chromatograms taken before and after the forced degradation of Peptide 1. Additionally, mass spectrometry data were used for peak identification (see Figure 41, Figure 42 in chapter 7) and the results are listed in Table 5. The peak names represent the Peptide 1 variants/fragments. In addition to P1, a small amount of $P1_D$, succinimide dimer and VYPN fragment were detected in unstressed sample (black trace). The not defined peak between P1 and P1 dimer could represent an intermediate dimer.

Four deamidated variants (with elution order: $P1_{D,\ iso}$, $P1_D$, succinimide and succinimide dimer), P1 and P1 dimer were observed in the chromatogram of stressed Peptide 1 (blue trace). The same elution order was reported by Nilsson et al. [132] under similar chromatographic conditions. Comparing the findings in Figure 1 with the ones reported by Nilsson et al., we were able to separate Asn, Asp and isoAsp peptide variants of Peptide 1 when using the above described separation conditions. Results illustrated in Figure 1 and discussed above differ significantly from HPLC results published by Lai et al. [79]. Lai described the presence of only three Peptide 1 variants (P1, $P1_D$ and $P1_{D,\ iso}$ in their chromatograms. The missing succinimide could be due to several reasons, including the fact that their forced degradation conditions differed from the conditions used in this study (they

degraded the peptide in 50 mM ammonium bicarbonate, pH 12). Also Lai's separation conditions were not the same; a flow rate was 1.2 mL/min, whilst Figure 1 represents the separation using the shallow gradients with a lower flow rate of 0.2 mL/min. Steep gradient could lead to co-elution of some signals. Unfortunately Lai had not discussed the absence of succinimide.

Table 5: Comparison of theoretical m/z values [131] with observed masses in unstressed/stressed Peptide 1 (HPLC UV/MS).[10]

Peak name	RT [min]	Theoretical m/z	Measured m/z
VYPN	21.4	492.24	492.38
P1	24.5	620.30	620.38
P1 dimer §	25.5	1221.58	1221.72
$P1_{D, iso}$ §	24.9	621.28	621.34
$P1_D$	26.5	621.28	621.31
$P1_{succinimide}$ §	26.9	603.30	603.42
$P1_{succinimide, dimer}$ §	29.0	1187.58	1187.69

z = 1 for all signals; § found in stressed sample only.

It is obvious that small amount of $P1_D$ (black trace, 26.5 min) has been already detected in unstressed test sample. The presence of such peptide modification might be caused by e.g. long storage in freezer or sample manipulation. Compared to the unstressed sample a much higher $P1_D$ signal was observed in the stressed sample (26.5 min). The signal with the elution time of 24.9 min was assigned to $P1_{D, iso}$. The molecular masses found for this signal do not differ from $P1_D$ and the peak assignment will be discussed in section Asp-N digestion (Figure 3). The following new signal (blue trace, 26.9 min), which was eluted in the subsequent neighbourhood of $P1_D$, represents succinimide. Succinimide converted from asparagine leads to a mass decrease of 17 Da due to the release of ammonia (see Scheme 5). Based on their masses also the presence of P1 dimer (25.5 min) and its succinimide (29.0 min) was confirmed. Some small hydrophilic fragments (black and blue trace, 21 min) in front of the P1 signal were assigned to amino acid sequence VYPN and are most likely a result of the unsuccessful attachment of G and A amino acids during production.

As discussed above, the presence of the deamidated species was verified by the described HPLC method. In order to prevent long analysis times and to achieve the best possible separation of the deamidated products CZE was chosen for further investigations. The application of appropriate electrophoretic conditions allows the separation of closely related species such as Asp and isoAsp (as described in detail in chapter 3.1.1, Separation

[10] LTQ XL typical accuracy +/- 0.5 m/z.

and identification of deamidated forms) in a short period of time. As published by Lai et al. [79] the resolution of Asp and isoAsp will be achieved by using a separation buffer with a pH close to the pKa values of Asp and isoAsp peptide carboxylic acids. We optimised Lai's analytical method (instead of using phosphate buffer, pH 3.0 the separation was performed with 3 % acetic acid, pH 2.5) to study the deamidated forms of Peptide 1. Using the acetate running buffer system of pH 2.5 we expect the following migration order of peptides: P1: $P1_D$: $P1_{D,\ iso}$ ([79], Scheme 7).

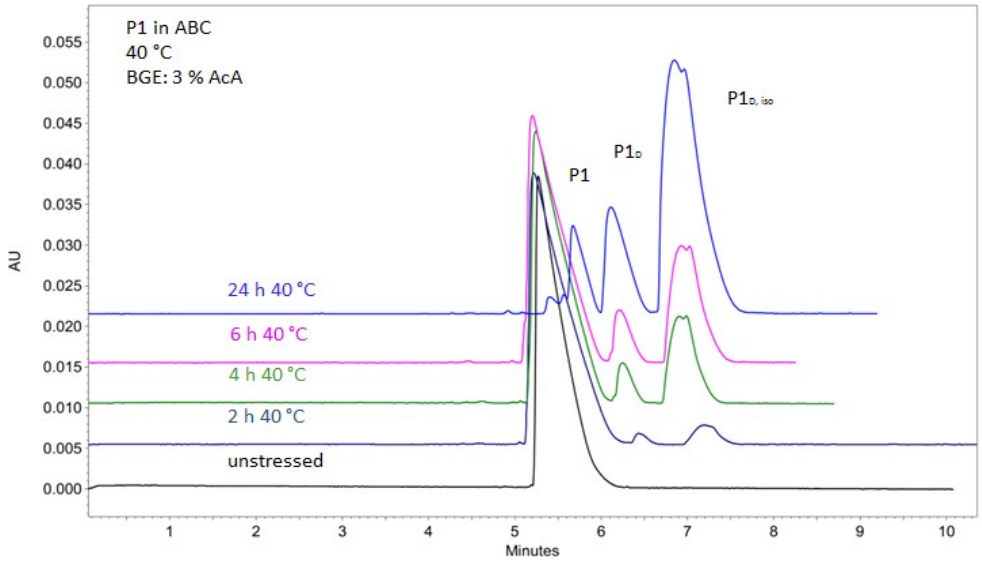

Figure 2: CZE: Full scale UV-electropherogram (214 nm wavelength) overlay from 0-10 min for Peptide 1 (1 mg/mL). From bottom trace to top trace: unstressed (black), 2 h 40 °C (dark blue), 4 h 40 °C (green), 6 h 40 °C (pink), 24 h 40 °C (light-blue). Experimental conditions: BGE: 3 % AcA pH 2.5, 40/50 cm 50 µm fused silica capillary, dynamic coating with capillary conditioning solution, separation temperature: 25 °C, separation voltage: 30 kV, injection 0.5 psi 10 s.

A series of CZE measurements was performed to monitor the deamidation of Peptide 1 during the incubation period of 24 hours (shown in Figure 2). The peaks were identified on the basis of the known migration order in this separation system and of the expected isoAsp:Asp ratio 1:3 [80]. The signal decrease of P1 (5.5 min) is clearly visible during the whole incubation procedure. The amount of deamidated products increased with time judging from the peak areas of two new signals in electropherograms ($P1_D$ 6.5 min and $P1_{D,\ iso}$ 7 min).

When applying CZE, a faster separation of asparagine peptide and both main deamidation variants ($P1_D$ and $P1_{D,\ iso}$) was achieved compared to HPLC. The pH value of the background electrolyte (2.5) used in this analysis resulted in an unwanted peak broadening. Increasing the pH to 3.0, (as reported by Lai [79]), led to an impaired peak resolution. The separation of only three signals was achieved using acetate buffer. The

additional signals (succinimide, dimers) present in Figure 1 were not observed, even with further modifications of the running buffer.

Following the strategy introduced in chapter 3.1.1 (Separation and identification of deamidated forms), the site-specific enzymatic cleavage of unstressed and stressed material was performed. The application of Asp-N enzymatic digest on samples of interest should lead to the presence of new peptides, if there is some aspartate present in stressed sample (Scheme 6, Scheme 7). As performed with intact Peptide 1 samples (Figure 1 and Figure 2), the chromatographic signals were identified according to their masses after Asp-N digestion. Further experiments with Asp-N digested samples were performed using CZE with UV detection after identification by LC-MS.

The Asp-N enzyme cleavage of partially deamidated Peptide 1 yields peptides as illustrated in Scheme 10.

P1: VYPNGA
$P1_{D,\ iso}$: VYPD_{iso}GA
P2: VYP
P3: DGA

Scheme 10: Expected signals after heating stress and complete Asp-N digestion of Peptide 1. P1: no deamidation, $P1_{D,\ iso}$: N4 position deamidated and isomerized, P2, P3 cleavage products of Asp-N digested deamidated Peptide 1. Presented Asp-N cleavage products were expressed with respect on partial peptide deamidation or deamidation, isomerization.

Asp-N enzyme creates new peptides only in the presence of aspartate. Therefore it is anticipated that the chromatographic profile of unstressed digested Peptide 1 will not differ from the profile of samples, which have not been digested (black trace, Figure 1). Because the presence of aspartate ($P1_D$) was confirmed in the stressed sample (blue trace, Figure 1) $P1_D$ signal should be cleaved by Asp-N enzyme. In addition to the presence of $P1_{D,\ iso}$, two new peaks (P2 and P3) should be detected in the HPLC chromatogram with the properties stated in Table 6.

Table 6: Calculated [131] monoisotopic masses and pI values for in-silico Asp-N digested deamidated Peptide 1.

Peak name / Sequence	Mass [Da]	pI
P2: VYP	377.20	5.49
P3: DGA	261.11	3.80

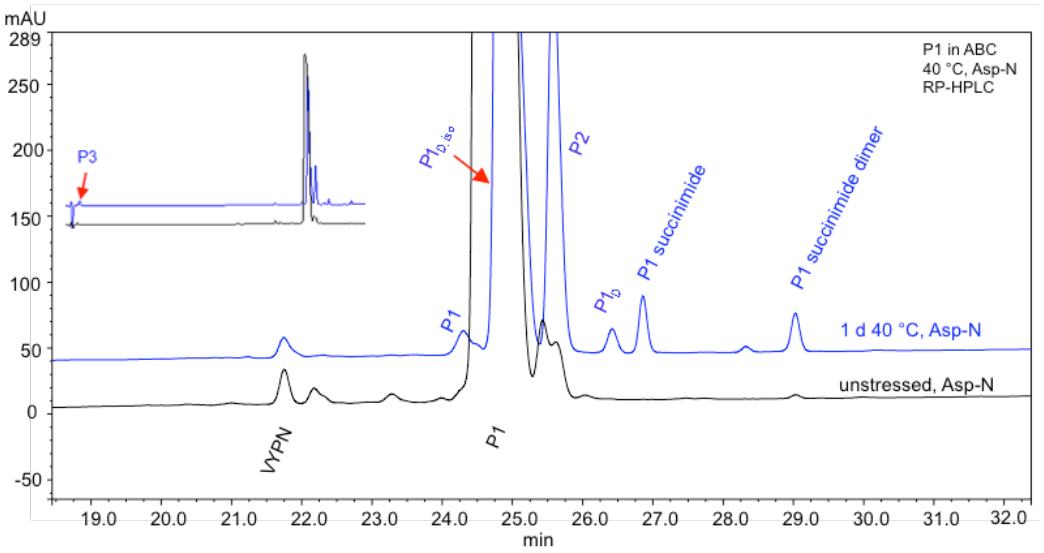

Figure 3: RP-HPLC: Full scale (0-32 min) and zoomed UV-chromatogram (214 nm wavelength) overlay for Peptide 1 digested by Asp-N. From bottom trace to top trace: unstressed, Asp-N (black), 24 h 40 °C, Asp-N (blue). Experimental conditions: X-Bridge BEH300 C18, 3.5 µm, 2.1 x 150 mm column, H_2O/ACN with 0.1 % TFA, flow rate 0.2 mL/min, column temperature 50 °C.

The chromatograms obtained after Asp-N digestion of Peptide 1 (unstressed and stressed) are shown in Figure 3. In addition to P1 peptide (24.4 min), VYPN fragment (21.6 min), succinimide dimer (29.1 min) and traces of P2 and P3 signals were detected in the mass spectrum of unstressed Asp-N digested sample. The presence of VYPN fragment was already discussed above. The observation of P2 and P3 peptides can be explained by the presence of low $P1_D$ signal in unstressed sample (Figure 1).

In comparison with results obtained for stressed non-digested Peptide 1 (Figure 1) a significant decrease of the $P1_D$ signal (blue trace, 26.5 min) and two additional peaks were detected (blue trace, 2.5 and 25.5 min) in chromatogram of stressed Asp-N digested sample. The molecular weights of these two signals were determined by mass spectrometry and the peaks were assigned to P2 and P3 peptide fragments. This demonstrates clearly that Asp-N enzyme cuts selectively at the N-terminal side of aspartate. In addition to the new created peptides, P1 (blue trace, 24.4 min) and $P1_{D,\ iso}$ signals (blue trace, 24.9 min) were identified in the chromatogram. The MS data evaluation is shown in Table 7.

Table 7: Comparison of theoretical m/z values [131] with observed masses in unstressed/stressed Asp-N digested Peptide 1 (HPLC UV/MS).[11]

Peak name	t_R [min]	Theoretical m/z	Measured m/z
P3	2.5	378.20	378.34
VYPN	21.6	492.24	492.32
P1	24.4	620.30	620.42
$P1_{D,\ iso}$ §	24.9	621.28	621.41
P2	25.5	262.10	262.18
$P1_{D}$ §	26.5	621.28	621.38
$P1_{succinimide}$ §	26.9	603.30	603.42
$P1_{succinimide,\ dimer}$	29.1	1187.58	1187.71

z = 1 for all signals; § found in stressed sample only

It became apparent after the chromatographic study of Asp-N digested samples, that the present deamidation can be clearly detected using UV detection. This can be achieved by visual comparison of chromatograms of the unstressed and stressed digested samples. A major benefit of this method is the detection of deamidation without using mass spectrometry.

The previous CZE experiments with intact Peptide 1 samples demonstrated the ability of this method to visualize the deamidated variants within a short period of time. The electrophoretic analysis of Asp-N digested samples will complete the whole investigation strategy. As illustrated in Scheme 7, there should not be any further signals present in unstressed digested Peptide 1, except of P1. The situation for stressed digested Peptide 1 should offer a greater variety of signals; presence of P1, $P1_{D,\ iso}$ and P2 or P3 (or both) peaks is expected in the electropherogram.

[11] LTQ XL typical accuracy +/- 0.5 m/z

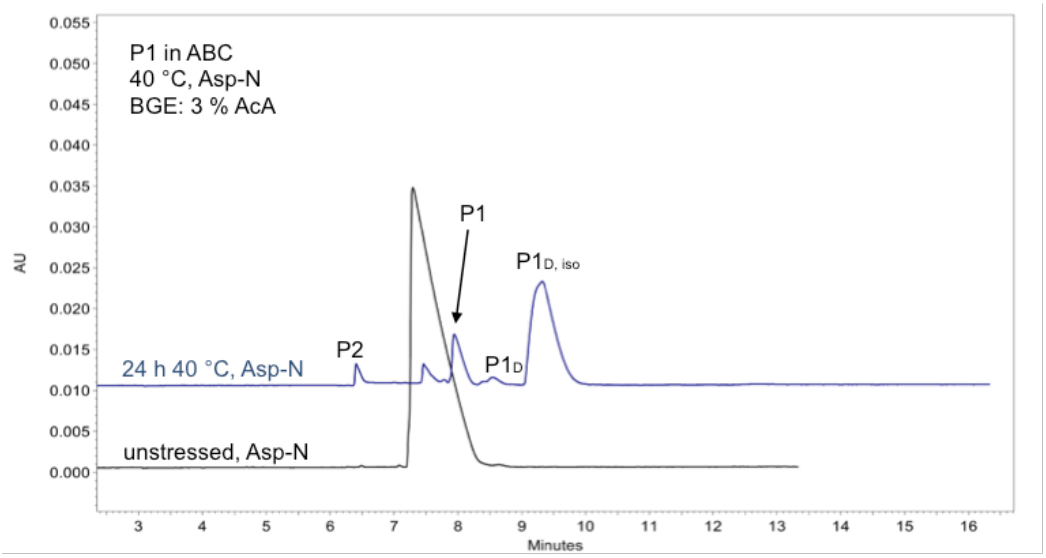

Figure 4: CZE: Full scale UV-electropherogram (214 nm wavelength) overlay for Peptide 1 digested by Asp-N(0.8 mg/mL). From bottom trace to top trace: unstressed, Asp-N (black), 24 h 40 °C, Asp-N (blue). Experimental conditions: BGE: 3 % AcA pH 2.5, 40/50 cm 50 µm fused silica capillary, dynamic coating with capillary conditioning solution, separation temperature: 25 °C, separation voltage: 30 kV, injection 0.5 psi 20 s.

As apparent from electropherograms of unstressed and stressed Peptide 1 (Figure 4), P1 (both 7.5 min) was not subjected to enzymatic hydrolysis. The same situation was observed for $P1_{D,\ iso}$ (blue trace, 9.5 min). As expected the $P1_D$ (blue trace, 8.5 min) was enzymatically cleaved and one new signal – P2[12] was found in electropherogram (blue trace, 6.5 min). The low $P1_D$ signal found after Asp-N digestion corresponds with the situation in Figure 3. The not labelled peak (7.5 min) is presumed to be a VYPN signal found in MS spectrum (Figure 1 and Figure 3).

Factors involved in deamidation process

As specified in more detail in chapter 3.1.1, the deamidation process is affected by many factors. The deamidation rate depends, i.a., on primary sequence. Asparagine can be degraded easily to aspartate and isoaspartate form, if the side chain of the C-flanking amino acid is relatively small and hydrophilic [80, 87]. It was expected that asparagine in Peptide 1 undergoes rapid deamidation reaction due to N-G motif. The fast aspartate and isoaspartate formation was observed in the degradation study monitored by CZE (Figure 2). But there are further factors having an influence on deamidation rate of peptides and proteins that would be worthwhile to study (e.g. buffer type and buffer concentration, pH, temperature). Many of them were miscellaneously combined and used for the deamidation studies of Peptide 1.

[12] The peak assignment was done after the electrophoretic run using the wavelength of 280 nm (fragment VYP consist of aromatic amino acid).

How the three of them influenced the asparagine degradation is presented in Table 8 and the results are discussed below.

Table 8: Observed degradation of Peptide 1 within 24 hours in 50 mM ammonium bicarbonate, pH 8.0 at 40 °C, within 3 days in 20 mM ammonium bicarbonate, pH 8.0 at 40 °C and within 24 hours in 50 mM Tris-HCl, pH 8.0 at 40 °C.

50 mM ABC pH 8.0, 40 °C				
Incubation period	A_{corr} % P1	A_{corr} % $P1_D$	A_{corr} % $P1_{D, iso}$	$P1_{D, iso}$ / $P1_D$
2 h	95.2	1.2	3.6	3.0
4 h	79.1	4.6	16.3	3.5
6 h	69.3	6.6	24.2	3.6
24 h	13.3	18.3	68.4	3.7
20 mM ABC pH 8.0, 40 °C				
Incubation period	A_{corr} % P1	A_{corr} % $P1_D$	A_{corr} % $P1_{D, iso}$	$P1_{D, iso}$ / $P1_D$
1 d	64.9	6.8	28.3	4.2
2 d	39.2	12.1	48.7	4.0
3 d	10.5	18.6	70.9	3.8
50 mM Tris-HCl pH 8.0, 40 °C				
Incubation period	A_{corr} % P1	A_{corr} % $P1_D$	A_{corr} % $P1_{D, iso}$	$P1_{D, iso}$ / $P1_D$
2 h	93.8	1.5	4.7	3.1
4 h	83.7	4.1	12.2	3.0
6 h	70.0	7.7	22.3	2.9
24 h	14.2	24.2	61.6	2.5

Results are reported as means of duplicate determinations.

The acceleration effect of all three buffers on deamidation of Peptide 1 was tested. As apparent from $P1_{D, iso}$ / $P1_D$ (isoAsp/Asp) results, the succinimide hydrolysis to isoaspartate varied not only between studies, but also during the incubation period. Patel and Borchardt [133] studied the effect of pH and buffer concentration on the ratio of isoAsp/Asp in hexapeptides at 37 °C and observed that this ratio varied in the range of 3.2 to 4.2 in the basic pH (6.0-12.0) depending on deamidation buffer. When comparing different molarities of ammonium bicarbonate deamidation buffer the same degree of deamidated variants was achieved after an incubation time of 24 hours in 50 mM ammonium bicarbonate, whereas an incubation time of 3 days is needed when using 20 mM bicarbonate. The results of the degradation study in 50 mM Tris-HCl are comparable with 50 mM ammonium bicarbonate. Tris-HCl conditions seem to affect the succinimide hydrolysis resulting in the production of more aspartate, than it has been observed by ammonium bicarbonate. The highest deamidation rate was observed for 50 mM ammonium bicarbonate, pH 8.0 – within 24 hours almost 70 % of asparagine was deamidated. Because it was reported that elevated

temperatures could lead to the formation of formaldehyde using Tris-HCl [94], the 50 mM ammonium bicarbonate will be the preferred choice for further degradation studies.

3.1.3.2 Forced degradation of Peptide 2 - GSNSG

Using the same degradation conditions as described in chapter 3.1.3.1, the slower deamidation rate was expected due to the present N-S motif [15, 87] in contrast to the Peptide 1. Partial deamidation of N3 asparagine leads to presence of three peptide variants: P2 (Asn), $P2_D$ (Asp) and $P2_{D,\ iso}$ (isoAsp) as illustrated in Scheme 11[13].

P2: GSN^{3}SG
$P2_D$: GSDSG
$P2_{D,\ iso}$: GSD_{iso}SG

Scheme 11: Expected signals after heating stress of Peptide 2 (no enzyme digest) with possible peptide modifications: P2: no deamidation, $P2_D$: N3 position deamidated, $P1_{D,\ iso}$: N3 position deamidated and isomerized.

It has been shown on Peptide 1 sample that capillary electrophoresis combined with Asp-N digestion is a very effective method in detection of asparagine deamidation. Similarly as described above, firstly, the measurements of intact (unstressed and stressed) samples were planned. If some indication of deamidation is found, the electrophoretic examination of Asp-N digested samples will follow.

To induce asparagine deamidation in Peptide 2, the peptide was subjected to elevated temperature (40 °C) and degradation buffer (50 mM ammonium bicarbonate, pH 8.0). For the estimation of the deamidation rate the incubated peptide was analysed by CZE in intervals of approximately 2 days. As shown in Figure 5 about 30 % of Peptide 2 was degraded in almost one week.

[13] The presence of succinimides is not demonstrated, because this unstable intermediate product is according to literature quickly hydrolysed to the aspartyl or the isoaspartyl residue.

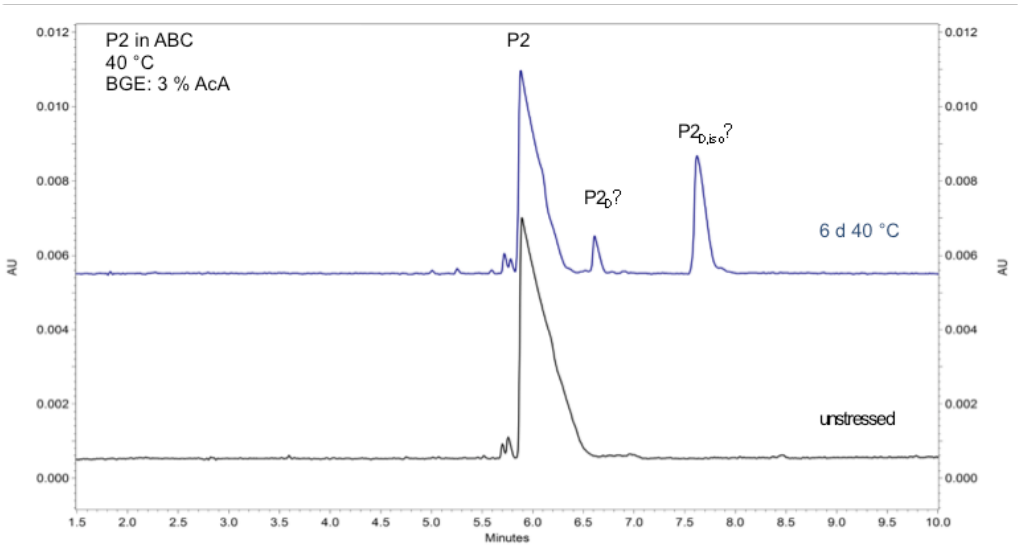

Figure 5: CZE: Full scale UV-electropherogram (214 nm wavelength) overlay for Peptide 2 (1 mg/mL). From bottom trace to top trace: unstressed (black), 6 d 40 °C (blue). Experimental conditions: BGE: 3 % AcA pH 2.5, 40/50 cm 50 µm fused silica capillary, dynamic coating with capillary conditioning solution, separation temperature: 25 °C, separation voltage: 30 kV, injection 0.5 psi 10 s.

In addition to the main signal P2 (6.0 min) being found in unstressed and stressed samples, there were two further signals: $P2_D$? (blue trace, 6.7 min) and $P2_{D,\ iso}$? (blue trace, 7.7 min) detected in electropherogram of stressed sample in Figure 5. In comparison to the CZE deamidation profile of Peptide 1 in Figure 2 these three signals are not separated in typical distances. Especially the $P2_{D,\ iso}$? deviates from the expected separation profile and does not migrate in the close proximity of $P2_D$?. Besides generating different electrophoretic profile of degradation products a $P2_{D,\ iso}$?:$P2_D$? (isoAsp:Asp) peak area percentage ratio was approximately 5:1 after 3 weeks of incubation (see Table 9). The described situation is nevertheless possible, because the stress conditions differ from nature conditions. Despite of this fact, aforementioned result is surprising when compared to the isoAsp:Asp ratio 3:1 findings from studies of other peptides [80, 87, 88] or to Peptide 1 results (stated in Table 8).

Table 9: Observed degradation of Peptide 2 within 21 days in 50 mM ammonium bicarbonate, pH 8.0 at 40 °C.

50 mM ABC pH 8.0, 40 °C				
Incubation period	A_{corr} % P2	A_{corr} % $P2_D$?	A_{corr} % $P2_{D,\ iso}$?	$P2_{D,\ iso}$? / $P2_D$?
2 d	90.5	3.0	6.2	2.1
8 d	70.1	5.2	21.5	4.1
15 d	52.1	7.7	36.2	4.7
21 d	46.5	7.8	41.6	5.3

As performed with Peptide 1 (Figure 4), the unstressed and stressed Peptide 2 was digested with Asp-N enzyme and analysed by CZE. It is expected that the enzyme will cause the hydrolysis of $P2_D$? if $P2_D$? represents the aspartate form of Peptide 2.

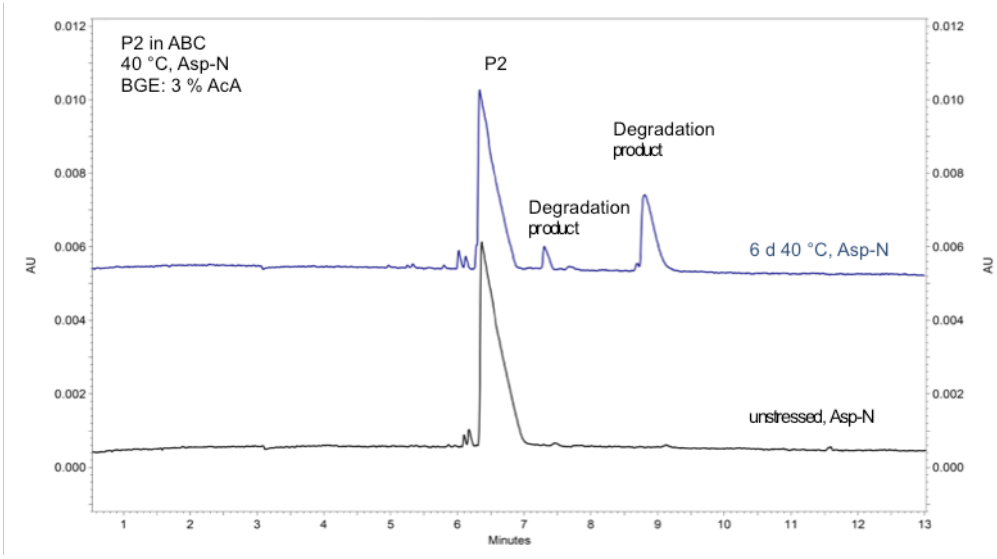

Figure 6: CZE: Full scale UV-electropherogram (214 nm wavelength) overlay for Peptide 2 digested by Asp-N (1 mg/mL). From bottom trace to top trace: unstressed, Asp-N (black), 6 d 40 °C, Asp-N (blue). Experimental conditions: BGE: 3 % AcA pH 2.5, 40/50 cm 50 µm fused silica capillary, dynamic coating with capillary conditioning solution, separation temperature: 25 °C, separation voltage: 30 kV, injection 0.5 psi 10 s.

Two electropherograms of Asp-N digested samples (Figure 6) are practically identical to the data introduced in Figure 5. Based on these results it can be presumed, that the peaks labelled as degradation products (7.5 and 9.0 min) do not represent any form of deamidated asparagine. The CZE signals demonstrate with a relatively high probability some fragments formed by hydrolysis of N- or C-terminal amino acid. Further HPLC-MS investigation of intact and Asp-N digested samples proved neither presence of deamidated variants nor aspartate cleavage products in MS spectrum (data not shown). The knowledge derived from these experiments might be helpful to recognize deamidation in further research. Besides appearing new signals, the particular attention must be given also to the peak distances and isoAsp:Asp ratio.

3.1.3.3 Forced degradation of Glu1-Fibrinopeptide

The application of CZE and Asp-N digestion for the investigation of deamidation will be demonstrated on more complex molecule than Peptide 1 or Peptide 2.

To induce deamidation, the Glu1-Fibrinopeptide was exposed to a degradation buffer consisting of 50 mM ammonium bicarbonate, pH 8.0 and an elevated temperature (40°C). The peptide degradation was monitored by CZE-UV of intact samples. Mass spectrometry

(CZE-MS, HPLC-MS) was introduced to identify the degradation products and to determine the number of deamidated asparagines. Afterwards, the CZE-UV (CZE-MS) analysis of Asp-N digested samples completed the investigation.

As apparent from the primary structure of Glu1-Fibrinopeptide (referred to as a signal variant F in Scheme 12), there are two potential deamidation sites (asparagines) located on the N- and C-terminal side of aspartate. Under certain circumstances the D5 aspartate can be converted into isoaspartate and/or the N4, N6 asparagine(s) can undergo deamidation/isomerization as demonstrated by possible scenarios in Scheme 12.

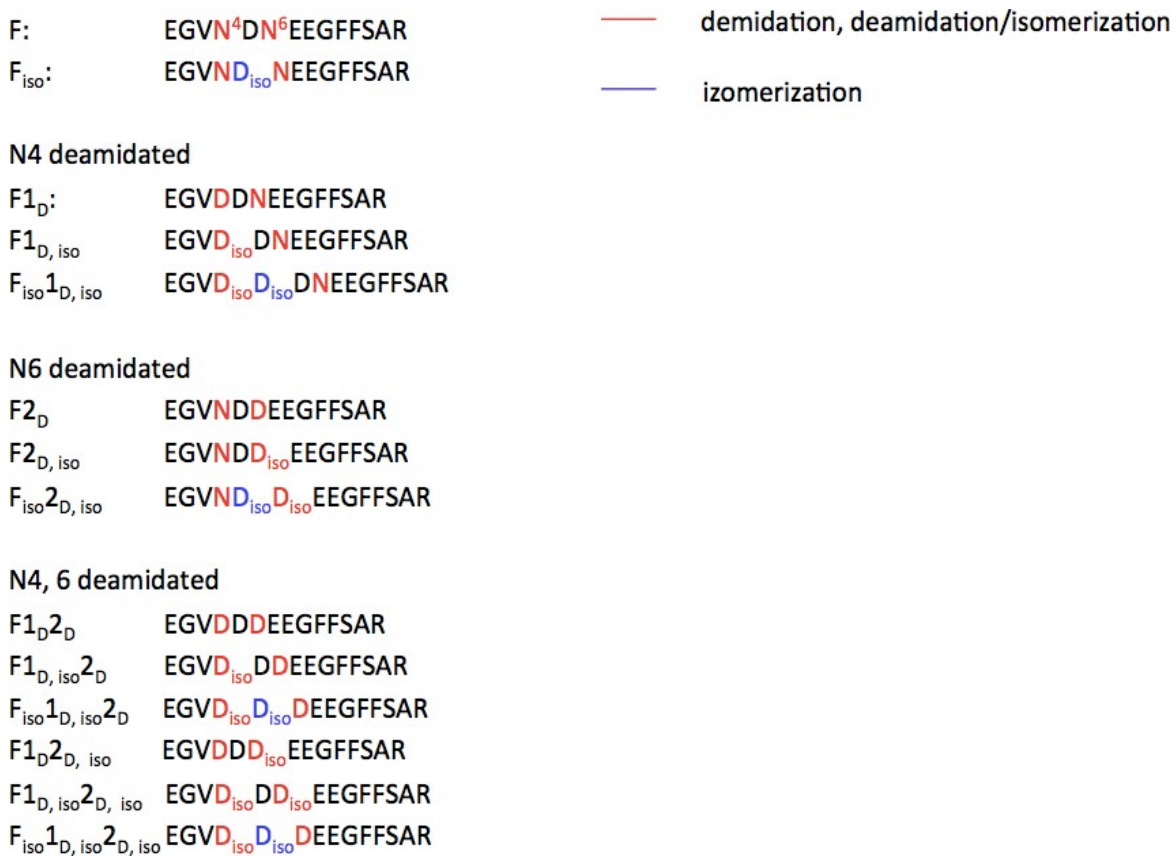

Scheme 12: Possible signals variants after forced degradation of Glu1-Fibrinopeptid: no deamidation, D5 position isomerized, N4 position deamidated/isomerized, N6 position deamidated/isomerized and its combinations.

The variability of the degradation products increases with each deamidated asparagine. If both of the asparagines will be partially deamidated/isomerized and D5 partially isomerized there is the possibility to observe 18 different forms of this peptide. Including the presence of succinimide, the amount of possible peptide variants will continue to grow.

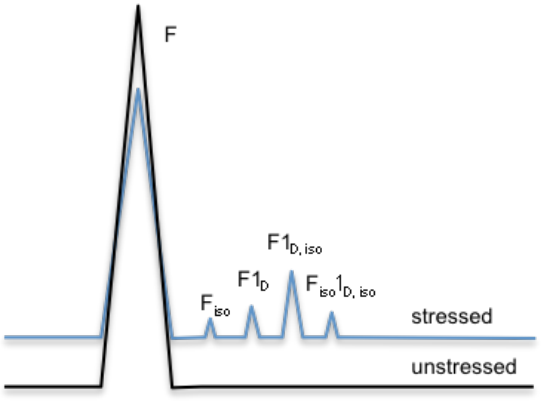

Scheme 13: Visualization of electrophoretic separation of unstressed and stressed Glu1-Fibrinopeptide. In addition to the main signal (F), further signals can be observed after forced degradation leading to a partial N4 deamidation/isomerization and partial D5 isomerization.

Exemplary, an electropherogram (Scheme 13), where N4 asparagine is partially deamidated/isomerized and D5 aspartate is partially isomerized[14], would appear as described subsequently. Because of the partial degradation, the peak representing Glu1-Fibrinopeptide (F) can still be detected in the electropherogram. This F signal will be lower than the one in unstressed sample, because it is reduced by the amount of all degradation products. $F1_D$ and $F1_{D,\ iso}$ as two expected N4 deamidation products will be visible as two peaks under optimal electrophoretic conditions in the electropherogram. Is the isomerization of D5 faster than deamidation of N4, F_{iso} variant will be participating on reduction of the F signal. Should the isomerization of D5 occur simultaneously with N4 asparagine deamidation, the $F_{iso}1_D$ and $F_{iso}1_{D,\ iso}$ peaks will be also found between degradation products.

Using the acidic buffer (pH 2.5) and normal polarity, at least three peaks (in the separation order Asn, Asp and isoAsp) are expected in electropherograms of stressed samples. Should the N4 and N6 deamidated variants be present (labelled as $F1_D$ and $F2_D$ in Scheme 12), it is quite likely that these signals will co-migrate. As listed in Table 10, the $F1_D$ and $F2_D$ deamidated forms have the same physicochemical properties and will possess the same charge. It is anticipated that the variant $F1_D2_D$ will be separated later than $F1_D$ or $F2_D$ due its lower pI value.

[14] The presence of succinimides is not demonstrated, because this unstable intermediate product is according to literature quickly hydrolysed to the aspartyl or the isoaspartyl residue.

Table 10: Calculated [131] monoisotopic masses and pI values for undigested Glu1-Fibrinopeptide: non-deamidated and N4, N6 deamidated.

Peak name / Sequence	Mass [Da]	pI
F: EGVN^{4}DN^{6}EEGFFSAR	1570.59	4.00
F1$_D$: EGVDDNEEGFFSAR	1571.58	3.83
F2$_D$: EGVNDDEEGFFSAR	1571.58	3.83
F1$_D$2$_D$: EGVDDDEEGFFSAR	1572.56	3.71

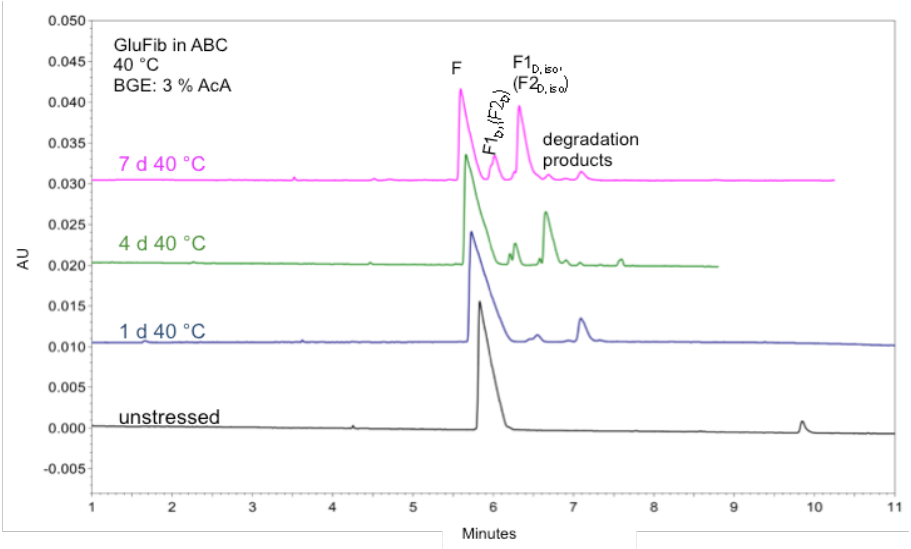

Figure 7: CZE: Full scale UV-electropherogram (214 nm wavelength) overlay for Glu1-Fibrinopeptide (2 mg/mL). From bottom trace to top trace: unstressed (black), 1 d 40 °C (blue), 4 d 40 °C (green), 7 d 40 °C (pink). Experimental conditions: BGE: 3 % AcA pH 2.5, 40/50 cm 50 µm fused silica capillary, dynamic coating with capillary conditioning solution, separation temperature: 25 °C, separation voltage: 30 kV, injection 0.5 psi 10 s.

As illustrated by electropherograms in Figure 7, the forced degradation of Glu1-Fibrinopeptide resulted in the presence of a couple of new peaks. As the F signal decreases the signals representing the deamidation and degradation products are concurrently increasing during the whole incubation. Derived from previous experiences (the CZE study of stressed Peptide 1), some of these signals could represent the deamidated variants. The molecular weights of present peaks were determined by mass spectrometry and the main three signals were assigned to F (5.7 min), F1$_D$, F2$_D$ (6.2 min) and F1$_{D,\ iso}$, F2$_{D,\ iso}$ (6.7 min). Also, the presence of F1$_D$2$_D$ was detected (observable as peak shoulder at F1$_D$. Using this method it cannot be distinguished between F1$_D$ and F2$_D$ signals, as well as between F1$_{D,\ iso}$ and F2$_{D,\ iso}$, therefore the present peaks were assigned to both variants. The corresponding MS data are summarised in Table 11.

Table 11: Comparison of theoretical m/z values [131] with observed masses in unstressed/stressed Glu1-Fibrinopeptide (CZE-ESI-MS).[15]

Peak name	t_m [min]	Theoretical m/z	Measured m/z
F	5.7	786.29	786.31
$F1_D$, ($F2_D$) §	6.2	786.79	786.79
$F1_D2_D$ §	6.2	787.28	787.30
$F1_{D,\ iso}$, ($F2_{D,\ iso}$) §	6.7	786.79	786.76

z = 2 for all signals; § found in stressed sample only.

The peptide degradation was monitored within a period of one week. As shown in Table 12, the incubation of Glu1-Fibrinopeptide led to degradation of about 50 % of F signal after 7 days. In addition to the above-described Glu1-Fibrinopeptide variants there were also some signals present in the more acidic area. These degradation products were mostly fragments formed by hydrolysis of N- or C-terminal amino acids and participated on F degradation from almost 10 % after 7 days (data not shown). The ratio of isoAsp/Asp[16] ($F_{D,\ iso}/F_D$) increased from 2.9:1 after one day to 3.2:1 after one week and it could be presumed, that this ascending trend in the succinimide hydrolysis to isoAsp would continue with further incubation.

Table 12: Observed degradation of Glu1-Fibrinopeptide within 7 days in 50 mM ammonium bicarbonate, pH 8.0 at 40 °C. [16]

50 mM ABC pH 8.0, 40 °C				
Incubation period	A_{corr} % F	A_{corr} % F_D[16]	A_{corr} % $F_{D,\ iso}$	$F_{D,\ iso}/F_D$
1 d	89.4	2.5	7.3	2.9
4 d	73.4	5.8	17.6	3.0
7 d	51.8	9.7	30.7	3.2

Results are reported as means of triplicate determinations.

As demonstrated in Table 11, the presence of two deamidated asparagines was confirmed using CZE-ESI-MS. Additionally, chromatographic investigations of intact samples were performed in order to verify the results (data not shown). A molecular mass representing the $F1_D2_D$ variant (m/z = 787.11^{2+}) was found in mass spectrum after chromatographic separation. MS/MS was applied for further confirmation of multiple deamidation (for ion chromatogram see Figure 43 in chapter 7). The b4-ion was observed

[15] Micro-TOF typical accuracy +/- 100 ppm.

[16] F_D demonstrates the $F1_D$ or $F2_D$ variant (or both if they co-migrate), $F_{D,\ iso}$ represents $F1_{D,\ iso}$ or $F2_{D,\ iso}$ (or both).

after low-energy CID fragmentation with m = 401.3 Da, whereby the N4 deamidation has been proved. The y9-ion at m = 1057.4 Da confirms the N6 deamidation site.

Because the separation of the multiple deamidated products was not achieved using current electrophoretic conditions, the electrophoretic method was optimized. Gennaro and Solano reported [134], that the multiple N→D[17] substitutions could be separated using a 20 mM acetic acid, pH 4.5 as a running buffer. Exemplary, three synthetic peptides with nearly equal amino acid chains (NN, ND, DD) were examined and the separation resulted in superior resolution of charged peptide variants. To achieve the optimal separation conditions for multiple deamidated species of Glu1-Fibrinopeptide, the following aspects were considered:

(1) Using of higher pH than pI value of peptide variants will affect the ion charges; they became a negative and therefore the reverse polarity will be applied for separation.

(2) Dynamic coating will control the peptide adsorption onto capillary wall.

Based on previous experience and applying the above-mentioned conditions to double deamidated Glu1-Fibrinopeptide, the order of separation can be predicted: $F1_DF2_D$:$F1_D(F2_D)$:F[18]. In addition to these peaks, the presence of isomerized variants is also expected in electropherogram.

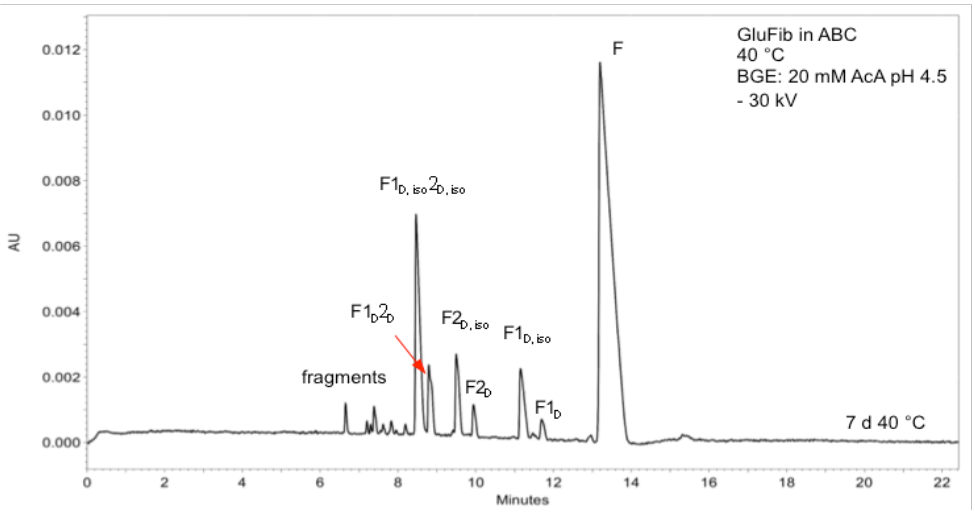

Figure 8: CZE: Full scale UV-electropherogram (214 nm wavelength) of Glu1-Fibrinopeptide stressed for 7 d at 40 °C. Experimental conditions: BGE: 20 mM AcA pH 4.5, 40/50 cm 50 µm fused silica capillary, dynamic coating with capillary conditioning solution, separation temperature: 25 °C, separation voltage: -30 kV, injection 0.5 psi 10 s.

[17] one letter abbreviation system: N for asparagine and D for aspartate

[18] Using the one letter abbreviations then DD:DN(ND):N represent the $F1_DF2_D$:$F1_D(F2_D)$:F Glu1-Fibrinopeptide variants.

A significant improvement of former peak resolution (Figure 7) was achieved using 20 mM acetic acid as BGE for the separation of stressed Glu1-Fibrinopeptide. As evident from the electropherogram in Figure 8, it is not only possible to separate DD:D:N signals [134], but also their isomerized products. Using the above-described conditions, the Glu1-Fibrinopeptide - F is separated with the longest migration time (13.5 min). As introduced in Table 10, F has the highest pI value and is the weakest anion of all present peptide variants. Based on the MS results (summed in Table 13), the peaks with migration time between 8 and 13 minutes were assigned to the various Glu1-Fibrinopeptide variants. The separation order was following: $F1_{D,\ iso}\ 2_{D,\ iso}$, $F1_D2_D$, $F2_{D,\ iso}$, $F2_D$, $F1_{D,\ iso}$, $F1_D$. The deamidated peptide variants have lower pI values (Table 10), a more negative charge and are separated with shorter migration times than F. The $F1_D$ and $F2_D$ signals (DN, ND variants) cannot be determined from the UV profile. The peak assignment was established as described below. The peak with the migration time of 11.7 min was labelled as $F1_D$ and the other deamidated form as $F2_D$ (10.0 min). The explanation for the peak resolution of two peptides with same amino acid sequences is seen in different physical properties (hydrodynamic radii) of DN and ND variants. The signal with migration time of 11.3 min was assigned to the $F1_{D,\ iso.}$. Iso determination was based on the known migration order of isoAsp and Asp forms and approximately 3:1 isoAsp:Asp ratio. The same principle was applied to the $F2_{D,\ iso}$ variant. The possibility to separate the $F1_D$ and $F1_{D,\ iso}$ ($F2_D$ and $F2_{D,\ iso}$) from each other is explained by slight differences in pKa's of aspartate and isoaspartate. The DD form represented by $F1_D2_D$ peak (8.8 min) migrated with the lowest migration time in relation to the DN or ND variant. As stated in Table 10, this molecule has the lowest pI value, therefore a strongest negative charge and moves fastest towards the anode. The peak $F1_{D,\ iso}\ 2_{D,\ iso}$ (8.5 min) was considered to be an isomerized form of $F1_D2_D$.

Contrary to the improved peak resolution demonstrated in Figure 8, these electrophoretic conditions led to an unstable current during the MS runs. This fact mainly disturbed the peak identification via ESI-MS[19]. Higher concentration of running buffer (50 mM) offered the same electrophoretic profile and significantly more stable current during the MS run. Despite of this improvement, the identification of peptides with a migration time lower than 8.3 min was not achieved.

[19] CZE MS results provided K. Jooss, University Aalen.

Table 13: Comparison of theoretical m/z values [131] with observed masses in stressed and stressed Asp-N digested Glu1-Fibrinopeptide (CZE-ESI-MS).[20]

Peak name	mt [min]	Theoretical m/z	Measured m/z
$F1_{D,\,iso}\,2_{D,\,iso}$	8.5	787.28	787.32
$F1_D2_D$	8.8	787.28	787.38
$F2_{D,\,iso}$	9.7	786.79	786.83
$F2_D$	10.0	786.79	786.79
$F1_{D,\,iso}$	11.3	786.79	786.85
$F1_D$	11.7	786.79	786.79
F	13.5	786.29	786.30

z = 2 for all signals.

Further electrophoretic experiments with Asp-N digested samples should help to improve the introduced peak assignment. It is expected that all Glu1-Fibrinopeptide variants will be cut into smaller peptides; except one: $F_{iso}1_{D,\,iso}\,2_{D,\,iso}$. Despite of the short amino acid chain of Glu1-Fibrinopeptide, many peptide variants may be present in electropherogram after analysis. It must be taken into account that the studied stressed molecule will not be very likely fully degraded. The partially isomerized aspartate and partially deamidated/isomerized asparagine will increase the number of present signals after Asp-N digestion. An example will be introduced in detail below the Scheme 14. This scheme describes the specific Asp-N cleavage of Glu1-Fibrinopeptide with partially isomerized D5 aspartate and/or deamidated/isomerized N4 and N6 asparagines.

[20] microTOF-Q typical accuracy +/- 100 ppm.

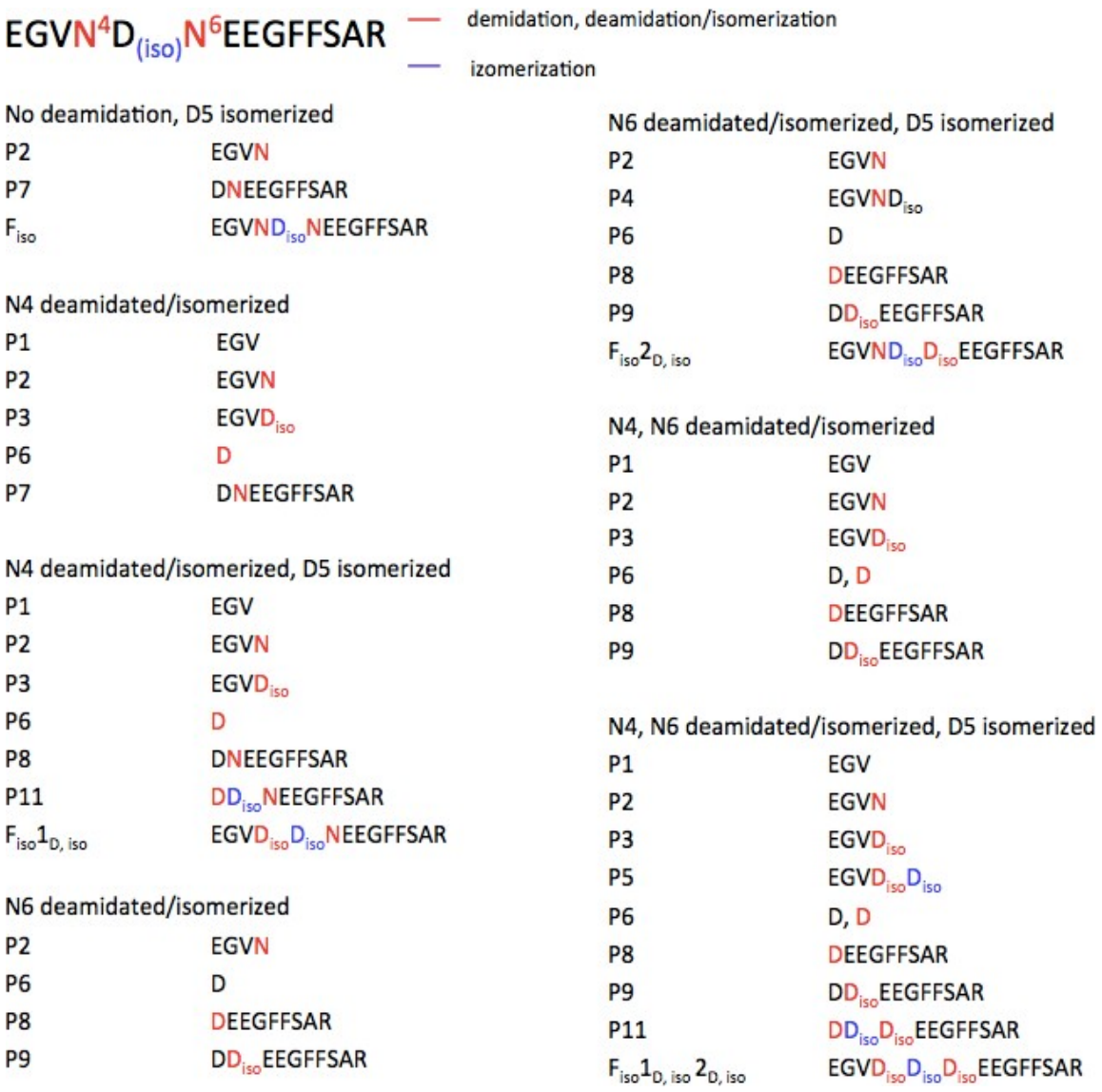

Scheme 14: Possible signal variants after Asp-N digest of forced degraded Glu1-Fibrinopeptide: no deamidation, D5 position isomerized, N4 position deamidated/isomerized, N6 position deamidated/isomerized and its combinations. Presented Asp-N cleavage products were expressed with respect on partial/fully peptide isomerization, deamidation or deamidation, isomerization.

For example, if N4 partially deamidates/isomerizes and D5 partially isomerizes, 6 variants of Glu1-Fibrinopeptide could be observable – F, F_{iso}, $F1_D$, $F_{iso}1_D$, $F1_{D,\ iso}$, $F_{iso}1_{D,\ iso}$. Because of the Asp-N enzyme specificity, the F_{iso} and $F_{iso}1_{D,\ iso}$ variants do not undergo enzymatic cleavage. The other Glu1-Fibrinopeptide variants will be enzymatically hydrolysed to P1, P2, P3, P6, P8 and P11 peptides. pI values and masses of all peptide fragments are listed in Table 14.

Table 14: Calculated [131] monoisotopic masses and pI values for in-silico Asp-N digested Glu1-Fibrinopeptide: not-deamidated, N4, N6 deamidated/isomerized.

Peak name / Sequence	Mass [Da]	pI
P1: EGV	303.32	4.00
P2: EGVN	417.42	4.00
P3: $EGVD_{iso}$	418.40	3.67
P4: $EGVND_{iso}$	532.51	3.67
P5: $EGVD_{iso}D_{iso}$	533.49	3.49
P6: D – not visible	133.10	3.80
P7: DNEEGFFSAR	1171.19	4.14
P8: DEEGFFSAR	1057.08	4.14
P9: DD_{iso}EEGFFSAR	1172.17	3.92
P10: DD_{iso}NEEGFFSAR	1286.28	3.92
P11: $DD_{iso}D_{iso}$EEGFFSAR	1287.26	3.77

Asp-N enzyme should cleave the unstressed Glu1-Fibrinopeptide at the N-terminal side of D5 aspartate leading to the generation of two new peptides (P2 and P7). The same electrophoretic conditions as for the examination of stressed sample in Figure 8 will be applied. Due to different physicochemical properties, P2 and P7 should appear as two separated peaks in electropherogram, P7 as a weaker anion with longer migration time than P2. Presence of $F1_{D,\ iso}$ $2_{D,\ iso}$, $F1_D2_D$, $F2_{D,\ iso}$, $F2_D$, $F1_{D,\ iso}$ and $F1_D$ peaks, demonstrated in stressed sample (Figure 8), is no longer anticipated in electropherogram after Asp-N digestion. In addition to the presence of P2 and P7, some other peptide variants illustrated in Scheme 14 are expected.

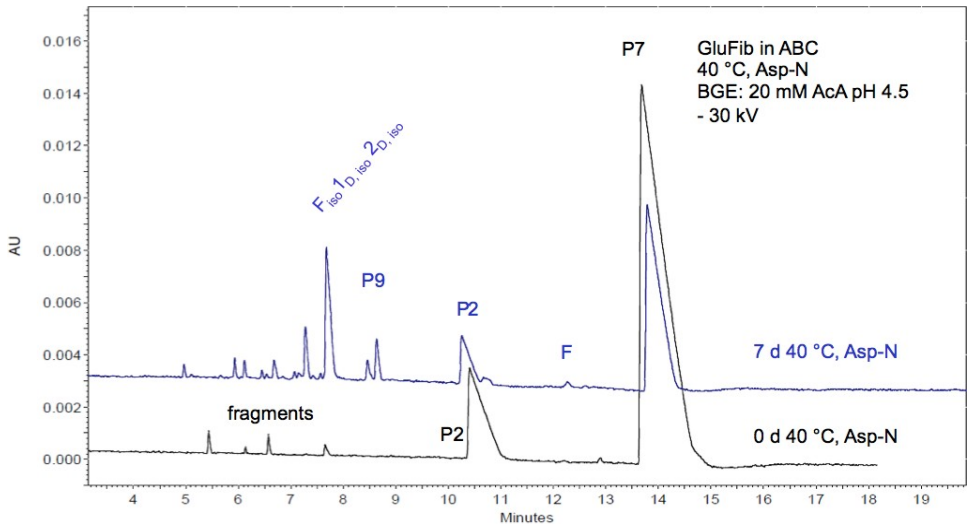

Figure 9: CZE: Full scale UV-electropherogram (214 nm wavelength) overlay for Glu1-Fibrinopeptide unstressed and stressed for 7 d at 40 °C, Asp-N digestion (1.0 mg/mL). From bottom trace to top trace: unstressed, Asp-N (black), 7 d 40 °C, Asp-N (blue). Experimental conditions: BGE: 20 mM AcA pH 4.54, 40/50 cm 50 µm fused silica capillary, dynamic coating with capillary conditioning solution, separation temperature: 25 °C, separation voltage: -30 kV, injection 0.5 psi 10 s.

An electrophoretic separation of Asp-N digested unstressed and stressed sample is illustrated in Figure 9. MS was used to identify the present electrophoretic signals and the mass spectrometric data obtained for the two Asp-N digests are listed in Table 15. Data concerning the Asp-N digest of unstressed sample show the presence of both expected digestion products P2 (11.3 min) and P7 (14.8 min). The peptide at a migration time of 8.5 min (previously determined as $F1_{D,\ iso}\ 2_{D,\ iso}$) remained undigested. Because Asp-N enzyme does not hydrolyse the isoaspartates the former peak description was stated more precisely to $F_{iso}1_{D,\ iso}\ 2_{D,\ iso}$. Some peaks ($F1_D2_D$, $F2_{D,\ iso}$, $F2_D$, $F1_{D,\ iso}$ and $F1_D$) that were present in non-digested sample (Figure 8) disappeared after Asp-N digestion and a series of new peptides became detectable. Peptide P9 (9.5 min) could be assigned to a digestion product of deamidated Glu1-Fibrinopeptide. The rest of the peptides detected at a migration time between 5.0 to 7.5 min could not be identified using MS (this was most likely caused by the current problems in this time interval). The new occurred signals were considered as P3, P4, P5 or P11 (5.0-7.5 min) peptides on the basis of their low pI values. Based on the remaining peptide F signal (13.5 min), it should be emphasized that some changes occurred in enzyme action compared to the unstressed sample. It was presumed that the cleavage sites of stressed peptide are not easily accessible for enzyme as it was seen for unstressed sample. Although the amount of the undigested F peptide was minimal, this observation should be, in the future, kept in mind.

Table 15: Comparison of theoretical m/z values [131] with observed masses in stressed and stressed Asp-N digested Glu1-Fibrinopeptide (CZE-ESI-MS).[21]

Peak name	mt [min]	Theoretical m/z	Measured m/z
$F_{iso}1_{D,\,iso}2_{D,\,iso}$	8.5	787.28	787.32
P9 *	9.5	587.08	586.74
P2	11.4	418.42^{1+}	418.18^{1+}
F *	13.5	786.29	786.30
P7	15.0	586.60	586.23

z = 2 for all signals (unless otherwise stated); * found in stressed sample only.

In order to gain a better idea of disappearing and new present signals after Asp-N digestion the electropherograms of stressed undigested and stressed digested samples were compared in Figure 10.

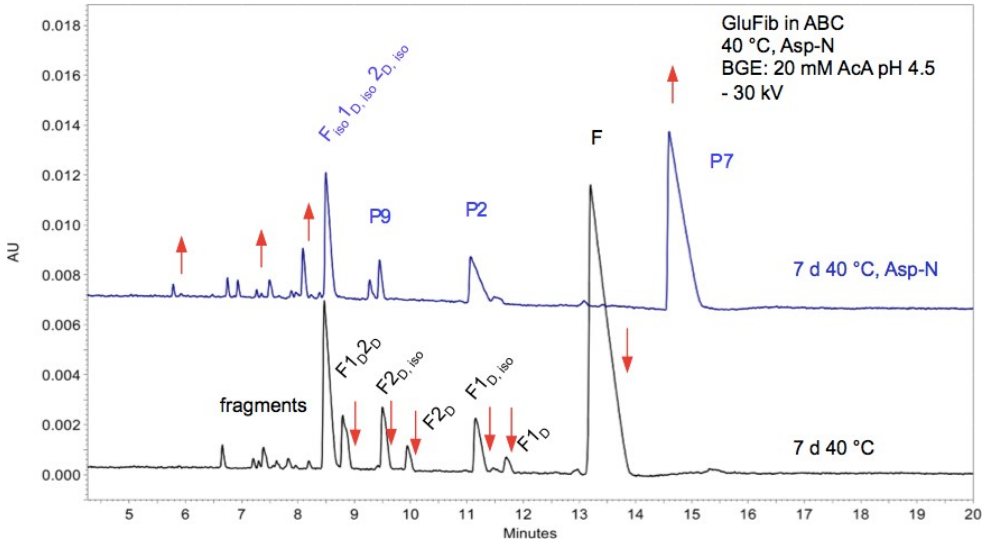

Figure 10: CZE: Full scale UV-electropherogram (214 nm wavelength) overlay for intact (2 mg/mL) and Asp-N digested (1 mg/mL) stressed Glu1-Fibrinopeptide. From bottom trace to top trace: 7 d 40 °C (black), 7 d 40 °C, Asp-N (blue). Experimental conditions: BGE: 20 mM AcA pH 4.5, 40/50 cm 50 µm fused silica capillary, dynamic coating with capillary conditioning solution, separation temperature: 25 °C, separation voltage: -30 kV, injection 0.5 psi 10 s.

The data illustrated in Figure 10 were already discussed in detail above (Figure 8 and Figure 9). By the visual comparison of these two experiments it is easier to detect all deamidated variants.

Because there were a couple of nonspecific cleaved peptides present in Glu1-Fibrinopeptide, some attempts were made to optimize the digestion procedure. The producer recommendation [135] of using Tris buffer and pH about 8.0 was followed. The cleavage of

[21] microTOF-Q typical accuracy +/- 100 ppm.

cysteine residues can be protected by alkylation and this step was carried out after sample denaturation and reduction before digestion buffer exchange. To minimize the cleavage at the N-terminus of glutamate the concentration of enzyme and incubation time should be optimized. It was observed, that the aspartyl specific cleavage is the 2000-fold faster than the glutamyl side activity of Asp-N [136]. The prevention of additional cleavage can be achieved by reducing the enzyme concentration (enzyme/substrate ratio of 1:1000, (w/w) and incubation time of 2-6 h. The fact is that the specificity and nonspecificity of the endoproteinase Asp-N is tested on two different peptides by the producer (glucagon and melittin), which do not include any glutamate in their amino acid sequences [135]. The enzyme concentrations used for the digestion procedure are relatively high (1:10 and 1:20). The incubation of Glu1-Fibrinopeptide has been done at 1:200 (enzyme/substrate ratio) and the incubation was performed at 37 °C for 3 h. Despite of the short digestion time the cleavage at the N-terminal side of glutamyl was observed.

3.1.3.4 Forced degradation of Hirudin

After the study of deamidation in short peptides the investigation strategy was further implemented on larger molecule – Hirudin. This complex polypeptide consists of 65 amino acids with three disulphide bonds between the thiol groups of six cysteine residues (C6-C14, C16-C28, C22-C39). Five asparagines are equally distributed among the whole molecule with one most probably deamidation site: N52 [130]. As observed in previous deamidation studies, the isomerization of aspartates has to be also considered.

To induce deamidation, Hirudin was exposed to a degradation buffer consisting of 170 mM disodium hydrogen phosphate, pH 8.0 and elevated temperature (40°C). The polypeptide degradation was monitored by CZE-UV of intact samples. Mass spectrometry (CZE-MS) was introduced to identify the degradation products. Afterwards, the CZE-UV (CZE-MS) analysis of Asp-N digested samples completed the investigation.

Scheme 15 illustrates the all expected signals as a result of partial deamidation of N52 asparagine. Masses and pI values of Hirudin with N52 deamidation/isomerization are listed in Table 16.

H: VVYTDCTESGQN^{12}LCLCEGSN^{20}VCGQGN^{26}KCILGSDGEKN^{37}QCVTGEGTPKPQSHN^{52}DGDFEEIPEEYLQ
H_D: VVYTDCTESGQNLCLCEGSNVCGQGNKCILGSDGEKNQCVTGEGTPKPQSHDDGDFEEIPEEYLQ
$H_{D,\ iso}$: VVYTDCTESGQNLCLCEGSNVCGQGNKCILGSDGEKNQCVTGEGTPKPQSHD_{iso}DGDFEEIPEEYLQ

Scheme 15: Expected signals after forced degradation (Asn deamidation) of undigested Hirudin. H: no deamidation, H_D: N52 position deamidated, $H_{D,\ iso}$: N52 position deamidated and isomerized.

Table 16: Calculated [131] monoisotopic masses and pI values of not-deamidated and N52 deamidated Hirudin.

Peak name / Sequence	Mass [Da]	pI
H: VVYT DCTESGQNLCLCEGSNVCGQGNKCILGS DGEKNQCVTGEGTPKPQSHN^{52}DG DFEEIPEEYLQ	6969.53	4.04
H_D: VVYT DCTESGQNLCLCEGSNVCGQGNKCILGS DGEKNQCVTGEGTPKPQSHD^{52}DG DFEEIPEEYLQ	6970.51	3.97

Using acetate of pH 2.5 as a BGE and normal polarity, the following migration order of Hirudin variants is expected: H, H_D, $H_{D,\,iso}$. As apparent from listed H and H_D pI values (Table 16) the difference between these two variants is marginal. Due to the long amino acid chain, in addition to deamidated products, also a presence of various peptide fragments can be expected after forced degradation.

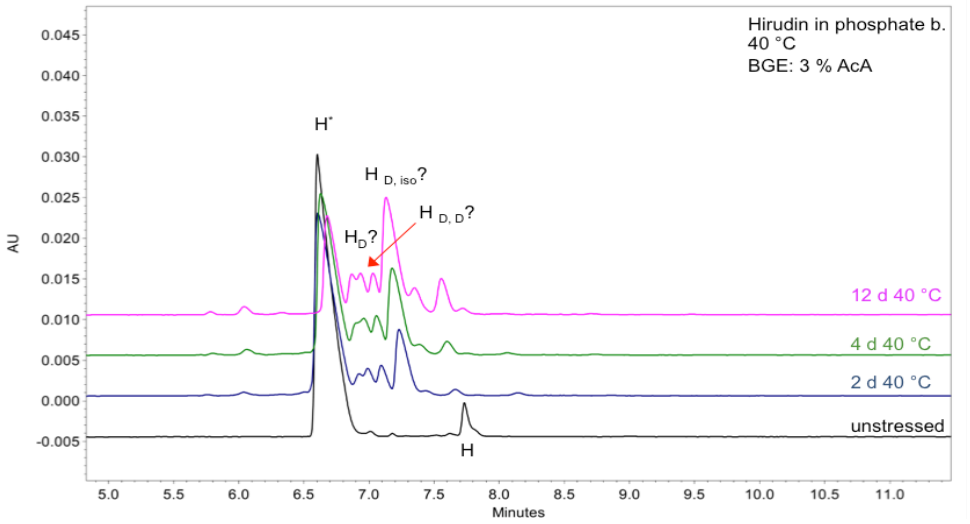

Figure 11: CZE: UV-electropherogram (214 nm wavelength) overlay for Hirudin (5 mg/mL). From bottom trace to top trace: unstressed (black), 2 d 40 °C (blue), 4 d 40 °C (green), 12 d 40 °C (pink). Experimental conditions: BGE: 3 % AcA pH 2.5, 40/50 cm 50 µm fused silica capillary, dynamic coating with capillary conditioning solution, separation temperature: 25 °C, separation voltage: 30 kV, injection 0.5 psi 10 s.

As demonstrated by electropherograms in Figure 11, the forced degradation of Hirudin resulted in the presence of some new peaks. As the H^* signal decreases the signals representing the deamidation and degradation products are concurrently increasing during the whole incubation. About 66 % of Hirudin was degraded in almost two weeks. MS was used to identify the present electrophoretic signals of unstressed and stressed sample. The mass spectrometric data obtained for unstressed and 12 days stressed samples are listed in Table 17. As apparent from results the observed molecular weights differ from the theoretical. Applying the typical instrument accuracy of 100 ppm, a maximal mass difference of 0.7 Da can be expected for protonated $[M + 1H]^+$ Hirudin sample (this would be then 0.14 Da for the charge state of $^{5+}$). Despite of low accuracy, the mass found for the signal at

6.7 min represents very likely the alkylated H^* form. A significant decrease of H^* signal was observed with some concurrently increasing signals in the acidic region during the whole incubation period. The non-alkylated form (H) was not directly identified. However, the UV signal with the migration time of 7.7 min was regarded as non-alkylated Hirudin. A couple of peaks (H_D?, $H_{D,D}$?, $H_{D,\ iso}$?) detected between 6.9 to 7.4 min (blue, green and pink trace) are supposed to be a demonstration of deamidation of one or more asparagines. Other peaks represent very likely peptide fragments.

The presence of H is explained by incomplete alkylation of free thiols by IAA due to excess amount of DTT. When IAA was added to the reaction, the remaining DTT in the sample competed with the cysteinyl thiols to react with alkylating agent. Based on previous experiments (data not shown), the use of concentrations of DTT lower than 50 mM led to an insufficient reduction of disulfide bonds.

The peptide denaturation and reduction was achieved using mild conditions to avoid further sample degradation. This decision was taken because even a short heating period over 50 °C led to the peptide degradation (new signals were present in electropherogram, data not shown). Therefore the sample was reduced using incubation temperature of 37 °C (sample was incubated for 1 h instead of the more usual 10-15 min at 60 °C).

Table 17: Comparison of theoretical m/z values [131] with observed masses in unstressed Hirudin (CZE-ESI- MS).[22]

Peak name	Rt [min]	Theoretical m/z	Measured m/z
H^*	6.7	1463.51^{5+} / 1219.75^{6+}	1462.98^{5+} / 1219.36^{6+}
H	7.7	1743.38^{4+} / 1394.91^{5+}	1741.68^{4+} / 1393.55^{5+}
$H^{*\S}$	6.7	1463.51^{5+} / 1219.75^{6+}	1463.19^{5+} / 1219.62^{6+}

* alkylated; § found in stressed sample only.

Further electrophoretic experiments with Asp-N digested samples should help to improve the introduced peak assignment. It is anticipated that unstressed Hirudin will be cleaved into five smaller peptides (P1-P5) as illustrated in Scheme 16. In addition to the aforementioned cleavage products the presence of further peptides (P6-P8) is expected after digestion of partially deamidated Hirudin.

[22] microTOF-Q typical accuracy +/- 100 ppm.

No deamidation
P1: VVYT
P2: DCTESGQN^{12}LCLCEGSN^{20}VCGQGN^{26}KCILGS
P3: DGEKN^{37}QCVTGEGTPKPQSHN^{52}
P4: DG
P5: DFEEIPEEYLQ

N52 deamidated/isomerized
P6: DGEKN^{37}QCVTGEGTPKPQSH
P7: D^{52}
P8: DGEKN^{37}QCVTGEGTPKPQSHD$^{52}_{iso}$

Scheme 16: Possible signals variants after Asp-N digest of forced deamidation of Hirudin. P1-P5: no deamidation, P6-P7: N52 position deamidated, P8: N52 position deamidated/isomerized. Presented Asp-N cleavage products were expressed with respect on no/partial/fully peptide deamidation or deamidation, isomerization.

It was assumed, that the Asp-N enzyme would not cleave the unstressed and stressed Hirudin variants as shown in Scheme 16. As reported by Šlechtová et al. [137], the missed cleavage sites in protein digestions using trypsin are frequently observed, if the cleavage sites are close to each other. Therefore it is presumed that also the sequence motifs with successive aspartates (or aspartates in the close proximity to each other) can represent a source of miscleavages. Skipping a cleavable residue D53 would lead to the formation of a new peptide P9 (P3+P4). Miscleavage of a D55 residue would create other peptide variant P10 (P4+P5). The situation can be even more complicated if N52 asparagine is deamidated. Three aspartates are now located close to each other: D52, D53 and D55 and therefore the presence of further miscleavage products is quite likely. In case of the specific enzyme cleavage, the deamidation can be proven by signal decrease of P5 and finding the P6 peptide. Signal for P7 will not be visible in UV spectrum. Using the visual comparison of both electropherograms to detect deamidation becomes almost impossible. Therefore the MS data will be required to identify the digestion products.

Corresponding masses and pI values of peptides produced by specific Asp-N cleavage are listed in Table 18, Table 19.

Table 18: Calculated [131] monoisotopic masses and pI values for in-silico Asp-N digested not-deamidated Hirudin.

Peak name / Sequence	Mass [Da]	pI
P1 1-4: VVYT	480.56	5.49
P2 5-32: DCTESGQNLCLCEGSNVCGQGNKCILGS	2833.15	4.14
P3 33-52: DGEKNQCVTGEGTPKPQSHN	2126.24	5.45
P4 53-54: DG	190.16	3.80
P5 55-65: DFEEIPEEYLQ	1411.49	3.45

Table 19: Calculated [131] monoisotopic masses and pI values for in-silico Asp-N digested N52 deamidated/isomerized Hirudin.

Sequence	Mass [Da]	pI
P6: DGEKNQCVTGEGTPKPQSH	2012.14	5.45
P7: D – not visible	133.10	3.80
P8: DGEKNQCVTGEGTPKPQSHD_{iso}	2127.23	4.75

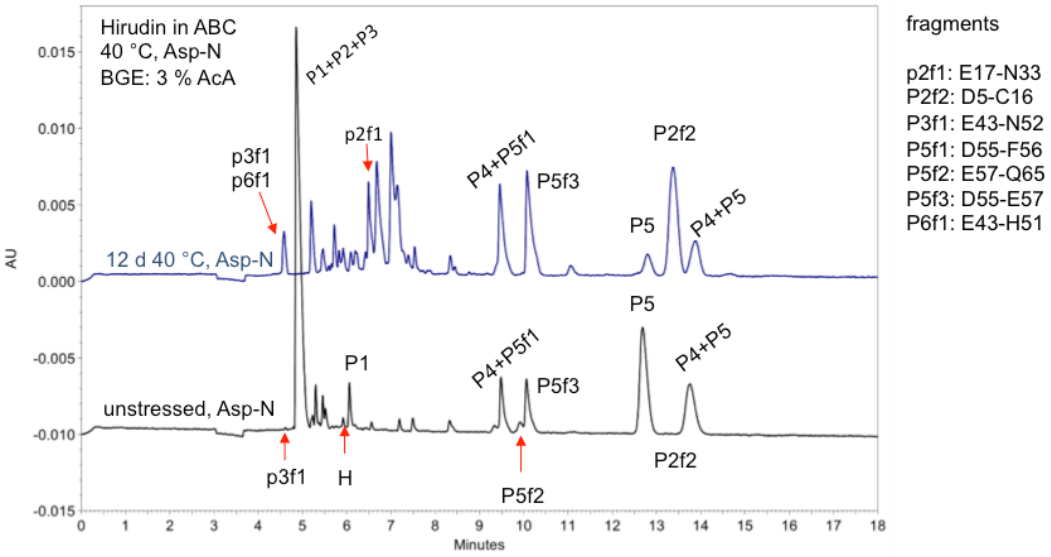

Figure 12: CZE: UV-electropherogram (214 nm wavelength) overlay for Hirudin, Asp-N digestion (1.5 mg/mL). From bottom trace to top trace: unstressed, Asp-N (black), 12 d 40 °C, Asp-N (blue). Experimental conditions: BGE: 3 % AcA pH 2.5, 40/50 cm 50 µm fused silica capillary, dynamic coating with capillary conditioning solution, separation temperature: 25 °C, separation voltage: 30 kV, injection 0.5 psi 20 s.

An electropherogram overlay of unstressed and stressed Asp-N digested Hirudin samples is shown in Figure 12. The peak identification based on the knowledge of pI peptide values was not possible. MS evaluation[23] of present signals has brought interesting findings and is summarised in Table 20. There were only two signals found in their expected form: P1 (6.1 min), and P5 (12.8 min). The other peptides were present as miscleavage products or as products of unspecific enzyme cleavage. As apparent from the amino acid sequences of newly present products, cutting the molecule at the N-terminal side of glutamyl residue created many peptides. One important observation from these experiments is that none of the identified peptides was cleaved at peptide bond N-terminal to asparagine. The focus was primarily placed on finding the P6 peptide or its fragment. The presence of the P6f1 (E43-H51) peptide fragment – EGTPKPQSH (blue trace, 4.7 min) demonstrates the deamidation of N52. Finding the e.g. P8 signal or EGTPKPQSHD_{iso} peptide fragment would confirm the

[23] CZE MS results provided K. Jooss, University Aalen.

deamidation statement based on the presence of P6f1. Unfortunately these measurements did not yield relevant results and no other signals verifying deamidation were found.

Table 20: Matching theoretical m/z values [131] with observed masses and corresponding sequences in unstressed and stressed Asp-N digested Hirudin (CZE-ESI-MS).[24]

Peak name	t_m [min]	Calculated m/z	Measured m/z	Sequence
P3f1	4.7	1095.15^{1+}	1094.49^{1+}	EGTPKPQSHN
P6f1	4.7	491.02^{2+}	490.74^{2+}	EGTPKPQSH
P1+P2+ P3*	4.9	1436.58^{4+}	1436.23^{4+}	VVYTDCTESGQNLCLCEGSNVC GQGNKCILGSDGEKNQCVTGEG TPKPQSHN
H*	6.0	1463.51^{5+}	1463.11^{5+}	VVYTDCTESGQNLCLCEGSNVC GQGNKCILGSDGEKNQCVTGEG TPKPQSHNDGDFEEIPEEYLQ
P1	6.1	481.56^{1+}	481.27^{1+}	VVYT
P2f1*	7.0	897.37^{2+}	897.41^{2+}	EGSNVCGQGNKCILGSN
P4+P5f1	9.5	452.52^{1+}	453.15^{1+}	DGDF
P5f2	10.0	1149.22^{1+}	1149.53^{1+}	EEIPEEYLQ
P5f3	10.1	409.15^{1+}	409.12^{1+}	DFE
P5	12.8	1411.48^{1+}	1411.58^{1+}	DFEEIPEEYLQ
P2f2*	13.6	1456.42^{1+}	1456.50^{1+}	DCTESGQNLCLC
P4+P5	13.8	1583.63^{1+}	1583.60^{1+}	DGDFEEIPEEYLQ

*alkylated; $^{1+}$ z = 1, $^{2+}$ z = 2 etc.

As previously described in chapter 3.1.3.3, the Asp-N digestion Glu1-Fibrinopeptide led to the presence of unspecific digested peptides. For Hirudin the enzyme/substrate ratio was also 1:200, but the incubation duration of three hours (as used for Glu1-Fibrinopeptide) was too short (undigested protein was still present). Because the Asp-N is a zinc metallo protease, the digestion of Hirudin was accomplished in the presence of zinc with various incubation times. Zinc ion should improve the catalytic ability of enzyme by directly participation in the catalytic mechanism (interacts with the substrate molecules) [138]. Presence of the undigested Hirudin was minimal after 18 hours and therefore this incubation period was adopted.

The interpretation of the data was challenging after Hirudin Asp-N digestion (too many cleavages at glutamates, miscleavages, co-migrations in CZE). Therefore the polypeptide digestion by some other enzyme was considered. Lys-C was chosen as an appropriate cleavage agent creating four peptides (P1-P4) as illustrated in Scheme 17. On account of the deamidation of N52, the presence of further P4 forms ($P4_D$ and $P4_{D,\ iso}$) was expected. The newly formed peptides produced by Lys-C digestion were separated by capillary

[24] microTOF-Q typical accuracy +/- 100 ppm.

electrophoresis using UV detection and the signals were identified by MS. The molecular masses and pI values of the digestion products are listed in Table 21.

No deamidation
P1: VVYTDCTESGQNLCLCEGSNVCGQGNK
P2: CILGSDGEK
P3: NQCVTGEGTPK
P4: PQSHN^{52}DGDFEEIPEEYLQ

N52 deamidated/isomerized
$P4_D$: PQSHD^{52}DGDFEEIPEEYLQ
$P4_{D,\ iso}$: PQSHD$^{52}_{iso}$DGDFEEIPEEYLQ

Scheme 17: Possible signals variants after forced degradation and Lys-C digest of Hirudin: no deamidation: P1-P4 signals, N52 position deamidated/isomerized: $P4_D$, $P4_{D,\ iso}$.

Table 21: Calculated [131] monoisotopic masses and pI values for in-silico Lys-C digested not-deamidated and N52 deamidated Hirudin.

Sequence	Mass [Da]	pI
P1: VVYTDCTESGQNLCLCEGSNVCGQGNK	2820.18	4.14
P2: CILGSDGEK	920.43	4.37
P3: NQCVTGEGTPK	1132.52	5.99
P4: PQSHNDGDFEEIPEEYLQ	2145.91	3.77
$P4_D$: PQSHDDGDFEEIPEEYLQ	2146.90	3.66

Considering the presence of three P4 variants, using the acetate buffer of pH 2.5 as BGE and normal polarity, this migration order is expected in electropherogram: P4, $P4_D$ and $P4_{D,\ iso}$.

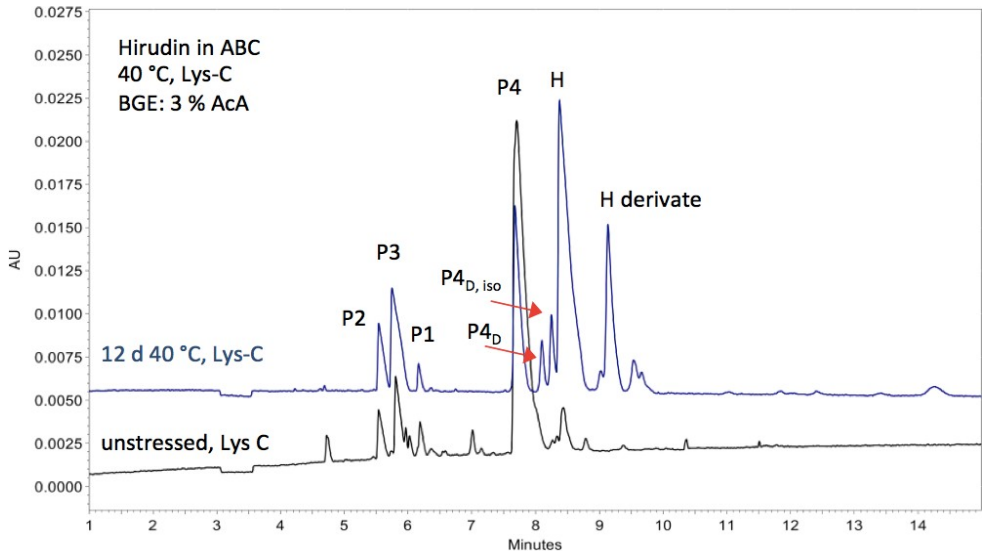

Figure 13: CZE: UV-electropherogram (214 nm wavelength) overlay for Hirudin digested by Lys-C (1.5 mg/mL). From bottom trace to top trace: unstressed, Lys-C (black), 12 d 40 °C, Lys-C (blue). Experimental conditions: BGE: 3 % AcA pH 2.5, 40/50 cm 50 µm fused silica capillary, dynamic coating with capillary conditioning solution, separation temperature: 25 °C, separation voltage: 30 kV, injection 0.5 psi 10 s.

An overlay of two CZE electropherograms of Lys-C digested unstressed and stressed sample is shown in Figure 13. The MS data evaluation[25] (summarised in Table 22) led to the identification of P2 (5.6 min), P3 (5.8 min) and P4 (7.8 min) peptides. Evidence of P1 mass was found (6.2 min) but could not be confirmed within the MS accuracy 100 ppm. Also two signals separated between 8.0 and 8.4 minutes were identified. These peaks represent the deamidated forms of P4 peptide. An accurate assignment of $P4_D$ and $P4_{D,\ iso}$ signals was done based on the known migration order of Asp and isoAsp peptide variants.

As apparent from the electropherogram of stressed Hirudin, only partial enzymatic hydrolysis of this sample was achieved, because there was still the H signal present (8.5 min). The other signal with longer migration time (9.3 min) was assigned to H derivate. The present peptide could not be identified from MS spectra. The assumption that this signal represents some H derivate was verified by a spiking experiment. The stressed sample was spiked to the digested one and the signal representing the H derivate increased significantly.

[25] CZE MS results provided K. Jooss, University Aalen.

Table 22: Comparison of theoretical m/z values [131] with observed masses in Lys-C digested Hirudin (CZE-ESI-MS).[26]

Peak name	t_m [min]	Calculated m/z	Measured m/z
P1*	6.2	1017.06^{3+}	1017.74^{3+}
P2*	5.6	978.43^{1+}	978.41^{1+}
P3*	5.8	1133.52^{1+}	1133.49^{1+}
P4	7.8	1074.60^{2+}	1074.44^{2+}
$P4_D$ §	8.0	1075.09^{2+}	1074.93^{2+}
$P4_{D,\ iso}$ §	8.4	1075.09^{1+}	1074.91^{1+}

$^{1+}$ z = 1, $^{2+}$ z = 2 etc.; * alkylated; § found in stressed sample only.

3.1.3.5 Deamidation of proteins

Deamidation of protein P

The idea of employing of the Asp-N enzyme for determination of deamidation of asparagine in proteins came couple years ago during the extensive study of therapeutic protein P within work on unspecified customer project in Solvias. PD Dr. Maria Schwarz as a leading scientist has performed this investigations with her group and at the end of this work the CZE method could be established for qualitative analysis of this protein including the determination of the deamidation factor of the sample.

Use of CZE to study deamidated intact protein P was disabled by the tendency of protein to form aggregates. The separation profile was diffuse and the deamidated variants co-migrated with various aggregation forms. Therefore the enzyme digest (e.g. Lys-C, Glu-C and trypsin) was necessary to cleave the protein into peptides which enabled the individually peptide identification and localization of deamidation site(s).

Enzyme cleavage by Asp-N introduces aspartate specificity in the digest enzymes and allows fast peak identification by visual comparison of separation patterns of unstressed and stressed sample. If some signal of unstressed sample decrease after digest and some new signals are present in stressed sample, presence of deamidation can be predicted. Deamidated variant(s) will lead after enzyme digestion to generation of new peptides, because some new cleavage sites were formed (Scheme 6, Scheme 7).).

Table 23 represents peptides after in-silico Asp-N digestion of non-deamidated protein P (because we demonstrate the study of the customer protein, only fictive protein sequence is stated. Amino acid sequence provides information about deamidation sites in corresponding peptides; therefore no mass and pI values are included in this table).

[26] microTOF-Q typical accuracy +/- 100 ppm.

Table 23: Generated peptides of in-silico Asp-N digested not-deamidated protein P.

Peak name / Sequence
P1 1-8: QAVKSWIL
P2 9-15: DSYLWEG
P3 16-36: DKILAHKMSN^{25}TYQPGN^{31}FGAKR
P4 37-49: DTYGQN^{42}YPWTHSA
P5 50-57: DSFTRENQ
P6 58-71: DTYGQN^{63}YPWETHSA
P7 72-83: DLSAYEQHTILS
P8 84-97: DTHSGEHQN^{92}HAVTR
P9 98-106: DKLAASIKL

In P1, P2, P5, P7 and P9 peptides no deamidation sites are present. But also each aspartate isomerization possibility has to be considered. If D9 would be partially isomerized, then P1 and P2 will be observable after Asp-N digestion and also some signal for P1+P2 (with mass increase of 1 Da) will be present.

Scheme 18: Expected signals after heating stress of Peptide P with possible P3 peptide modifications: no deamidation, N25 position deamidated/isomerized, N31 position deamidated/isomerized and its combinations.

Moderate deamidation of both N25 and N31 asparagines in P3 could result in all illustrated deamidation variants (Scheme 18). Considering partial isomerization, it is possible to obtain 8 different peptides (including not-deamidated variant P). Some of them would vary only in presence D/D_{iso}. The presence of isoaspartate determines if Asp-N will cleave at this site or not (see Scheme 19). Also in the presence of asparagine the enzyme would not cleave at this site, but now the isoAsp-peptide fragment is carrying the more negative charge and structurally differs from Asn-peptide (DTYQPGD_{iso}FGAKR x DTYQPGNFGAKR). Therefore it can be distinguished by means of CZE.

No deamidation — demidation, deamidation/isomerization

P3: DKILAHKMSN[25]TYQPGN[31]FGAKR

N25 deamidation/isomerization

dP3-1: DKILAHKMS

dP3-2: DTYQPGNFGAKR

P3,$1_{D,iso}$: DKILAHKMSD_{iso}TYQPGNFGAKR

N31 deamidation/isomerization

dP3-3: DKILAHKMSNTYQPG

dP3-4: DFGAKR

P3-$2_{D,iso}$: DKILAHKMSNTYQPGD_{iso}FGAKR

N25,31 deamidation/isomerization

dP3-1: DKILAHKMS

dP3-5: DTYQPG

dP3-4: DFGAKR

P3-$1_{D,\ iso}2_{D}$: DKILAHKMSD_{iso}TYQPG

P3-$1_{D}2_{D,\ iso}$: DTYQPGD_{iso}FGAKR

P3-$1_{D,\ iso}2_{D,\ iso}$: DKILAHKMSD_{iso}TYQPGD_{iso}FGAKR

Scheme 19: Possible signal variants after Asp-N digest of forced deamidated Peptide P (focused on P3 deamidation): no deamidation, N25 position deamidated/isomerized, N31 position deamidated/isomerized and its combinations.

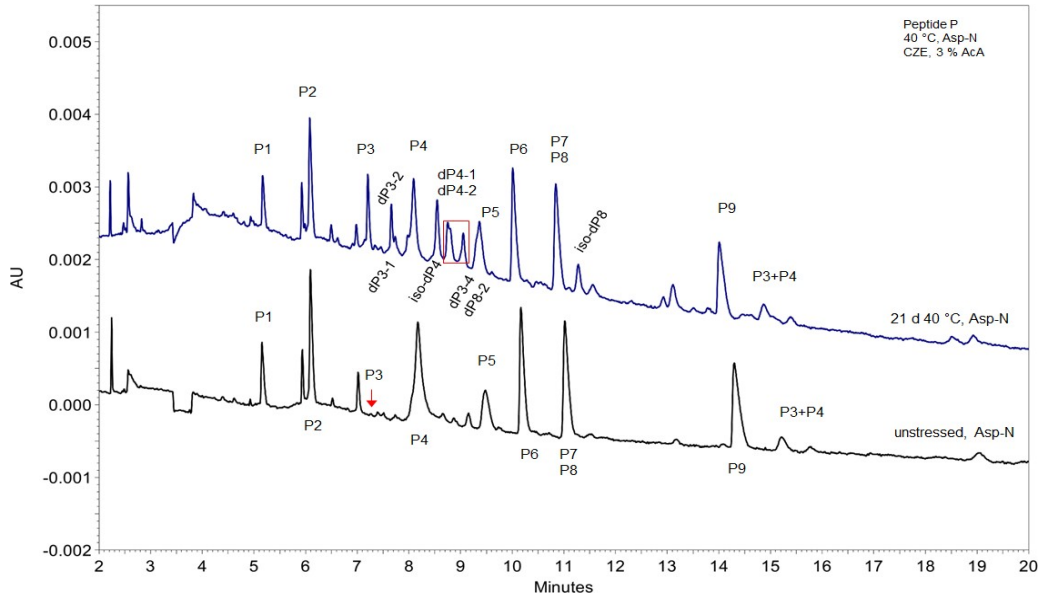

Figure 14: CZE: Full zoomed UV-electropherogram (214 nm wavelength) overlay for Protein P stressed for 21 d at 40 °C, Asp-N digestion (2.0 mg/mL). From bottom trace to top trace: unstressed, Asp-N (black), 21 d 40 °C, Asp-N (blue). Experimental conditions: BGE: 3 % AcA pH 2.5, 40/50 cm 50 µm neutral coated capillary, separation temperature: 25 °C, separation voltage: 30 kV, injection 0.5 psi 20 s.

In order to monitor the deamidation process in Protein P the sample was incubated in deamidation buffer for 3 weeks at 40 °C. The unstressed and stressed samples were than

digested with Asp-N and analysed by CZE-UV (Figure 14). Presence of a couple of decreasing/increasing or completely new signals in electropherogram indicates deamidation of not only one asparagine.

MS data evaluation of digested Peptide P led to identification of present signals and enabled also the recognition of some co-migrating signals (P7 and P8, 11 min). P3 signal is present only as a low signal in unstressed sample, but after the forced degradation, this signal is clearly visible (7.2 min). P3+P4 signal in both samples determines the partial isomerization of D37 in P4, because the Asp-N enzyme was not able to cleave at this site. It is possible, that this degradation took place during protein production. As mentioned above, the amount of increasing/new peaks signalizes the multiple deamidation and actually four deamidation sites were detected. Deamidation of P3 asparagines N25 and N31 followed by Asp-N digestion was demonstrated by identification of dP3-1, dP3-2 (blue trace, 7.5 min) and dP3-4 (blue trace, 9.5 min). dp3-4 signal co-migrates with P5, but the signal increase is obvious. P4 peptide possesses 1 possible deamidation site, which is also partially deamidated and isomerized after 3 weeks of incubation. The presence of iso-dP4 (blue trace, 8.5 min) and also the two Asp-N cleavage products dp4-1 and dp4-2 (blue trace 8.5-9.5 min) is evidence for N42 deamidation. Deamidation of N92 asparagine of P8 was confirmed by identification of iso-dP8 (blue trace, 11.5 min) and also presented dP8-2 fragment that co-migrates with P5.

Forced deamidation of other proteins

Some model proteins were chosen for further investigation of forced deamidation. This study material varied in composition; simple proteins (with shorter amino acid sequence – Aprotinin, Interferon, Lysozyme or longer amino acid chains – BSA, Hemoglobin) and antibodies (IgG1-Avastin, Erbitux), with and without presence of disulfide bridges, with diverse amino acid motifs, where the deamidation of asparagines can be expected.

In general, the portion of deamidation was too small in protein studies. By applying the Asp-N enzymatic hydrolysis on unstressed and stressed sample followed by CZE separation, there were often no noticeable differences (indicating deamidation) between both digested samples.

The forced degradation study of Hemoglobin represents the above-described situation. The CZE-UV examination of intact stressed samples did not lead to the detection of any newly formed aspartates/isoaspartates. Also further electrophoretic investigation of Asp-N digested samples did not yielded results verifying the presence of deamidated variants (data not shown). Based on our previous experience with Hirudin, the further investigations were

carried out using Lys-C digestion. The properties of Lys-C cleavage products are stated in Table 24.

Table 24: Calculated [131] monoisotopic masses and pI values for in-silico Lys-C digested not-deamidated Hemoglobin.

Peak name / Sequence	Mass [Da]	pI
Hb1: MVLSPADK	860.04	5.59
Hb2: TNVK	460.53	8.41
Hb3: AAWGK	531.61	8.80
Hb4: VGAHAGEYGAEALERMFLSFPTTK	2582.91	5.50
Hb5: TYFPHFDLSHGSAQVK	1834.02	6.61
Hb6: GHGK	397.43	8.76
Hb7: K – not visible	146.19	8.75
Hb8: VADALTNAVAHVDDMPNALSALSDLHAHK	2997.33	5.10
Hb9: LRVDPVNFK	1087.29	8.75
Hb10: LLSHCLLVTLAAHLPAEFTPAVHASLDK	2968.51	6.26
Hb11: FLASVSTVLTSK	1252.47	8.75
Hb12: YR	337.38	8.75

As apparent from Table 24, there are three peptides containing asparagine: Hb2, Hb8 and Hb9. Therefore the focus will be placed on these peptides. Based on the results of intact and Asp-N digested samples, it can be expected that the level of the asparagine deamidation will be very low or no aspartates were created during the forced degradation.

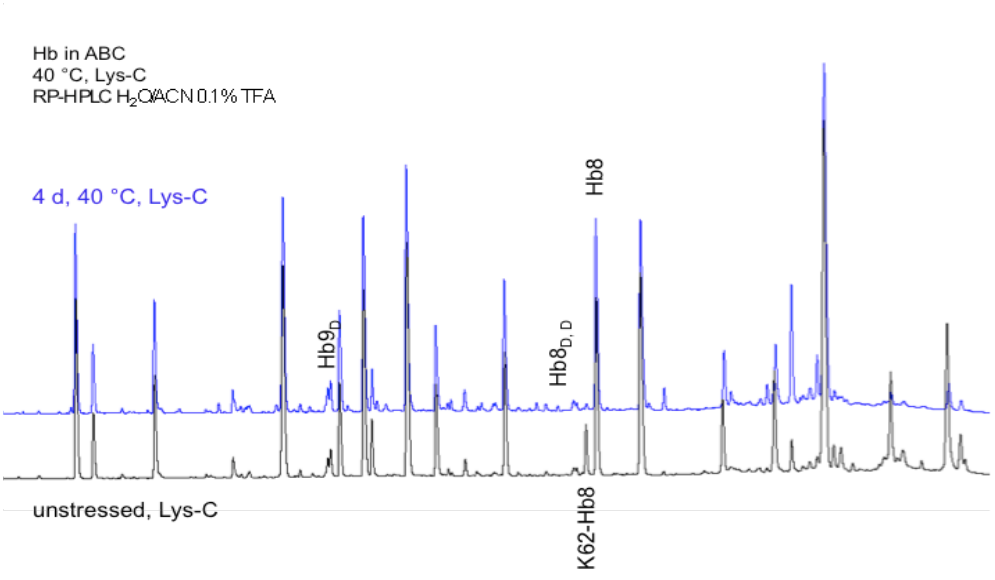

Figure 15: RP-HPLC: UV-chromatogram (214 nm wavelength) overlay for Hemoglobin, Lys-C digestion. From bottom to top: unstressed, Lys-C (black trace), 4 d 30 °C, Lys-C (blue trace). Experimental conditions: X-Bridge BEH300 C18, 3.5 µm, 2.1 x 150 mm column, H_2O/ACN with 0.1 % TFA, flow rate 0.2 mL/min, column temperature 50 °C.

Resulting from the interpretation of the chromatographic data demonstrated in Figure 15, the deamidation could not be clearly detected from a signal decrease of some asparagine peptide (in unstressed sample) or presence of new signals (in stressed sample). The employment of MS detection allowed the identification of two deamidated peptides $Hb9_D$ (N98 deamidated) and $Hb8_{D,D}$ (N69 and N79 deamidated). The signal representing the peptide K62-Hb8 was significant higher in unstressed sample than in stressed sample. The apparent signal decrease was not caused by deamidation. The presence of two successive lysines K61 and K62 led to a miscleaved peptide bond between K62 and Hb8 and production of K62-Hb8 peptide in unstressed peptide. The digestion reaction in unstressed sample differed from the situation observed for stressed sample, where only small amount of K62-Hb8 peptide was found as a result of more accurate enzyme cleavage.

Due to low level of deamidation, the deamidated variants could not be recognized by visual comparison of electropherograms/chromatograms of unstressed and stressed Hemoglobin samples (intact or digested). Therefore some attempts have been made to increase the level of the deamidation. Further prolongation of the incubation time of proteins or using of higher pH of degradation buffer led often to the protein degradation. Therefore other possibilities were considered to accelerate the aspartate deamidation.

3.1.3.6 L-Asparaginase deamidation of peptides and proteins by CZE UV

As discussed in previous chapter, the accelerated creation of deamidated samples was requested. Avoiding the long incubation process would decrease the risk of possible test sample decomposition. Targeted deamidation would offer faster results and minimize side effects (fragmentation/degradation) caused by long incubation. To achieve the objective, L-Asparaginase (L-Asp) enzyme was applied to enhance the generation of aspartate peptides. The introduced approach should help with the creation of deamidated samples in short period.

Zhang et al. [139] reported the optimal conditions (50 °C) for L-asparaginase produced in Escherichia coli. The deamidation rate of two Peptide 1 samples was studied in the presence or absence L-Asp. Samples were exposed to a degradation buffer consisting of 50 mM Tris-HCl pH 8.6 and a temperature of 50 °C.

As previously introduced in chapter 3.1.3.1, it is expected that the incubation without enzyme would lead to the presence of three Peptide 1 variants: P1, $P1_D$ and $P1_{D,\ iso}$. Using L-Asp, the creation of $P1_D$ should be favoured over $P1_{D,\ iso}$ formation, but the isomerization of $P1_D$ cannot be excluded.

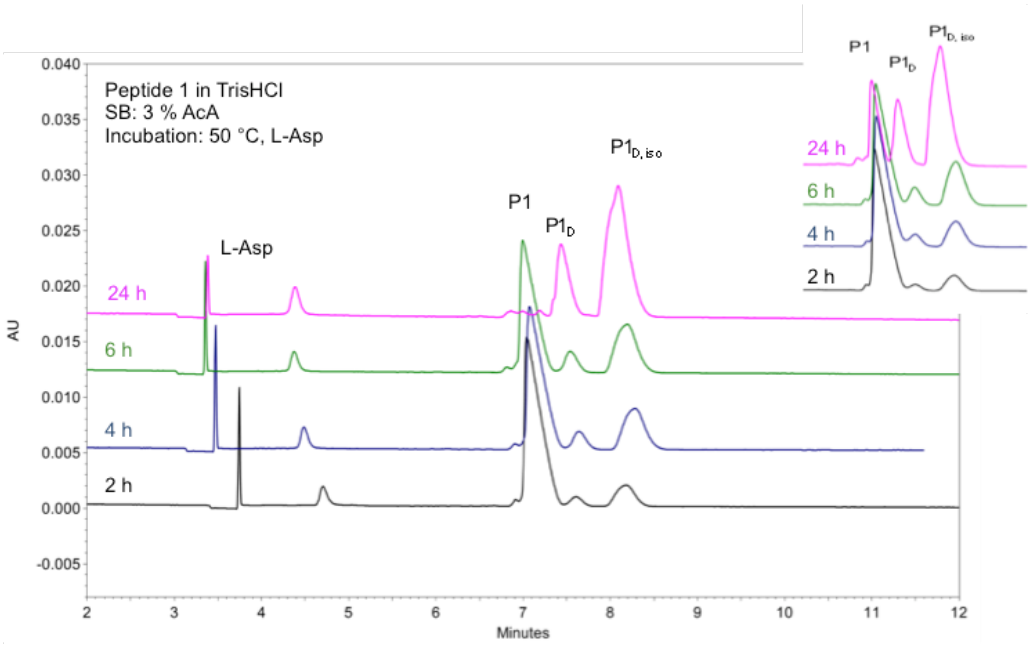

Figure 16: CZE: UV-electropherogram (214 nm wavelength) overlay for Peptide 1 (2 mg/mL) incubated with L-Asp in 50 mM Tris-HCl pH 8.6 at 50 °C. From bottom trace to top trace: 2 h (black trace), 4 h (blue trace), 6 h (green trace) and 24 h (pink trace) of incubation. Incubated Peptide 1 without L-Asp is shown in upper right corner. Experimental conditions: BGE: 3 % AcA pH 2.5, 40/50 cm 50 µm fused silica capillary, dynamic coating with capillary conditioning solution, separation temperature: 25 °C, separation voltage: 30 kV, injection 0.5 psi 10 s.

An overlay of four electropherograms illustrates the degradation of Peptide 1 in the presence of L-Asp enzyme (Figure 16). To compare the impact of L-Asp on peptide deamidation, an overlay of four electropherograms was attached showing the peptide degradation without L-Asp enzyme (upper right corner). L-Asp was visible as two separated peaks in electropherogram (between 3-5 minutes) followed by three Peptide 1 variants in the well-known migration order: P1, $P1_D$, $P1_{D,\ iso}$. The deamidation rate of P1 in the presence of L-Asp was in the first three measurements comparable to the results obtained after incubation without enzyme (Table 25). The degradation process was slightly accelerated in the presence of L-Asp. The most significant difference was noticed after 24 hours of incubation. Whilst the deamidation of the incubated Peptide 1 reached the level of about 75 %, Peptide 1 was almost completely converted to $P1_D$ and $P1_{D,\ iso}$ in the presence of L-Asp.

Table 25: Corrected area percentages of P1, $P1_D$, $P1_{D,iso}$; Peptide 1 incubated without / with L-Asp at 50 °C for 2, 4, 6 and 24 h.

50 mM Tris-HCl pH 8.6, 50 °C				
Incubation period	A_{corr} % P1 no L-Asp / L-Asp	A_{corr} % $P1_D$ no L-Asp / L-Asp	A_{corr} % $P1_{D, iso}$ no L-Asp / L-Asp	$P1_{D, iso}$ / $P1_D$ no L-Asp / L-Asp
2 h	88.6 / 86.3	2.6 / 3.3	8.8 / 10.5	3.4 / 3.2
4 h	79.2 / 70.9	5.7 / 6.7	15.1 / 22.4	2.7 / 3.3
6 h	66.8 / 60.7	7.1 / 8.9	26.0 / 30.4	3.7 / 3.4
24 h	22.4 / 0.7	20.0 / 25.8	57.6 / 73.5	2.9 / 2.8

Results are reported as the means of triplicate determinations.

As apparent from the $P1_{D, iso}$ / $P1_D$ results, the creation of $P1_D$ was not favoured over $P1_{D, iso}$ formation. The approximate isoAsp:Asp ratio of 3:1 was comparable to the results obtained after incubation using the elevated temperature only. In the study on Peptide 1 the temperature optimum was found between 50 and 60 °C (data not shown).

Because the deamidation rate in Peptide 1 was accelerated in the presence of L-Asp enzyme, the deamidation experiments succeeded also with proteins, which were not able to deamidate previously without L-Asp, like Aprotinin, BSA, Interferon and Lysozyme.

As an example, the deamidation study of Lysozyme is shown. In this experiment the studied material was subjected to incubation with and without L-Asp. The results are demonstrated in Figure 47 (chapter 7). As compared to the unstressed sample (black trace), no signals of deamidated variants could be detected. Even the higher concentration of enzyme, prolonged incubation time or enzyme immobilization (over 24 h) did not lead to expected result. The explanation for this fact could be the steric hindrance of the adjacent amino acids and the protein conformation[27].

3.1.4 Conclusion

The CZE separation of asparagine, aspartate and isoaspartate variants was achieved using 3 % AcA pH 2.5 as a background electrolyte and applied dynamic coating for fused silica capillary. The utilization of Asp-N enzyme for the hydrolysis of newly formed aspartate(s) was demonstrated on deamidated samples. The Asp-N enzyme digestion in the combination with CZE/HPLC-UV technique is a very attractive tool for the determination of

[27] Supposing that the L-Asp cannot access the asparagines in the intact proteins, the structure of lysozyme was unfolded by denaturation and cleaved by Lys-C. The newly created peptide fragments are thought to be accessible for the L-Asp enzyme. Comparison of two electropherograms (Figure 48 in chapter 7) demonstrates clearly the presence of some new signals in L-Asp digested sample. It is possible that some of them represent deamidated variants. Unfortunately the reproducibility of these results was not achieved in following experiments, but this idea could be followed in the future.

present aspartates in small peptides as demonstrated on Peptide 1 and Glu1-Fibrinopeptide. Increasing number of aspartates in polypeptides and proteins lead to the presence of many signals after the molecule hydrolysis by Asp-N and electrophoretic/chromatographic separation. The risk of co-migration/co-elution is higher; new signals (from deamidated asparagines) can stay hidden behind the signals of other peptide fragments. If the portion of deamidated asparagine(s) is too small, the signal decrease of the former peptide/protein will not be clearly visible and the presence of new signals of deamidated and deamidated/isomerized sample variants might not exceed the noise level. An application of Asp-N enzyme to such deamidated sample will produce even smaller signals from deamidated asparagine variants. Therefore the Asp-N in the combination with UV detection is well suited for samples in which the deamidation reached the particular degree. The investigation of Asp-N hydrolysed Glu1-Fibrinopeptide and Hirudin (analysed by HPLC and CZE) confirmed the published enhanced specificity of the Asp-N enzyme, namely the ability to cleave also at the N-terminus of glutamyl residues. The production of unspecific cleaved peptide fragments and also the miscleavages (as there are three potential cleavage sites in the close proximity) increased the amount of peaks present in Hirudin. This situation made the visual comparison of the electrophoretic signals more difficult. The optimization of the Asp-N digestion conditions did not lead to any significant improvement of the enzyme specificity. Finally, an application of Lys-C enzyme to Hirudin followed by CZE analysis of produced peptide fragments allowed the separation of deamidated variants from their non-deamidated counterpart. The Asn, Asp and isoAsp variants were clearly visible in electropherogram.

It is apparent that buffer type and its concentration have an effect on deamidation rate of peptides as many researchers reported it. In addition to the aforesaid property the buffer concentration has an influence on hydrolysis of succinimide during the deamidation process. Diverse deamidation buffers also affected the hydrolysis of succinimide and led to various isoAsp/Asp ratios despite of the same pH and concentration. If we consider the complex structure of proteins (secondary, tertiary, quaternary) and the influence of buffer on the opening of this protective mechanism, then it is difficult to predict, how the deamidation behaviour will develop.

The CZE separation of multiple deamidated variants was achieved using the acetate buffer (20 mM, pH 4.5) with pH value above the pI values of deamidated species and by applying a negative polarity. An increase of the buffer concentration to 50 mM provided better current stability during the CZE-ESI-MS run but this improvement still did not allow the identification of all present signals.

According to the ICH guidelines on impurities in new drug product, the classification of organic impurities (process- and drug related-) below the 0.1 % level is considered as not necessary [140]. In peptides where only few signals are present, even a small portion of the deamidated asparagine can be apparent in the UV-electropherogram/chromatogram. In larger molecules multiple deamidation can be expected. Such partially deamidated asparagines are subjected to the Asp-N hydrolysis together with all present aspartates of the protein. This digestion procedure leads to the creation of a mixture of cleaved signals – some have their origin in normal aspartates and some originate from the deamidated asparagines. The more aspartates, the more created peptide fragments and very likely the lower signals in electropherograms/chromatograms. As a consequence it is very likely that these new signals do not achieve limit of detection and will not be recognized using UV detection.

We saw that many proteins were frequently completely degraded before the deamidation of asparagine reached some detectable level. Use of L-Asparaginase for the faster creation of deamidated samples was examined. The deamidation rate was accelerated in the presence of L-Asparaginase enzyme in Peptide 1. This method could not be successfully transferred to the proteins. The explanation for it is that the steric hindrance of present amino acids does not allow the enzyme's nucleophile to attack the C-atom of amide leading to the release of ammonia.

3.2 Evaluation of a CZE method for the analysis of charge variants in antibodies alternative and complementary to cIEF

Monoclonal antibodies are large proteins, whose molecular structure is very heterogeneous as a result of multiple posttranslational modifications and degradation events. Such variants differ in charge and can be commonly designated as acidic or basic compared with the main species. Chromatography methods (ion-exchange chromatography – IEX) or (capillary) isoelectric focusing (IEF, cIEF) are generally employed for the study of charge-related heterogeneity of biopharmaceuticals. Since He et al. [141] have made known the CZE method, which allows the separation of mAb isoforms in coated fused silica capillary; the method variety applicable for the analysis of charge variants has increased. The benefits of using such an analytical method for isoform separation as e.g. low cost material (no coated capillaries, no ampholytes or special HPLC columns needed) attract scientists from all over the world and many studies have been introduced employing CZE instead of IEX or IEF (15, 141, 142, 143).

The aim of this study is to evaluate and validate the CZE method applicable for the analysis of charge variants in antibodies complementary to cIEF. The analytical method published by He et al. [141] was optimised and applied to study the isoforms of two monoclonal antibodies: Avastin and Erbitux.

The charge variants and their alterations (such as deamidation) upon e.g. storage cannot always be monitored in intact molecules due a co-migration with main signals; therefore the samples of interest are frequently enzymatically hydrolysed. Instead of commonly used peptide mappings where enzymes such as trypsin, Lys-C, Glu-C etc. are generally applied, the selective cleavages of monoclonal antibodies into Fab and Fc portions using papain or pepsin can be accomplished. The study of papain and pepsin digested Avastin and Erbitux samples, followed by the CZE analysis will be introduced and discussed.

In this chapter also a novel utilization of the optimised CZE method of He et al. [141] will be presented as suitable for the investigation of de-glycosylated antibody portions as an alternative to gel capillary electrophoresis.

3.2.1 Introduction

Charge heterogeneity analysis of proteins is a necessary step in characterization of biopharmaceuticals. It provides important information about product quality (different types of charge variants include antibody fragmentation, deamidation, formation of N-terminal pyroglutamate, glycation at lysine residues, sialylation etc.) [144]. These changes could

affect e.g. the biological activity of the drug, the affinity of monoclonal antibodies towards antigens or their shelf life [145].

Despite thorough understanding of the degradation pathways that could be present during production by cell cultures, such as purification, formulation and storage of the biologics; the biopharmaceutical industry is obliged to characterize the microheterogeneities of drugs exhaustively in order to demonstrate batch-to-batch consistency. In the case of monoclonal antibodies, these microheterogeneities may have effect on clearance, efficacy, immunogenicity and potency [139].

Monoclonal antibodies (mAbs) were discovered by Köhler and Milstein in 1975 [146]. This breakthrough raised great expectations of many scientists in various research fields (biochemistry, cell structure, immunology and cell genetics [147]. After overcoming the technical difficulties of the monoclonal antibody production these molecules with high specificity for antigens found their place in medical and industrial use.

The market for mAbs continues to grow steadily. Pharmacological therapeutics are able to precisely identify the key targets and found application in cancer therapy and treatment of autoimmune and inflammatory diseases [7, 148]. The most currently marketed mAb is the IgG class antibody. The molecular weight is approximately 150 kDa, composed of two identical light chains (2x 25 kDa) and two identical heavy chains (2x 50 kDa) in the Y shape motif (see Scheme 20). The composition can also be described as two antigen-binding fragments (Fab, 55 kDa) and one crystallisable fragment (Fc, 35 kDa) [139, 149]. The antigen specificity is defined by the complementary determining regions (CDRs), which are located in the variable fragment portion (Fv) of the Fab. The hinge region is an amino acid area situated in the central part of the heavy chains linking these two chains by disulphide bridges. It confers the mobility of two Fabs and enables the bivalent antigen binding and activation of Fc.

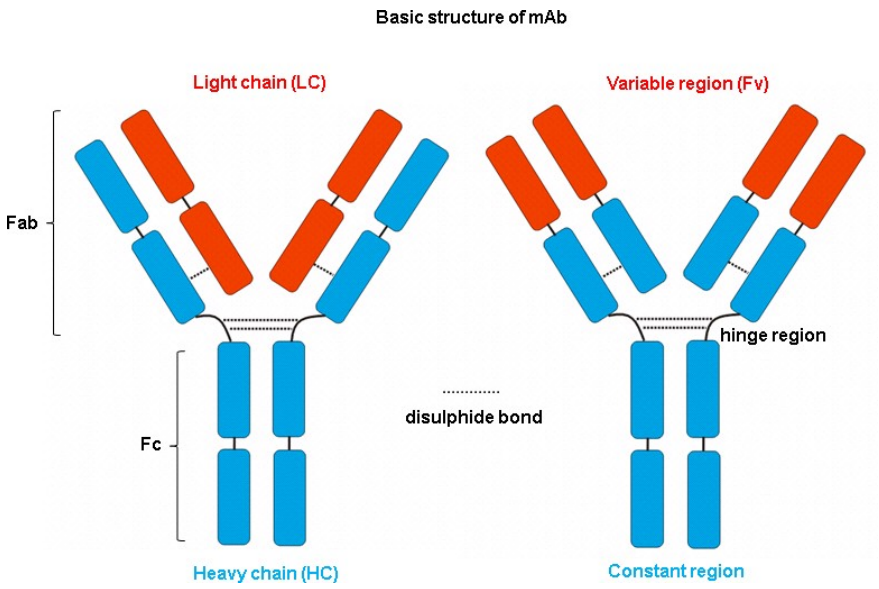

Scheme 20: Schematic representation of monoclonal antibody structure.

Most of the heterogeneity generates alterations in the surface charge of the molecule [13]. An overview of the sources of charge-related heterogeneity in monoclonal antibodies [150] is presented in Table 26.

Table 26: Sources of charge heterogeneities in mAbs.

Degradation pathways	**charge variants**	**source of pI shift**
Cyclization of Glu	acidic	loss of primary amine
Deamidation	acidic	gain of carboxylic group
Glycation	acidic	loss of basicity of Lys-ε-amino group
Fragments	acidic/basic	-
Sialylation	acidic	gain of carboxylic group
C-terminal Lys cleavage	acidic	loss of Lys-ε-amino group
Amidation	basic	replacing the -OH group by -NH_2
Desialylation	basic	loss of carboxylic group
Incomplete removal of C-terminal Lys	basic	presence of Lys-ε-amino amino group

Classification of these alterations can be done according to the properties they possess. These variants can be organized into 2 categories: acidic and basic species. For example deamidation, C-terminal Lys cleavage or glycation result in an increase in the net negative charge. This could be observed as a decrease of pI value and formation of acidic species. On the other hand desialylation or amidation cause an additional positive charge or remove negative charges leading to an increase of pI value and formation of basic species. Several studies have shown that also e.g. cysteinylation, presence of trisulfide bonds (formation of acidic species), oxidation of methionine or isomerization of Asp (formation of basic species)

can also contribute to the alteration of the charge distribution [151, 152]. The explanation for this phenomenon refers to the conformational differences that affect the surface charge properties.

Analytical methods for charge heterogeneity need to detect small changes reproducibly. Charge-related heterogeneity characterization requires high throughput analytical methods like ion-exchange chromatography - IEX (anion exchange chromatography – AEX, cation exchange chromatography – CEX) or isoelectric focusing (IEF, or its capillary form capillary isoelectric focusing – cIEF).

Given both the large size and the structural complexity of an intact mAb may hinder the efficient analytical work. An overlapping of charge variant signals with main peak signal in intact mAbs lead often to the fact that a lot of important information stays hidden. The main point of the interest – deamidation of asparagine (studied in 3.1) is one of the protein modifications, which can be determined, inter alia, by charge-based analytical techniques. As described in chapter 3.1 the determination of deamidation in biologics requires financial investment and time, not solely because many HPLC runs are often mandatory before adequate separation is achieved. Although use of analytical techniques as RP-HPLC/CZE with MS and MS/MS data analysis is crucial for the characterization of biotherapeutics, at the same time, operating a mass spectrometer requires specialised operators and is also expensive to run. It might be helpful, if there would be an objective indication that demonstrates some molecule alterations, before beginning the mass spectrometry analytical works. At present, the optimised CZE method can be used for the examination of the charge variant profiles. Because the charge variants and their alterations (such as deamidation) upon e.g. storage cannot always be monitored in intact monoclonal antibodies due a co-migration with main signals, generally it is useful to study the molecule fragmented into peptides (to perform peptide mappings). A variety of specific enzymes can be employed for this purpose (e.g. Arg-C, Glu-C, Lys-C, trypsin etc.) [153]. The aforesaid enzyme types require frequently certain procedures, that have to be done prior to digestion, such as denaturation, sample reducing, alkylation, multiple changing of buffer etc. and especially an enzyme purchase (such enzymes with high specificity are expensive; in case of less expensive trypsin, the cleavage is often performed in the presence of Lys-C to achieve the improved digestion). Some inexpensive enzymes exist that are able to reduce the protein (mAb) complexity: papain and pepsin. Both of these enzymes are routinely employed for the production of antibody fragments, because such enhanced molecules allow a targeted programming of therapeutics [154].

This chapter focuses on fast, inexpensive and straightforward analytical methods, which can be employed for the study of isoform distribution. Isoelectric focusing (IEF) as a charge-

sensitive method provides the information about charge heterogeneities. It is important to notice that IEF is an irreplaceable method for pI value determination in routine quality control [155]. Capillary isoelectric focusing (cIEF) found its place in the protein analytics because of the automation, high resolution and fast run times [156]. If the knowledge of the pI value is not obligatory and only the separation profile of charge variants is requested then it is not mandatory to use all the quite expensive cIEF equipment (coated FC-cartridges, transfer lines) and chemicals (ampholytes). The routine experiences from the past have shown in the Solvias lab that independence from such special products (like ampholytes) can save a lot of time and money. Occasionally the production of ampholytes can be discontinued, products replaced by another (similar) one and consequently, the routine analysis of a sample of interest might lead to different isoelectric patterns using the new product. Capillary zone electrophoresis (CZE) with ε-aminocaproic acid as the background electrolyte is able to meet all named requirements at the beginning of this paragraph. It was proved that this analytical tool could be used if the isoelectric profile of whole mAbs is required [141]. In this work papain and pepsin are used to reduce the complexity of monoclonal antibodies Avastin and Erbitux.

Avastin is a recombinant humanized monoclonal IgG1 antibody. This glycoprotein is composed of two equal light chains (214 AA) and two heavy chains (453 AA) [157]. Heterogeneity of heavy chains is caused by the presence of C-terminal lysine residues and also N-linked glycosylation at N303. The amino acid sequences of light and heavy chains of Avastin received from [158] is presented in Table 42 (chapter 7) and served for calculation of pI values (whole mAb or Fab and Fc fragments).

Erbitux is a chimeric mouse-human monoclonal IgG1 antibody. This glycoprotein consists of two light chains (213 AA) and two heavy chains (452 AA) [159]. The amino acid sequence of cetuximab has two different glycosylation sites at Asn88 and Asn299 of the heavy chain. The heavy chains demonstrate also C-terminal lysine heterogeneity [160]. Properties of light and heavy chain are described in Table 43 (chapter 7).

As introduced above the structure of IgG class antibody can be described by two different ways. Composition can be seen as presence of two heavy (HC) and two light chains (LC) or two antigen binding fragments (Fab) and one crystallisable fragment (Fc) [139, 149] as illustrated in Scheme 21.

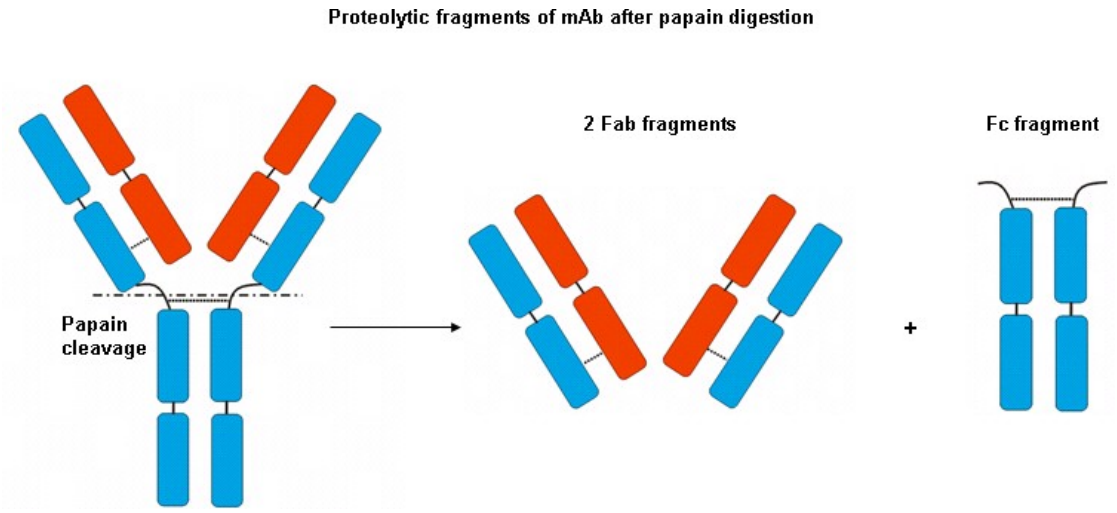

Scheme 21: Papain cleavage scheme of monoclonal antibody.

The application of Fab fragments found its place in the medical praxis, because these molecules are smaller in size than whole IgGs (provide better penetration into tissues) and show lower immunogenicity in many diagnostic applications [161]. Fab and Fc fragments are generally produced by enzymatic digestion of IgGs using papain [162, 163]. For therapeutic uses, Fabs can be purified from the digestion mixture by various analytical techniques (e.g. affinity chromatography, gel filtration chromatography, ion exchange or their combination [164].

Papain as a thiol protease cleaves the monoclonal antibody at the heavy chain hinge region. Amino acid sequences of upper, core and lower hinge of humanized IgG1 are well known [165]. The upper hinge amino acid sequence (EPKSCDKTHT) will be cleaved behind the histidine and in front of disulfide bonds [166]. The hydrolysis leads to the creation of two equal Fab fragments (two heavy chains are present) and one Fc fragment and will be demonstrated on amino sequence of Avastin in Scheme 24 (page 96).

Treatment with papain can also yield to partial cleaving of monoclonal antibody [167]. Brown et al. [168] observed predominant production of $F(ab)_2$ portion in IgG antibody, if the cysteine was absent in digestion procedure, and explained this fact by impossibility to reduce the hinge region disulphide.

Many researchers use an Immunopure Fab preparation Kit from Pierce to produce the Fab fragments. We developed a cheap fast method to obtain Fab and Fc fragments using papain digestion. Using this method the handling is relatively straightforward (e.g. no replacement of formulation buffer is required) and the duration of the entire digestion procedure is relatively short.

Pepsin can be used for a more thorough investigation of charge variants in monoclonal antibodies. Analogous to Fab fragments the $F(ab)_2$ also found utilization in medicine. Because murine monoclonal antibody therapy can lead to the formation of an unwanted immune response in patients when applied in vivo [161], using of immunoglobulin fragments ($F(ab)_2$) can be advantageous for immunotherapeutic application. Application of $F(ab)_2$ fragments to patients minimizes the risks of immunogenic properties of IgGs, because these are predominantly located on the Fc part of the molecule [169] and Fc subfragments are removed after digestion. Smaller size of $F(ab)_2$ molecules enables better penetration into tissue and provide less steric hindrance [170].

Acidic endopeptidase pepsin cleaves monoclonal antibodies in the hinge region generating the $F(ab')_2$ an Fc subfragments [170] as illustrated in Scheme 22.

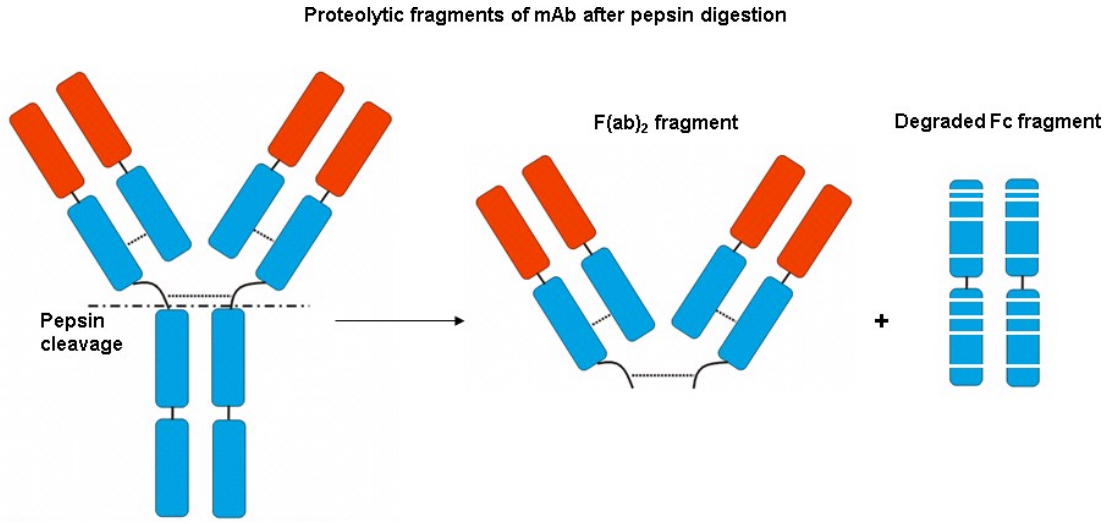

Scheme 22: Pepsin cleavage scheme of monoclonal antibody.

It is known, that pepsin is active only at acid pH being irreversibly denatured at neutral or alkaline pH [171]. Pepsin cleaves preferentially C-terminal hydrophobic, aromatic residues like phenylalanine and leucine. To look closely into the digestion process pepsin cuts the monoclonal antibody at the heavy chain lower hinge region. The lower hinge amino acid sequence (APELLGGP) will be cleaved behind the disulfide bonds between two leucines as illustrated in Scheme 25 on amino sequence of Avastin leading to creation of one $F(ab)_2$ fragment and one (segmented) Fc fragment.

Further utilization of EACA running buffer

Carboxypeptidase B digestion

C-terminal lysines are commonly present on the heavy chain of monoclonal antibodies. Their impact on bioactivity is not well understood until now, but the degree of heterogeneity

of C-terminal lysine variants indicates the manufacturing consistency [172]. Heterogeneity of C-terminal lysine residues is believed to result from varying degree of proteolysis by endogenous carboxypeptidase(s) during cell culture production [173].

Carboxypeptidase B is a metallocarboxypeptidase (Zn) that catalyses the hydrolysis of the basic amino acids as lysine, arginine and ornithine from the C-terminal position of polypeptides [174] as illustrated in Scheme 23.

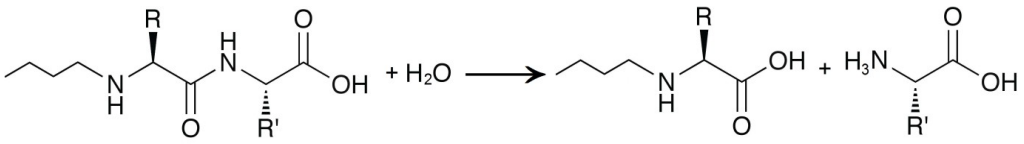

R = organic substituent
R' = K, R and ornithin

Scheme 23: Carboxypeptidase B cleavage scheme of polypeptide.

3.2.2 Materials and Methods

Materials

Test samples used in this study were purchased from Roche (Avastin) and from Merck (Erbitux). Papain and pepsin were obtained from Sigma, PNGase from NEB, and Carboxypeptidase B from Worthington. Acetic acid, ε-aminocaproic acid (EACA), ammonium bicarbonate, disodium hydrogen phosphate, dithiothreitol (DTT), ethylenediaminetetraacetic acid (EDTA), hydroxypropyl methylcellulose (HPMC), iodoacetamide (IAA), L-cysteine, phosphoric acid (H_3PO_4) were purchased from Sigma. Acetonitrile (ACN), ammonium hydroxide, hydrochloric acid (HCl), sodium hydroxide (NaOH), trifluoroacetic acid (TFA), tris(hydroxymethyl)aminomethane (Tris-HCl) were purchased from Fluka. Conditioning solution, SDS-MW gel buffer, SDS sample buffer and internal standard (10 kDa) were purchased from AB Sciex, RapiGest from Waters, Pharmalyte 3-10, 5-8.5 from GE, 1 % methylcellulose (MC) and pI markers (4.65, 10.10) from ProteinSimple.

Fused silica capillary was obtained from CM scientific, neutral coated capillary from AB Sciex, FC-coated cIEF cartridges from ProteinSimple, 3 and 10 kDa filters from Millipore, air displacement pipettes, thermomixer and centrifuge from Eppendorf.

Methods

Papain digestion. Papain enzyme was added to the protein at a ratio 1:10 (w/w) for Avastin and 1:20 for Erbitux and the digestion was performed in presence of 25 mM final concentration L-Cys. The protein/enzyme mixture was then diluted to a final concentration of 2.5 mg/mL with the milli-Q water and incubated at 37 °C for 5 h.

Pepsin digestion. Samples were transferred into 0.2 M sodium acetate buffer pH of 4.0 using 10 kDa filters and centrifugation. Pepsin enzyme was added to the protein at a ratio 1:20 (w/w) in presence of 0.1 % final concentration of RapiGest (w/v). The protein/enzyme mixture was then diluted to a final concentration of 2.5 mg/mL with 0.2 M sodium acetate buffer and incubated at 37 °C for 18 h.

Carboxypeptidase B digestion. Erbitux (60 µg) was mixed with 5 µg of carboxypeptidase B and incubated at 37 °C for 3.5 h in formulation buffer.

Papain, PNGase digestion. 1.5 µg of PNGase were added to Papain digested Erbitux (preparation see above) and the mixture was incubated at 37 °C for 1 h.

Electrophoretic conditions. CZE was carried out on the PA800 Beckman Coulter (AB Sciex) instrument with temperature controlled autosampler using fused silica capillary (50 cm of length, 50 µm id) with normal polarity. The cathode was at the detector end of the capillary for the analyses with lower pH. The capillary was flushed (by HCl, NaOH and milli-Q water) from appropriate buffer reservoirs using pressure (50 psi) prior to each run. The capillary was filled with running buffer (600 mM EACA, 0.1 % HPMC, pH 6.0, unless otherwise stated) using pressure (50 psi). The sample was injected using pressure (0.5 psi) for 10 s, the constant voltage of 30 kV was applied and the operation temperature of 25 °C was kept. Electropherograms were UV-monitored at 214 nm and the data were processed with 32 Karat.

cIEF conditions. The cIEF runs were carried out using a Convergent Bioscience iCE280 Analyzer (Protein Simple) with temperature controlled Prince autosampler on fluorocarbon-coated fused silica capillary. Electropherograms were UV-monitored at 280 nm in whole column. The anolyte consists of 80 mM phosphoric acid in 0.1 % methylcellulose and the anolyte is 100 mM sodium hydroxide in 0.1 % methylcellulose.

A working ampholyte solution (AS) was prepared by mixing 2000 µl 0.35 % methylcellulose, 60 µl broad- and 10 µl narrow-range Pharmalytes 3-10 and 8-10.6 respectively and pI markers 4.65 and 10.10 at 5 µl each. The sample/ampholyte mixture was prepared by mixing 100 µl AS with 10 µl test solution and the mix was carefully transferred into glass insert vials avoiding bubbles.

All test samples were prefocused for 1.5 min using a voltage of 1500 V and focused for a variable periods of time (generally for 6-8 min, depending on analyte) using a voltage of 3000 V.

Chromatographic conditions. Reversed phase chromatography was carried out using an Agilent 1200 binary pump system with temperature controlled autosampler and vacuum degasser. The analytes were introduced onto Vydac C4 column from Grace and the flow rate was maintained at 1 mL/min. The column was equilibrated with mobile phase A (0.1 % TFA in H_2O). Mobile phase A and mobile phase B (0.1 % TFA in ACN) were used to establish the 50 min gradient as shown in Table 27.

The UV chromatograms were obtained by monitoring absorbance at 214 nm and the data were processed with Chromeleon software (Dionex).

Table 27: Gradient.

time [min]	mobile phase B [%]
0	5
5	20
30	45
45	90
50	5

3.2.3 Results and Discussion

Optimization of CZE background electrolyte providing the information about isoform pattern

Initially, the highly resolved reproducible isoelectric profiles (cIEF) of two monoclonal antibodies (Avastin and Erbitux) were obtained. Secondly, the CZE separation method based on [141] was adapted to achieve the electrophoretic (CZE) profiles analogous to the cIEF. During the examination the following parameters were optimized: (a) pH value of the ε-aminocaproic acid (EACA) running buffer; (b) concentration of EACA and ionic strength; (c) concentration of hydroxypropyl methylcellulose (HPMC); (d) capillary length, separation temperature and field strength; (e) sampling rate and (f) flushing and equilibration conditions.

It is expected that in addition to the main variant also some acidic and basic variants will be visible in the isoelectric profile of Avastin due to N-linked glycosylation and C-terminal heterogeneity (lysines). Based on the amino acid sequence of Avastin [158], the pI value was calculated using Expasy software [131]. As stated in Table 42, the calculated value of 8.1 differs from value that was experimentally determined to 8.3 by Kaja et al. [175]).

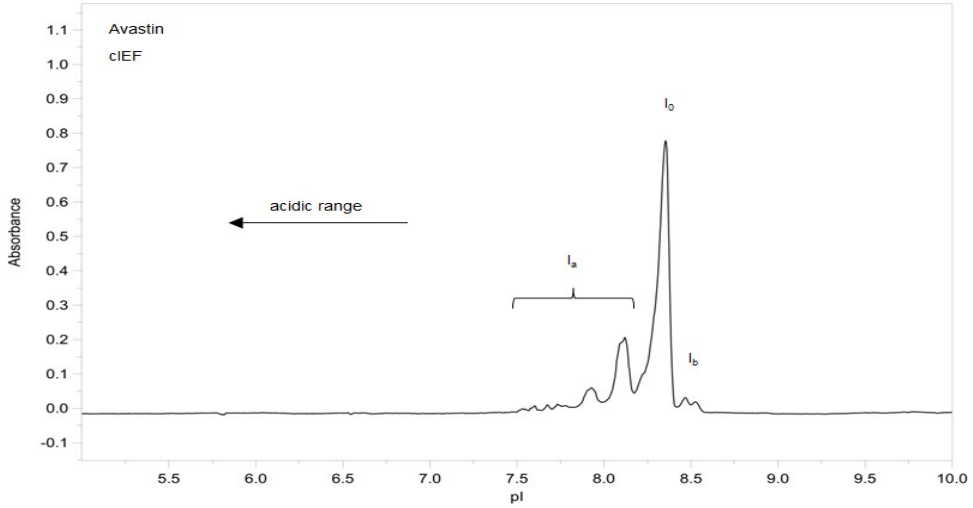

Figure 17: cIEF of Avastin: c_{end} = 0.5 mg/ml, basic AS with Pharmalyte 3-10, 8-10.5, pI M 4.65, 10.10 and 0.35 % MC.

Charge distribution of unstressed Avastin sample is represented by Figure 17 (using cIEF conditions 3.2.2). Main (I_0), acidic (I_a) and basic (I_b) species can be evaluated and the appropriate relative percentage peak areas used for quality control. The pI values of the present isoforms were determined using pI markers (pI markers at pI 4.65 and 10.10 are not shown in Figure 17). Consequently, the pI of I_0 was calculated with 8.3. Information about the pI value generally provides sufficient specificity and serves as identity assay on a control system. There are couple of signals visible in the acidic range representing probably presence of glycans with sialic acids. Signals for basic variants might indicate e.g. presence of lysines, amidation or some fragments.

As discussed below, the presence of ε-aminocaproic acid and HPMC should provide a sufficient dynamic capillary coating. Therefore the initial focus of the work lay first in avoiding the application of TETA and optimizing various parameters to achieve the best possible peak resolution using CZE.

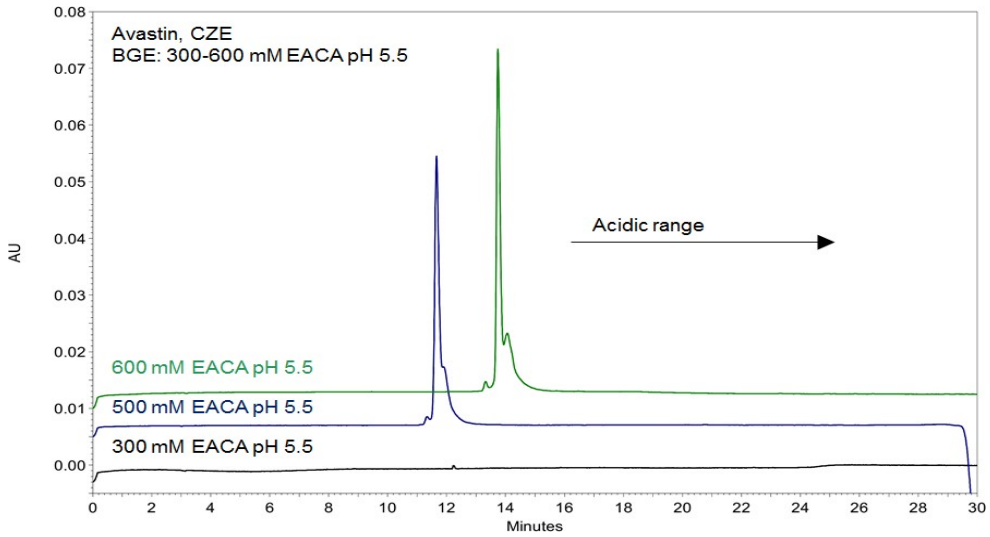

Figure 18: CZE, Avastin (unstressed) in formulation buffer (2 mg/mL). From bottom to top: 300 mM (black trace), 500 mM (blue trace), 600 mM EACA (green trace), pH 5.5. Experimental conditions: BGE: 300-600 mM EACA, 0.1 % HPMC, pH 5.5, 40/50 cm 50 µm fused silica capillary, separation temperature: 25 °C, separation voltage: 30 kV, injection 0.5 psi 10 s.

CZE separation of intact unstressed Avastin with EACA, 0.1 % HPMC running buffer is demonstrated in Figure 18. The pH was fixed at 5.5 and the concentration varied from 300-600 mM. By the contrast with [141] in the CZE experiments from Figure 18 no additionally capillary coating was applied. He et al. [141] reported using of TETA, because in their previous experiments [177] an undesirable peak broadening was observed without additional coating of the capillary. Positively charged aliphatic oligoamines (such as TETA) are able to adsorb at the interface between the capillary wall and the background electrolyte. That situation leads to the drastic variation of the positive charge density in the Stern layer, which decreases the zeta potential and, hence, reduces the EOF.

In the electrophoretic measurements in Figure 18, using the background electrolyte containing 300 mM EACA led to the presence of a very low signal, most likely as a result of analyte adsorption to a capillary wall. Further increase in buffer concentration resulted in an improvement of the signal height and also of the resolution of acidic and basic species. The adsorption of zwitterionic EACA onto the capillary wall deactivates the electrochemical double layer. This is apparent also from the electropherograms shown in Figure 18. With the increasing EACA concentration the adsorption of the Avastin onto capillary wall decreased and the signal intensity of Avastin grew until the EACA concentration achieved the certain level (600 mM). A further increase had no impact on the signal intensity. The most appropriate conditions of EACA were therefore set to 600 mM. The presence of HPMC in background electrolyte appears to mask efficiently the silanol groups of the fused silica capillary as it has been published by various researchers [178, 179]. Even small amounts of

polysaccharide derivates (such as HPMC) can significantly improve the resolution of protein separations by decreasing the zeta potential. High concentrations of polysaccharide derivates (e.g. dextran, HPMC, MC) increase the buffer viscosity to a large extent and cause molecular sieving [180]. However, the HPMC concentration of 0.2 % and lower is below the entanglement point and therefore the improvement of the peak resolution is thought to be due to differential reduction of the protein mobility and attenuation of electroosmotic flow [181, 182, 183]. The most appropriate concentration of HPMC, which participated on the best charge isoform separation of Avastin, was experimentally set to 0.1 %.

It is expected that the separation of charge variants will be significantly improved when the pH of the 600 mM EACA background electrolyte will rise closely to the pI value of Avastin. As reported by He [141], such conditions improves separation, because the relative charge differences among charge variants increase. If the pH value of the BGE is too close to the pI value of the protein analyte, attention must be paid to the possibility of an increased protein adsorption to the capillary wall or of the limited protein solubility [184].

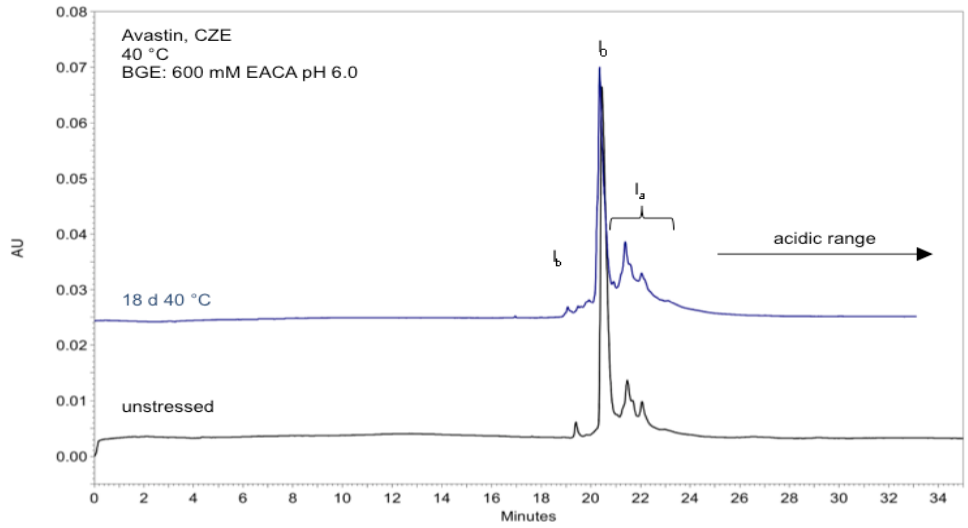

Figure 19: CZE, Avastin (unstressed, stressed) in formulation buffer (2 mg/mL): From bottom to top: unstressed (black trace), 18 d 40 °C (blue trace). Experimental conditions: BGE: 600 mM EACA, 0.1 % HPMC, pH 6.0, 40/50 cm 50 µm fused silica capillary, separation temperature: 25 °C, separation voltage: 30 kV, injection 0.5 psi 10 s.

The final background electrolyte properties and CE parameters (3.1.2) led to the reproducible separation of main, acidic and basic isoforms and allowed analysis of Avastin within 30 minutes for unstressed and also stressed test sample (Figure 19). Compared to the unstressed profile a signal increase in range of the acidic isoforms could be observed. By matching the CZE profile of an unstressed sample with cIEF (Figure 17) the improvement of isoform distribution was achieved for basic variants only.

As shown in the Table 28 the CZE and cIEF corrected area percentages of main isoforms of intact unstressed Avastin were comparable. The CZE acidic and basic charge variant distribution differed from cIEF. Presence of acidic variants was higher in CZE than it was observed in cIEF. At the same time it was observed that the amount of basic variants was lower.

Table 28: Corrected area percentage of main [I_0], acidic [I_a] and basic [I_b] isoform of unstressed intact Avastin.

	cIEF	CZE
A % [I_0]	69.4	68.3
A % [I_a]	26.6	29.9
A % [I_b]	4.0	1.8

Results are reported as the means of triplicate determinations.

It is anticipated that the experiments with Erbitux will offer more heterogeneous charge variant profile than it was observed for Avastin due to presence of two different glycosylation sites and also C-terminal lysine heterogeneity.

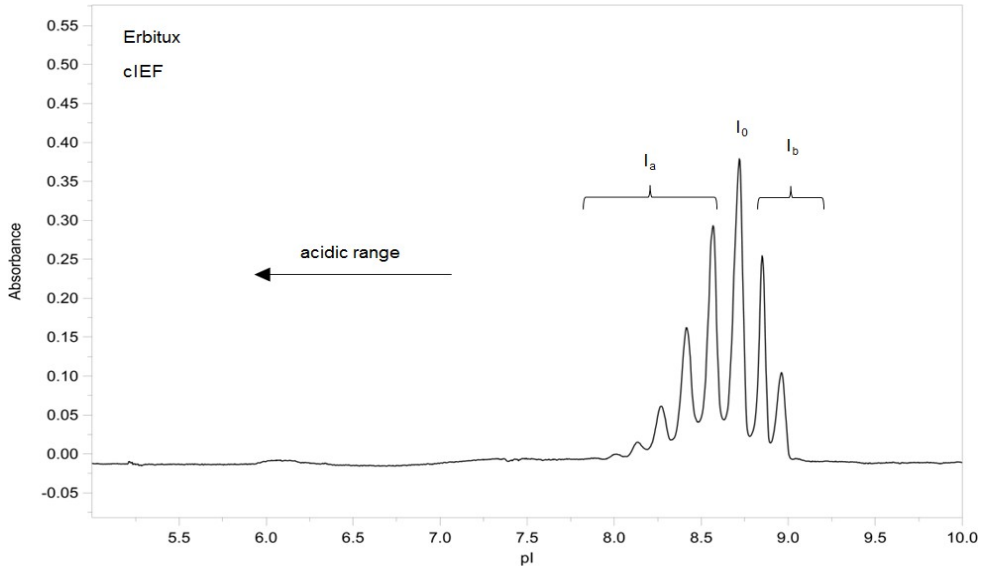

Figure 20: cIEF of Erbitux: c_{end} = 0.5 mg/ml, basic AS with Pharmalyte 3-10, 8-10.5, pI M 4.65, 10.10 and 0.35 % MC.

The charge isoform distribution of non-stressed Erbitux (using the cIEF conditions described in chapter 3.2.2) is shown in Figure 20. The annotations of acidic and basic species are congruent to the annotations made in case of Avastin (Figure 17). pI markers at pI 4.65 and 10.10 are not shown in Figure 20. High amount of acidic isoforms can be explained by the presence of various glycans with attached sialic acids (Quian et al. [185] adverts to 21 distinct oligosaccharides in Erbitux) and basic isoforms demonstrate probably presence of lysines. The isoelectric point of the main isoform (I_0) was experimentally

determined to 8.75, which is slightly differing from the calculated value of 8.48 (as listed in Table 43). As reported by Shaw et al. [176] this situation is not uncommon and the explanation for it can be seen in the different ionization of single amino acid groups in model and folded proteins.

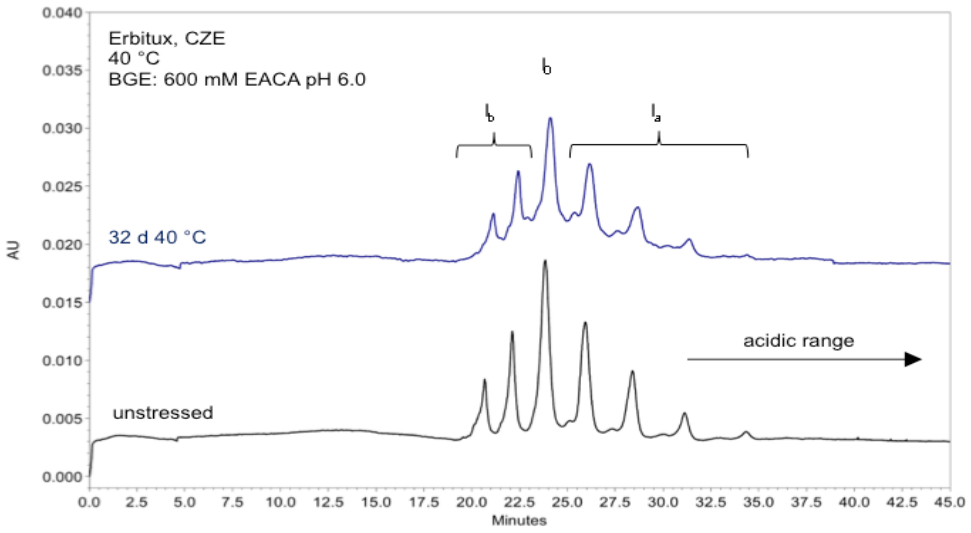

Figure 21: CZE, Erbitux (unstressed, stressed) in formulation buffer (2 mg/mL). From bottom to top: unstressed (black trace), 32 d 40 °C. Experimental conditions: BGE: 600 mM EACA, 0.1 % HPMC, pH 6.0, 40/50 cm 50 µm fused silica capillary, separation temperature: 25 °C, separation voltage: 30 kV, injection 0.5 psi 10 s.

The CZE separation with the most suitable conditions (for details see 3.2.2) is demonstrated in Figure 21 on unstressed and stressed Erbitux sample. All above-mentioned parameters (e.g. running buffer concentration, pH etc.) were also here tested with the conclusion, that the same background electrolyte composition as for Avastin offers the most convenient isoform resolution. Buffers with pH greater than 6.0, led to peak broadening and long analysis times (above one hour, data not shown). Compared to the electropherogram in Figure 17, the resolution of charge variants is even better than that achieved with isoelectric focusing. Calculating the area percentages, the relative proportion of isoforms of unstressed Erbitux is comparable to cIEF (Table 29). Analysis of stressed Erbitux sample did not detect any increase of acidic charge variants. With increasing degree of sample degradation, the baseline resolution suffered, but the individual isoforms could be clearly separated from each other.

Table 29: Corrected area percentage of main [I_0], acidic [I_a] and basic [I_b] isoform of unstressed intact Erbitux.

	cIEF	CZE
A % [I_0]	30.0	31.1
A % [I_a]	46.2	44.9
A % [I_b]	23.8	24.0

Results are reported as the means of triplicate determinations.

CZE assay after papain digestion

Expecting that papain digestion of Avastin and Erbitux will allow a better visualization of charge variants both monoclonal antibodies were examined by cIEF and CZE after the enzymatic digestion.

Initially, the papain fragmentation of Avastin and Erbitux into Fab and Fc portions was optimized. Based on [163, 186, 187] the following parameters were enquired: (a) enzyme:substrate ratio (w/w); (b) digestion temperature and incubation time; (c) formulation buffer; (d) additives; and (e) enzyme pre-activation.

As introduced above, using papain, the upper hinge amino acid sequence of some humanized IgG1 will be cleaved behind histidine. If the hydrolysis rules will be applied on some specific target, under the condition that heavy and light chain sequences are known, then it is possible to obtain the exact Fab and Fc amino acid sequences. The cleavage site of the investigated Avastin is introduced in Scheme 24. The properties of new emerged fragments (as e.g. molecular weight and isoelectric point) can be calculated. As apparent from Table 30, the pI values of both fragments differ by ≥one unit; therefore a clearly visible separation of both signals can be expected.

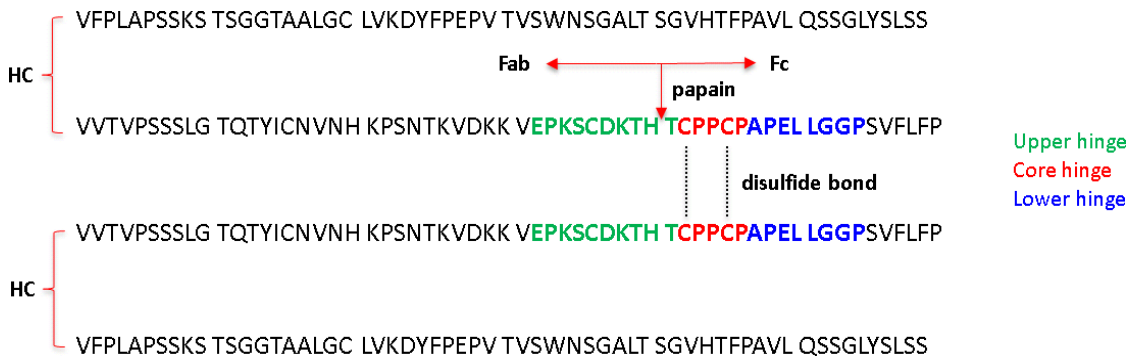

Scheme 24: The hinge region and part of heavy chains of Avastin with expected papain digestion site.

Table 30: Calculated [131] average molecular weights and pI values of Fab and Fc fragments of Avastin.

Fragment	Mw [kDa]	pI
Fab	48.2	8.21
Fc	25.1	6.95

Optimization of the papain digestion process on Avastin and Erbitux was monitored by cIEF method. The aim was achieved when the complete hydrolysis of IgGs resulted in the production of two products (Fab and Fc) and no IgG signal was visible anymore. The charge distribution of the fragments was finally analysed by CZE, simultaneously optimizing the electrophoretic parameter to achieve the best possible resolution.

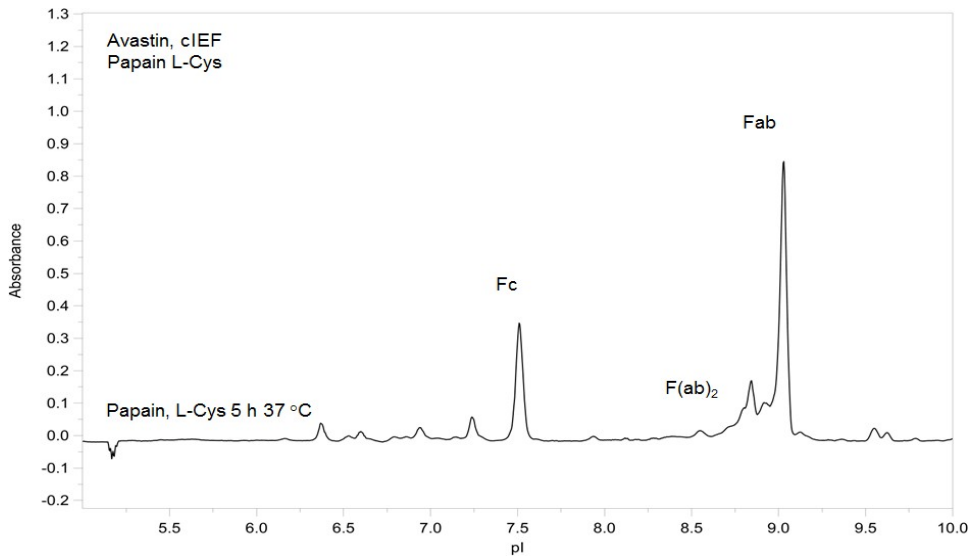

Figure 22: cIEF of papain digested Avastin: c_{end} = 0.3 mg/ml, digestion in 1 mM at 37 °C for 5 h, basic AS with Pharmalyte 3-10, 8-10.5, pI M 4.65, 10.10 and 0.35 % MC.

Charge distribution of Fab and Fc fragments of papain digested unstressed Avastin sample is demonstrated in Figure 22. Sample preparation and isoelectric conditions are

described in chapter 3.1.2. Firstly, the signal identification was carried out on the basis of knowledge of the isoelectric points (Table 30). The pI values of Fab and Fc fragments were set experimentally using two pI markers. Although observed isoelectric points of the fragments were higher than expected, the signal assignment was straightforward. The difference between Fab and Fc pI values of almost 1 pH unit allowed dramatic separation of both main signals. Secondly, the spiking of single fractions was performed (Fab and Fc fragments were collected using RP-HPLC separation of papain digested Avastin, subjected to vacuum to dry, dissolved again in a minimum volume of water and used for spiking); for results see Table 44. As apparent from Figure 22 the Fc fragment is present in the more acidic region of the electropherogram and its pI value was experimentally determined to 7.54. All further acidic forms are clearly baseline separated. Two signals with pI values of 6.90 and 7.25 result very likely from present glycans with attached sialic acids. Remaining acidic signals could not be identified, but it is presumed that these are also result of papain digestion. As described in [162], papain exhibits some specificity for leucine and glycine. The enzyme could therefore partially hydrolyse the molecule at other positions than at the C-terminal side of the histidine residue in the hinge region. The peak at 9.05 with some unresolved acidic variants was assigned as Fab. The acidic isoforms in the Fab region were considered to be a result of Fab microheterogeneity or co-migration of some other papain cleavage products. Based on research results from Bennet [165], it was expected that the signal at 8.6 represents the $F(ab)_2$ fragment (spiking experiments with intact Avastin did not approve some remaining signal of the undigested molecule). Bennet published the predominant production of $F(ab)_2$ if cysteine (L-Cys) is absent during the papain digestion procedure. Using lower concentrations of L-Cys (or its omission) in the digestion process led to the increment of the $F(ab)_2$ signal. The signal at 9.60 represents papain.

The above-introduced CZE separation conditions (in detail described in chapter 3.2.2) were seen as the most appropriate for the analysis of digested samples. It is expected that using normal polarity and running buffer at pH 6.0, the fragments will be positively charged and appear in the reverse order than it was observed by isoelectric focusing.

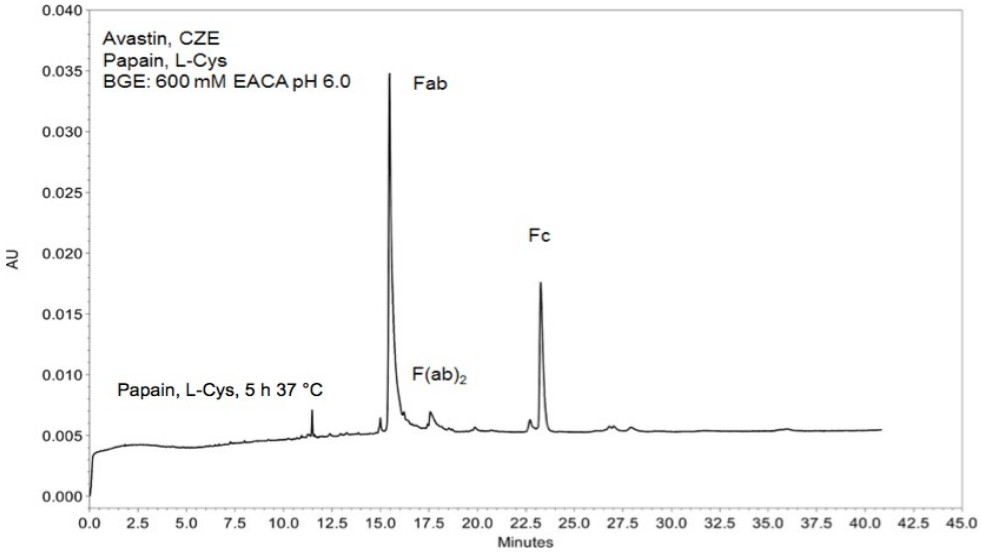

Figure 23: CZE of papain digested Avastin (c_{end} = 2.5 mg/mL), digestion in 1 mM L-Cys at 37 °C for 5 h. Experimental conditions: BGE: 600 mM EACA, 0.1 % HPMC, pH 6.0, 40/50 cm 50 µm fused silica capillary, separation temperature: 25 °C, separation voltage: 30 kV, injection 0.5 psi 10 s.

As demonstrated in Figure 23, the Fab (16.0 min) and Fc (24.5 min) fragments were separated within 25 minutes. The electrophoretic signal with the migration time of 17.5 min represents very likely the $F(ab)_2$ fragment. It is apparent, that the isoform profiles differ from these obtained by isoelectrofocusing. In comparison with Figure 22 a worse separation of acidic Fab signals was observed, but as introduced in Table 31 the area percentages of single fragments were comparable.

Table 31: cIEF and CZE corrected area percentage of Fab + $F(ab)_2$ and Fc fragments.

	cIEF	CZE
A % [Fab + $F(ab)_2$]	69.6	68.4
A % [Fc]	30.4	31.6

Results are reported as the means of triplicate determinations.

As presented in introduction section, this method should allow the better visualization of the charge variant alterations. The presence of new signals is expected in stressed sample due to possible deamidation or fragmentation. Worthwhile to noting is that the deamidation has been widely reported for asparagines in the variable domains of monoclonal antibodies [82, 83, 150, 188]. Variable domains are situated in the Fab fragments.

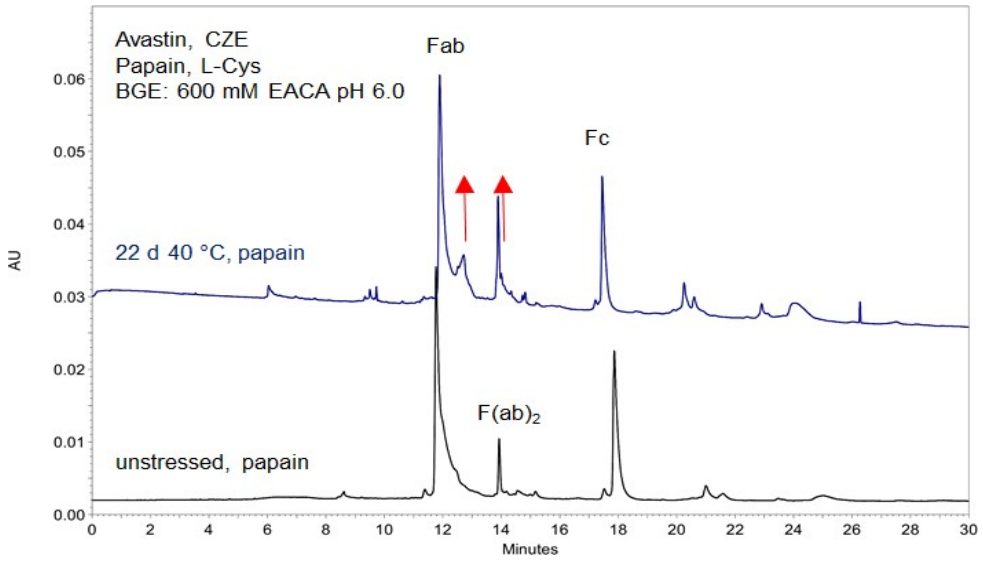

Figure 24: CZE of papain digested unstressed and stressed Avastin, digestion in 1 mM L-Cys at 37 °C for 5 h (c_{end} = 2.5 mg/mL). From bottom to top: unstressed, papain (black trace) and 22 d at 40 °C, papain (blue trace). Experimental conditions: BGE: 600 mM EACA, 0.1 % HPMC, pH 6.0, 40/50 cm 50 µm fused silica capillary, separation temperature: 25 °C, separation voltage: 30 kV, injection 0.5 psi 10 s.

Using papain digestion to reduce the protein complexity of unstressed and stressed Avastin and subsequent CZE separation of resulting fragments is introduced in Figure 24. From both electropherograms it is apparent, that some differences could be observed between these digested samples. The signals in the acidic region of the Fab fragment (blue trace, 12.8 min) indicate the presence of some new charge variants. Presumably, such signals represent deamidation of asparagine(s) after forced degradation. This sample can be a regarded for further investigations e.g. peptide-mapping with MS detection or Asp-N digestion. Also an increment of the $F(ab)_2$ signal of stressed sample (blue trace, 14 min) was noticed. This observation could be explained by some molecule conformational changes due to forced stress. An access of the enzyme to the target can be aggravated and therefore a diminished ability of the enzyme ability to reduce the hinge region disulphide could be observed.

Interesting results were observed after using a second enzyme in the test sample preparation: Protein N-Glycosidase (PNGase). PNGase digest was performed after papain digestion followed by CZE analysis. This enzyme facilitates the release of N-glycans from glycoproteins by the cleavage of the link between asparagine and N-acetylglucosamines [189, 190]. Applying PNGase digestion the attached N-glycans will be released and the remaining Asn residue will by hydrolysed (deaminated) to Asp. If there are no sialic acids attached to glycans then due deamination, the deglycosylated protein will be more acidic as its glycosylated counterpart.

As mentioned in introduction section (3.2.1), there are two N-glycans present at N303 of both heavy chains (which corresponds to Fc fragments). According to Fuller et al. [191], who investigated labelled N-glycans of various Avastin lots by chromatography, no Avastin glycoforms had sialylated structures. Boeggman et al. [192], who performed the MALDI analysis of the biantennary Avastin N-glycans, obtained the same results as Fuller et al. Based on this fact it can be expected that the N303 deaminated Fc part of Avastin will migrate as a weaker cation with higher migration time than its glycosylated counterpart when applying positive polarity and using 600 mM EACA running buffer of pH 6.0.

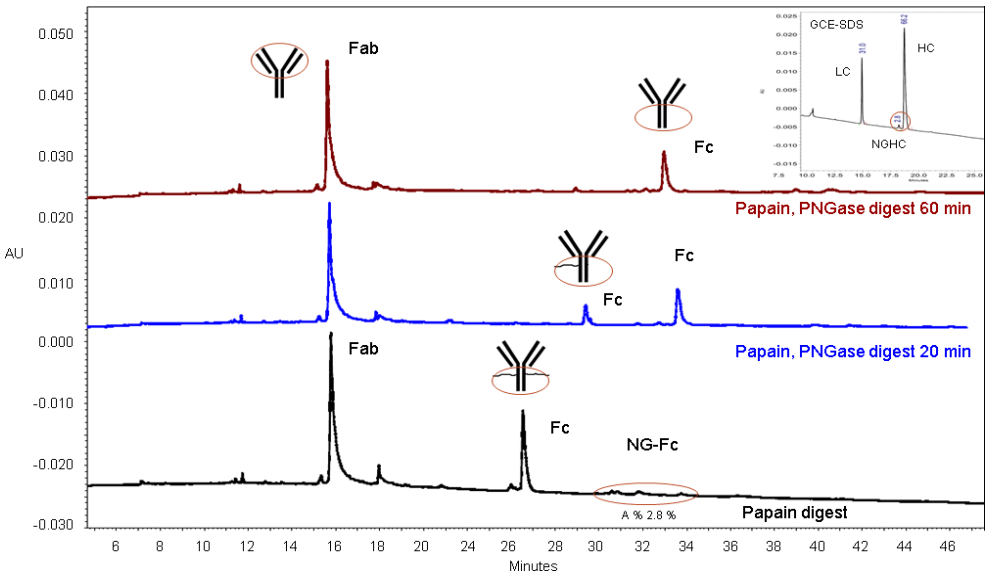

Figure 25: CZE of papain, PNGase digested Avastin (c_{end} = 2.5 mg/mL), papain digestion in 1 mM L-Cys at 37 °C for 5 h. From bottom to top: Papain digest without PNGase (black trace), Papain, PNGase digest: 20 min 37 °C (blue trace), Papain, PNGase digest: 1 h 37 °C (red trace). Experimental conditions: BGE: 600 mM EACA, 0.1 % HPMC, pH 6.0, 40/50 cm 50 µm fused silica capillary, separation temperature: 25 °C, separation voltage: 30 kV, injection 0.5 psi 10 s.

The electrophoretic separation profile of papain digested Avastin was already introduced in Figure 23 and this sample is represented by black trace in Figure 25 (the CGE-SDS separation of reduced Avastin is shown in electropherogram (upper right corner) to visualize the non-glycosylated (NGHC) and glycosylated heavy chain (HC) forms). In addition to presumed $F(ab)_2$ signal (18.0 min) and two dominant peaks: Fab (16.0 min) and Fc (26.7 min) some further peaks of low signal intensities were detected with migration time of 30-34 min (black trace). These peaks were supposed to represent the non-glycosylated Fc portion (NG-Fc) with zero, one or two attached lysines. Deglycosylation led to a loss of the initial Fc signal and to a creation of two new Fc fragment variants (blue trace, 30 and 34 min) after 20 minutes of incubation. With longer incubation (one hour), only deglycosylated Fc signal is observable (red trace, 33.2 min) in addition to Fab fragment (16.0 min), which stayed unchanged. The shift to the higher migration time indicates no terminal sialylation of

the Fc fragment. The enzymatic hydrolysis of N-glycans in the presence of sialic acids would contribute towards the creation of more basic Fc fragment and towards shift in the opposite direction. These observations correlate with the results published by Fuller and Boeggman [191, 192]. Because the deglycosylated signal appears now in the more acidic region than it was observed for its glycosylated form some additional anionic character can be attributed to this molecule. The explanation for this effect is that the asparagine residue from which the glycan was removed is deaminated to aspartate.

Routinely the CGE-SDS is used for the separation of the glycosylated species from their non-glycosylated counterparts [193, 194] after reduction of the monoclonal antibody. CGE-SDS assay enables the control of the non-glycosylated (NG) variant of heavy chain in the presence of gel, which allows separation according to differences in molecular weight. Therefore the non-glycosylated species migrate with lower migration times than their glycosylated counterparts. CZE separates the analyte based on differences in their electrophoretic mobilities. As described above, it was presumed, that the signals at 30-34 min (black trace) represent the NG-Fc portion. The calculated area percentage of NG-Fc (A % 2.0) correlated with the result obtained for NGHC. However, the NG-Fc peak heights were not much above the level of background noise. The CZE results indicate the possibility to examine the non-glycosylated and glycosylated forms by CZE using papain digestion and EACA background electrolyte.

After successful papain digestion and CZE separation of Fab and Fc fragments of humanized monoclonal antibody (Avastin) the chimeric monoclonal antibody (Erbitux) was studied. Papain cleavage at the C-terminal side of histidine residue in upper hinge region lead to the creation of the Fab and Fc fragments. The properties of new emerged Fab and Fc fragments (molecular weight and isoelectric point) were calculated; for results see Table 32. A clearly visible separation of both signals can be expected, because the difference between pI values of both fragments is large.

Table 32: Calculated [131] average molecular weights and pI values of Fab and Fc fragments of Avastin.

Fragment	Mw [kDa]	pI
Fab	47.8	8.70
Fc	50.1	7.12

A high degree of heterogeneity of Fc portion of Erbitux can be expected due to the presence of C-terminal lysines and glycosylation at Asn299 [195]. The glycosylation at Asn88 [195, 196] with present sialic acids will be among other post-translational changes a source of acidic heterogeneity of Fab.

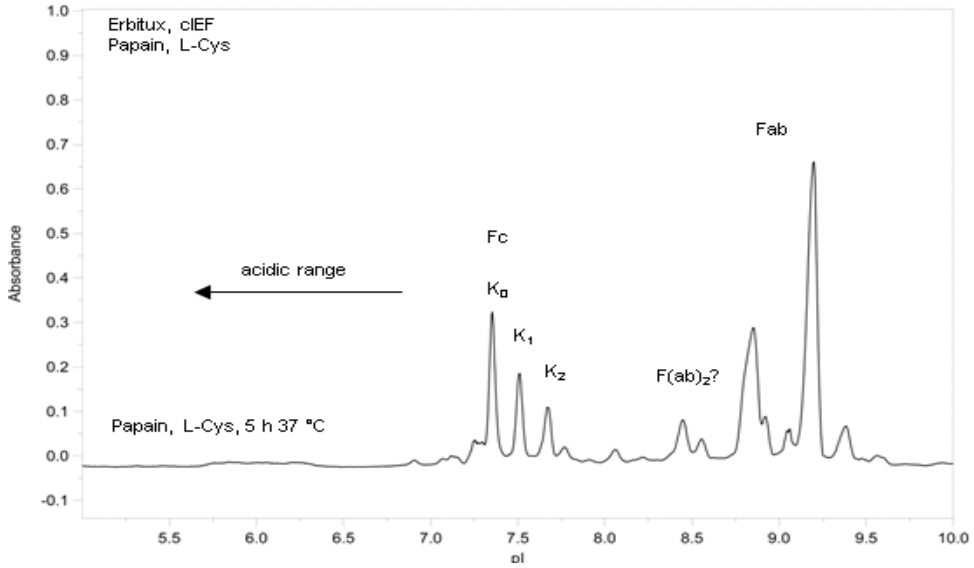

Figure 26: cIEF of papain digested Erbitux: c_{end} = 0.3 mg/ml, papain digest 37°C with L-Cys for 5 h, AS with Pharmalyte 3-10, 8-10.5, pI M 4.65, 10.10 and 0.35 % MC.

The IEF-electropherogram in Figure 26 represents papain digested Erbitux. In comparison to Avastin there are much more isoforms observable in both portions (as also shown in Figure 21). The basic isoforms of Fc portion result from two present C-terminal lysines (K_1, K_2) and the acidic not-resolved form represents very likely the glycosylation at Asn299. The acidic heterogeneity of Fab was explained by the glycosylation at Asn88. Release of such glycans by PNGase (data not shown) led to some minor changes in the isoelectrophoretic profile. This can be explained by simultaneously deamination and creation of further acidic signals. The signal at 9.60 represents papain. Other signals in the acidic region of the Fab portion (pI of 8.5) were presumed to be a product of papain nonspecific cleavage. To control the protein hydrolysis and the resulting final products, the digestion procedure was monitored by CGE-SDS (Figure 49). The peak identification was done based on the knowledge of molecular weights of the possible cleavage products. The digestion conditions applied in Figure 26 resulted in the formation of two main portions (Fab) of 50 kDa and of only minute amounts of $F(ab)_2$, non-digested IgG and some unidentified fragments of approximately 30 kDa.

As observed for papain digested Avastin experiments, it was expected that the above-introduced CZE separation conditions (in detail described in chapter 3.2.2) would lead to comparable results using cIEF and CZE for the analysis of papain digested Erbitux.

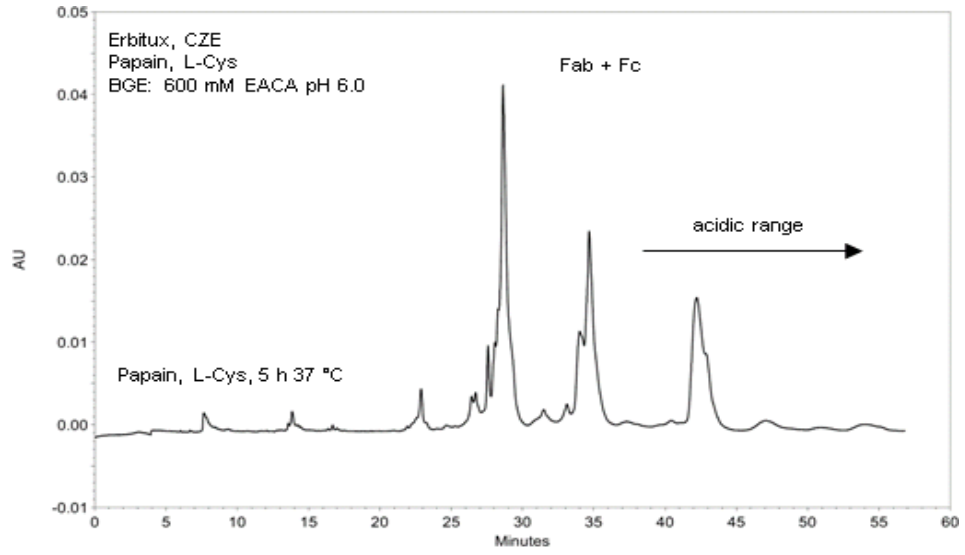

Figure 27: CZE of papain digested Erbitux (c_{end} = 2.5 mg/mL), digestion in 1 mM L-Cys at 37 °C for 5 h. Experimental conditions: BGE: 600 mM EACA, 0.1 % HPMC, pH 6.0, 40/50 cm 50 µm fused silica capillary, separation temperature: 25 °C, separation voltage: 30 kV, injection 0.5 psi 10 s.

The CZE electropherogram of papain digested Erbitux is demonstrated in Figure 27. The profiles of Fab and Fc portions are not comparable to cIEF results (Figure 26). The explanation for this fact was seen in a co-migration of some present signals. Most likely the Fab portions are represented by two signals (29 and 35 min). The split peaks of the acidic Fab signal (35 min) seem to be also present in Figure 26 at pI of 8.7. The Fc lysine isoforms were not detected. Various buffer pH values and concentrations, separation temperatures, voltages or analysis using the neutral coated capillary did not contribute to any improvement of the separation profile. Because the peak determination cannot be done in CZE run and the CZE and cIEF separation profiles were not comparable further steps were taken to identify the Fab and Fc portions. The fragments of papain digested Erbitux were collected using RP-HPLC separation, fractions were subjected to vacuum to dry, reconstituted in a minimum volume of water and used for individual CZE runs and later for spiking experiments (Figure 50). Electrophoretic investigation of the single fractions offered complex electrophoretic profiles of both Erbitux fragments. The CZE analysis of the Fab portion manifested the presence of two main peaks and further three clearly visible peaks were detected after examination of the Fc portion. In addition to the clearly visible peaks, there were also some signals observed as peak shoulders (data not shown). The combination of the Fab and Fc fragment resulted in the electrophoretic profile obtained for the papain digested sample (shown in Figure 27).

CZE assay after pepsin digestion

The interpretation of the electrophoretic signals of papain digested Erbitux turned out to be difficult due numerous co-migrations. Therefore, the complexity of the protein was reduced by pepsin digestion. If the information about the crystallisable region (Fc) is not required, pepsin can be taken for the mAb hydrolysis. After digestion, the Fc peptide fragments are removed from the test sample prior to analysis. Doing so, the problem of co-migration of Fab signals with Fc signals (as seen in Figure 27) will be eliminated.

It is known, that pepsin is active only at acid pH being irreversibly denatured at neutral or alkaline pH [171]. Pepsin cleaves preferentially at the C-terminal side of hydrophobic, aromatic residues like phenylalanine and leucine. To look closely into the digestion process the pepsin cuts the monoclonal antibody at the heavy chain lower hinge region. The lower hinge amino acid sequence (APELLGGP) will be cleaved behind the disulfide bonds between two leucine hinge [166]. As illustrated in Scheme 25 of the amino sequence of Erbitux the enzymatic hydrolysis leads to a creation of one $F(ab)_2$ fragment and one (segmented) Fc fragment.

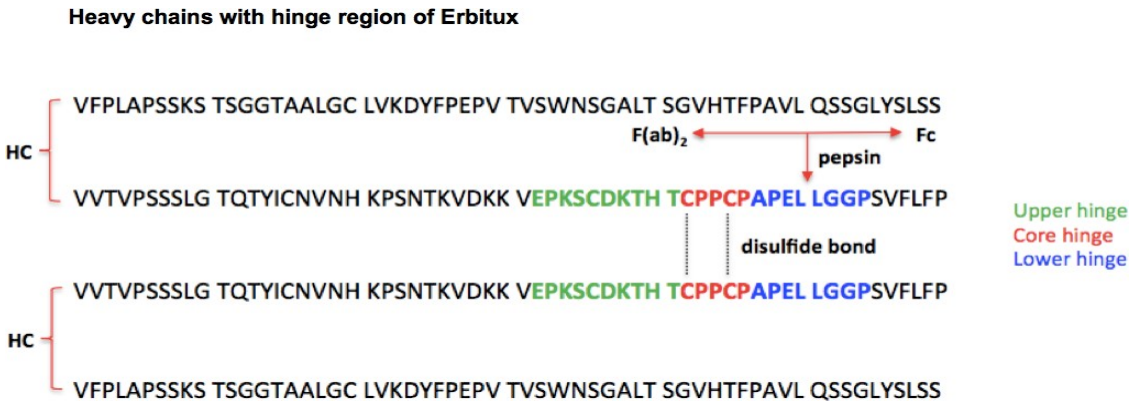

Scheme 25: The hinge region and part of heavy chains of Erbitux with expected pepsin hydrolysis.

Using Erbitux as the study material the pepsin digestion conditions were optimized. Based on published works [169, 170, 171, 197] the influence of the following parameters was investigated: (a) pepsin and test sample concentration ratio; (b) digestion temperature and duration; (c) formulation buffer; (d) additives; and (e) enzyme pre-activation. The charge isoform distribution of pepsin digested unstressed Erbitux sample was studied by cIEF and the isoelectrophoretic run using the final method is shown in Figure 28. The sample preparation and the isoelectric conditions are described in 3.1.2.

As previously described in chapter 3.2.1 and illustrated in Scheme 22, pepsin cleaves monoclonal antibodies in the hinge region generating the $F(ab')_2$ and Fc subfragments. These small fragments can be removed from the digestion mixture and $F(ab')_2$ can be further investigated.

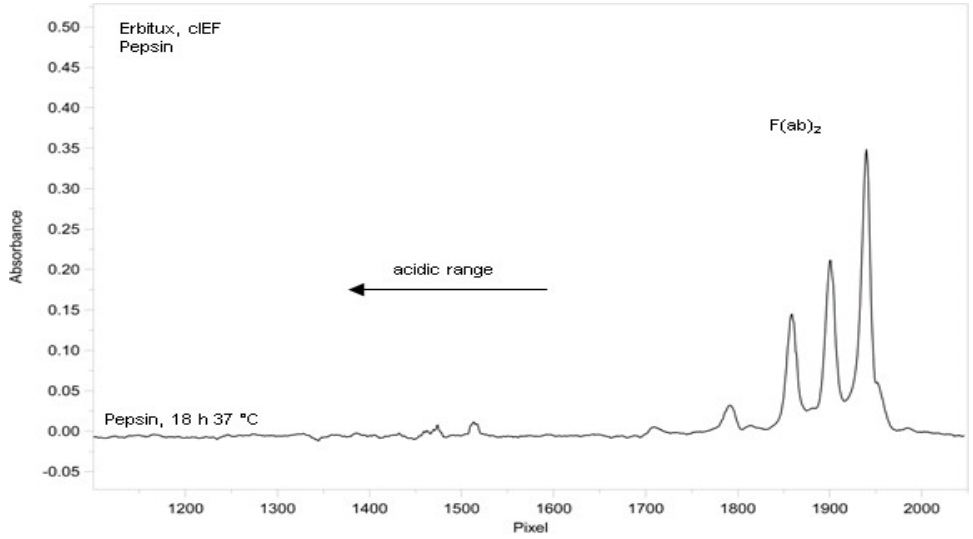

Figure 28: cIEF of pepsin digested Erbitux: c_{end} = 0.3 mg/ml, digest 37 °C 18 h with RapiGest: basic AS with Pharmalyte 3-10, 8-10.5 and 0.35 % MC.

As apparent from the IEF-electropherogram of pepsin digested Erbitux (Figure 28), the Fc portion clearly visible in Figure 26 does not appear in the acidic range anymore. The Fc subfragments created by the enzyme were effectively removed from the digestion mixture by ultracentrifugation. The acidic charge variants of the $F(ab)_2$ part are well resolved compared to the peak shoulder slightly visible in the basic range of the highest $F(ab)_2$ peak. The presence of the various acidic charge variants can be explained by attached sialic acids.

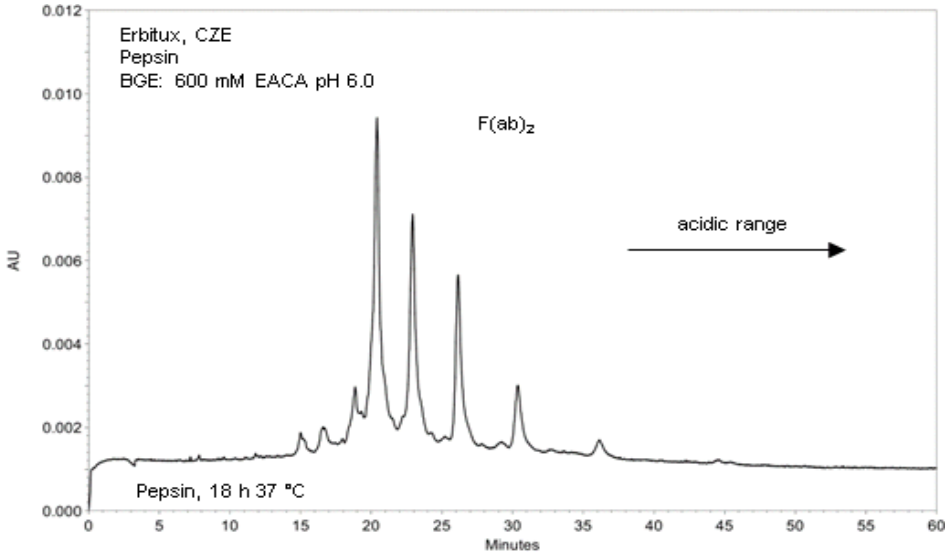

Figure 29: CZE of pepsin digested Erbitux (c_{end} = 2.6 mg/mL), digestion at 37 °C for 18 h. Experimental conditions: BGE: 600 mM EACA, 0.1 % HPMC, pH 6.0, 40/50 cm 50 µm fused silica capillary, separation temperature: 25 °C, separation voltage: 30 kV, injection 0.5 psi 10 s.

The electrophoretic profile of $F(ab)_2$ charge variants is illustrated in Figure 29. The present isoforms exhibit very great similarities with previously discussed cIEF profile (Figure 28). In comparison to cIEF the CZE method led to a significant improvement of the resolution of acidic and also basic variants. The acidic variants were already discussed above. The detected basic variants could indicate a presence of some peptide fragments or represent some conformational changes that lead to the creation of further charged isoforms [151, 152].

Monitoring the extend of Lysine cleavage by carboxypeptidase B activity

The presented CZE method can also be utilized for the investigation of the C-terminal lysines. As introduced in chapter 3.2.1 and illustrated by Scheme 23, carboxypeptidase B cleaves basic amino acids such as Lys and Arg from C-terminus of a protein [174].

Applying the enzyme carboxypeptidase B to Erbitux, the C-terminal lysines can be cleaved and the molecule can be investigated by CZE using EACA. Compared to the undigested molecule, some differences can be expected in the migration pattern, namely in the I_b range. The microheterogeneity pattern created i.a. by the lysine variants will be reduced by an amount of the removed lysines.

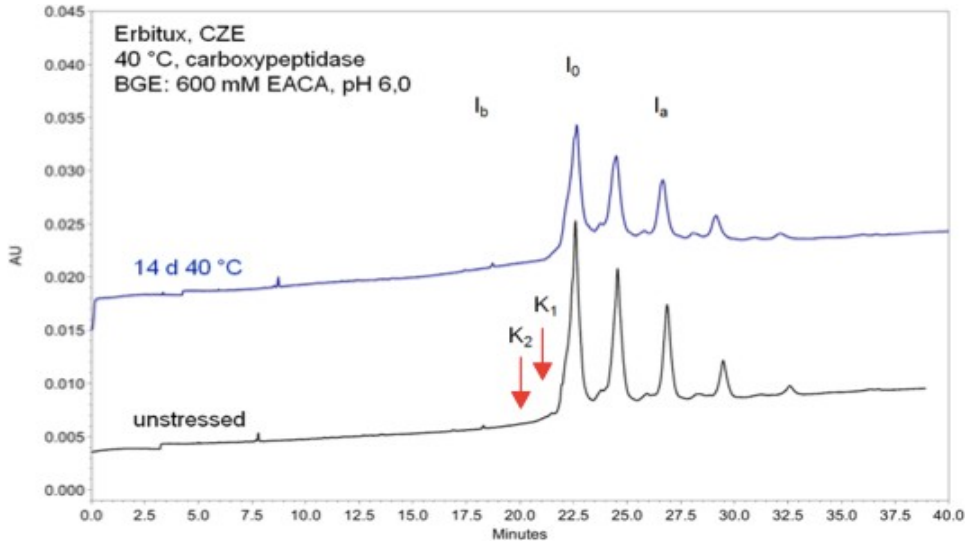

Figure 30: CZE of carboxypeptidase digested unstressed and stressed Erbitux (c_{end} = 2.5 mg/ml), digest 37 °C 3.5 h. From bottom to top: unstressed, carboxypeptidase (black trace), 14 d 40 °C, carboxypeptidase (blue trace). Experimental conditions: BGE: 600 mM EACA, 0.1 % HPMC, pH 6.0, 40/50 cm 50 µm fused silica capillary, separation temperature: 25 °C, separation voltage: 30 kV, injection 0.5 psi 10 s.

The reference for these experiments was introduced above in Figure 21. The carboxypeptidase treated unstressed and stressed Erbitux samples were analysed using EACA running buffer as shown in Figure 30. Two missing signals (labelled as I_b) clearly visible in the electropherogram of undigested Erbitux verify the former presence of two C-terminal lysines (as previously seen using isoelectrofocusing – data not shown).

As apparent from CZE electropherograms in Figure 30, the presence/absence of C-terminal lysines can be monitored by utilization of EACA running buffer and carboxypeptidase digestion. This method can be applied for unstressed samples and also stressed samples.

3.2.4 Conclusion

Objective of this study was to find out whether the application of a simple analytical CZE method would be appropriate for the study of charge variants of two monoclonal antibodies, intact and also enzymatically hydrolysed. Method, we were trying to develop, should be complementary to the cIEF, reproducible, free of oligoamines coating or neutral coated capillary and also independent of using ampholytes.

The EACA running buffer (600 mM, 0.1 % HPMC pH 6.0) provided very similar CZE profiles to these obtained by isoelectrofocusing in the study of intact monoclonal antibodies; in case of Erbitux even better resolution of acidic and basic isoforms was achieved. Closely associated with this finding is the increased probability to monitor even small microheterogeneity alterations e.g. lot-to-lot dissimilarities or presence of new charge

variants in stressed samples. Although the results obtained for intact mAbs were very promising, the separation of papain-digested samples led to a partial success only. Whilst the CZE resolution and the area percentages of Avastin Fab and Fc portions were comparable with the cIEF method, the exact Erbitux peak assignment to the specific portions was made difficult by co-migrating signals. It was demonstrated on Avastin sample, that the CZE method in the combination with papain digestion could be utilized in the study of degraded (potentially deamidated) samples, because the pre-localization of new acidic charge variants was made possible. Applying the CZE for the analysis of $F(ab)_2$ Erbitux portion (obtained after pepsin digestion) provided better resolution of present isoforms than it could be reached by isoelectrofocusing. Pepsin digestion leads to the partial fragmentation of the Fc portion, therefore is this method suitable for the investigation of charge variants of $F(ab)_2$ portions only.

Broad analytical application of EACA running buffer was demonstrated by the combination of papain digestion with PNGase. We manifested the power of this technique on separation of glycosylated and deglycosylated Avastin Fc fragments. Also the presence or absence of C-terminal side lysine residues can be demonstrated as shown in the example of the carboxypeptidase digested Erbitux.

CZE method is preferred compared to cIEF because cIEF does not allow detection at wavelengths below 250 nm (absorption of ampholytes) and cannot be directly coupled to MS.

3.3 Evaluation of a CZE method for the analysis of protein PEGylation in erythropoietin

The aim of this work is to establish the number of attached PEG moieties to erythropoietin (PEGylation degree), to localize the PEG attachment sites and to estimate the PEG occupancy (PEGocc). The study involves the development of capillary electrophoretic methods for the detection of intact erythropoietin (native and PEGylated) and also for the enzymatically cleaved molecule. Firstly, the CZE and CGE-SDS were applied for the investigations of the intact mAb. In further steps the focus was turned on the enzymatically-digested (Lys-C) sample; first of all the native (EPO) peptides were identified using various tools such RP-HPLC-MS and MALDI-TOF. In the following work the attention was aimed at the analysis of the generated peptides using CZE-UV. Spiking of the HPLC collected fractions to the digested EPO provided the identification of the present signals. Later, the peak assignment was performed and confirmed by CZE-ESI-MS analysis. After completion of the examination of the native mAb further investigations were proceed on the PEGylated mAb.

3.3.1 Introduction

Since the first successful genetic engineering product was introduced - human insulin in 1978 [198] the biotechnology manufacturing processing of drugs grew rapidly. Until 2013, more than 90 recombinant drug substances have been approved and many new products are still under development [199]. Many years of detailed study brought progress in production technology and pharmacological understanding of biologics [200].

Despite the many advantages that the protein therapeutics offer (e.g. highly specific functions which cannot be imitated by small drugs; less potential to interfere with normal biologic processes and to induce unwanted immune response; replacement treatment of mutated or deleted gene [201]), the risk of immunogenicity, in vitro and vivo instability and short half-life can be a limiting factors of using such therapy [202]. To improve the current limitations several strategies have been developed creating the second generation of protein therapeutics. Attachment of poly(ethylene glycol) (PEG) moiety is one of the drug modifications which can overcome above listed issues. Polyethylenglycol, a synthetic polyether with the general formula illustrated in Scheme 26 is a water-soluble polymer with wide range of molecular weights (typical 500 - 20000 Da [18]).

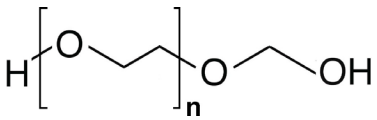

Scheme 26: Formula of polyethylenglycol.

These non-immunogenic non-toxic molecules are amphiphilic (soluble also in most organic solvents e.g. ethanol, toluene, acetone) and reactive with the nucleophile of amino groups of peptides and proteins through susceptible hydroxyl group creating often covalent conjugates. The presence of PEG enhances the therapeutic and biotechnological potential of peptides and proteins by masking of protein's surface and increasing of molecular size [203]. Concurrently the biological functions (enzymatic activity, receptor recognition) may be maintained. Derivates of biologics are prepared by reaction of an activated PEG moiety leading to the attachment of this water-soluble polymer to specific sites of peptides or proteins [204]. PEG is usually linked to proteins at the α-amino and ε-amino groups of lysines and the linkage can be accomplished by acylation or alkylation [205].

The PEG-attachment to the molecule is the problematical part of the drug modification. PEGylation process can result in molecular heterogeneity in terms of the number (leading to mono-, di-, three- up to polyPEGylation) and positions of attached PEG molecules (one position fully PEGylated, several sites partial PEGylated) forming the various protein-PEG conjugates [206, 207]. The biological properties may be influenced by these heterogeneities, therefore the development of analytical methods for PEGylated drugs has become more important [208].

Various analytical methods can used for the quantitative measurement of PEG molecules and their conjugates with peptides/proteins. Some of them have been in use for many decades e.g. colorimetric methods [20] and some have been introduced in recent years e.g. asymmetrical-flow field-flow fractionation (AF4) [209]. PEGylated peptides and proteins can be separated by various electrophoretic and chromatographic methods. The electrophoresis is represented by e.g. microchip electrophoretic separation [210], CGE-SDS and CZE [211]. Chromatography (e.g. size exclusion chromatography (SEC), hydrophobic interaction chromatography (HIC) and electrostatic interaction chromatography (IEC)) has been successfully employed to characterize PEG-protein conjugates [212]. Reversed-phase high-performance liquid chromatography (RP-HPLC) is mainly used for study of enzymatic digested PEG conjugates [213]. In this work it is discussed, how these methods can be employed for the establishment of the number of attached PEG moieties to erythropoietin (PEGylation degree) and for the localization of PEG attachment sites with calculation of PEG occupancy (PEGocc).

Erythropoietin and its PEGylated form

Erythropoietin (EPO) is a glycoprotein hormone that controls formation of red blood cells (erythropoiesis) [214]. Glycosylation of proteins depends on several factors such as the organism or cell line in which they are produced. N-glycosidic linkage of glycoproteins occurs via the asparagine amido group and N-acetyl-D-glucosamine residue, for O-glycosidic linkage binding to hydroxyl group of serine or threonine is typical [215]. Erythropoietin has also other biological functions as wound healing [216] or prevents neuronal apoptosis after cerebral injury [217]. The kidney predominantly produces human erythropoietin, although the liver production prevails in the fetal and perinatal period [218].

The mature protein consists of 165 amino acids resulting in a molecular mass of 30-34 kDa (18 kDa can be assigned the protein portion and the rest depends on amount of attached carbohydrates) [214, 218]. The polypeptide chain is linked through two disulfide bridges, one between cysteines at position seven and 161 and one between cysteines at position 29 and 33 in the amino acid sequence (Scheme 27). About 40 % of molecular mass can be attributed to carbohydrate residues: three N-linked (attached to asparagines at position 24, 38 and 83) and one O-linked (attached to serine at position 126). The carbohydrates (hexoses and N-acetylhexoseamines) induce a high molecular heterogeneity leading to a numerous glycoforms. Several isoforms are formed with respect to sialylation, glycan size, modifications like O-acetylation of sialic acids, deamidation of protein etc. Taichrib et al. [219] presented glycoform profiling of erythropoietin using CE-TOF MS and observed that erythropoietin molecule represents a complex mixture of various naturally occurring isoforms (>100).

Sasakis group [220] conducted a study of carbohydrate structure of human urine and Chinese hamster ovary cell erythropoietin and published interesting results. The N-linked glycans of recombinant erythropoietin are bi-, tri- and tetra-antennary glycans, which typically terminate with sialic acid residues: biantennary (1.4 %), triantennary (10 %), tetraantennary with one N-acetyllactosaminyl repeat (3.5 %), tetraantennary with one (32.1 %), two (16.5 %), or three (4.7 %) N-acetyllactosaminyl repeats. All of these saccharides are sialylated via 2→3 linkages. The O-linked glycans were monosialyl trisaccharide and disialyl tetrasaccharide. There are many published works about recombinant human erythropoietin (rHuEPO) describing the lot-to-lot variability of glycans or differences between various rHuEPO products [219, 220, 221]. Glycans attached to erythropoietin play a key role in the protein bioactivity. Their structure and profiles influence the activity in vivo and in vitro, the half-life in blood and stability of this protein. But also the sialylation of glycans participates in biological activity. Higher sialic acid content induces

prolonged half-life in vivo, the nature of the linkage prevents the clearance of erythropoietin from circulation, if bound to galactose or tetraantennary N-glycans. For that reasons, the glycosylation and sialylation have to be controlled for appropriate erythropoietin function.

Recombinant human erythropoietin was introduced into the market at the end of the 1980s [222]. Since then a large-scale biotechnological production spread this medicinal drug worldwide. Increasing production of biosimilars lead to increased erythropoietin product variations since glycosylation depends on producing organism or culture conditions [223].

In this chapter, an investigation of two erythropoietin forms will be introduced: NeoRecormon – EPO-β (EPO) and its PEGylated form Mircera (pegEPO). As compared to NeoRecormon, due PEGylation the Mircera is an erythropoiesis stimulating agent with reduced specific activity in vitro, increased activity in vivo and also increased half-life. The PEGylation is carried out through integration of an amide bond between methoxypolyethylene glycol-succinimidyl butanoic acid (PEG-SBA with molecular weight around 30 000 g/mol) and either the N-terminal amino group, or the ε-amino group of lysine, predominantly K52 and K45 [224]. This results in a molecular weight of around 60 kDa. The erythropoietin used in the manufacturing process is the active substance of the centrally authorized product (CAP[28]) NeoRecormon (Roche) produced by Chinese hamster ovary cell line. Group of G. W. Somsen [226] studied the structure of NeoRecormon and found out that this molecule possesses 77 different glycoforms even with up to 15 sialic acids attached to some oligosaccharides.

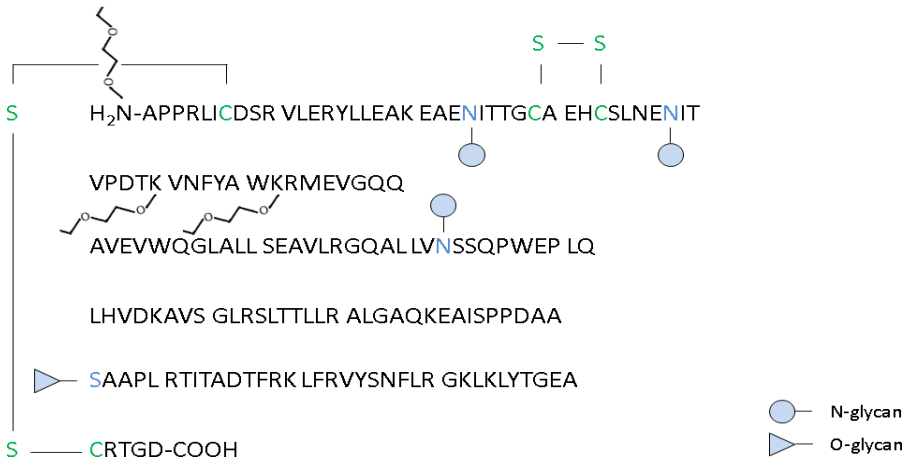

Scheme 27: Amino acid sequence of erythropoietin and its glycosylation, disulfide bonds and PEGylation sites.

[28] CAP products can be marketed in all EU/EEA Member States and undergo a co-ordinated quality control system [225].

Electrophoretic peptide mapping

The procedure for the localization of PEGylation sites using the Lys-C digestion and CZE peptide mapping is explained in the following text and is illustrated on native (P) and PEGylated protein (pegP) in Scheme 28. The endoproteinase Lys-C is a protease that hydrolyses proteins at the C-terminal side of lysine. Lys-C in comparison to trypsin cleaves also lysines followed by prolines [227]. The enzyme digestion is followed by electrophoretic (chromatographic) separation with direct UV detection. The peptide mappings of P and pegP samples are visually compared. If no PEG moiety is attached to the peptide (for example P1) then the area of P1* peptide will be comparable with the area of P1 peptide (if the concentration of P and pegP sample is nearly similar). Partial PEGylation is demonstrated on P2 peptide of pegP. The non-PEGylated P2 of pegP will migrate with the same migration time as P2* in electropherogram. The P2 signal (peak area) will be lower compared to the P2* peptide. The PEGylated P2-PEG will migrate later (as a consequence of the larger hydrodynamic radius) than its native counterpart with typically broader shape. As all synthetic polymers, also PEGs contain polymer chains of unequal lengths – the distribution of PEG chain lengths explains the signal broadening.

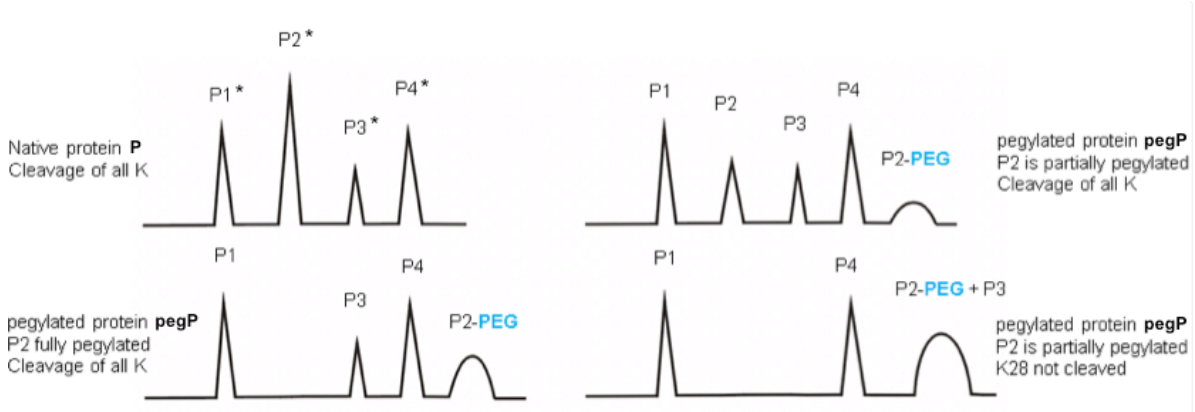

Sequence P/pegP	pI
P1: Y1-K14 YLVCGLALEGSLQK	10.5
P2: R15-K28 RGIVEERGFFYTP**K**	8.3
P3: T29-K38 TRREAEDTPK	6.5
P4: G39-K48 GERGEAEDTP	4.4
K – pegylated K	

Scheme 28: Visualization of Lys-C peptide mapping of native (P) and PEGylated (pegP) protein with 1 PEG molecule at K28 analysed by CZE.

Use of acidic background electrolyte for the CZE separation of Lys-C digested native and PEGylated protein is demonstrated on four exemplary electropherograms in Scheme 28. For native protein a complete enzyme digestion is expected to lead to a formation of four peptides whose signals are separated according to a net charge and hydrodynamic radius

(upper left panel). One PEG molecule bound to the K28 (P2) affects the separation of digested PEGylated protein. The altered (larger) hydrodynamic radius of P2-PEG causes lower electrophoretic mobility and leads to greater migration time (lower left panel) than it can be observed for P2* (upper left panel). Despite of higher pI value (and therefore higher positive charge using acidic running buffer) than P3 and P4, the P2-PEG will be separated most likely behind the P3 and P4 in the basic region. This separation behaviour could be observed, if the enzymatic digest works as expected. Proteins linked to a PEG molecule can be inaccessible for enzymes, because the PEG molecule may turn around the cleavage site or lead to the steric hindrance due a bulky chain, which would cause a limited access of enzyme to the cleavage site [228]. This fact could be resulting in missed cleavage and creation of longer peptide (P2-PEG + P3) as shown in Scheme 28 (lower right panel). It is also important to take into account some aspects of PEGylation. This covalent conjugation can lead to various number of PEG-protein adducts. If the P2 peptide is not fully PEGylated, then the signal for P2 peptide would be still observable (upper right panel). P2 signal will be lower than demonstrated in the native form (P2*, upper left panel) and also other signal – P2-PEG will be present. Partial PEGylation of K28 results in additional PEGylation of other peptide, for example P3 (not shown in Scheme 28). The electrophoretic profile of peptides would be similar to the pep-map of the native counterpart with P2* and P3* signals lower than it was observed for the native counterparts. Also one new signal will be present (P3-PEG) additional to the P2-PEG.

Since the PEGylation of Mircera is predominantly present on lysines, there is a possibility to cleave directly beyond this amino acid using the Lys-C enzyme. Use of an enzyme with other cleavage specificity (for example Glu-C) can lead to incomplete information about PEGylation. This fact is amino acid sequence dependent. If no glutamic acid is present between two PEGylated lysines, only one peptide can be created by Glu-C and the exact localization of PEG attachment will be impossible.

In the case of erythropoietin, the presence of attached glycans and sialylation should be considered. The glycosylation is beneficial for the protein stability, but its presence complicates the direct peptide identification after Lys-C digestion. Therefore the PNGase enzymatic digestion will also be applied to remove the N-glycans. The asparagine residues from which the glycans are removed are simultaneously deaminated, because the PNGase converts the asparagine site [229], within the N-glycosylation sequon (N-X-S/T/C, where X is any amino acid except proline) of glycan attachment to aspartic acid. In case of one deaminated asparagine the mass increment of Δ M = 0.9840 Da will be observable [229].

Therefore other steps are necessary (using PNGase to remove the N-glycans, combination of RP-HPLC with collecting of fractions and MALDI or additional cleavage of

glycosylated peptide by other enzyme and consecutive peptide mapping) to obtain the complete information about Lys-C digested products.

Capillary electrophoresis of erythropoietin

Electrophoretic methods are well suited for quality monitoring of proteins; the glycoproteins could be analysed even further by these techniques (IEF, SDS-PAGE, 2-D PAGE, CE: CZE MEKC, cIEF) [230].

As mentioned above, erythropoietin is a biopolymer with attached carbohydrates via N- and O-glycosidic linkages. Micro-heterogeneity of post-translational modifications in proteins facilitates the separation of a broad range of glycosylated isoforms with high efficiency using a capillary zone electrophoresis or isoelectric focusing [231]. The main features of capillary electrophoresis are the low costs, high speed of analysis and small sample amount, but it is crucial to solve the problem of glycoprotein adsorption onto capillary walls. Insufficient separation efficiency, poor reproducibility of the migration times and peak areas can be dealt by coating of capillary wall with various substances. Targeted on EPO, the application of such chemicals suppresses the glycoprotein adsorption on the capillary surface and control the electroosmotic flow (EOF) [215, 229, 232]. Most of the recent work on CE analysis has been carried out using fused silica capillary and dynamic coating like diaminoalkanes (for example putrescine) [233], UltraTrol LN [234, 235] or carboxymethyl chitosan [236]. There is also possibility to use the amine coated capillary (eCAP) [237], but the costs are much higher than self-prepared dynamic coating.

3.3.2 Materials and Methods

Materials

Test samples used in this study were purchased from Roche: NeoRecormon (EPO) and its PEGylated form Mircera (pegEPO).

Acetic acid, 2,5-dihydroxybenzoic acid (DHB), dithiothreitol (DTT), ε-aminocaproic acid (EACA), ethylenediaminetetraacetic acid (EDTA), hydroxypropyl methylcellulose (HPMC) and 1 M Tris-HCl pH 8.0 were purchased from Sigma. Acetonitrile (ACN), hydrochloric acid (HCl), sodium hydroxide (NaOH) and trifluoroacetic acid (TFA) were purchased from Fluka. Conditioning solution, SDS-MW gel buffer, SDS sample buffer, molecular weight and internal standard (10 kDa) were purchased from AB sciex, RapiGest from Waters, MALDI calibrants PepMix1 (1000-2500), PepMix2 (1500-6000) from LaserBio Labs. Enzyme Lys-C was obtained from WAKO, PNGase F from NEB.

Comassie blue R-250, MES SDS running buffer 20x, LDS Sample buffer, SDS-PAGE, gel, Mark 12 ladder 2.5-200 kDa, Novex Bis-Tris gel 4-12 % were obtained from ThermoFisher.

Fused silica capillary was obtained from CM scientific, 10 kDa filters from Millipore, air displacement pipettes, thermomixer and centrifuge from Eppendorf.

Methods

Lys-C digestion of EPO. Prior to Lys-C digestion, EPO sample was incubated after addition of 50 mM final concentration DTT at 37 °C for 1 h. Current buffer was changed to digestion buffer containing 50 mM Tris-HCl/2mM EDTA, pH 8.0 using 10 kDa filter and centrifugation. Lys-C enzyme was added to the peptide at a ratio 1:20 (w/w), the protein/enzyme mixture was then diluted to a final concentration of 0.8 mg/mL with the digestion buffer and incubated at 37 °C for 4 h.

SDS-PAGE. Gel and 1 gel substitution were mounted on electrophoresis apertures fitted and MES running buffer was introduced into the chambers.

Test samples were mixed with LDS sample buffer and incubated at 70 °C for 10 min. Protein size standard and samples were loaded into wells and the apparatus was attached to the power supply unit. For the first 10 minutes the voltage of 70 V was applied, that allowed the samples to stack, followed by separation using the voltage of 200 V. The electrophoresis was continued until the Comassie blue of ladder reached the bottom of the gel. The gel was rinsed for three five-minute washes with water and the bands were visualised by immersing the gel in a staining solution using gently shacking for one hour. The destaining and fixing step was performed for one hour using acetic acid/methanol/water solution.

Electrophoretic conditions. CZE was carried out on the PA800 Beckman Coulter (AB Sciex) instrument with temperature controlled autosampler on fused silica capillary (40/50 cm 50 µm) with normal polarity (sample components would migrate toward the detector either as cations at pH 2.4. The cathode was at the detector end of the capillary for the analyses with lower pH. The capillary was flushed (by HCl, NaOH and milli-Q water) from appropriate buffer reservoirs using pressure (50 psi) prior to each run. The dynamic coating was applied (conditioning solution, 20 psi) and the capillary was filled with running buffer using pressure (50 psi). The sample was injected using pressure (0.5 psi), the constant voltage of 30 kV was applied and the operation temperature of 25 °C was kept. Electropherograms were UV-monitored at 214 nm and the data were processed with 32 Karat.

Mass spectrometry analyses were carried out in positive mode on Agilent G1600 AX and Bruker microTOF-Q instruments using sheath Liquid: IPA/H_2O 60:40 + 1 % FAc.[29]

CGE-SDS was carried out on fused silica capillary (20/30 cm 50 µm) with reverse polarity. The capillary was flushed (by HCl, NaOH and milli-Q water) from appropriate buffer reservoirs using pressure (70 psi) prior to each run. The capillary was filled with running buffer using pressure (70 psi). The sample was injected using voltage (-5 kV), the constant voltage of -15 kV was applied and the operation temperature of 25 °C was kept.

Chromatographic conditions. Reversed phase chromatography was carried out using an Waters Acquity UPLC with temperature controlled autosampler and vacuum degasser coupled to Thermo Scientific™ Q Exactive™ hybrid quadrupole-Orbitrap.

The analytes were injected onto X-Bridge BEH300 C18 (Waters) column and the flow rate was maintained at 0.2 mL/min. The column was equilibrated with mobile phase A (0.1 % TFA in H_2O). Mobile phase A and mobile phase B (0.1 % TFA in ACN) were used to establish the 120 min gradient as shown in Table 33. The UV chromatograms were obtained by monitoring absorbance at 214 nm and the data were processed with Chromeleon software (Dionex). Peptides were then analysed on the Orbitrap equipped with Thermo Scientific™ HESI-II probe at an electrospray potential of 3.5 kV, S-lens RF Voltage of 60 V and capillary temperature of 275 °C, sheath gas pressure 25 psi, auxiliary gas flow 10 arb units. The Orbitrap was set to perform data acquisition in the positive ion mode (m/z full scan range 200-2000). The most intense ion was selected for Zoom Scan and then for MS/MS by using a data dependent scheme and dynamic exclusion. MS data acquisition was carried out on Thermo Scientific™ Xcalibur™ software. Data analysis was performed using Thermo Scientific™ PepFinder™.

Table 33: Gradient.

time [min]	mobile phase B [%]
0	0
5	0
85	50
86	90
96	90
97	0
120	0

MALDI-TOF. Model MALDI time-of-flight (TOF) mass spectrometer Autoflex 111 from Bruker Daltonics equipped with 200 Hz, Nd:YAG laser was used. Acquisitions were

[29] CZE MS results provided K. Jooss, University Aalen.

performed in positive ion reflectron mode. For all MALDI TOF analyses a saturated DHB matrix was prepared in a mixture of ACN: 1 % aqueous TFA (1:1, v/v). For the sample preparation the volume technique was utilized: 2 µl of matrix and 2 µl of sample solution were mixed thoroughly in an Eppendorf tube prior to deposition onto the stainless steel plate (MTP 384 target plate ground steel). Afterwards, 0.5 µl of the homogeneous solution was deposited on the spot of the sample plate (the solution was dropped onto at least two spots) and let dry under ambient conditions. Acquisition of mass spectra is done in Flex Control (using RP_PepMix method with these parameters: high voltage ion source 1: 20 kV, ion source 2: 18.55 kV, lens 9.0 kV, Delay 0-130 ns, pulsed ion extraction: 200 ns, laser attenuation 50-70 %, in the mass range of m/z 200 to 2000 and 1500 to 5000 and with approximately 1000 laser shots per spectrum). Spectrum processing and annotation was carried out in Flex Analysis.

3.3.3 Results and Discussion

3.3.3.1 Analysis of intact EPO and pegEPO

Capillary zone electrophoresis

Acetic acid represents a running buffer, providing a fast separation with the possibility of MS detection of even minor isoforms [234]. The isoform resolution is apparently sufficient for correct MS identification of the glycans and the possible sample modification as acetylation, oxidation and sulfation [234]. It has been demonstrated, that this technique is useful for carbohydrate characterization and for demonstration of differences between various erythropoietin products or lot-to-lot variability [219].

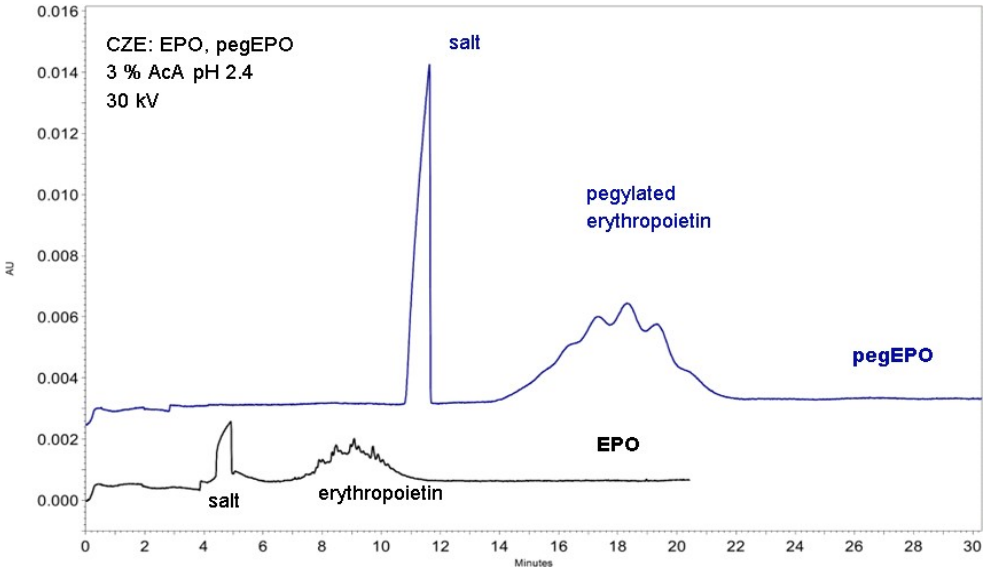

Figure 31: CZE: Full scale UV-electropherogram (214 nm wavelength) overlay for Erythropoietin; EPO and pegEPO (0.8 mg/mL). From bottom trace to top trace: not PEGylated form (black), PEGylated form (blue). Experimental conditions: BGE: 3 % AcA pH 2.4, 40/50 cm 50 µm fused silica capillary, dynamic coating with capillary conditioning solution, separation temperature: 25 °C, separation voltage: 30 kV, injection 0.5 psi 20 s.

Capillary zone electrophoretic (214 nm) profiles of both erythropoietin forms in formulation buffer are demonstrated in Figure 31. Although the employed conditions provided a sufficient resolution of different glycoforms (containing various numbers of sialic acids) of EPO and allowed a direct MS characterization, the not-well resolved charge isoform pattern was not suitable for the evaluation of individual signals. Separation of pegEPO revealed the presence of isoforms, even if they were not completely resolved. The improvement of the peak resolution was not achieved by the utilization of various pH values and concentrations of the acetate running buffer, therefore several BGEs were applied for the analysis of EPO and pegEPO.

As previously described above in chapter 3.2, the CZE can be applied for the separation of charge variants using ε-aminocaproic acid as BGE. Utilization of the EACA method for the investigation of EPO and pegEPO samples can provide several benefits over the introduced methods. Baseline separation of eight isoforms (I1-I8 from the most acidic to the most basic) suitable for the direct analysis of erythropoietin can be achieved using the Pharmacopoeia CZE method [233]. The significant advantage of the EACA method is the avoidance of using special chemicals (the Pharmacopeia method demands sophisticated composition of BGE, consisting of putrescine, tricine and urea). Other method known for EPO isoform separation is the Bietlot-Girard technique [238] using a relatively high ionic strength of 200 mM phosphate applicable also in the presence of human serum albumin as an excipient. Lee and Na [211] reported the use of 100 mM phosphate buffer, pH 2.5 (thus similar conditions as described by Bietlot) for the investigation of PEGylated protein.

There the most appropriate running buffer has been 300 mM EACA, 0.1 % HPMC, pH 4.7. The pH value of BGE was close to the pI value of erythropoietin that was reported as 3.7-4.7 [239]).

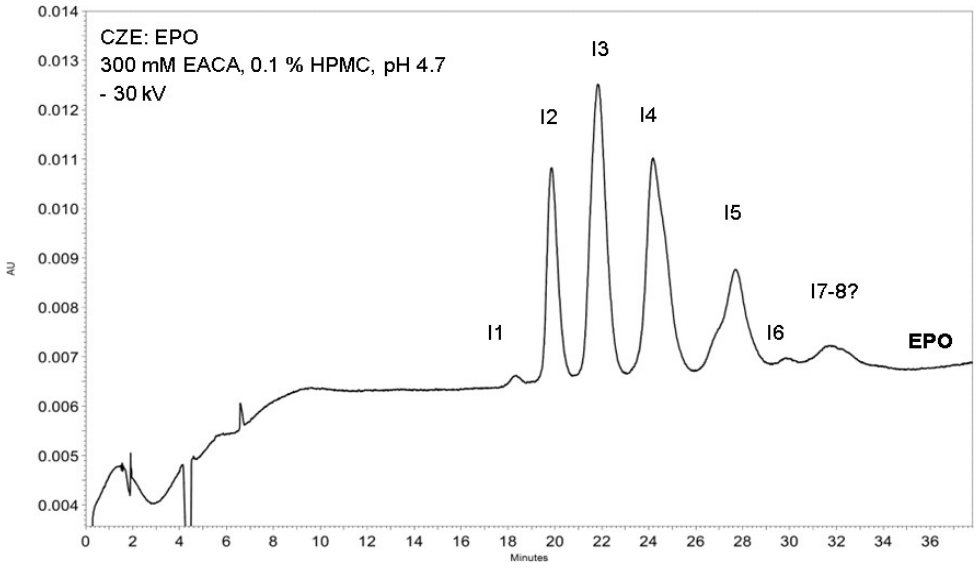

Figure 32: CZE: Full scale UV-electropherogram (214 nm wavelength) of EPO (0.8 mg/mL). Experimental conditions: BGE: 300 mM EACA, 0.1 % HPMC, pH 4.7, 40/50 cm 50 µm fused silica capillary, dynamic coating, separation temperature: 25 °C, separation voltage: -30 kV, injection 0.5 psi 10 s.

EPO was reproducibly separated into 7 isoforms within 35 minutes as apparent from electrophoretic profile in Figure 32. Although the peak resolution of EPO isoforms was comparable to the method described by Bietlot-Girard [238] and was very promising for further investigations of the PEGylated counterpart, its application for the examination of pegEPO was not effective (data not shown). However, also the aforesaid methods could not be employed for direct analysis of pegEPO (the analysis took a long time and the signals were low or missing). Further the conditions (100 mM phosphate buffer) described by Lee and Na [211] were tested. After some experiments with EPO and pegEPO, it has been stated, that the phosphate buffer is not well suited for this product because the molecule very likely precipitates and therefore no signal could be observed (data not shown).

As shown in Figure 31, the acetic acid running buffer was not suitable for the sufficient resolution of EPO and pegEPO isoforms. Further investigations with the ε-aminocaproic acid have shown the potential of this method for the separation of EPO. The conditions that allowed a good visualization of present EPO isoforms did not provided the same for pegEPO. Although CZE is a very powerful method for the separation of PEGylated products [211] and could be effective in separation of PEGylated species from their non-PEGylated counterparts, it is not suitable for every protein. It is important to bear in mind that an improvement of baseline separation of PEGylated peptides and proteins [206, 240, 241] is

not the only problem to solve. Some proteins can precipitate using an inappropriate running buffer, or by applying the voltage; or tend to stick to the capillary wall.

Capillary gel electrophoresis

Na et al. [242] have studied a PEGylated interferon alpha by CGE-SDS and have shown, that this technique has a great potential in size-based separations of PEGylated proteins. As demonstrated below, D. H. Na's method can also be applied for separations of PEGylated glycoproteins from their non-PEGylated forms.

Using SDS as an anionic detergent leads to the linearization of proteins, as previously described in chapter 2.2.1. For glycoproteins the lower than predicted charge-to-mass ratio was observed, which leads to overvaluation of molecular masses. Because the intrinsic charge of single glycoforms is masked, only the mass differences might contribute to the separation. This has the consequence that a successful separation can be obtained only for glycoproteins having large differences between shape, number and site of attached glycans. [243]. The following experiment demonstrates, that the separation of EPO can be still achieved and the explanation for it is seen in the presence of sialic acid anions.

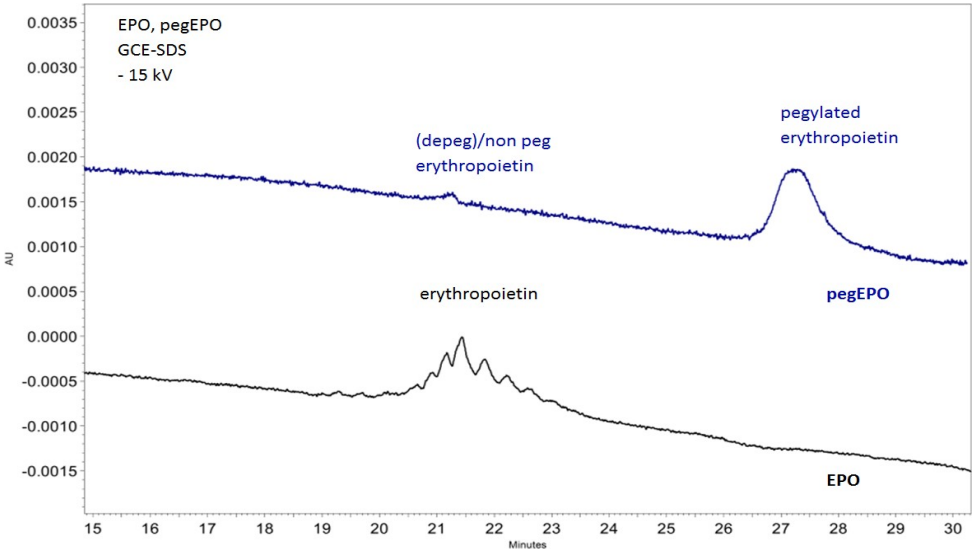

Figure 33: CGE-SDS: Full scale UV-electropherogram (214 nm wavelength) overlay for Erythropoietin; EPO and pegEPO (0.4 mg/mL). From bottom trace to top trace: not PEGylated form (black trace), PEGylated form (blue trace). Experimental conditions: BGE: gel buffer (Beckman), 20/30 cm 50 µm fused silica capillary, separation temperature: 25 °C, separation voltage: -15 kV, injection 5 kV 20 s.

An example of CGE-SDS analysis of EPO and pegEPO is demonstrated in Figure 33. The separation of EPO isoforms (black trace) is clearly visible, but better peak resolution as shown above (Figure 32) was not achieved. Also the low signal of EPO was typical for this method, but use of higher concentration of sample (>0.4 µg/µL) or higher amount of sample

injected into the capillary could solve this problem. It is possible to separate the non-, mono-, di-, tri- etc. PEGylated conjugates from each other based on the different molecular weights using a gel-sieving matrix. This situation represents the pegEPO sample (blue line), where the native (21 min.) and PEGylated forms (27 min.) of size 31 and 61 kDa were completely separated. Separation of isoforms, however, could not be achieved anymore. It was obvious, that only one PEG molecule was attached to the molecule (another signal was not observed having a longer migration time which would be typical for a molecule of higher molecular weight). Only a small signal was detected for non-PEGylated erythropoietin at 21 min. The question, that remained unanswered, was, if this signal represents the molecule that was not PEGylated from the beginning, or if some dePEGylation occurred during the storage over time, or if this was an artefact caused by heating during the test sample preparation.

3.3.3.2 Peptide mapping after Lys-C digestion

As previously described in detail in chapter 3.3.1 (Electrophoretic peptide mapping) the digestion of the molecule into smaller peptides followed by electrophoretic separation allows the detection of PEG moieties.

The Lys-C cleavage of EPO (pegEPO) yields peptides of different lengths as demonstrated in Scheme 29. The physicochemical properties (mass and pI value) of newly created peptide fragments after Lys-C digest are listed in Table 34. The masses and pI values were calculated for their amino acid sequences only, without additional attachments of oligosaccharides and sialic acids.

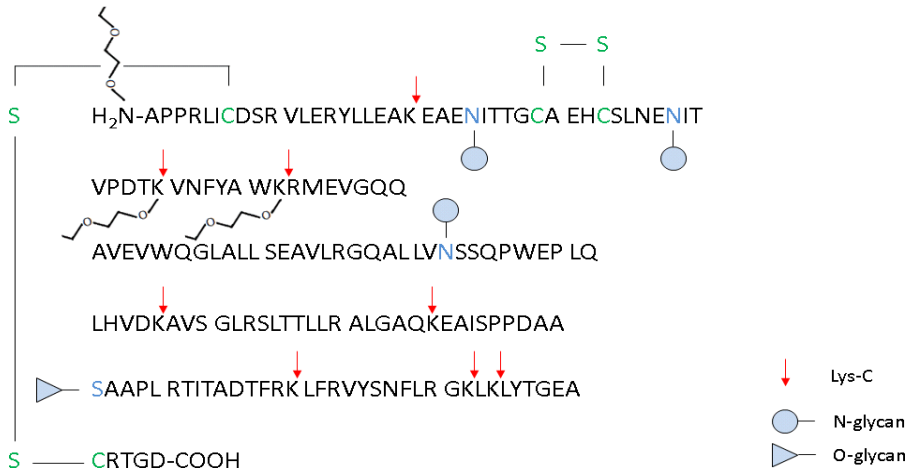

Scheme 29: PEGylated glycosylated erythropoietin with expected Lys-C cleavage sites.

Table 34: Calculated [131] monoisotopic masses and pI values for in-silico Lys-C digested EPO/pegEPO (without attached oligosaccharides and sialic acids). Blue highlighted pI values represent the peptide properties after removing of glycans.

Peak name / Sequence	Mass [Da]	pI
P1: A1-K20 **N**H_2-APPRLICDSRVLERYLLEAK	2341.29	8.24
P2: E21-K45 EAENITTGCAEHCSLNENITVPDT**K**	2688.20	4.25
P3: V46-K52 VNFYAW**K**	927.07	8.56
P4: R53-K97 RMEVGQQAVEVWQGLA LLSEAVLRGQALLVNSSQPWEPLQLHVDK	5021.65	4.96
P5: A98-K116 AVSGLRSLTTLLRALGAQK	1954.17	12.01
P6: E117-K140 EAISPPDAASAAPLRTITADTFRK	2498.31	6.22
P7: L141-K152 LFRVYSNFLRGK	1498.84	11.00
P8: L153-K154 LK	259.19	8.75
P9: L155-D165 LYTGEACRTGD	1184.51	4.37

X – PEGylated site; N, S – glycosylation (+ sialic acids), C – disulphide bridges

Firstly, the digestion procedure was monitored by SDS-PAGE as demonstrated in Figure 51. The molecular weight size marker was used for the calibration of the gel. Blank in the fourth lane represents a digestion mixture without test sample. Lys-C was identified based on the knowledge of the molecular size (33 kDa, [244]). As a result of attached glycans the band representing EPO migrates with an apparent molecular mass of about 40 kDa (lane five and six). Because only the traces of intact EPO were observed after the incubation of four hours (lane eight), this digestion period was chosen for further experiments.

HPLC-HESI-MS, MALDI-TOF

In order to precisely affirm the conjunction of PEG moiety to the individual peptides the reversed phase high-performance liquid chromatography directly coupled to the mass spectrometer (and also UV detector) was utilized. The chromatographic conditions for EPO Lys-C peptide mapping reported previously in [245, 246] were optimized with respect to the highest peak resolution, (needed for fraction collection).

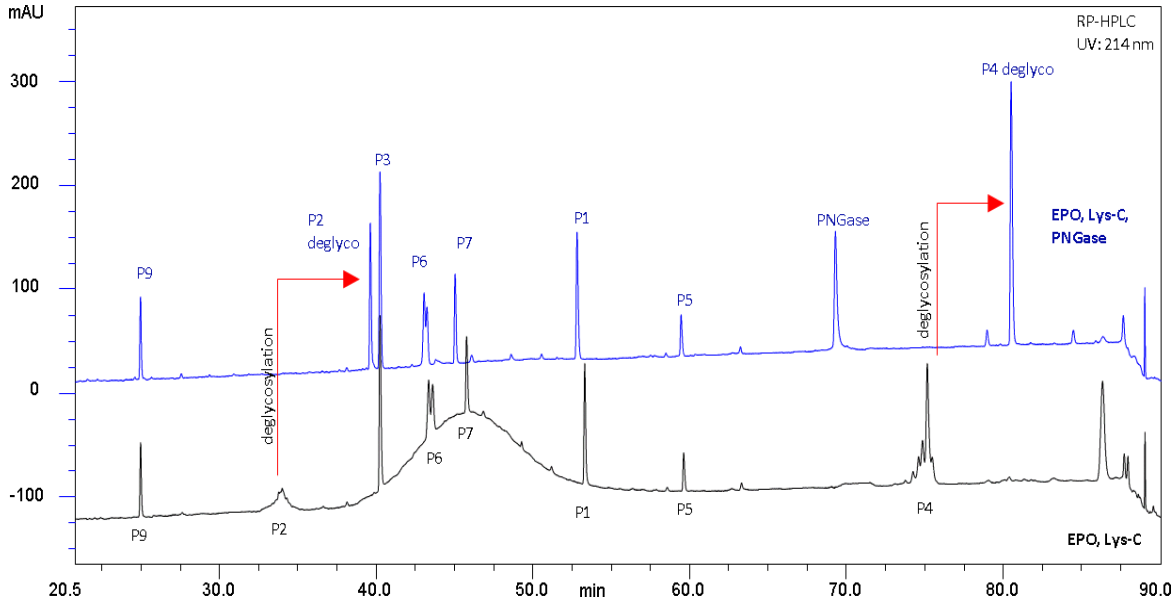

Figure 34: Zoomed UV-chromatogram (20-90 min, 214 nm wavelength) of Lys-C (black trace), and Lys-C, PNGase (blue trace) digested EPO (c_{end}= 0.7 µg/µL). Experimental conditions: X-Bridge BEH300 C18, 3.5 µm, 2.1 x 150 mm column, H_2O/ACN with 0.1 % TFA, flow rate 0.2 mL/min, column temperature 50 °C.

After the RP-HPLC separation and the MS analysis the non-glycosylated signals were directly assigned to the peptide fragments (P1, P3, P5, P7, P8, P9 – with retention time of 9 min, the P8 was not visible in the zoomed chromatogram) as illustrated in Figure 34. The observed molecular masses are listed in Table 35. The instability of the baseline was induced by an interruption of the blank injection before the EPO, Lys-C sample run and did not have any impact on the peak areas of single signals (based on results from earlier experiments with LTQ-DECA – data not shown). The glycopeptides of EPO, Lys-C sample (black trace) eluted as typically broader peaks (resulting from heterogeneous glycans). To identify the N-glycosylated peptides directly by HPLC-MS the PNGase digestion was performed after the Lys-C protein hydrolysis (blue trace). It was expected, that deglycosylated peptides elute later than their glycosylated counterparts [247], because the deglycosylation increases the hydrophobicity of the peptides carrying glycans. This shift was observed for P2 (34 min) and P4 peptides (75 min). P2 peptide with two attached glycans at N24 and N38 eluted at 40 min after PNGase treatment (blue trace). Because the mass increment of about 2 Da was observed the deamination of both asparagines to aspartic acids could be authenticated. The similar situation was also seen after deglycosylation of P4 at 80 min with only one deamidated asparagine. All peptides were collected as single fractions for further spiking experiments and their masses were double-checked by MALDI-

TOF for eventual presence of some impurities. The PNGase digestion was also applied for the glycan hydrolysis from two collected fractions followed by MALDI-TOF analysis[30].

The fraction of the presumed P6 peptide (43 min) with attached O-glycans was investigated by MALDI-TOF MS. As demonstrated in chapter 7, Figure 53 the typical O-glycan fragmentation pattern -18/+203/+162 could be obtained; despite of low signals. Resemann [251] demonstrated the MALDI MS spectra using the Anchorchip plate with hydrophilic anchors, but the cleavage between galactose, N-acetylgalactosamine and the peptide with an additional loss of water was also detected in our experiment. The non-glycosylated form of Peptide 6 is also present as a low signal at 47 min. The presence of further low signals is induced by nonspecific cleaved peptides in negligible or very small amounts.

Table 35: Matching theoretical m/z values [131] with observed masses and corresponding sequences in Lys-C (PNGase) digested EPO/pegEPO (HPLC-HESI-MS).[31]

Peak name	t_R [min]	Calculated m/z	Measured m/z	Sequence
P5 f1	17.45	587.34^{1+} / 294.18^{2+}	587.36^{1+} / 294.18^{2+}	ALGAQK
P5 f2	18.53	743.44^{1+} / 372.22^{2+}	743.45^{1+} / 372.23^{2+}	RALGAQK
P5 f3	22.50	602.35^{1+} / 301.68^{2+}	602.36^{1+} / 301.69^{2+}	AVSGLR
P2 f1*§	24.47	538.25^{2+}	538.31^{2+}	EDITTGCAEH
P9	25.00	1185.5^{1+}	1185.52^{1+}	LYTGEACRTGD
P7 f2	27.67	821.46^{1+}	821.46^{1+}	SNFLRGK
P2 trunc*§	33.00	1281.57^{2+}	1281.60^{2+}	AEDITTGCAEHCSLN EDITVPDTK
P2f2	33.50	537.72^{2+}	537.77^{2+}	ENITTGCAEH
P1 f3	31.97	736.42^{1+}	736.42^{1+}	YLLEAK
P1 f4	32.32	892.52^{1+} / 446.76^{2+}	892.52 / 446.77^{2+}	RYLLEAK
P1 f5	32.71	564.30^{2+}	564.30^{2+}	APPRLICDSR
P1 f6	39.0	617.36^{2+}	617.36^{2+}	VLERYLLEAK
P2*	39.45	897.73^{3+}	897.52^{3+}	EAENITTGCAEHCSL NENITVPDTK
P1 f7	39.95	812.96^{2+}	812.95^{2+}	APPRLICDSRVLER
P5 f4	34.15	903.52^{1+} / 452.26^{2+}	903.53^{1+} / 452.27^{2+}	AVSGLRSLT

[30] Singly and doubly charged ions of deglycosylated P4 are demonstrated in Figure 52. This RP-HPLC fraction was treated by PNGase to remove the glycans and analysed in presence of 2,5-dihydroxybenzoic acid (DHB). This commonly used water soluble MALDI matrix [248] is suitable for protein digests, small proteins and glycopeptides below 10 kDa building large heterogeneous white crystal needles [249] in presence of acetonitrile (ACN) and trifluoroacetic acid (TFA). TFA added to the matrix solution in a concentration of 0.1 % assists the protonation of peptide/protein and serves for better ionization of studied molecule [250].

[31] OrbiTrap typical accuracy +/- 2 ppm.

Peak name	t_R [min]	Calculated m/z	Measured m/z	Sequence
P5 f5	34.85	802.47^{1+}	802.48^{1+}	AVSGLRSL
P5 f6	37.30	535.83^{2+}	535.84^{2+}	TLLRALGAQK
P3	40.35	927.07^{2+}	927.47^{2+}	VNFYAWK
P6	46.93	1250.16^{2+} / 833.7^{3+}	1250.66^{2+} / 834.11^{3+}	EAISPPDAASAAPLRT ITADTFRK
P7	45.81	1499.84^{1+} / 750.42^{2+}	1500.85^{1+} / 750.43^{2+}	LFRVYSNFLRGK
P7 f5	38.18	697.40^{1+} / 349.20^{2+}	697.40^{1+} / 349.21^{2+}	LFRVY
P7 f6	41.17	693.88^{2+}	693.89^{2+}	FRVYSNFLRGK
P7 f7	47.96	657.86^{2+}	657.87^{2+}	LFRVYSNFLR
P5f7	50.00	686.41^{2+} / 457.94^{3+}	686.42^{2+} / 457.95^{3+}	SLTTLLRALGAQK
P1	53.36	1171.65^{2+} / 781.77^{3+}	1172.16^{2+} / 781.77^{3+}	APPRLICDSRVLERYL LEAK
P5	59.67	978.09^{1+}	978.09^{1+}	AVSGLRSLTTLLRAL GAQK
P5 f8	62.96	785.98^{2+} / 524.32^{3+}	785.99^{2+} / 524.32^{3+}	AVSGLRSLTTLLRAL
P4*	75.58	1256.91^{4+} / 1005.53^{5+}	1257.04^{4+} / 1005.71^{5+}	RMEVGQQAVEVWQ GLA LLSEAVLRGQALLVN SSQPWEPLQLHVDK

$^{1+}$ z = 1, $^{2+}$ z = 2 etc.; * PNGase, §pegEPO.

Further experiments were performed with PEGylated substance, after the peptide identification of the non-PEGylated sample has been carried out. The presence of PEG moieties is highly expected in P1, P2 and P3 peptides as specified by the manufacturer and illustrated in Scheme 29.

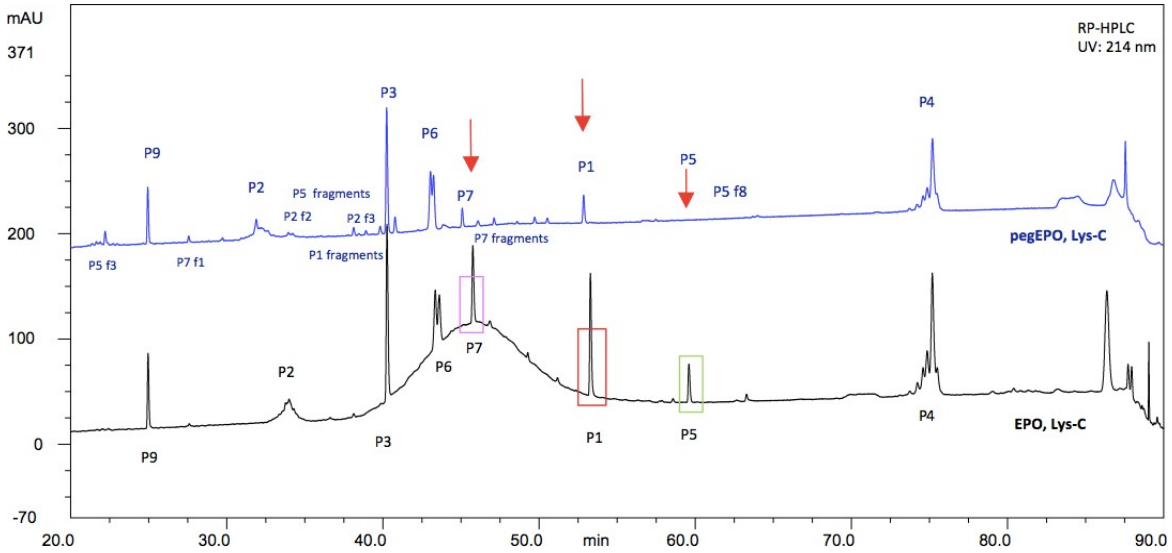

Figure 35: Full scale UV-chromatogram (214 nm wavelength) of Lys-C digested EPO (black trace) and pegEPO (blue trace) (c_{end}= 0.7 µg/µL). Experimental conditions: X-Bridge BEH300 C18, 3.5 µm, 2.1 x 150 mm column, H_2O/ACN with 0.1 % TFA, flow rate 0.2 mL/min, column temperature 50 °C.

As illustrated in Figure 35 (blue trace), besides the presence of main signals, nonspecific cleaved peptide fragments were detected. The first impression may lead to the assumption that P1, P5 and P7 can be PEGylated, because the P1, P5 and P7 pegEPO, Lys-C signals are significantly reduced in comparison with EPO, Lys-C sample. The Peptide 5 (blue trace, 60 min) was even completely degraded and no remaining signal was present. Closer examination of the amino acid sequences around the nonspecific cleavage sites revealed that the Lys-C digestion yielded many peptides cleaved at the arginine residues (1/3 of all identified signals) using the above introduced digestion conditions. Gershon and Raijimakers [252, 253] have studied the Lys-C and Lys-N hydrolyses of different substrates, but only the Lys-N enzyme exhibited some arginine specificity. Jekel et al. [254] demonstrated in their study the Lys-C cleavage of two different arginine bonds on ribonuclease. Protein PEGylation may explain the presence of larger quantity of the nonspecific cleaved fragments in the pegEPO sample. The attached PEG molecule acts as a barrier and the enzyme is not capable of reaching its typical cleavage site, therefore some other amino acid will be attacked for so long until the nonspecific hydrolysis will not be completed.

The presence of numerous non-specific fragments besides the expected P1-P9 signals makes the calculation of the PEG molecule occupancy (PEGocc, Table 36) more difficult. Therefore the results predicate more of the PEGylation trend than of the exact PEGocc. Despite of this fact, we tried to calculate the PEGocc for every peptide. For the determination of the PEG molecule occupancy (PEGocc), a stable signal (without attached PEG moiety) has to be chosen as a reference. The lowest probability of PEG attachment was presumed for the P9 because no lysine is present in the amino acid sequence of this peptide. Practically no nonspecific cleaved P9 fragments were observed in this RP-HPLC analysis. Each peptide was individually compared to the P9 (P1/P9, P2/P9 and so forth) resulting in the area percentages of P1-P7 (P8 was excluded for its low signal) as listed in Table 36. Areas of nonspecific cleaved fragments were summed with corresponding main signals. The pair area percentages (EPO P1 A% - pegEPO P1 A%, EPO P2 A% - pegEPO P2 A% etc.) of both samples were used for the evaluation of PEGocc of pegEPO (Table 36). Peptide 6 was excluded from the evaluation, because the pegEPO A % of P6 was higher than the value of the non-PEGylated form. Some nonspecific cleaved fragments co-eluted with P6 and caused increase of the peak area. For the calculation of P5 A% the signals of nonspecific cleaved P5 fragments were summed with the specific digested P5 signal. The same principle was applied for the calculation of P7 A%. Results in Table 36 point at high PEGocc of peptides P1 and P5. From the results can also be derived that only a minute amount of PEG is attached to the other peptides leading to a total PEGocc of 86 %. The missing 14 % may be comprised of P6, because the PEGylation of P6 could not be

evaluated. As described by the manufacturer [224], the PEGylation of P1 (N-terminal amino group) and also of P2 (K45) and P3 (K52) can be expected. The high value of PEGocc of P5 is slightly surprising, but as mentioned in chapter 3.3.1, it is difficult to control the attachment process of the PEG moiety to the molecule [206, 207].

Table 36: Area percentage of single peptides of Lys-C digested EPO and pegEPO (Figure 35) and PEGocc over single peptides (P9 as reference signal) analysed by RP-HPLC.

HPLC	EPO	pegEPO	PEGocc/P9[32]
Peptide	A % [Px/P9]	A % [Px/P9]	
P1	66.1	36.6	0.45
P2	72.0	68.7	0.05
P3	74.1	71.9	0.03
P4	86.7	83.4	0.04
P5	58.3	41.0	0.30
P6	70.7	74.8	-
P7	50.2	50.4	0.00
total			**0.86**

Furthermore the PEGocc can be calculated from the deglycosylated samples. The removal of N-linked oligosaccharides from glycoproteins leads to the creation of narrow peaks (P2 and P4) and allows the detection of possible non-specific cleaved peptides. These signals would co-elute with broader glycopeptides and could not be later used for calculation of PEGocc. Therefore the EPO and pegEPO were deglycosylated using PNGase F after Lys-C digestion. The resulting peptides were investigated by RP-chromatography. The peak areas of EPO and pegEPO peptides were used for the calculation of PEGocc.

[32] PEGocc calculation: $100 - \frac{\text{! \% !"\#\$\%\&}}{\text{!\% !"\#}} \cdot 100$

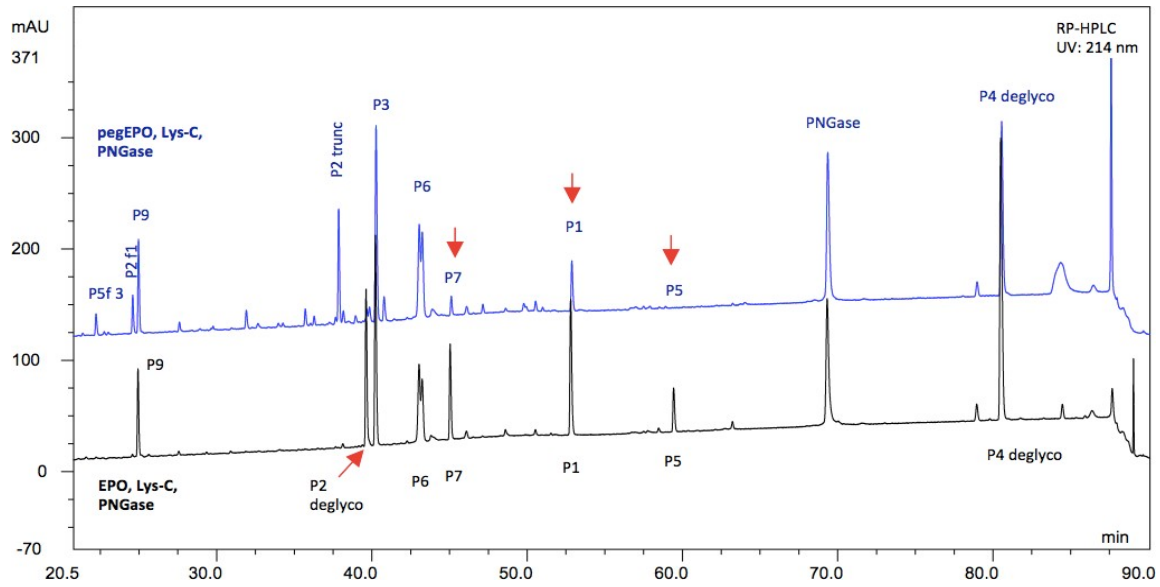

Figure 36: Full scale UV-chromatogram (214 nm wavelength) of Lys-C, PNGase digested EPO and pegEPO (c_{end}= 0.7 µg/µL). Experimental conditions: X-Bridge BEH300 C18, 3.5 µm, 2.1 x 150 mm column, H_2O/ACN with 0.1 % TFA, flow rate 0.2 mL/min, column temperature 50 °C.

Many similarities were observed after comparing the data of deglycosylated Lys-C digested EPO (black trace) and pegEPO samples (blue trace) in Figure 36. The greater quantity of nonspecific cleaved fragments was obvious also in the deglycosylated Lys-C digested pegEPO sample. The PNGase treatment of Lys-C digested pegEPO led to a formation of N-terminal truncated peptide P2 (P2 trunc, 38 min) and further P2 variants (24.5 min, 39.5 min). The N-terminal P2 truncation could be explained by the attached PEG moiety to this peptide. It can be calculated if the area of the P2 peptide has been effectively reduced. The area of the truncated peptide was converted to the area, which this signal would have as a non-truncated. Because the detection wavelength of 214 nm was used, the area of non-truncated peptide can be calculated from the known truncated peptide using the number of peptide bonds as shown in the following equation:

$$A_{!"!!!"\#\$\%} = \frac{!_{!"\#\$\%}}{!"_{!"\#\$\%}} \cdot PB_{!"!!!"\#\$\%} \qquad (3.1)$$

where A is the area of peptide and PB is the amount of peptide bonds in peptide.

The recalculated area of the P2 trunc (non-truncated) was summed with the area of the P2 (and present fragments) giving the total P2 area needed for the comparison with P9. The evaluation of the single peptides compared to the P9 is listed in Table 37. The pegEPO A % of P6 was higher than the value of non-PEGylated form and was excluded from the evaluation (observed also for EPO P6, Table 36). For the calculation of A % of P5 (P7) the corresponding nonspecific cleaved fragments were summed with the specific digested P5 (P7). The results in Table 37 demonstrate a high amount of attached PEG molecule to P1

and P5 peptides, also observed for the Lys-C digested molecule (Table 36), but some differences between the results were noticed. Peptide P1 (Lys-C) seems to be PEGylated from 45 % whilst P1 (Lys-C, PNGase) only from 41 %. In case of P5 the difference became even more distinct (30 % of attached PEG to Lys-C P5 and 38 % of attached PEG to Lys-C, PNGase P5). An increase of PEGocc of 8 % was also observed for deglycosylated P4. Please note, the co-elution of some signals has been observed (mainly nonspecific cleavage fragments) influencing the measure of A% P1-P9 by up to several A %. The total PEGocc of 104 % (Table 37) differs from the observation in Table 36 (86 %), where only Lys-C digested samples were evaluated.

Table 37: Area percentage of single peptides of Lys-C, PNGase digested EPO and pegEPO (Figure 36) and PEGocc over single peptides (P9 as reference signal) analysed by RP-HPLC.

HPLC	EPO	pegEPO	PEGocc/P9[33]
Peptide	A % [Px/P9]	A % [Px/P9]	
P1	65.8	38.7	0.41
P2	66.3	64.1	0.03
P3	73.8	71.0	0.04
P4	83.6	73.6	0.12
P5	56.2	35.0	0.38
P6	70.7	74.6	-
P7	43.5	43.3	0.00
total			**1.04**

CZE-UV, CZE-ESI-MS

The presence of PEG moieties was further investigated by capillary zone electrophoresis. The individual peptides, created by Lys-C digestion were separated using various buffer systems until the best peak resolution was achieved. As illustrated in Scheme 28, the great advantage of CZE over RP-HPLC is the possibility of the visualization of attached PEGs. In addition to the presence of the native peptides also their PEGylated variants can be expected in the electropherogram. The distinguishing characteristics that make the PEGylated variants clearly recognizable from non-PEGylated ones are broader peaks and higher migration times. Later also the PNGase digested samples will be introduced.

As indicated in Table 34 some peptides have similar pI values. Additionally, three glycopeptides (P2, P4 and P6) are sialylated and have therefore lower pI values than stated in table. Using acetate at pH 2.5 as running buffer the sialylated glycopeptides will be

[33] PEGocc calculation: $100 - \frac{\text{! \% !"\#\$\%\&}}{\text{!\% !"\#}} \cdot 100$

separated with higher migration times than P1, P3, P5, P7 or P9 peptides. As specified by the manufacturer, the presence of PEG moieties is highly expected in P1, P2 and P3 peptides (as illustrated in Scheme 29). Performing the Lys-C cleavage of EPO and pegEPO samples, then in the case of the presence of PEG moieties attached to P1 and P2, these peaks are also expected in pegEPO, Lys-C sample. Peptides P1, P2 will appear with lower intensity than P1 and P2 of EPO, Lys-C sample and in addition to these signals also pegP1 and pegP2 should be observed with in the electropherogram (with typically broader shape and higher migration time than non-PEGylated peptides). It is important to take into account that the presence of PEG moieties could restraint the access of the enzyme to the cleavage site. This can result in the creation of the non-specific cleaved peptide pegP1-pegP2 as previously shown in Scheme 28 and discussed below the scheme. The presence of sialic acids attached to the P2 peptide may also have an effect on the quantity of P2 signals (non-PEGylated and PEGylated).

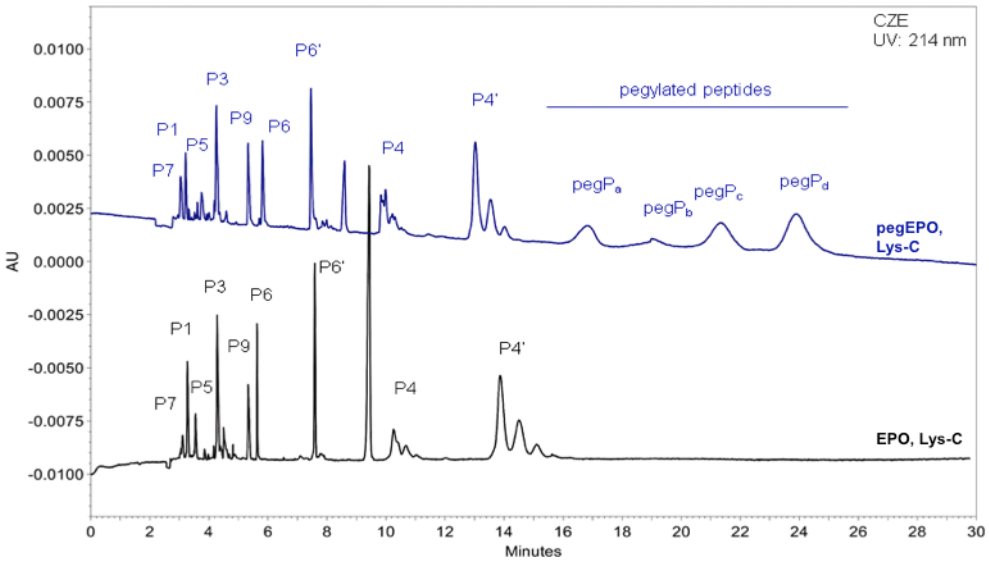

Figure 37: Full scale UV-electropherogram (214 nm wavelength) of Lys-C digested EPO and pegEPO (c_{end} = 0.7 µg/µL). Experimental conditions: BGE: 3 % AcA pH 2.4, 40/50 cm 50 µm fused silica capillary, dynamic coating with capillary conditioning solution, separation temperature: 25 °C, separation voltage: 30 kV, injection 0.5 psi 20 s.

The capillary zone electropherograms of the Lys-C digested EPO and pegEPO are shown in Figure 37. The separation profiles of both analytes are similar except for the presence of PEGylated signals of pegEPO. The pI values based pre-assignment of the signals to the single peptides was not possible. The first identification of peptides was performed by spiking of single high concentrated RP-HPLC fractions leading to the signal increase of respective peaks. The peptides P1, P3, P5, P7 and P9 were identified as single signals. P4 is present at 10.5 and 14.0 min representing a glycopeptide differing by the number of sialic acids. The variability of each signal (oligosaccharide pattern) is given by the

antennary complexity. Similar situation as for P4 was observed for P6 peptide (where two P6 peaks were separated at 5.8 and 7.8 min). The identity of P4 and P6 peptides was also verified by the spiking experiment.

Spiking of the Peptide 2 fraction did not induce an increase of any peak signal height. Using negative polarity or acidic phosphate buffer were not beneficial, the signal was not present. The peak assignment was later verified using the more elegant tool: CZE-ESI-MS[34] and the results are summarised in Table 38. Also the MS data evaluation did not confirm any presence of P2 peptide in the electropherogram. The CZE peptide mapping of the Lys-C digested pegEPO (blue trace) showed many similarities to the HPLC analysis (Figure 35, blue trace). The presence of a few nonspecific cleaved fragments (primary P5 and P7) was detected, although any of them could not be separated clearly from other signals. However, the CZE run compared to the RP-HPLC offers an excellent visualization of PEGylated signals and therefore might be considered as preferred tool for the comparison of reference with its PEGylated conjugate. There are at least four signals present symbolizing the PEGylated peptides labelled as $pegP_a$ - $pegP_d$ between 25-55 min. Comparing the non-PEGylated signal intensities of EPO and pegEPO Lys-C digested samples, the signal reduction is obvious for P1 and P5 in pegEPO, Lys-C sample. These two peptides can be represented e.g. by $pegP_a$ and $pegP_b$ signals at 17 and 19 min. As introduced above, it is highly expectable that PEG moiety is attached to the P2 peptide. The sialylation of P2 could lead to the observation of two P2 signals (as it can be seen for P4 and P6 peptides) after electrophoretic separation. Therefore it can be presumed that the remaining PEGylated peaks $pegP_c$ and $pegP_d$ represent the variously sialylated forms of PEG-P2 peptide.

Table 38: Matching theoretical m/z values [131] with observed masses and corresponding sequences in Lys-C (PNGase) digested EPO/pegEPO (CZE-ESI-MS).[35]

Peak name	t_m [min]	Calculated m/z	Measured m/z	Sequence
P7	3.0	750.42^{2+}	750.38^{2+} / 500.59^{3+}	LFRVYSNFLRGK
P1	3.2	781.77^{3+} / 586.57^{4+}	781.73^{3+} / 586.55^{4+}	APPRLICDSRVLERYLLEAK
P5	3.5	489.55^{2+}	489.67^{2+}	AVSGLRSLTTLLRALGAQK
P7 f7	3-5	657.86^{2+} / 438.57^{3+}	657.83^{2+} / 438.89^{3+}	LFRVYSNFLR
P1 f6	3-5	617.36^{2+}	617.32^{2+}	VLERYLLEAK
P5 f1	3-5	587.34^{1+}	587.32^{1+}	ALGAQK
P5 f3	3-5	602.35^{1+}	602.32^{1+}	AVSGLR
P5 f7	3-5	686.41^{2+}	686.38^{2+}	SLTTLLRALGAQK

[34] CZE MS results provided K. Jooss, University Aalen.

[35] Micro-TOF typical accuracy +/- 100 ppm.

Peak name	t_m [min]	Calculated m/z	Measured m/z	Sequence
P7 f6	3-5	693.88^{2+}	693.88^{2+}	FRVYSNFLRGK
P7 f5	3-5	349.20^{2+}	349.19^{2+}	LFRVY
P1 f3	3-5	736.42^{1+}	736.37^{1+}	YLLEAK
P2 f1*§	6.0	538.25^{2+}	538.31^{2+}	EDITTGCAEH
P3	4.2	464.04^{2+}	464.21^{2+}	VNFYAWK
P9	5.7	593.25^{2+}	593.23^{2+}	LYTGEACRTGD
P6	5.8, 7.8	833.77^{2+} / 626.08^{3+}	834.06^{2+} / 625.80^{3+}	EAISPPDAASAAPL RTITADTFRK
P4*	6.0	1257.41^{4+} / 1006.13^{5+}	1257.43^{4+} / 1005.95^{5+}	RMEVGQQAVEVW QGLA LLSEAVLRGQALLV NSSQPWEPLQLHV DK
P2*	7.5	897.73^{3+}	897.40^{3+}	EAEDITTGCAEHCS LNEDITVPDTK

$^{1+}$ z = 1, $^{2+}$ z = 2 etc.; * PNGase; § pegEPO.

As previously seen in the HPLC section, for the calculation of the PEGocc the area percentages of single peptides were matched. Corrected areas of EPO (pegEPO) peptides were compared with corrected area of P9 resulting in e.g. A_{corr} % of P1 EPO and A_{corr} % of P1 pegEPO as listed in Table 39. Then the PEGocc in pegEPO could be calculated. Peptide 2 was not detected in electropherogram (Figure 37) and therefore its evaluation was not possible. As previously seen in Table 36 the A_{corr} % of pegEPO Peptide 6 was higher than A % of EPO P6. If there is no attached PEG moiety present on P6 lysine then the peak areas have to be comparable. A decrease in peak area of pegEPO would point at PEG linked to this peptide whereas an increase of pegEPO signal is not expected and could be explained by different sialylation of P6 of both samples. These two erythropoietin samples were produced as two different batches and slight lot-to-lot variability could be observed between these products. The second explanation for this observation might be a presence of a co-migrating signal with pegEPO P6 peptide increasing the corrected area of this signal. The results in Table 39 indicate the PEGylation of predominantly P1 and P5 peptides. It was not possible to sum all the P1 and P5 peptide fragments with their main signals, because some of them co-migrated with other nonspecific cleaved fragments. This fact led to differences in PEGocc of P1 and P5 between HPLC and CZE results. Minute amount of attached PEG molecule was detected for P3 and P4 peptide, P7 seems to be non-PEGylated.

Table 39: Area percentage of single peptides of Lys-C digested EPO and pegEPO and PEGocc (Figure 37) over single peptides (P9 as reference signal) analysed by CZE.

CZE	EPO	pegEPO	PEGocc/P9[36]
Peptide	A_{corr} % [Px/P9]	A_{corr} % [Px/P9]	
P1	49.2	33.9	0.31
P2	-	-	-
P3	63.6	60.6	0.05
P4	92.2	90.3	0.02
P5	29.3	15.8	0.46
P6	72.3	74.0	-
P7	34.1	34.2	0.00
total			**0.86**

Results are reported as the means of triplicate determinations.

Applying the PNGase enzyme to the Lys-C digested EPO a migration time shift of the N-deglycosylated peptides is expected. This effect can be observed due to loss of a negative charge caused by the removal of sialic acids attached to glycans. Using acetic acid at pH 2.5 as BGE and positive polarity, these deglycosylated peptides are separated with lower migration times than their glycosylated/sialylated counterparts (please note, P2 peptide was not found in Lys-C digested sample).

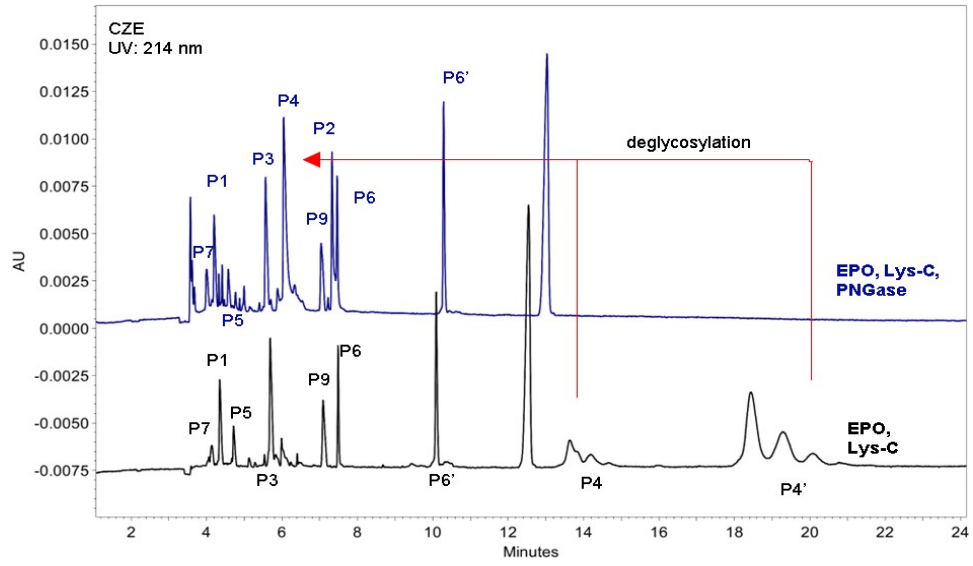

Figure 38: Zoomed UV-electropherogram (214 nm wavelength) of Lys-C and Lys-C, PNGase digested EPO (c_{end}= 0.7 µg/µL). Experimental conditions: BGE: 3 % AcA pH 2.4, 40/50 cm 50 µm fused silica capillary, dynamic coating with capillary conditioning solution, separation temperature: 25 °C, separation voltage: 30 kV, injection 0.5 psi 20 s.

[36] PEGocc calculation: $100 - \frac{!\ \%\ !"\#\$\%\&}{!\%\ !"\#} \cdot 100$

The peptide mapping of the deglycosylated EPO Lys-C digested sample is demonstrated by the blue trace in Figure 38. This sample treatment led to visible changes in the migration pattern of peptide P4. This pair of signals is visible between 13 and 22 min (black trace) migrates after deglycosylation as a single signal (6 min, blue trace). Besides the P4 peptide migration time shift, there is also another new signal noticeable between P9 and P6 after PNGase digestion. After CZE-MS analysis this peak was identified as P2. As previously shown in Table 34 the peptides P2 and P9 are part of the group of acidic peptides having pI values of 4.25 and 4.37 respectively. Using the above described separation conditions; both of them migrate as weak cations (behind the peptides with high pI values which are carrying strong positive charges).

The deglycosylated pegEPO Lys-C sample was subject to further electrophoretic investigation. Although nowadays it is possible to characterize the PEGylated proteins directly using the newest generation of Orbitrap instruments [255] such state-of-the-art instrument for online CZE-MS identification of PEGylated signals was not available. As previously demonstrated above (Figure 38), the deglyco peptide variants of EPO are separated with lower migration times than their glycosylated counterparts. The same principle can be expected for the glycopeptides with attached PEG moieties ($pegP_a$ - $pegP_d$). Such migration time shift would represent very likely one of the two-glycosylated peptides: P2 or P4 (PNGase does not hydrolyse the O-linked glycans of P6).

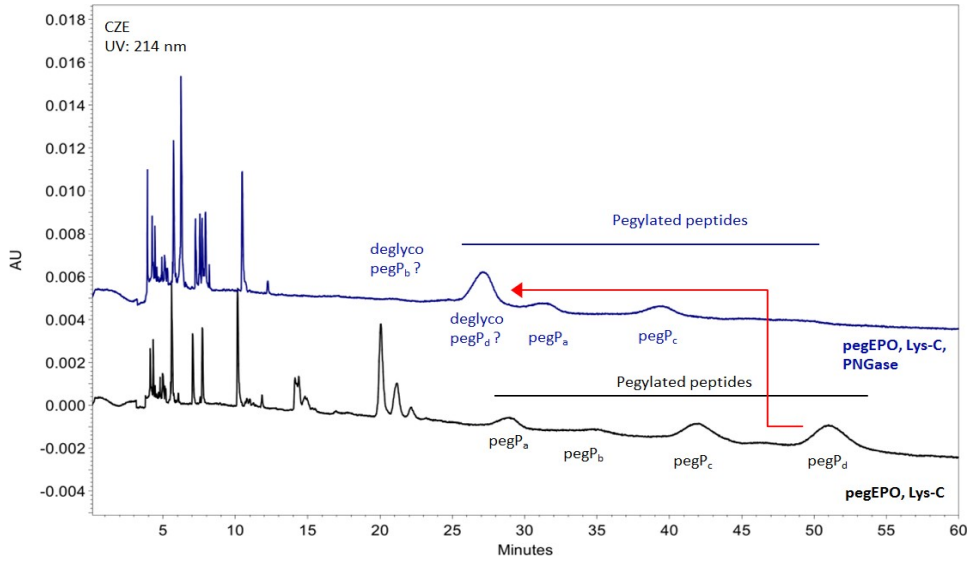

Figure 39: Full scale UV-electropherogram (214 nm wavelength) of Lys-C and Lys-C, PNGase digested EPO (c_{end}= 0.7 µg/µL). Experimental conditions: BGE: 3 % AcA pH 2.4, 40/50 cm 50 µm fused silica capillary, dynamic coating with capillary conditioning solution, separation temperature: 25 °C, separation voltage: 30 kV, injection 0.5 psi 20 s.

The comparison of electropherograms obtained after the analysis of Lys-C digested pegEPO samples is shown in Figure 39. Besides the Lys-C cleavage (black trace), PNGase

was used to remove the N-linked glycans from pegEPO sample (blue trace) and interesting results were observed. The migration pattern of the present signals changed significantly after deglycosylation. In addition to the migration time shift of the deglycosylated P4 peptide also P2 was present (as previously observed for EPO, Figure 38). Further some visible changes occurred between 25 and 55 minutes. As apparent from the electropherogram overlay, four broad peaks illustrating the presence of attached PEG moieties ($pegP_a$-$pegP_d$) were reduced to three signals after PNGase treatment. From the mobility shift of $pegP_d$ it can be presumed that this signal represents some N-glycosylated, sialylated peptide (P2 or P4).

Furthermore the PEGocc can be calculated from the deglycosylated EPO and pegEPO samples as it has been already introduced for chromatography.

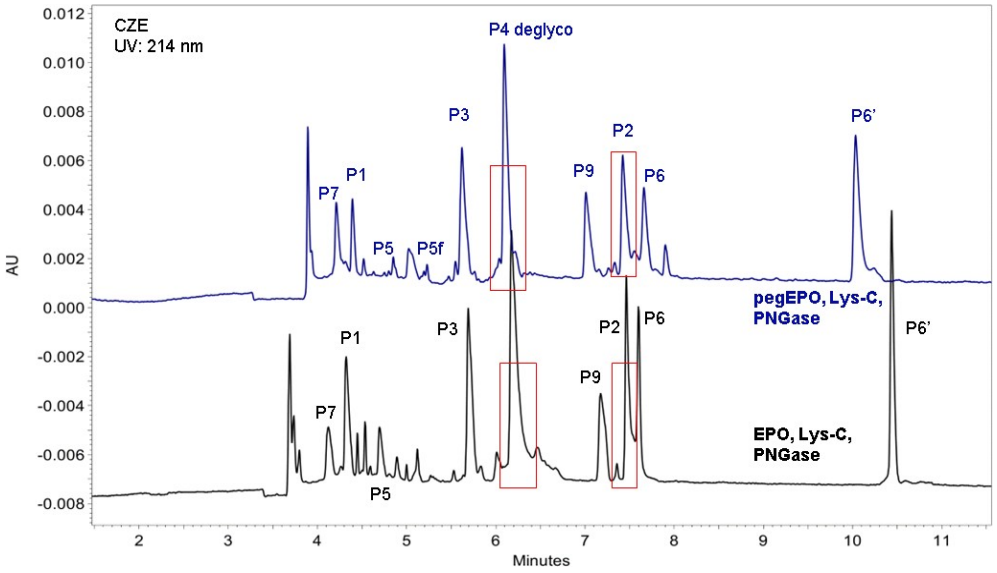

Figure 40: Zoomed UV-electropherogram (214 nm wavelength) of Lys-C, PNGase digested EPO (black trace) and pegEPO (blue trace) (c_{end}= 0.7 µg/µL). Experimental conditions: BGE: 3 % AcA pH 2.4, 40/50 cm 50 µm fused silica capillary, dynamic coating with capillary conditioning solution, separation temperature: 25 °C, separation voltage: 30 kV, injection 0.5 psi 20 s.

The electrophoretic examination of EPO and pegEPO Lys-C digested deglycosylated samples has been already introduced in Figure 38 and Figure 39. The Figure 40 represents zoomed overlay of these two electropherograms. As previously seen in Lys-C digested samples (Table 39), also here some P5 and P7 peptide fragments were detected. The CZE/MS peptide mapping evidenced a few co-migrations of these peptide fragments, which impended the precise calculation of PEGocc[37]. As previously seen in HPLC experiment with

[37] To avoid the presence of unspecific cleaved fragments the digestion conditions were modified by the group of Maria Schwarz (2015) and further CZE experiments were performed. It can be stated

PNGase treated EPO and pegEPO Lys-C digested samples (Figure 36.), the greater quantity of nonspecific cleaved fragments was present in pegEPO sample after electrophoretic separation.

The calculated PEGocc values for deglycosylated samples are demonstrated in Table 40. The results point at high PEGocc of P1 and P5 peptides and minute amount of attached PEG moieties to the P3 and P4 peptides. From very low P6 and P7 PEGocc value, it can be presumed that these peptides are completely non-PEGylated.

Table 40: Area percentage of single peptides of Lys-C, PNGase digested EPO and pegEPO and PEGocc (Figure 40) over single peptides (P9 as reference signal) analysed by CZE.

CZE	EPO	pegEPO	PEGocc/P9[38]
Peptide	A_{corr} % [P9]	A_{corr} % [P9]	
P1	49.6	30.9	0.38
P2	61.8	55.9	0.10
P3	63.5	60.1	0.05
P4	79.6	73.0	0.08
P5	25.6	14.1	0.45
P6	74.5	75.2	0.01
P7	31.6	31.8	0.01
total			**1.07**

Results are reported as the means of duplicate determinations.

3.3.4 Conclusion

An effective CZE method was introduced for the investigation of charge variants of native erythropoietin (EPO). Using EACA as BGE yields well resolved peaks and allows separation of 7 EPO isoforms. The advantage of the demonstrated CZE method consists of the possibility of isoform analysis without the need to coat the capillary or to use the pre-coated capillary as stated in other methods that are commonly used for routine quality control of

---

that the results from these measurements also pointed at high PEGocc of P1 and P5. But each digestion procedure leads to small differences between PEGocc of individual peptides. The inconsistency of the cleavage process is very likely caused by the linkage of PEG moieties to the EPO molecule. The PEGs impeded the access of the enzyme to its cutting positions leading to the inconsistent amounts of the generated peptides.

[38] PEGocc calculation: $100 - \frac{!\ \%\ !"\#\$\%\&}{!\%!"\#} \cdot 100$

erythropoietin. However the introduced method was suitable for the visualization of charge variants of native EPO, the method was not applicable for pegEPO.

Capillary gel electrophoresis was introduced for the study of EPO and pegEPO. Separation of the native molecule led to unexpected well-resolved glycosylated variants. Using this analytical method, a good peak resolution is anticipated only for glycoproteins having large differences between shape, number and site of attached glycans. Therefore the explanation for this observation is seen in the presence of sialic acid anions. Further, the capillary gel electrophoresis was used for the study of the PEGylation degree of pegEPO. Applying this method, minute amount of non-PEGylated and mono-PEGylated conjugates could be detected in pegEPO.

Capillary zone electrophoresis and reversed-phase chromatography were introduced for the investigation of the occurrence of PEG. Peptide mapping of the EPO reference sample and its PEG-conjugate were used for the investigation of the precise PEG site localization and the PEG occupancy (PEGocc). Both analytical techniques determined two main PEGylation sites (at peptide 1 and peptide 5) by comparing the A % of EPO and pegEPO peptides. The differences between the PEGocc values estimated by HPLC and CZE were explained by presence of high amount of unspecific cleaved fragments that co-eluted/co-migrated with other signals. The usability of this method requires an optimization of the digestion procedure (especially of the PEGylated molecule) to obtain the lowest possible amount of unspecific cleaved fragments. This would contribute to the simplification of the evaluation process. We have demonstrated that the CZE method is suitable for the visualization of PEGylated variants.

4 Conclusion

This thesis comprises three studies evaluating CZE-UV and HPLC-MS based methods for the characterization of post-translational modifications in therapeutic proteins.

The first study focused on the deamidation of proteins. Within this study we demonstrated the impact of various degradation conditions on the extent of deamidation in peptides and proteins. A buffer composed of 50 mM ammonium bicarbonate, pH 8.0, was chosen as the most appropriate buffer for studying deamidation. Excellent resolution of the main deamidated species could be achieved by using capillary zone electrophoresis of peptides. Targeted cleavage on the N-terminal side of aspartate by the enzyme Asp-N was introduced for cutting of newly formed aspartates followed by CZE/RP-HPLC separation. Comparison of the non-stressed with the stressed electrophoretic/chromatographic profiles allowed the visual detection of deamidation in peptides. The application of the Asp-N digestion to polypeptides and proteins was found being more difficult compared to peptides, because the presence of deamidated variants was not clearly recognisable in UV electropherograms/chromatograms. An acceleration of the asparagine deamidation rate was observed by applying L-asparaginase enzyme to the peptide. This procedure could not be successfully transferred to the proteins under the used conditions.

In the second study, a CZE-UV method was used for the study of charge variants present in IgG type immunoglobulins. The visualization of protein isoforms was facilitated in bare fused silica capillary using ε-aminocaproic acid (EACA) as BGE additive and detecting at a wavelength of 214 nm. Utilizing the CZE method, the isoform distribution of Avastin and Erbitux samples was comparable to the results obtained by capillary isoelectrofocusing. The CZE method was also employed for the examination of charge variants in unstressed and stressed papain digested Avastin. Although the efficient resolution of Avastin charge variants was performed using CZE, the signals of papain digested Erbitux co-migrated and the electrophoretic profile was not comparable to cIEF. A wider application range of EACA separation method is demonstrated on enzymatic (pepsin, lysine) hydrolysis of Erbitux and papain-PNGase digestion of Avastin.

Finally, in the third study, CZE-UV was introduced as a versatile analytical tool for the analysis of PEGylated proteins. Its power is demonstrated on the study of PEGylated glycosylated erythropoietin. CGE-SDS was applied for the investigation of the PEGylation degree, using EACA running buffer in bare fused silica capillary for isoform visualization) and also for the visualization of PEGylated variants (CZE using acetate). Using this method, the localization of PEGylation sites could be attained and the calculation of PEG occupancy was enabled. Because of the presence of many unspecific cleaved fragments,(especially in the

PEGylated molecule, the precise calculation of PEGocc was not possible and an optimization of the digestion procedure is required.

5 Abbreviations

Table 41: Table of standard amino acids and abbreviations.

Amino acid	1-Letter	3-Letter
Alanine	A	Ala
Arginine	R	Arg
Asparagine	N	Asn
Aspartic acid	D	Asp
Cysteine	C	Cys
Glutamic acid	E	Glu
Glutamine	Q	Gln
Glycine	G	Gly
Histidine	H	His
Isoleucine	I	Ile
Leucine	L	Leu
Lysine	K	Lys
Methionine	M	Met
Phenylalanine	F	Phe
Proline	P	Pro
Serine	S	Ser
Threonine	T	Thr
Tryptophan	W	Trp
Tyrosine	Y	Tyr
Valine	V	Val

d – day

Da – Dalton

h – hour

CHAPS – 3-((3-cholamidopropyl) dimethylammonio)-1-propanesulfonate

min – minute

mM – millimolar

pI – isoelectric point

pKa – acid dissociation constant

s – second

t_m – migration time

t_R – retention time

V - volt

6 References

1. T. M. Dall, P. D. Gallo, R. Chakrabarti, T. West, A. P. Semilla, M. V. Storm. An aging population and growing disease burden will acquire a large and specialized health care workforce by 2025. Health Aff 32 (2013): 2013-2020.
2. P. J. Carter. Introduction to current and future protein therapeutics: A protein engineering perspective. Exp Cell Res 317 (2011): 1261-1269.
3. B. Leader, Q. J. Baca, D. E. Golan. Protein therapeutics: a summary and pharmacological classification. Nat Rev Drug Discov 7 (2008): 21-39.
4. C. Krejsa, M. Rogge, W. Sadee. Protein therapeutics: new applications for pharmacogenetics. Nat Rev Drug Discov 5 (2006): 507-521.
5. A. L. Nelson, E. Dhimolea, J. M. Reichert. Development trends for human monoclonal antibody therapeutics. Nat Rev Drug Discov 9 (2010): 767-774.
6. http://www.statista.com/statistics/258022/top-10-pharmaceutical-products-by-global-sales-2011/
7. A. M. Scott. J. D. Wolchok, L. J. Old. Antibody therapy of cancer. Nat Rev Cancer 279 (2012): 278-287.
8. N. Jenkins, L. Murphy, R. Tyther. Post-translational Modifications of Recombinant Proteins: Significance for Bipharmaceuticals. Mol Biotechnol 39 (2008): 113-118.
9. N. Rathore, R. S. Rajan. Current perspectives on stability of protein drug products during formulation, fill and finish operations. Biotechnolog Prog 24 (2008): 504-514.
10. J. L. Reubsaet, J. H. Beijnen, A. Bult, R. J. van Maanen, J. A. Marchal, W. J. Underberg. Analytical techniques used to study the degradation of protein and peptides: chemical instability. J Pharm Biomed Anal 17 (1998): 955-978.
11. J. L. Reubsaet, J. H. Beijnen, A. Bult, R. J. van Maanen, J. A. Marchal, W. J. Underberg. Analytical techniques used to study the degradation of protein and peptides: physical instability. J Pharm Biomed Anal 17 (1998): 979-984.
12. H. Lodish, A. Berk, S. L. Zipursky, P. Matsudaira, D. Baltimore, and J. Darnell. Molecular cell biology, 4th edition, ISBN-10: 0-7167-3136-3 (2000): Section 3.2 Folding, Modification, and Degradation of Proteins.
13. J. Vlasak, R. Ionescu. Heterogeneity of monoclonal antibodies revealed by charge-sensitive methods. Curr Pharm Biotechnol 9 (2008): 468-481.
14. L. C. Santora, I. S. Krull, I.S., K. Grant. Characterization of recombinant human monoclonal tissue necrosis factor-α antibody using cation-exchange HPLC and capillary isoelectric focusing. Anal Biochem 275 (1999): 98-108.
15. Y. He, J. Mo, X. He, M. Ruesch. Rapid analysis of charge heterogeneity of monoclonal antibodies by capillary zone electrophoresis and imaged capillary isoelectric focusing. Capillary Electrophoresis and Microchip Capillary Electrophoresis: Principles, Applications, and Limitations. Online ISBN: 9781118530009 (2013): 293-308.
16. K. D. Ratanji, J. P. Derrick, R. J. Dearman, I. Kimber. Immunogenicity of therapeutic proteins: Influence of aggregation. J Immunotoxicol 11 (2014): 99-109.
17. M. M. C. van Beers, M. Sauerborn, F. Gilli, V. Brinks, H. Schellekens, W. Jiskoot. Oxidized and aggregated recombinant human interferon beta is immunogenic in human interferon beta transgenic mice. Pharm Res 28 (2011): 2393-2402.
18. Y. Kodera, A. Matsushima, M. Hiroto, H. Nishimura, A. Ishii, T. Ueno, Y. Inada. PEGylation of proteins and bioactive substances for medical and technical applications. Prog Polym Sci 23 (1998): 1233-1271.
19. F. M. Veronese. Peptide and protein PEGylation: a review of problems and solutions. Biomaterials 22 (2001): 405-417.
20. T. L. Cheng, K. H. Chuang, B. M. Chen, S. R. Roffler. Analytical Measurement of PEGylated Molecules. Bioconjug Chem 23 (2012): 881-899.
21. M. Kamionka. Engineering of therapeutic proteins production in Escherichia coli. Curr Pharm Biotechnol 12 (2011): 268-274.

22. M. Peipp, J. J. Lammerts van Bueren, T. Schneider-Merck, W. W. K. Bleeker, M. Dechant, T. Beyer et al. Antibody fucosylation differentially impacts cytotoxicity mediated by NK and PMN effector cells. Blood 112 (2008): 2390-2399.
23. J. E. Nettleship, N. Rahman-Hug, R. J. Owens. The production of glycoproteins by transient expression in mammalian cells. Methods Mol Biol 498 (2009): 245-263.
24. F. Altmann, E. Staudacher, I. B. Wilson, L. März. Insect cells as hosts for expression of recombinant glycoproteins. Glyconj J 16 (1999): 109-123.
25. A. Croset, L. Delafosse, J-P. Gaudry, Ch. Arod, L. Glez, Ch. Losberger, D. Begue, A. Krstanovic, F. Robert, F. Vilbois, L. Chevalet, B. Antonsson. Differences in thy glycosylation of recombinant proteins expressed in HEK and CHO cells. J Biotechnol 161 (2012): 336-348.
26. H. Mellstedt, D. Niederwieser, H. Ludwig. The challenge of biosimilars. J Anal Oncol 19 (2008): 411-419.
27. S. A. Berkowitz, J. R. Engen, J. R. Mazzeo, G. B. Jones. Analytical tools for characterizing biopharmaceuticals and the implications for biosimilars. Nat Rev Drug Discov. 11 (2012): 527-540.
28. C. D. Garcia, K. Y. Chumbimuni-Torres, E. Carrilho. Capillary electrophoresis and microchip capillary electrophoresis: Principles, applications, and limitations. Wiley, ISBN: 978-0-470-57217-7 (2013): 229-245.
29. A. J. Chirino, A. Mire-Sluis. Characterizing biological products and assessing comparability following manufacturing changes. Nat Biotechnol 22 (2004): 1383-1391.
30. http://www.ema.europa.eu/docs/en_GB/document_library/Presentation/2011/06/WC500107827.pdf
31. K. D. Altria. Overview of capillary electrophoresis and capillary electrochromatography. J Chromatogr A 856 (1999): 443-463.
32. P. G. Righetti, W. S. Hancock, B. Karger, C. Horvath, F. Regnier, D. B. Wetlaufer. Capillary electrophoresis in analytical biotechnology. CRC Press, ISBN 0-8493-7825-7 (1996): 12-20.
33. V. Dolnik. Recent developments in capillary zone electrophoresis. Electrophoresis 20 (1999): 3106-3115.
34. M. Graf, M. G. Garcia, H. Wätzig. Protein adsorption in fused silica and polyacrylamide-coated capillaries. Electrophoresis 26 (2005): 2409-2417.
35. F. Tagliaro, G. Manetto, F. Crivellente, F. P. Smith. A brief introduction to capillary electrophoresis. Forensic Sci Int 92 (1998): 75-88.
36. E. Katz, R. Eksteen, P. Schoenmakers, N. Miller. Handbook of HPLC. CRC Press ISBN: 978-0-8247-9444-6 (1998): 79.
37. Y. Xu. Tutorial: Capillary electrophoresis. Chem Educ 1 (1996): 2023-2037.
38. B. J. Smith. SDS polyacrylamide gel electrophoresis of proteins. Methods Mol Biol 1 (1984): 41-55.
39. Z. Zhu, J. J. Lu, S. Liu, Protein separation by capillary gel electrophoresis: A review. Analytica Chimica Acta 709 (2012): 21-31.
40. K. Ganzler, K. S. Greve, A. S. Cohen, B. L Karger. High-performance capillary electrophoresis of SDS-protein complexes using UV-transparent polymer networks. Anal. Chemistry 64 (1992): 2655-2671.
41. Y. Shen, F. Xiang, T. D. Veenstra, E. N. Fung, R. D. Smith. High-resolution capillary isoelectric focusing of complex protein mixtures from lysates of microorganisms. Anal Chem 71 (1999): 5348-5353.
42. T. Wehr, M. Zhu, R. Rodriguez-Diaz. Capillary isoelectric focusing. Methods Enzymol 270 (1996): 358-374.
43. D. Garfin, S. Ahuja. Handbook of isoelectric focusing and proteomics. ISBN: 0-12-088752-5 (2005): 37.
44. B. R. Fonslow, S. A. Kang, D. R Gestaut, B. Graczyk, T. N. Davis, D. M. Sabatini, J. R. Yates. Native capillary isoelectric focusing for the separation of protein complex isoforms and subcomplexes. Anal Chem 82, (2010): 6643-6651.

45. A. V. Stoyanov, Ch. Das, C. K. Fredrickson, Z. H. Fan. Conductivity properties of carrier ampholyte pH gradients in isoelectric focusing. Electrophoresis 26 (2005): 473-479.
46. http://www.proteinsimple.com/ice280.html
47. S. Lindsay. High performance liquid chromatography, 2nd edition. John Wiley and sons, ISBN: 0-471-93115-2 (1992): 63-71.
48. http://www.chromacademy.com/chromatography-HPLC-Column-Dimensions.html
49. R. E. Majors. Column pressure considerations in analytical HPLC. LCGC North America 25 (2007): 1074-1092.
50. W. J. Lough, I. W. Wainer. High performance liquid chromatography. Fundamental principles and practice. Blackie academic and professional. ISBN: 0-7514-0076-9 (1996), Chapters: Modes of chromatography, Support materials and solvents, Instrumentation.
51. Y. Luo, T. Matejic, CH. K. Ng, B. Nunnally, T. Porter, S. Raso, J. Rouse, T. Shang, J. Steckert. Characterization and analysis of biopharmaceutical proteins. Separ Sci Technol 10 (2011): 283-359.
52. D. Corradini. Handbook of HPLC. CRC Press, ISBN: 978-1-4200-1694-9 (2010): 48.
53. L. M. L. Nollet. Handbook of food analysis, 2nd edition. Marcel Dekker, ISBN: 0-8247-5036-5 (2004), Chapters: Peptides, Proteins.
54. T. Taylor. Reversed-phase HPLC mobile-phase chemistry – explained. LCGC North America 32 (2014): 894.
55. J. N. Herron, W. Jiskoot, D. J. A. Chromelin. Physical amethods to characterize pharmaceutical proteins. Pharmaceutical Biotechnology. ISBN: 978-1-4899-1081-3, (1995): 243.
56. D. M. A. M. Luykx, S. S. Goerdayal, P. J. Dingemanse, W. Jiskoot, P. M. J. M. Jongen. HPLC and tandem detection to monitor conformational properties of biopharmaceuticals. J Chrom B 821, (2005): 45-52.
57. P. Hong, S. Koza, E. S. P. Bouvier. A review. Size-exclusion chromatography for the analysis of protein biotherapeutics and their aggregates. J Liq Chromatogr R T 35 (2012): 2923-2950.
58. https://www.shodex.com/en/kouza/f.html
59. http://www.materials-talks.com/blog/2014/08/12/multi-angle-light-scattering-mals
60. H. Schwartz, T. Pritchett. Separation of proteins and peptides by capillary electrophoresis: Application to analytical biotechnology. Available as pdf: http://sciex.com/Documents/manuals/SeparationofProteinsandPeptidesbyCapillaryElectrophoresisApplicationtoAnalyticalBiotechnologyVol-V.pdf, page 91.
61. R. C. Willis. CE gets an A-plus in drugmaking. Today's chemists at work 2 (2003): 34-39.
62. J. R. Petersen, A. A. Mohammad. Clinical and forensic application of capillary electrophoresis. Springer science ISBN: 978-1-59259-120-6 (2001). Chapter: Basic principles and modes of capillary electrophoresis.
63. J. Griffiths. A Brief history of mass spectrometry. Anal Chem 80 (2008): 5678-5683.
64. M. Mann, R. C. Hendrickson, A. Pandey. Analysis of proteins and proteomes by mass spectrometry. Annu Rev Biochem 70 (2001): 437-473.
65. G. Siuzdak. The emergence of mass spectrometry in biochemical research. Review. Proc Natl Acas Sci USA 91 (1994): 11290-11297.
66. M. Kinter, N. E. Sherman. Protein sequencing and identification using tandem spectrometry. John Wiley and sons, ISBN: 0-471-32249-0 (2000): 32.
67. R: E: March. An introduction to quadrupole ion trap mass spectrometry. J Mass Spectrom 32 (1997): 351-369.
68. E. D. Hoffmann. Tandem mass spectrometry: A primer. J Mass Spectrom 31 (1996): 129-137.
69. F. Sobott, S. J. Watt, J. Smith, M. J. Edelmann, H. B. Kramer, B. M. Kessler. Comparison of CID versus ETD based MS/MS fragmentation for the analysis of protein ubiquitination. Am Soc Mass Spectrom 20 (2009): 1652-1659.

70. K. Strupat. Molecular weight determination of peptides and proteins by ESI and MALDI. Methods Enzymol 405 (2005): 1-36.
71. http://www.waters.com/waters/en_US/Mass-Accuracy-and-Resolution/nav.htm?cid=10091028&locale=en_US
72. M. P. Balogh. Debating resolution and mass accuracy in mass spectrometry. Spectroscopy 19 (2004): 34-40.
73. H. S. Gadgil, G. D. Pipes, T. M. Dillon, M. J. Treuheit, P. V. Bondarenko. Improving mass accuracy of high performance liquid chromatography/electrospray ionization time-of-flight spectrometry of intact antibodies. J Am Soc Mass Spectrom 17 (2006): 867-872.
74. J. Cai, J. Henion, Review. Capillary electrophoresis-mass spectrometry. J Chromat A 703 (1995): 667-692.
75. R. Haselberg, G. J. de Jong, G. W. Somsen. Review. Capillary electrophoresis-mass spectrometry for the analysis of intact proteins 2007-2010. Electrophoresis 2011, 32 (2010): 66-92.
76. R. Haselberg, G. J. de Jong, G. W. Somsen. Review. CE-MS for the analysis of intact proteins 2010-2012. Electrophoresis 34 (2913): 99-112.
77. P. Hommerson, A. M. Khan, G. J. de Jong, G. W. Somsen. Ionization techniques in capillary electrophoresis-mass spectrometry: Principles, design and application. Mass Spectrom Rev 30 (2011): 1096-1120.
78. S. De Boni, G. K. E. Scriba. Capillary electrophoresis analysis of hydrolysis, isomerization and enantiomerization of aspartyl model tripeptides in acidic and alkaline solution. J Pharm Biomed Anal 43 (2007): 49-56.
79. M. Lai, D. Skanchy, J. Stobaugh, E. Topp. Capillary electrophoresis separation of an asparagine containing hexapeptide and its deamidation products. J Pharm Biomed Anal 18 (1998): 421-427.
80. N. E. Robinson, A. B. Robinson, Molecular clocks – deamidation of asparaginyl and glutaminyl residues in peptides and proteins. ISBN: 1590872509 (2004): 33
81. T. Geiger, S. Clarke. Deamidation, isomerization and racemization at asparaginyl and aspartyl residues in peptides – succinimide-linked reactions that contribute to protein degradation. J Biol Chem 262 (1987): 785-794.
82. R. J. Harris, B. Kabakoff, F. D. Macchi, F. J. Shen, M. Kwong, J. D. Andya, S. J. Shire, N. Bjork, K. Totpal, A. B. Chen. Identification of multiple sources of charge heterogeneity in a recombinant antibody. J Chromatogr B Biomed Sci Appl. 2001 752(2):233-45.
83. J. Vlasak, M. C. Bussat, S. Wang, E. Wagner-Rousset, M. Schaefer, C. Klinguer-Hamour, M. Kirchmeier, N. Corvaïa, R. Ionescu, A. Beck. Identification and characterization of asparagine deamidation in the light chain CDR1 of a humanized IgG1 antibody. Anal Biochem 392 (2009):145-154.
84. H. Liu, G. Gaza-Bulseco, Ch. Chumsae. Glutamine deamidation of a recombinant monoclonal antibody. Rapid Commun Mass Spectrom 22 (2008): 4081-4088.
85. S. Capasso, L. Mazzarella, F. Sica, A. Zagari. Deadamitadion via cyclic imide in asparaginyl peptides. J Pept Res 2 (1989): 195-200.
86. Boston university school of medicine. http://www.bumc.bu.edu/ftms/research/isoaspartome/
87. R. Tyler-Cross, V. Schirch. Effects of amino acid sequence, buffers, and ionic strength on the rate and mechanism of deamidation of asparagine residues in small peptides. J Biol Chem 266 (1991): 22549-22556.
88. D. Chelius, D. S. Rehder, P. V. Bondarenko. Identification and characterization of deamidation sites in the conserved regions of human immunoglobulin gamma antibodies. Anal Chem 77 (2005): 6004-6011.
89. H. Yang, R. A. Zubarev. Mass spectrometric analysis of asparagine deamidation and aspartate isomerization in polypeptides. Electrophoresis 31 (2010): 1764-1722.
90. N. E. Robinson. Protein Deamidation, Proc Natl Acad Sci 99 (2002): 5283-5288.
91. P. Hao, Y. Ren, A. Datta, J. P. Tam, S. K. Sze. Evaluation of the Effect of Trypsin Digestion Buffers on Artificial Deamidation. J Proteome Res 14 (2015), 1308–1314.

92. J. H. McKerrow, A. B. Robinson. Deamidation of asparaginyl residues as a hazard in experimental protein and peptide procedures. Anal Biochem 42 (1971): 565-568.
93. Y. Song, R. L. Schowen, R. T. Borchardt, E. M. Topp. Effect of pH on the rate of asparagine deamidation in polymeric formulations: pH – rate profile. J Pharm Sci 90 (2001): 141-156.
94. L. P. Stratton, R. M. Kelly, J. Rowe, J. E. Shively, D. D. Smith, J. F. Carpenter, M. C. Manning. Controlling deamidation rates in a model peptide: effects of temperature, peptide concentration, and additives. J Pharm Sci 90 (2001): 2141-2148.
95. S. Capasso, L. Mazzarella, F. Sica, A. Zagari. First evidence of spontaneous deamidation of glutamine residue via cyclic imide to α- and γ-glutamic residue under physiological conditions J Chem Soc, Chem Commun 23 (1991): 1667-1668.
96. T. Flatmark. On the heterogeneity of beef heart cytochrome c. Acta Chem Scand 20 (1966):1487-1496.
97. K. Patel, R. T. Borchardt. Chemical pathways of peptide degradation. III. Effect of primary sequence on the pathways of deamidation of asparaginyl residues in hexapeptides, Pharmaceutical research 7 (1990): 787-793.
98. N. E . Robinson, A. B. Robinson. Deamidation of human proteins, Proc Natl Acad Sci 98 (2001):12409-12413.
99. M. Xie, R. L. Showen. Secondary structure and protein deamidation. J Pharm Sci 88 (1999): 8-13.
100. A. A. Kossiakoff. Tertiary structure is a principial determinant to protein deamidation. Science 240 (1988): 191-194.
101. J. Cacia, R. Keck, L. G. Presta, J. Frenz. Isomerization of an aspartic acid residue in the complementarity-determining regions of a recombinant antibody to human IgE: identification and effect on binding affinity. Biochemistry 35 (1996):1897-903.
102. O. Takahashi, R. Kirikoshi. Intramolecular cyclization of aspartic acid residues assisted by three water molecules: a density functional theory study. Comput Sci & Discovery 7 (2014)
103. B. A. Johnson, J. M. Shirokawa, W. S. Hancock, M. W. Spellman, L. J. Basa, D. W. Aswad. Formation of Isoaspartate at Two Distinct Sites during in Vitro Aging of Human Growth Hormone. J Biol Chem 264 (1989): 14262-14271
104. D. W. Aswad, V. Paranandi, B. T. Schurter. Isoaspartate in peptides and proteins: formation, significance and analysis. J Pharm Biomed Anal 21 (2000): 1129-1136.
105. G. C. Chu, D. Chelius, G. Xiao, H. K. Khor, S. Coulibaly, P. V. Bondarenko. Accumulation of succinimide in a recombinant monoclonal antibody in mildly acidic buffers under elevated temperatures. Pharm Res 6 (2007): 1145-1156.
106. H. Frenz, S.-L. Wu, W. S. Hancock. Characterization of human growth hormone by capillary electrophoresis. J Chromatogr 480 (1989): 379-391.
107. S. De Boni, Ch. Oberthür, M. Hamburger, G. K. E. Scriba. Analysis of aspartyl peptide degradation products by high-performance liquid chromatography and high-performance liquid chromatography-mass spectrometry. J Chromatogr A 1022 (2004): 95-102.
108. R. Bischoff, P. Lepage, M. Jaquinod, G. Cauet, M. Acker-Klein, D. Clesse, M. Laporte, A. Bayol, A. van Dorsselaer, C. Roitsch. Specific dedamidation: Isolation and biochemical characterization of succinimide intermediates of recombinant hirudin. Biochemistry 32 (1993): 725-734.
109. D. Chelius, D. S. Rehder, P. V. Bondarenko. Identification and characterization of deamidation sites in the conserved regions of human immunoglobulin gamma antibodies. Anal Chem 77 (2005): 6004-6011.
110. A. di Donato, M. A. Ciardiello, M. de Nigris, R. Piccoli, L. Mazzarella, G. D'Alessio. Selective deamidation of ribonuclease A. J Biol Chem 268 (1993): 4745-4751.
111. Y. D. Liu, J. Zhang van Enk, G. C. Flynn. Human antibody Fc deamidation in vivo. Biologicals 37 (2009): 313-322.
112. J. Kyte, R. F. Doolittle. A simple method for displaying the hydropathic character of a protein. J Mol Biol 151 (1982): 105-132.

113. Y. F. Huang, Ch-Ch. Huang, Ch-Ch. Hu, H.-T. Chang. Capillary electrophoresis-based separation techniques for the analysis of proteins. Electrophoresis 27 (2006): 3503-3522.
114. D. Barcelo, M. L. Marina, A. Rios, M. Valcarcel. Analysis and detection by capillary electrophoresis, Elsevier 45, ISBN: 0-444-51718-9 (2005): 113
115. M. I. Aguilar. HPLC of peptides and proteins. Humana Press, ISBN: 0-89603-977-3 (2004): 17-20.
116. M. Liu, J. Cheetham, N. Cauchon, J. Ostovic, W. Ni, D. Ren, Z. S. Zhou. Protein isoaspartate methyltransferase-mediated 18O-labeling of isoaspartic acid formass spectrometry analysis. Anal Chem 84 (2012): 1056-1062.
117. J. F. Alfaro, L. A. Gillies, H. G. Sun, S. Dai, T. Zang, J. J. Klaene, B. J. Kim, J. D. Lowenson, S. G. Clarke, B. L. Karger, Z. S Zhou. Chemo-enzymatic detection of protein isoaspartate using protein isoaspartate methyltransferase and hydrazine trapping. Anal Chem 80 (2008): 3882-3889.
118. J. X. Zhu, D. W. Aswad. Selective cleavage of isoaspartyl peptide bonds by hydroxylamine after methyltransferase priming. Anal Biochem 364 (2007): 1-7
119. D. Kameoka, T. Ueda, T. Imoto. A method for the detection of asparagine deamidation and aspartate isomerization of proteins by MALDI/TOF-mass spectrometry using endoproteinase Asp-N 134 (2003): 129-135.
120. G. R. Drapeau. Substrate specificity of a proteolytic enzyme isolated from a mutant of Pseudomonas fragi. Journal of biological chemistry 259 (1980): 839-840.
121. G. Maier, G. R. Drapeau, K. H. Doenges, H. Postingl. Methods in protein sequence analysis (K.A. Walsh), 1986: 335-337.
122. J. Noreau, G. R. Drapeau. Isolation and properties of the protease from the wild-type and mutant strains of Pseudomonas Fragi. Journal of Bacteriology 140 (1979): 911-916.
123. D. Ingrosso, A. V. Fowler, J. Bleibaum, S. Clarke. Specificity of endoproteinase Asp-N (Pseudomonas fragi): Cleavage at glutamyl residues in two proteins. Biochem Biophys Res Commun 162 (1989):1528-1534.
124. B. J. Kuipers, H. Gruppen. Prediction of molar extinction coefficients of proteins and peptides using UV absorption of the constituent amino acids at 214 nm to enable quantitative reverse phase high-performance liquid chromatography-mass spectrometry analysis. J Agric Food Chem 55 (2007): 5445-5451.
125. A. L. Swain, M. Jaskolski, D. Housset, J. K. Mohana Rao, A. Wlodawer. Crystal structure of Escherichia Coli L-asparagine, an enzyme used in cancer therapy. Proc Natl Acad Sci 90 (1993): 1474-1478.
126. R: Pieters, S. P. Hungerm J. Boos, C. Rizzari, L. Silverman, A. Baruchel, N. Goekbuget, M. Schrappe, CH-H. Pui. L-Asparaginase treatment in acute lymphoblastic leukemia: A focus on Erwinia asparaginase. Cancer 117 (2001): 238-249.
127. K. Michalska, M. Jaskolski, Structural aspects of l-asparaginases, their friends and relations. Acta Biochim Pol 53 (2006) 53: 627-640.
128. http://www.sigmaaldrich.com/catalog/product/sigma/f3261?lang=de&region=CH
129. J. Dodt, H.-P. Müller, U. Seemüller, L-Y. Chang. The complete amino acid sequence of hirudin, a thrombin specific inhibitor. FEBS 165 (1983): 180-184.
130. A. Tuong, M. Maftouh, C. Ponthus, O. Whitechurch, C. Roitsch, C. Picard. Characterization of the deamidated forms of recombinant Hirudin. Biochemistry 31 (1992): 8291-8299.
131. http://web.expasy.org/compute_pi/
132. M. R. Nilsson, M. Driscoll, D. P. Raleigh. Low levels of asparagine deamidation can have a dramatic effect on aggregation of amyloidogenic peptides: Implications for the study of amyloid formation, Prot Sci 11 (2002): 342-349.
133. K Patel, R. T. Borchardt. Chemical pathways of peptide degradation. II. Kinetics of deamidation of an asparaginyl residue in a model hexapeptide. Pharm Res 7 (1990): 703-711.

134. L. A. Gennaro, O. Salas-Solano. Characterization of deamidated peptide variants by micro-preparative capillary electrophoresis and mass spectrometry, J Chromatogr A 1216 (2009): 4499-4503.
135. https://pim-eservices.roche.com/LifeScience/Document/c9df15d9-23f2-e311-98a1-00215a9b0ba8
136. Deuss et al. Eight international conference on methods in protein sequence analysis. J Prot Chem 9 (1990): 299-300.
137. Šlechtová T., Gilar M., Kalíková K., Tesařová E. Insight into trypsin miscleavage: Comparison of kinetic constants of problematic peptide sequences, Anal Chem 87 (2015): 7636-7643.
138. K. A. McCall, Ch. Huang, C. A Fierke. Function and mechanism of zinc metalloenzymes. J Nutr 130 (2000): 1437-1446.
139. Y. Q. Zhang, M. L. Tao, W. D. Shen, Y. Z. Zhou, Y. Ding, Y. Ma, W. L. Zhou. Immobilization of L-asparaginase on the microparticles of the natural silk sericin protein and its characters. Biomaterials 25 (2004): 3751-3759.
140. K. Pilaniya, H. K. Chandrawanshi, U. Pilaniya, P. Manchandani, P. Jain, N. Singh. Recent trends in the impurity profile of pharmaceuticals. J Adv Technol Res 3 (2010): 302-310.
141. Y. He, C. Isele, W. Hou, M. Ruesch. Rapid analysis of charge variants of monoclonal antibodies with capillary zone electrophoresis in dynamically coated fused-silica capillary. J Sep Sci 34 (2011): 548-555.
142. S. Babu. Monoclonal antibody charge heterogeneity analysis by CZE and CZE/MS. Agilent Technologies (2015), publication number 5991-6141.
143. Y. Y. Zhao, N. Wang, W. H. Liu, W. J. Tao, L. L. Liu, Z. D. Shen. Charge Variants of an Avastin Biosimilar. Isolation, Characterization, In Vitro Properties and Pharmacokinetics in Rat. PLoS ONE 11 (2016): 1-13.
144. L. A. Khawli et al. Charge variants in IgG1. mAbs 2 (2010): 613-624.
145. M. Perkins, R. Theiler, S: Lunte, M. Jeschke. Determination of the origin of charge heterogeneity in a murine monoclonal antibody. Pharm Res 17 (2000): 1110-1117.
146. A. Funaro, A. L. Horenstein, P. Santoro, C. Cinti, A. Gregorini, F. Malavasi. Monoclonal antibodies and therapy of human cancer. Biotechnol Adv 18 (2000): 385-401.
147. D. H. Marguilies. Monoclonal antibodies: Producing magic bullets by somatic cell hybridization. J Immunol 174 (2005): 2451-2452
148. A. C. Chan, P. J. Carter, Therapeutic antibodies for autoimmunity and inflammation. Nat Rev Immunol 10 (2010): 301–316.
149. Monoclonal antibodies. Unibas semester lectures (2013).
150. Y. Du, A. Walsh, R. Ehrick, W. Xu, K. May, H. Liu. Chromatographic analysis of the acidic and basic species of recombinant monoclonal antibodies. MAbs 4 (2012): 578-585.
151. C. Chumsae, G. Gaza-Bulseco, J. Sun, H. Liu. Comparison of methionine oxidation in thermal stability and chemically stressed samples of a fully human monoclonal antibody. J Chromatogr B. 850 (2007): 285–294.
152. J. Wypych, M. Li, A. Guo, Z. Zhang, T. Martinez, M. J. Allen et al. Human IgG2 antibodies display disulfide-mediated structural isoforms. J Biol Chem. 283 (2008):16194–16205.
153. K. F. Medzihradsky. In-solution digestion of proteins for mass spectrometry. Method Enzymol 405 (2005): 50-65.
154. A. L. Nelson. Antibody fragments. Hope and Hype. mAbs 2 (2010): 77-83.
155. J. M. Pezzuto, M. E: Johnson, H. R. Manasse. Biotechnology and Pharmacy. ISBN: 978-94-015-8135-6 (2013): 82.
156. Z. Sosic, D. Houde, A. Blum, T. Carlage, Y. Lyubarskaya. Application of imaging capillary IEF for characterization and quantitative analysis of recombinant protein charge heterogeneity. Electrophoresis 29 (2008): 4368-4376.
157. http://www.ema.europa.eu/docs/en_GB/document_library/EPAR_-_Scientific_Discussion/human/000582/WC500029262.pdf

158. http://www.drugbank.ca/drugs/DB00112
159. http://www.drugbank.ca/drugs/DB00002
160. C. H. Chung, B. Mirakhur, E. Chan, Q. T. Le, J. Berlin, M. Morse, B. A. Murphy, S. M. Satinover, J. Hosen, D. Mauro, R. J. Slebos, Q. Zhou, D. Gold, T. Hatley, D. J. Hicklin, T. Platts-Mills. Cetuximab-induced anaphylaxis and IgE specific for Galactose-α-1,3-galactose. N Engl J Med 358 (2008): 1109-1117.
161. R. J. Flanagan, A. L. Jones. Fab antibody fragments: some application in clinical toxicology. Drug Safety 27 (2004): 1115-33.
162. C. N. Phillip, Yoshio Osawa. Preparation and characterization of the Fab and F(ab)2 fragments of an aromatase activity-suppressing monoclonal antibody. Steroids 62 (1997): 776-781.
163. L. Coleman, S. M. Mahler. Purification of Fab fragments from a monoclonal antibody papain digest by Gradiflow electrophoresis. Protein Expr Purif 32 (2003): 246-251.
164. G. Rodrigo, M. Gruvegard, J. M. van Alstine. Antibody fragments and their purification by protein L affinity chromatography. Antibodies 4 (2015): 259-277.
165. W. R. Strohl, L. M. Strohl. Therapeutic antibody engineering. Current and future advances driving the strongest growth area in the pharmaceutical industry. Elsevier. ISBN: 9781907568374 (2012): 41.
166. R. E. Kontermann, S. Dubel. Antibody engineering 2. Springer. ISBN: 3642011462 (2010): 70.
167. K. L. Bennett, S. V. Smith, R. J. W. Truscott, M. M. Sheil. Monitoring Papain Digestion of a Monoclonal Antibody by Electrospray Ionization Mass Spectrometry. Anal Biochem 245 (1997): 245: 17-27.
168. B. A. Brown, R. D. Comeau, P. L. Jones, F. A. Liberatore, W. P. Neacy, H. Sands, B. M. Gallagher. Pharmacokinetics of the monoclonal antibody B72.3 and its fragments labeled with either ^{125}I or ^{111}I. Cancer Res 47 (1987): 1149-1154.
169. M. L. Hagmann, Ch. Kionka, M. Schreiner, Ch. Schwer. Characterization of the F(ab')2 fragment of a murine monoclonal antibody using capillary isoelectric focusing focusing and electrospray ionization mass spectrometry. J Chromatogr A 816 (1998) 49-58.
170. R. S. Stowers, J. A. Callihan, J. D. Bryers. Optimal Conditions for F(ab')2 Antibody Fragment Production from Mouse IgG2. JURIBE 8 (2008): 16-20.
171. http://www.piercenet.com/browse.cfm?fldID=4E03B016-5056-8A76-4ECA-982DA6CAAC8A#pepsin
172. http://www.chem.agilent.com/Library/applications/5991-0895EN.pdf
173. J. Luo, J. Zhang, D. Ren, W. L. Tsai, F. Li, A. Amanullah, T. Hudson. Probing of C-terminal lysine variation in a recombinant monoclonal antibody production using Chinese hamster ovary cells with chemically defined media. Biotechnol Bioeng 109 (2012): 2306-2315.
174. http://www.worthington-biochem.com/COB/
175. S. Kaja, J. D. Hilgenberg, E. Everett, S. E. Olitsky, J. Gossage, P. Koulen. Effects of dilution and prolonged storage with preservative in a polyethylene container on Bevacizumab (Avastin) for topical delivery as a nasal spray in anti-hereditary hemorrhagic telangiectasia and related therapies. Human antibodies 20 (2011): 95-101.
176. K.L. Shaw, G. R. Grimsley, G. I. Yakovlev, A. A. Makarov, C. N. Pace. The effect of net charge on solubility, activity and stability of ribonuclease Sa. Protein Sci 10 (2001): 1206-1215.
177. Y. He, N. A Lacher, W. Hou, Q. Wang, C. Isele, J. Starkey, M. Ruetsch. Analysis of identity, charge variants, and disulphide isomers of monoclonal antibodies with capillary zone electrophoresis with an uncoated capillary column. Anal Chem 82 (2010): 3222-3230.
178. M. R. Mohamadi, T. Yasui, N. Kaji, M. Tokeshi, Y. Baba. Quantitative evaluation of dynamic coating on plastic microchips for preventing protein adsorption. CBMS ISBN: 978-0-9798064-1-4 (2007): 495-497.

179. C. Aquilar, A. J. P. Hofte, U. R. Tjaden, J. van der Greef. Analysis of histones by on-line capillary zone electrophoresis–electrospray ionisation mass spectrometry. J Chromatogr A 926 (2001): 57-67.
180. H. Schwartz, T. Pritchett. Separation of proteins and peptides by capillary electrophoresis: Application to analytical biotechnology. Available as pdf: http://sciex.com/Documents/manuals/SeparationofProteinsandPeptidesbyCapillaryElectrophoresisApplicationtoAnalyticalBiotechnologyVol-V.pdf, page 56.
181. M. Chung, D. Kim, A. E. Herr. Polymer sieving matrices in microanalytical electrophoresis. Analyst 139 (2014): 5635-5654.
182. T. Yasui, M. Reza Mohamadi, N. Kaji, Y. Okamoto, M. Tokeshi, Y. Baba. Characterization of low viscosity polymer solution microchip electrophoresis of non-denatured proteins on plastic chips. Biomicrofluidics 5 (2011): 1-9.
183. J. L. Ford, Design and evaluation of hydroxypropyl methylcellulose matrix tablets for oral controlled release. A historical perspective. AAPS 16 (2014): 2
184. H. Wätzig, M. Degenhardt, A. Kunkel. Strategies for capillary electrophoresis: method development and validation for pharmaceutical and biological applications. Electrophoresis 19 (1999): 2695-2752.
185. J. Quian, T. Liu, L. Yang, A. Daus, R. Crowley, Q. Zhou. Structural characterization of N-linked oligosaccharides on monoclonal antibody cetuximab by combination of orthogonal matrix-assisted laser desorption/ionization hybrid quadrupole-quadrupole time-of-flight tandem mass spectrometry and sequential enzymatic digestion. Anal Biochem 364 (2007): 8-18.
186. K. G. Moorhouse, W. Nashabeh, J. Deveney, N. S. Bjork, M. G. Mulkerrin, T. Ryskamp . Validation of an HPLC method for the analysis of the charge heterogeneity of the recombinant monoclonal antibody IDEC-C2B8 after papain digestion. J Pharm Biomed Anal 16 (1997): 593-603.
187. M. Adamczyk, J. C. Gebler, J. Wu. Papain digestion of different mouse IgG subclasses as studied by electrospray mass spectrometry. J Immunol Methods 237 (2000): 237:95-104.
188. L. Huang, J. Lu, V. J. Wroblewski, J. M. Beals, R. M. Riggin. In vivo deamidation characterization of monoclonal antibody by LC/MS/MS. Anal Chem 77 (2005): 1432-1439.
189. M. Hamm, Y. Wang, R. R. Rustandi. Characterization of N-Linked Glycosylation in a Monoclonal Antibody Produced in NS0 Cells Using Capillary Electrophoresis with Laser-Induced Fluorescence Detection. Pharmaceuticals 6 (2013): 393–406.
190. Y. Kanda, T. Yamada, K. Mori, A. Okazaki, M. Inoue, K. Kitajima-Miyama, R. Kuni-Kamochi, R. Nakano, K. Yano, S. Kakita, K. Shitara, M. Satoh. Comparison of biological activity among nonfucosylated therapeutic IgG1 antibodies with three different N-linked Fc oligosaccharides: the high-mannose, hybrid, and complex types. Glycobiology 17 (2007): 104-118.
191. S. Fuller, T. Haxo, J. Hyche, M. Kimzey, S. Lockhart, S. Pourkaveh, Z. Szabo, J. Truong, J. Wegstein, V. Woolworth. Assessing the variability of an innovator molecule N-glycan profile. ProZyme Hayward, CA, USA: http://www.labhoo.com/brochures/B8306_Assessing_the_Variability_of_an_Innovator_Molecule_N-Glycan_Profile.pdf
192. E. Boeggman, B. Ramakrishnan, M. Pasek, M. Manzoni, A. Puri, K. L. Loomis, T. J. Waybright, P. K. Qasba. Site specific conjugation of fluoroprobes to the remodeled Fc N-glycans of monoclonal antibodies using mutant glycosyltransferases: Application for cell surface antigen detection. . Bioconjug Chem 20 (2009: 1228-1236.
193. G. Hunt, W. Nashabeh. Capillary electrophoresis sodium dodecyl sulfate nongel sieving analysis of a therapeutic recombinant monoclonal antibody: A biotechnology perspective. Anal Chem 71 (1999): 2390-2397.
194. O. Salas-Solano, B. Tomlinson, S. Du, M. Parker, A. Strahan, S. Ma. Optimization and validation of a quantitative capillary electrophoresis sodium dodecyl sulfate method for

quality control and stability monitoring of monoclonal antibodies. Anal Chem 78 (2006): 6583-6594.
195. Y. An, Y. Zhang, H. M. Müller, M. Shameem, X. Chen. A new tool for monoclonal antibody analysis. mAbs 6 (2014): 879-893.
196. X. Zhong, J. F. Weight. Biological insights into therapeutic protein modifications throughout trafficking and their biopharmaceutical applications. J Biochem Cell Biol 2013 (2013): 1-19.
197. P. J. Gauci, M. R. Alderton. Pepsin digestion of antibodies to produce functional antigen-binding fragments (Fab): A scientific fantasy? J Chromatogr A 816 (1998): 49-58.
198. D. V. Goeddel, D. G. Kleid, F. Bolivar, H. L. Heyneker, D. G. Yansura, R. Crea, T. Hirose, A. Kraszewski, K. Itakura, A. D. Riggs. Expression in Escherichia coli of chemically synthesized genes for human insulin. Proc. Natl. Acad. Sci, 76 (1979): 106-110.
199. M. S. Kinch. An overview of FDA-approved biologics medicines. Drug Discovery Today 20 (2015): 393-398.
200. R. J. Y. Ho, M. Gibaldi, Biotechnology and biopharmaceuticals: transforming proteins and genes into drugs. ISBN 0-471-20690-3(2003): 138
201. B. Leader, Q. J. Baca, D. E. Golan. Protein therapeutics: a summary and pharmacological classification. Nature reviews. Drug discover 8 (2008): 21-39.
202. D. S. Pisal, M. P. Kosloski, S. V. Balu-Iyer. Delivery of therapeutic proteins. J Pharm Sci 99 (2010): 2557-2575.
203. F. M. Veronese, Peptide and protein PEGylation: a review of problems and solutions. Biomaterials 22 (2001): 405-417.
204. S: Jevsevar, M. Kunstelj, V. G. Porekar. PEGylation of therapeutic proteins. Biotechnolog J 5 (2010): 113-128.
205. O. B. Kinstler, D. N. Brems, S. L. Lauren, A. G. Paige, J. B. Hamburger, M. J. Treuheit. Characterization and stability of N-terminally PEGylated rhG-CSF. Pharm Res 13 (1996): 996-1002.
206. D. H. Na, E. J. Park, Y. W. Jo, K. C. Lee. Capillary electrophoretic separation of high-molecular-weight poly(ethyleneglycol)-modified proteins. Analytical Biochemistry 373 (2008): 207–212.
207. K. Mayolo-Deloisa, J. Gonzalez-Valdez, D. Guajardo-Flores, O. Aguilar, J. Benavides, M. Rito-Palomares. Current advances in the non-chromatographic fractionation and characterization of PEGylated proteins. J. Chem Technol. Biotechnol, 86 (2011): 18-25.
208. C. J. Fee, J. M. van Alstine. PEG-proteins: reaction engineering and separation issues, Chemical engineering science, 61 (2006): 924-939..
209. K. Rebolj, D. Pahovnik, E. Žagar. Characterization of protein conjugate using an asymmetrical-flow field-flow fractionization and size exclusion chromatography with multi-detection system. Anal Chem 84 (2012): 7374-7383.
210. B. K: Seyfried, M. Marchetti-Deschmann, J. Siekmann, M. J. Bossard, F. Scheiflinger, P. L. Turecek, G. Allmaier. Microchip capillary gel electrophoresis of multiply PEGylated high-molecular mass glycoproteins. Biotechnol J 7 (2012): 635-641.
211. K. S. Lee, D. H. Na. Capillary electrophoretic separation of poly(ethylene glycol)-modified granulocyte-colony stimulating factor. Archives of pharmacal research 33 (2010): 491-495.
212. N. Yoshimoto, S. Yamamoto. PEGylated protein separations. Challenges and opportunities. Biotechnol J 7 (2012): 592-593.
213. C. Maullu, D. Raimondo, F. Caboi, A. Giorgetti. Site-directed enzymatic PEGylation of the human granulocyte colony-stimulating factor. FEBS 276 (2009): 6741-6750.
214. S. Chateauvieux, C. Grigorakaki, F. Morceau, M. Dicato, M. Diederich. Erythropoietin, erythropoiesis and beyond, Biochemical Pharmacology 82 (2011): 1291-1303.
215. V. Pacáková, S. Hubená, M. Tichá, M. Maděra, K. Štulík. Effects of electrolyte modification and capillary coating on separation of glycoprotein isoforms by capillary electrophoresis. Electrophoresis 22 (2001): 459-463.

216. Z. A. Haroon, K. Amin, X. Jiang, M. O. Arcasoy. A novel role for erythropoietin during fibrin-induced wound heling response, American Journal of Pathology, 163 (2003): 993-1000.
217. A.- L. Siren, M. Fratelli, M. Brines, Ch. Goemans, S. Casagrande, P. Lewczuk, S. Keenan, Ch. Gleiter, C. Pasquali, A. Capobianco, T. Mennini, R. Heumann, A. Cerami, H. Ehrenreich, P. Ghezzi. Erythropoietin prevents neuronal apoptosis after cerebral ischemia and metabolic stress, PNAS 98 (2001): 4044-4049.
218. S. B. Krantz. Erythropoietin. Blood journal 77 (1991) 419.
219. A. Taichrib, M. Pioch, C. Neusüss. Multivariate statistics for differentiation of erythropoietin preparations based on intact glycoforms determined by CE-MS. Anal Bioanal Chem 403 (2012): 797-805.
220. H. Sasaki, B. Bothner, A. Dell, M. Fukuda. Carbohydrate structure of erythropoietin expressed in Chinese hamsters ovary cells by a human erythropoietin cDNA. The journal of biological chemistry 262 (1987): 12059-12076.
221. Z. Shahrokh, L. Royle, R. Saldova, J. Bones, J. L. Abrahams, N. V. Artemenko, S. Flatman, M. Davies, A. Baycroft, S. Sehgal, M. W. Heartlein, D. J. Harvey, P. M. Rudd. Erythropoietin produced in a human cell line (Dynepo) has significant differences in glycosylation compared with erythropoietins produced in CHO cell lines. Molecular pharmaceutics 8 (2010): 286-296.
222. S. Boucher, A. Kane, M. Girard. Qualitative and quantitative assessment of marketed erythropoiesis-stimulating agents by capillary electrophoresis. Journal of pharmaceutical and biomedical analysis 71 (2012): 207.
223. M. Taverna, N. T. Tran, T. Merry, E. Horvath, D. Ferrier. Electrophoretic methods for process monitoring and the quality assessment of recombinant glycoproteins, Electrophoresis 19 (1998): 2572-2594.
224. http://www.ema.europa.eu/docs/en_GB/document_library/EPAR_-_Scientific_Discussion/human/000739/WC500033669.pdf
225. https://www.edqm.eu/en/CAP-programme-613.html
226. http://www.beckmancoultermedia.com/beckmancoultermedia/CE/Somsen_Presentation/index.htm
227. https://www.lifetechnologies.com/order/catalog/product/90051
228. B. Maiser, F. Kröner, F. Dismer, G. Brenner-Weiss, J. Hubbuch. Isoform separation and binding site determination of mono-PEGylated lysozyme with pH gradient chromatography. J Chromatogr A 1268 (2012): 102-108.
229. G. Palmisano, M. N. Melo-Braga, K. Enghol-Keller, B. L. Parker, M. R. Larsen. Chemical deamidation: A common pitfall in large-scale N-linked glycoproteomic mass spectrometry-base analyses. J Proteome Res 11 (2012): 1949-1957.
230. M. Taverna, N. T. Tran, T. Merry, E. Horvath, D. Ferrier. Electrophoretic methods for process monitoring and the quality assessment of recombinant glycoproteins. Electrophoresis 19 (1998): 2572-2594.
231. M. Girard, A. Puerta, J. C. Diez-Masa, M. de Frutos. High resolution separation methods for the determination of intact human erythropoiesis stimulating agents. A review. Analytica chimica acta 713 (2012): 7-22.
232. N. K. Klausen, T. Kornfelt. Analysis of the glycoforms of human recombinant factor VIIa by capillary electrophoresis and high-performance liquid chromatography, J. of Chromatography A, 718 (1995): 195-202.
233. European Pharmacopoeia 8.4, (2015): 4750–4754, 01/2008: 1316
234. E. Balaguer, U. Dmelbauer, M. Pelzing, V. Sanz-Nebot, J. Barbosa, C. Neusüss. Glycoform characterization of erythropoietin combining glycan and intact protein analysis by capillary electrophoresis – electrospray – time-of-flight mass spectrometry, Electrophoresis 27 (2006): 2638-2650.
235. E. Balaguer, C. Neusüss. Glycoform characterization combining intact protein and glycan analysis by capillary electrophoresis-electrospray ionization-mass spectrometry, Analytical Chemistry 78 (2006): 5384-5393.

236. X. Fu, L. Huang, F. Gao, W. Li, N. Pang, M. Zhai, H. Liu, M. Wu. Carboxymethyl chitosan-coated capillary and its application in CE of proteins, Electrophoresis 28 (2007): 1958-1963.
237. S. S. Park, J. Park, J. Ko, L- Chen, D. Meriage, J. Course-Zeineddini, W. Wong, B. A. Kerwin. Biochemical assessment of erythropoietin products from Asia versus US epoetin alfa manufactured by Amgen, J. of pharmaceutical sciences 98 (2008): 1688-1699.
238. H.P. Bietlot, M. Girard, Analysis of recombinant human erythropoietin in drug formulations by high performance capillary electrophoresis. J. Chromatogr. A 759 (1997): 177–184.
239. J. R. Delanghe, M. Bollen, M. Beullens. Testing for recombinant erythropoietin. Am J Hematol 83 (2008): 237-241.
240. W. Li, Y. Zhong, B. Lin, Z. Su. Characterization of polyethylene glycol-modified proteins by semi-aqueous capillary electrophoresis. J. of Chromatography A 805 (2001): 299-307.
241. J. Bullock, S. Chowdhury, D. Johnston. Characterization of Poly(ethylene glycol)-Modified Superoxide Dismutase: Comparison of Capillary Electrophoresis and Matrix-Assisted Laser Desorption/Ionization Mass Spectrometry. Analytical Chemistry 68 (1996): 3258-3264.
242. D. H. Na, E. J. Park, Y. S. Youn, B. W. Moon, Y. W. Jo, S. H. Lee, W-B. Kim, Y. Sohn, K. C. Lee. Sodium dodecyl sulfate-capillary gel electrophoresis of polyethylene glycosylated interferon alpha. Electrophoresis 25 (2004): 476-479.
243. Z. El-Rassi. Carbohydrate analysis by modern chromatography and electrophoresis. Elsevier, ISBN: 0-444-50061-8 (2002): 734.
244. http://www.wako-chem.co.jp/english/labchem/product/life/Lys-C/index.htm
245. M. A. Recny, H. A. Scoble, Y. Kim. Structural characterization of natural human urinary and recombinant DNA-derived erythropoietin. J Biol Chem 262 (1987): 17156-17163.
246. H. Rahbek-Nielsen, P. Roepstorff, H. Reischl, M. Wozny, H. Koll, A. Haselbeck. Glycopeptide profiling of human urinary erythropoietin by matrix-assisted laser desorption/ionization mass spectrometry. J Mass Spectrom 32 (1997): 948-958.
247. I. Dragan, R. Swart, R. van Ling, J. P. Chervet. Development of a verstatile method for the analysis of glycoproteins using monolithic capillary LC coupled to ESI-MS and MALDI-MS. Recent applications in LC-MS 17 (2004): 40-42.
248. K. Strupat, M. Karas, F. Hillenkampf. 2,5-Dihyxybenzoic acid: a new matrix for laser desorption-ionization mass spectrometry. Int J Mass Spectrom Ion Processes 111 (1991): 89-102.
249. D. J. Harvey. Matrix-assisted laser desorption/ionization mass spectrometry of carbohydrates. Mass Spectrom Rev 18 (1999): 349-451.
250. W. A. Korfmacher. Using mass spectrometry for drug metabolism studies, 2nd edition. ISBN: 9781420092219, (2009): 342.
251. A. Resemann, N. Tao, U. Schweiger-Hufnagel, K. Marx, S. Kaspar, Bruker Daltonics, Fremont, CA, Bruker Daltonik GmbH, Bremen, Germany. Comprehensive Study of O-Linked Glycans of Erythropoeitin, ASMS 2013, ThP 19 356.
252. P. D: Gershon. Cleaved and missed sites for trypsin, Lys-C and Lys-N can be predicted with high confidence on the basis of sequence context. J Proteome Res 13 (2014): 702-709.
253. R. Raijimakers, P. Neerincx, S. Mohammed, A. J. R: Heck. Cleavage specificities of the brother and sister proteases Lys-C and Lys-N. RSC 46 (2010): 8827-8829.
254. P. A. Jekel, W. J. Weijer, J. J. Beintema. Use of Lys-C endoproteinase from Lysobacter enzymogenes in protein sequence analysis. Anal Biochem 134 (1983): 347-354.
255. I. C. Forstenlehner, H. J. Holzmann, K. Scheffler, W. Wieder, H. Toll, Ch. G. Huber. A Direct-Infusion and HPLC-ESI-Orbitrap-MS approach for the characterization of intact PEGylated proteins. Anal Chem 86 (2014): 826-834.

7 Appendix

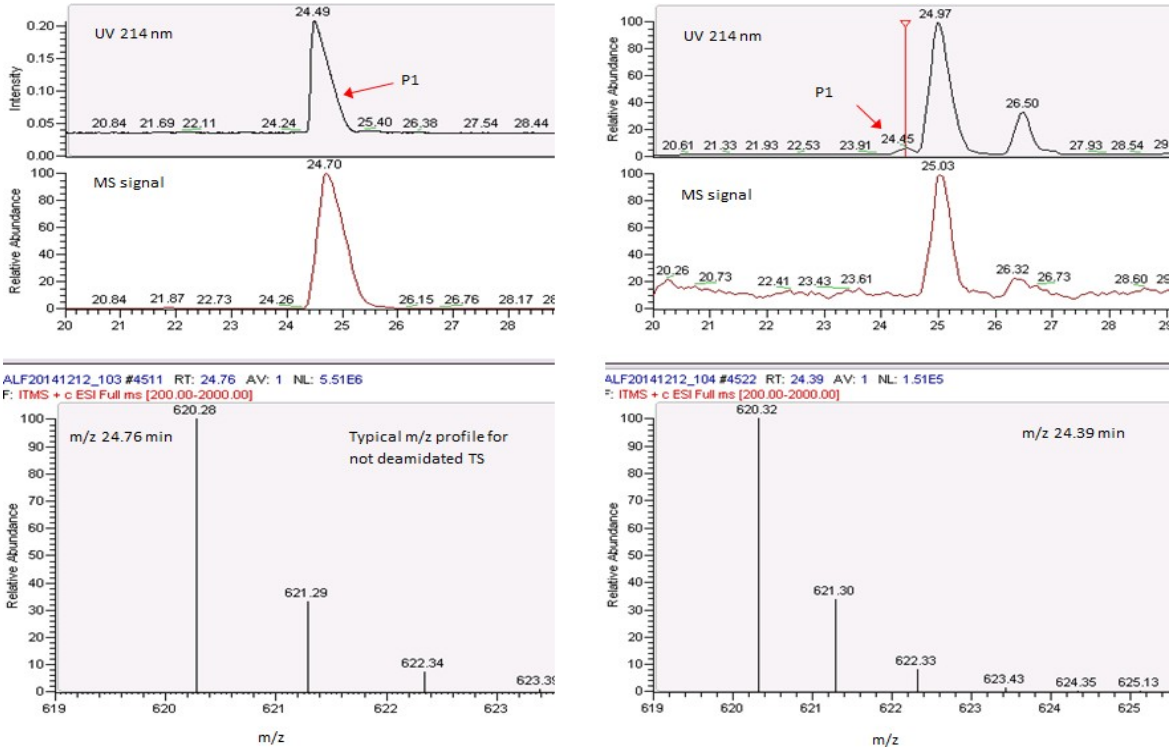

Figure 41: RP-HPLC MS: Analog chromatogram (214 nm wavelength, top trace), ion chromatogram (middle trace) and corresponding mass signals (bottom trace) overlay for Peptide 1. Unstressed (left), 24 h 40 °C (right). Experimental conditions: X-Bridge BEH300 C18, 3.5 µm, 2.1 x 150 mm column, H_2O/ACN with 0.1 % TFA, flow rate 0.2 mL/min, column temperature 50 °C.

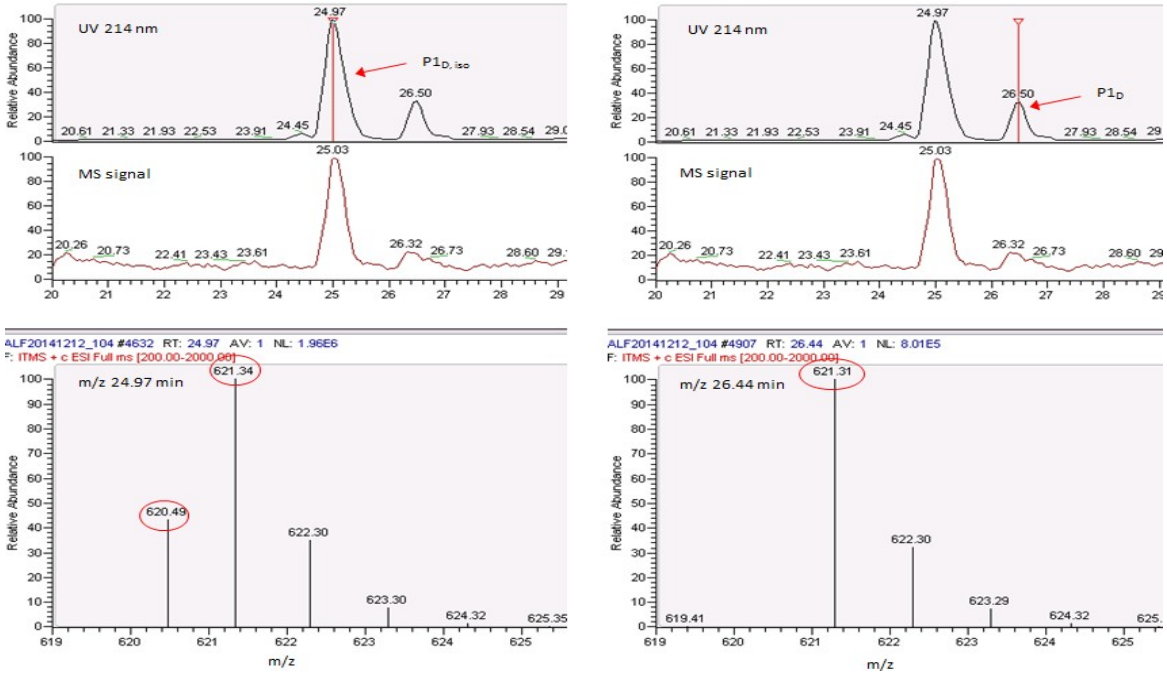

Figure 42: RP-HPLC MS: Analog chromatogram (214 nm wavelength, top trace), ion chromatogram (middle trace) and corresponding masses (bottom trace) overlay for Peptide 1. Unstressed (left), 24 h 40 °C (right). Experimental conditions: X-Bridge BEH300 C18, 3.5 µm, 2.1 x 150 mm column, H_2O/ACN with 0.1 % TFA, flow rate 0.2 mL/min, column temperature 50 °C.

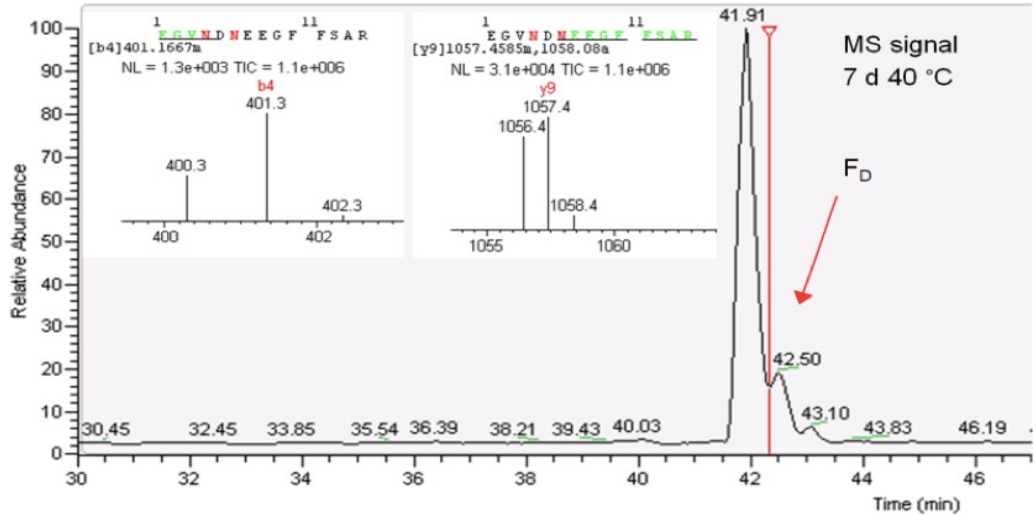

Figure 43: RP-HPLC MS: Ion chromatogram (top trace) with MS/MS spectra of stressed (7 d 40 °C) Glu1-Fibrinopeptide. Experimental conditions: X-Bridge BEH300 C18, 3.5 µm, 2.1 x 150 mm column, H_2O/ACN with 0.1 % TFA, flow rate 0.2 mL/min, column temperature 50 °C.

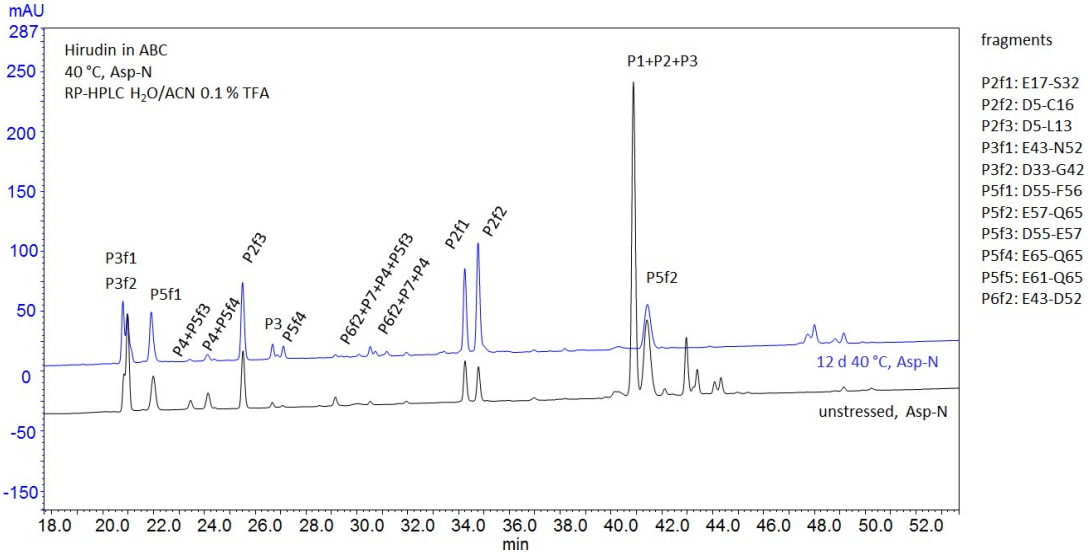

Figure 44: RP-HPLC: Zoomed (18.0-53.7 min) UV-chromatogram (214 nm wavelength) overlay for Hirudin. From bottom to top: unstressed, Asp-N (black), 12 d 40 °C, Asp-N (blue). Experimental conditions: X-Bridge BEH300 C18, 3.5 µm, 2.1 x 150 mm column, H_2O/ACN with 0.1 % TFA, flow rate 0.2 mL/min, column temperature 50 °C.

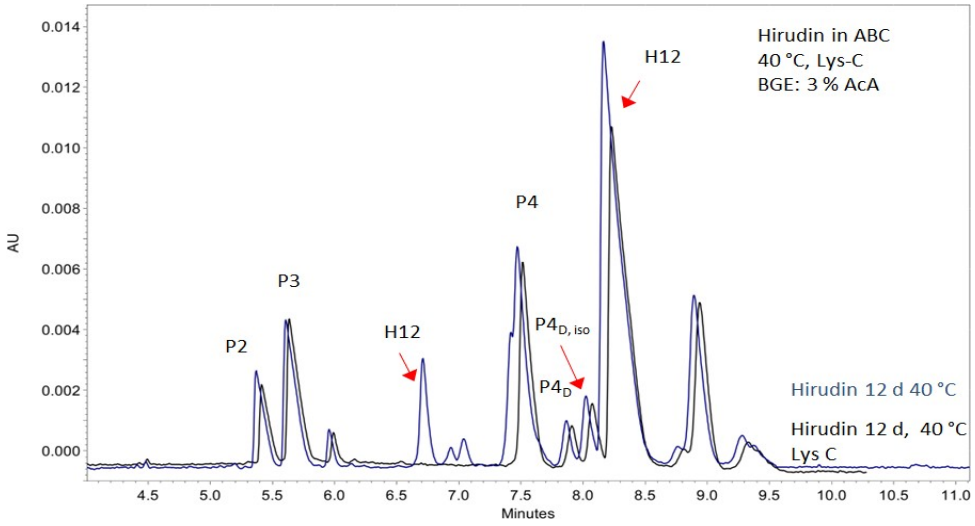

Figure 45: CZE: UV-electropherogram (214 nm wavelength) overlay for Hirudin (1.5 mg/mL). From bottom trace to top trace: 12 d 40 °C, Lys-C (black), 12 d 40 °C spiked to 12 d 40 °C, Lys-C (blue). Experimental conditions: BGE: 3 % AcA, 40/50 cm 50 µm fused silica capillary, dynamic coating with capillary conditioning solution, separation temperature: 25 °C, separation voltage: 30 kV, injection 0.5 psi 10 s.

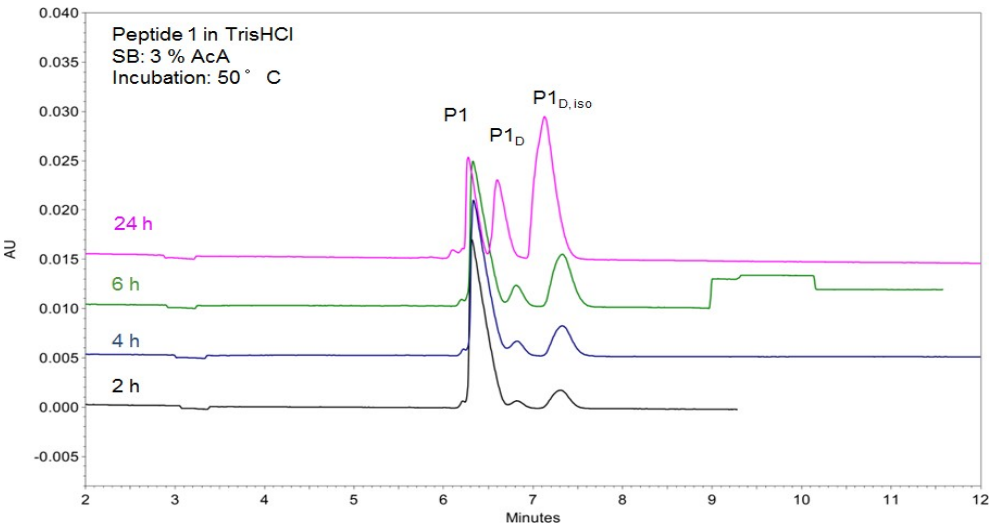

Figure 46: CZE, Peptide 1 in 50 mM Tris-HCl pH 8.6 (2 mg/mL), incubated at 50 °C for 2, 4, 6 and 24 h (no L-Asp); SB: 3 % AcA pH 2.5.

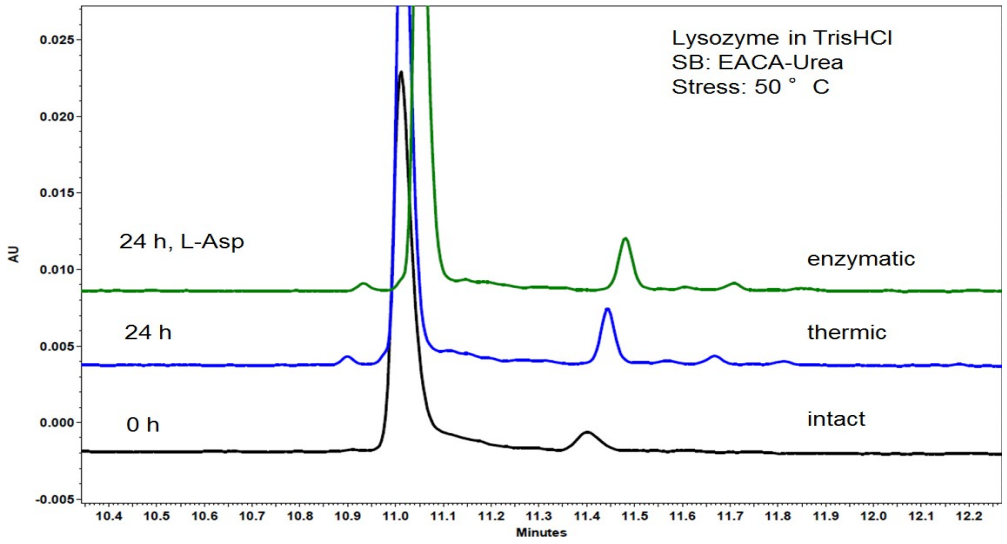

Figure 47: CZE, Lysozyme in 50 mM Tris-HCl pH 8.6 (2 mg/mL), unstressed (black trace), incubated without L-Asp at 50 °C for 24 h (blue trace), incubated in presence of L-Asp at 50 °C for 24 h (green trace); SB: 75 mM EACA/1 M Urea pH 3.5.

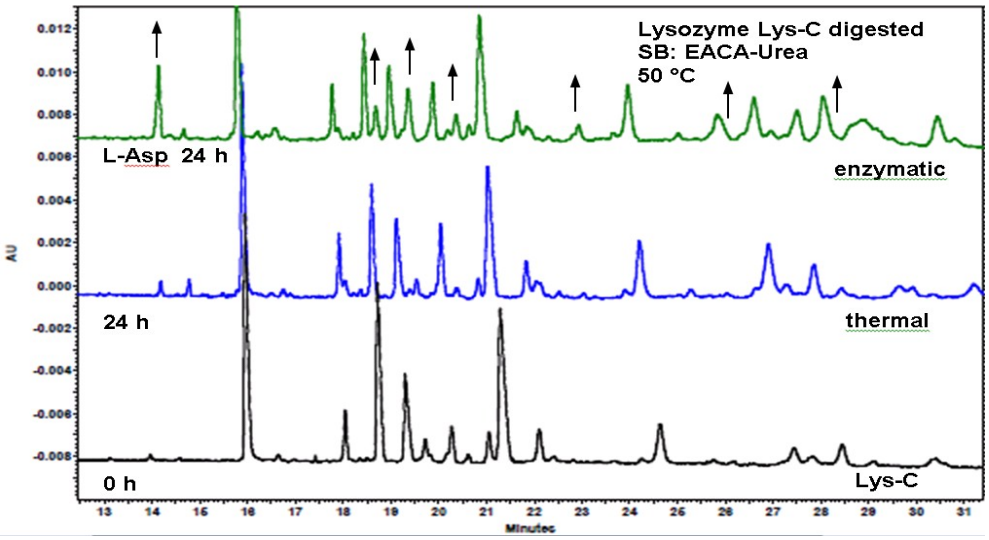

Figure 48: CZE, Lysozyme in 50 mM Tris-HCl pH 8.6 (2 mg/mL), Lys-C digested (black trace), incubated at 50 °C for 24 h (blue trace), incubated with L-Asp at 50 °C for 24 h (green trace); SB: 75 mM EACA/1 M Urea pH 3.5.

Table 42: Amino acid sequence of light (LC) and heavy chain (HC) of Avastin with calculated [131] average molecular weights and pI values.

Sequence	Mw [kDa]	pI
LC: DIQMTQSPSSLSASVGDRVTITCSASQDISNYLNWYQQKPGKA PKVLIYFTSSLHSGVPSRFSGSGSGTDFTLTISSLQPEDFATYYC QQYSTVPWTFGQGTKVEIKRTVAAPSVFIFPPSDEQLKSGTASV VCLLNNFYPREAKVQWKVDNALQSGNSQESVTEQDSKDSTYS LSSTLTLSKADYEKHKVYACEVTHQGLSSPVTKSFNRGEC	23.5	6.34
HC: EVQLVESGGGLVQPGGSLRLSCAASGYTFTNYGMNWVRQAP GKGLEWVGWINTYTGEPTYAADFKRRFTFSLDTSKSTAYLQMN SLRAEDTAVYYCAKYPHYYGSSHWYFDVWGQGTLVTVSSAST KGPSVFPLAPSSKSTSGGTAALGCLVKDYFPEPVTVSWNSGAL TSGVHTFPAVLQSSGLYSLSSVVTVPSSSLGTQTYICNVNHKPS NTKVDKKVEPKSCDKT**H**TCPPCPAPELLGGPSVFLFPPKPKDTL MISRTPEVTCVVVDVSHEDPEVKFNWYVDGVEVHNAKTKPREE QYNSTYRVVSVLTVLHQDWLNGKEYKCKVSNKALPAPIEKTISK AKGQPREPQVYTLPPSREEMTKNQVSLTCLVKGFYPSDIAVEW ESNGQPENNYKTTPPVLDSDGSFFLYSKLTVDKSRWQQGNVF SCSVMHEALHNHYTQKSLSLSPGK	49.8	8.35
Whole IgG	146.5	8.09

Table 43: Amino acid sequence of light (LC) and heavy chain (HC) of Erbitux with calculated [131] average molecular weights and pI values.

Sequence	Mw [kDa]	pI
LC: DILLTQSPVILSVSPGERVSFSCRASQSIGTNIHWYQQRTNGSP RLLIKYASESISGIPSRFSGSGSGTDFTLSINSVESEDIADYYCQQ NNNWTTFGAGTKLELKRTVAAPSVFIFPPSDEQLKSGTASVVCL LNNFYPREAKVQWKVDNALQSGNSQESVTEQDSKDSTYSLSS TLTLSKADYEKHKVYACEVTHQGLSSPVTKSFNRGA	23.5	6.34
HC: QVQLKQSGPGLVQPSQSLSITCTVSGFSLTNYGVHWVRQSPG KGLEWLGVIWSGGNTDYNTPFTSRLSINKDNSKSQVFFKMNSL QSNDTAIYYCARALTYYDYEFAYWGQGTLVTVSAASTKGPSVF PLAPSSKSTSGGTAALGCLVKDYFPEPVTVSWNSGALTSGVHT FPAVLQSSGLYSLSSVVTVPSSSLGTQTYICNVNHKPSNTKVDK RVEPKSPKSCDKT**H**TCPPCPAPELLGGPSVFLFPPKPKDTLMIS RTPEVTCVVVDVSHEDPEVKFNWYVDGVEVHNAKTKPREEQY NSTYRVVSVLTVLHQDWLNGKEYKCKVSNKALPAPIEKTISKAK GQPREPQVYTLPPSRDELTKNQVSLTCLVKGFYPSDIAVEWES NGQPENNYKTTPPVLDSDGSFFLYSKLTVDKSRWQQGNVFSC SVMHEALHNHYTQKSLSLSPGK	49.7	8.69
Whole IgG	145.6	8.48

Table 44: Area % of papain digested Avastin Fab, Fc fragments after spiking experiment.

Sample	Area % of Fc	Area % of Fab
Avastin	28.5	71.5
Avastin + 5 µl Fc	29.5	70.5
Avastin + 10 µl Fc	30.4	69.6
Avastin + 5 µl Fab	27.4	72.6
Avastin + 10 µl Fab	25.5	74.5

Papain digested Erbitux

Table 45: Area % of papain digested Erbitux Fab, Fc fragments after spiking experiment.

Sample	Area % of Fc	Area % of Fab
Erbitux	30.3	69.7
Erbitux + 5 µl Fc	33.7	66.3
Erbitux + 10 µl Fc	41.4	58.6
Erbitux + 5 µl Fab	29.0	71.0

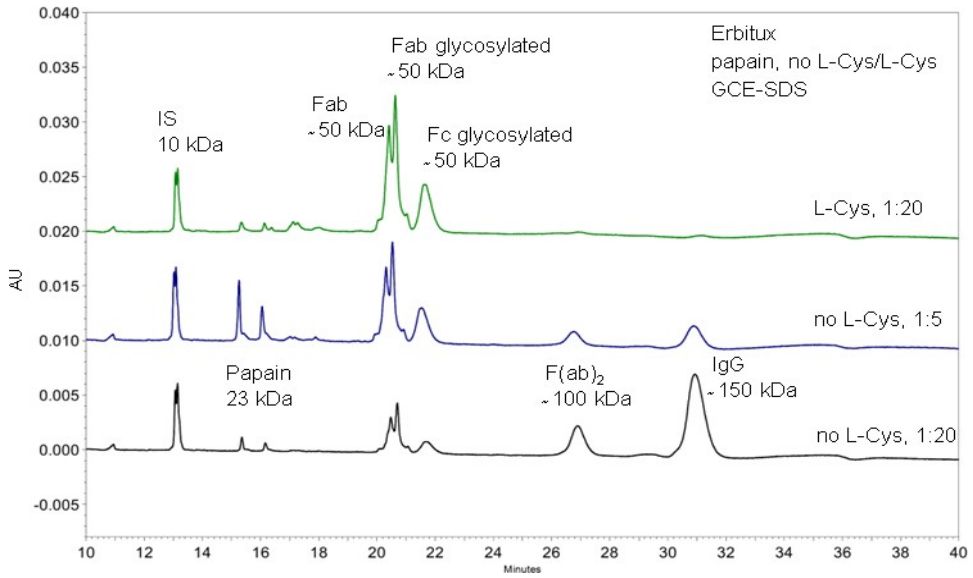

Figure 49: CGE-SDS of papain digested Erbitux: c_{end} = 0.9 mg/ml, papain digest 37 °C with/without L-Cys for 5 h.

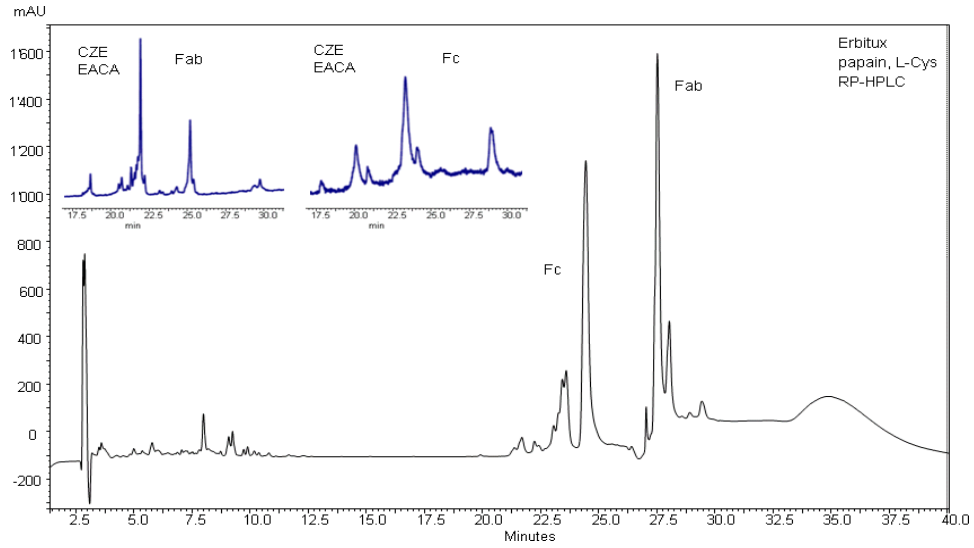

Figure 50: HPLC of papain digested Erbitux (c_{end} = 2.5 mg/mL), digestion in 1 mM L-Cys at 37 °C for 5 h and CZE separation of collected Fab and Fc fractions,. Experimental conditions: X-Bridge BEH300 C18, 3.5 µm, 2.1 x 150 mm column, H_2O/ACN with 0.1 % TFA, flow rate 0.2 mL/min, column temperature 50 °C. BGE: 600 mM EACA, 0.1 % HPMC, pH 6.0 ($I_{AcA, NaOH}$ = 4.5)

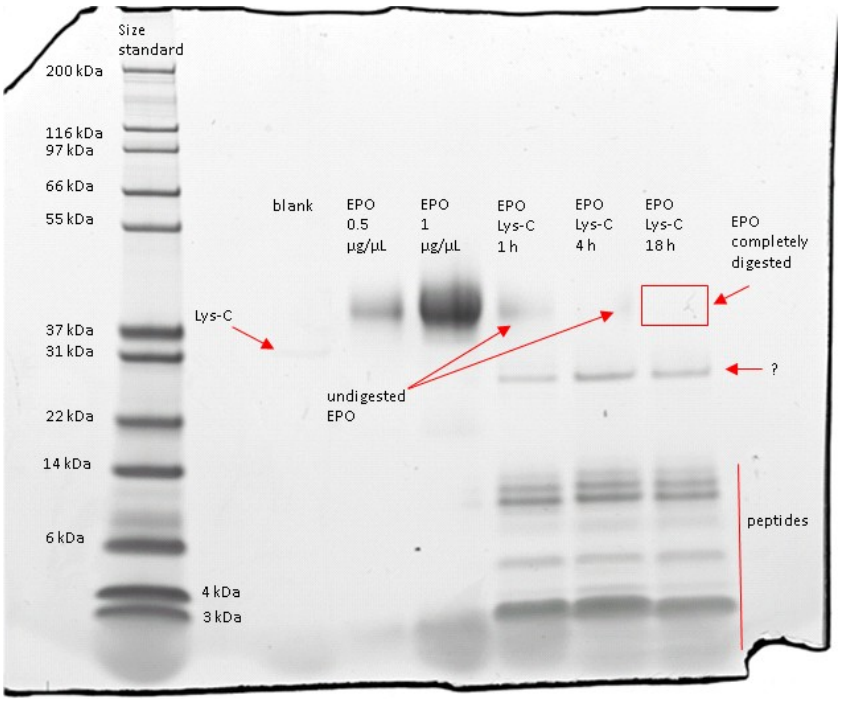

Figure 51: SDS-PAGE of Lys-C digested EPO.

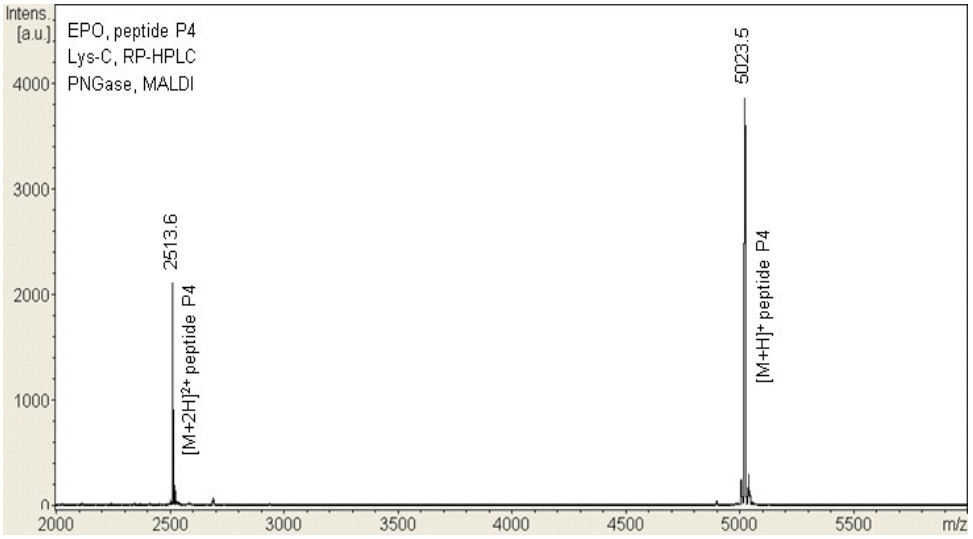

Figure 52: MALDI mass signals of Lys-C digested EPO, fraction of P4 after deglycosylation by PNGase: Experimental conditions: peptide II and protein I calibration standards, DHB matrix, positive mode, ground steel target.

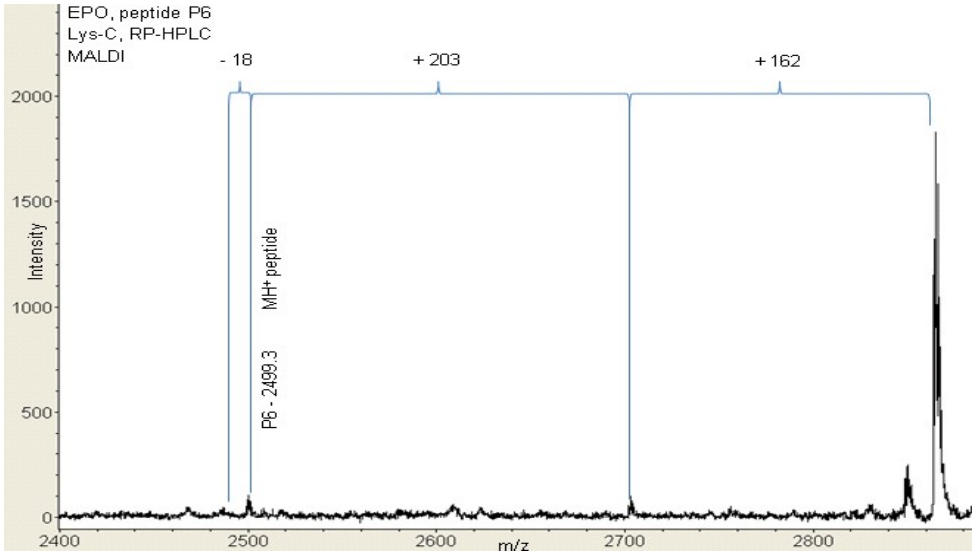

Figure 53: MALDI mass signals of Lys-C digested EPO, fraction of P6: Experimental conditions: peptide II and protein I calibration standards, DHB matrix, positive mode, ground steel target.